University of Alberta

Delivery of STAT3 Inhibitor Cucurbitacins to Tumor by Polymeric Nano-Carriers : Implications in Cancer Chemo- and Immunotherapy

by

Ommoleila Molavi

A thesis submitted to the Faculty of Graduate Studies and Research
in partial fulfillment of the requirements for the degree of

Doctor of Philosophy
in
Pharmaceutical Sciences

Faculty of Pharmacy and Pharmaceutical Sciences

Fall 2009
Edmonton, Alberta

Examining Committee

Dr. Afsaneh Lavasanifar, Faculty of Pharmacy and Pharmaceutical Sciences

Dr. Raymond Lai, Department of Laboratory Medicine and Pathology, Faculty of Medicine and Dentistry

Dr. Mavanur Suresh, Faculty of Pharmacy and Pharmaceutical Sciences

Dr. Ayman El-Kadi, Faculty of Pharmacy and Pharmaceutical Sciences

Dr. Colin Anderson, Department of Surgery, Faculty of Medicine and Dentistry

Dr. Satya Prakash, Department of Biomedical Engineering, Mcgill University

Dedication

"Ahead of all I humbly thank GOD, the Most Compassionate the Most Merciful, who gave me health, thoughts, supportive family, great mentors and co-operative people to enable me achieve this goal."

This Thesis is dedicated to:

My dear husband, Nasser Samadi and my lovely son, Amin Samadi, who offered me unconditional love and support throughout the course of this thesis. You are my blessings from GOD and I love you so much!

My wonderful father, Mohammad Hossien Molavi, who devoted his life to raising me to be the person I am today. You have been with me every step of the way, through good and bad times. Thank you for all the unconditional love, guidance, and support that you have always given me, helping me to succeed and instilling in me the confidence that I am capable of doing anything I put my mind to. Thank you for everything. I love you so much!

The memory of my mother, Sakineh Booterabi. She was the brightest star in the sky of my life but sadly disappeared very early in my life. Peace be upon her.

The memory of my great mentor, Professor John Samuel, a most extraordinary supervisor to whom I owe a vast debt. He provided me with the incentive and excellent advice to undertake this project and inspired in me a passion for cancer research. Prof. Samuel was a man of faith, great honor and integrity. His inquisitive and meticulous natures are traits I hope to exemplify. I will miss him greatly and hope I have made him proud. Peace be upon him.

ABSTRACT

Signal Transducer and Activator of Transcription 3 (STAT3), a common oncogenic mediator, is constitutively activated in many types of human cancers and plays a critical role in tumor growth and cancer immune evasion. The focus of this dissertation is the delivery of STAT3 inhibitor cucurbitacins to tumors using polymeric nano-carriers for the inhibition of tumor growth and modulation of tumor-induced immunosuppression.

The anticancer and immunomodulatory activity of STAT3 inhibitor JSI-124 (cucurbitacin I) was studied in mice carrying B16 tumor. The results showed that JSI-124 + CpG or 7-acyl lipid A combination therapy modulated immunosuppression in tumor environment and generated superior anti-tumor effects compared to monotherapy. In further studies, a sensitive and reproducible liquid chromatography-mass spectroscopy (LC-MS) method was developed and validated for quantitative analysis of STAT3 inhibitor cucurbitacins *in vitro* and in biological samples. Moreover, nano-delivery systems based on poly(ethylene oxide)-*block*-poly(ε-caprolactone) (PEO-*b*-PCL) micelles and its analogues containing physically encapsulated cucurbitacin and poly(D,L -lactic-co-glycolic acid) (PLGA) nanoparticles (NPs) containing chemically conjugated JSI-124 for the delivery of STAT3 inhibitor to tumor and dendritic cells (DCs) were developed and characterized. Polymeric micelles of different PCL based core structure were able to significantly increase the water solubility of STAT3 inhibitor cucurbitacins, and slow the rate of drug release by a diffusion dependent mechanism. The chemical structure of the micellar core was found to control the

release rate of cucurbitacin from the micelles. PLGA NPs containing conjugated JSI-124, on the other hand, demonstrated a degradation dependent drug release profile over a 1-month period. Both nanoparticulate formulations exhibited potent anticancer and STAT3 inhibitory activity against B16 cancer. Moreover PLGA-JSI-124 NPs suppressed STAT3 activation in immunosuppressed p-STAT3^{high}DCs and significantly improved their function in stimulating T cell proliferation *in vitro*. These findings show that JSI-124 esters of PLGA NPs can potentially provide a useful platform for JSI-124 delivery to tumor and its targeted delivery to DCs.

The results of this research not only proved the principle of STAT3 inhibition in tumors as an efficient intervention for enhancing the therapeutic efficacy of TLR ligand-based cancer immunotherapy, but led to development of nano-delivery systems with potential application in cancer chemo-and immunotherapy.

ACKNOWLEDGEMENTS

- The words fall short for my great mentor Dr. John Samuel, to express my gratitude. He was an incredible supervisor from whom I not only learned about scholarly conduct but got life lessons that extend far beyond the academic arena. He exemplified the true meaning of a mentor and made this degree process an experience that I will never forget.
- I am very indebted to my kind supervisor, Dr. Afsaneh Lavasanifar for her enormous support and guidance throughout my PhD program. The completion of this thesis would not have been possible without her assistance and support.
- I sincerely thank Dr. Raymond Lai, for serving on my supervisory committee and his active participation and support during my PhD program. I will never forget his generosity, care, and the time he took for helping me in this project.
- My sincere thanks go to Dr. Mavanur Suresh, my advisory committee member, for his support and contribution, Dr. Colin Anderson for serving on my candidacy and defense committee, and Drs. Ayman El-Kadi and Satya Prakash for serving on my defense committee.
- I thank Drs. Dion Brocks and Anooshirvan Shayeganpour for their help with pharmacokinetic studies, Dr. Vishwanatha Somayaji for assisting in LC/MS & NMR analysis, and Dr. Zengshuan Ma for helping me with the animal studies.
- I would like to thank Dr. Praveen Elamanchili for training me in the bench work at the beginning of my program and my dear friend Dr. Samar Hamdy for all her kindness during the course of this thesis.
- I am very grateful to all my previous and recent labmates for providing a friendly and happy environment in the group. Their ideas and suggestions for this project were always clever and useful.
- The words cannot express my gratitude to my family for their love, encouragement, and patience throughout the peaks and valleys of this journey.

Finally I am grateful to the Iranian Ministry of Health and Medical Education, Faculty of Pharmacy at the University of Alberta, and Rx & D Health Research Foundation / Canadian Institutes of Health Research, sponsors of this research.

TABLE OF CONTENTS

LIST OF TABLES

LIST OF FIGURES

LIST OF ABBREVIATIONS

Ab	antibody
ABL	Abelson leukaemia
ADCC	antibody-dependent cell mediated cytotoxicity
Ag	antigen
ALCL	anaplastic large cell lymphoma
AP1	activating protein 1
APC	antigen presenting cells
ANOVA	analysis of variance
ATCC	American Type Culture Collection
ATF1	activating transcription factor 1
AUC	area under the curve
B16CM-DCs	DCs treated with CM from B16 cells
BCA	bicinchoninic acid
BCR	the breakpoint-cluster region
BMDC	bone marrow derived dendritic cells
BSA	bovine serum albumin
Bu-Li	butyl lithium
CDC	complement dependent cytotoxicity
$CDCl_3$	deuterated chloroform
c.IAP2	the cellular inhibitor of apoptosis 2
CMC	critical micelle concentration
Con.	concentration

COX2	cyclooxygenase 2
CpG	cytosine-phosphate-guanine
cpm	counts per minute
CTL	cytotoxic T lymphocyte
DAB	3-3 diaminobenzidene
DAMP	damage associated molecular pattern
DCC	N,N- dicyclohexylcarbodiimide
DCs	dendritic cells
ddH_2O	distilled water
DLS	dynamic light scattering
DMAP	dimethylaminopyridine
DMSO	dimethyl sulfoxide
DNA	deoxyribonucleic acid
DOX	doxorubicin
DTT	dithiothreitol
EDTA	ethylenediamine tetra-acetic acid
EGTA	ethyleneglycotetraacetic acid
ELISA	enzyme-linked immunosorbent assay
EPR	enhanced permeability and retention
ER	endoplasmic reticulum
FACS	fluorescent activate cell sorting
FBS	fetal bovine serum
FCS	fetal calf serum

FDA	food & drug administration
FITC	fluorescene isothiocyanate
Foxp3	forked-head transcription factor 3
FSC	forward scatter
g	gravitation force
GAPDH	glyseraldehyde-3-phosphate dehydrogenase
G-CSF	granulocyte colony stimulating factor
GM-CSF	granulocyte-macrophage colony stimulating factor
GPC	Gel Permeation Chromatography
GRB2	growth factor receptor-bound protein 2
h	hour
HCl	hydrochloric acid
HEPES	4-(2-hydroxyethyl)-1-piperazineethanesulfonic acid)
HMGB	high mobility group box 1
HPLC	high performance liquid chromatography
HSLAS	health sciences laboratory animal facilities
HSP	heat shock protein
I	iodine
IC_{50}	50% inhibition in cell growth
IDO	indoleamine 2,3-dioxygenase
IFN-α	interferon-α
IFN-γ	interferon gamma
Ig	immunoglobulin

IKK	inhibitor of NF-κB kinase
IL	interleukin
IP	interferon inducible protein
i.p.	intraperitoneal
IRAK	interleukin receptor associated kinase
I.S	internal standard
i.v.	intravenous
JAK	Janus kinase
JNKK1	c-JUN N-terminal kinase (JNK) kinase 1
JSI-124	JAK/STAT inhibitor (cucurbitiacin I)
KDa	kilodaltons
KV	kilovoltage
L	litter
LC-MS	liquid chromatography-mass spectrometry
LNs	lymph nodes
LPS	lipopolysaccharide
µL	microlitre
µg	microgram
mAb	monoclonal antibody
MAPK	mitogen-activated protein kinase
M-CSF	macrophage colony stimulating factor
mDC	myeloid dendritic cells
[M-H]	deprotonated molecular ion

mg	milligram
MHC	major histocompatibility complex
min	minutes
mL	milliliter
MLR	mixed lymphocyte reaction
MMP	Matrix Metalloproteinas
MPLA	monophosphoryl lipid A
MR	mannose receptors
MTD	the maximum tolerated dose
MTT	3-(4,5-dimethylthiazole-2-yl)-2,5-biphenyl tetrazolium bromide
MUC1	mucin-1
MW	molecular weight
MyD88	myeloid differentiation factor-88
NaF	sodium fluoride
NaOH	sodium hydroxide
Na_3VO_4	sodium orthovanadate
NF-κβ	nuclear factor kappa beta
ng	nanogram
NIK	NF-κB-inducing kinase
NK cells	natural killer cells
nm	nanometer
NMR	nuclear magnetic resonance
NPs	nanoparticles

NPM-ALK	nucleophosmin-anaplastic lymphoma kinase
NRTK	non-receptor Tyr kinases
OD	optical density
ODN	oligodeoxynucleotide
OVA	ovalbumin
o/w	oil-in-water
PAMP	pathogen-associated molecular patterns
PBMC	peripheral blood mononuclear cells
PBS	phosphate buffered saline
PCCL	α-carboxyl-ε-caprolactone
pDCs	plasmacytoid dendritic cells
PE	phycoerythrin
PEO	poly(ethylene oxide)
PEO-*b*-PBCL	poly(ethylene oxide)-*block*-poly(α-benzyl carboxylate ε-caprolactone)
PEO-*b*-PCL	poly(ethylene oxide)-*block*-poly(ε-caprolactone)
PEO-*b*-PPO	poly(ethylene oxide)-*block*-polypropylene oxide
Pg	picogram
PI	propidium iodide
PIAS	proteins inhibitors of activated STAT
PIPase	Tyr phosphatase
PLAA	poly(L-amino acid)
PLGA	Poly(D,L-lactic-co-glycolic acid)

PRR	pattern recognition receptors
p-STAT	phosphorylated-STAT3
PVA	polyvinyl alcohol
PVDF	polyvinylidene fluoride
PXT	paclitaxel
RANTES	regulated on activation normal T cell expressed and secreted
RES	reticuloendothelial system
RP-HPLC	reverse phase HPLC
RNA	ribonucleic acid
RTK	receptor Tyr kinases
s	seconds
S	serine
s.c.	subcutaneous
SD	standard deviation
SDS-PAGE	sodium dodecyl sulfate polyacrylamide gel electrophoresis
SH2	Src-homology 2
SIR	selected ion recorder
SOCS	suppressor of cytokine signaling
Sol	soluble
SSC	side scatter
STAT	signal transducer and activator of transcription
TAA	tumor associated antigen
TBAP	tetrabutylammonium dihydrogenphosphate

TCR	T cell receptor
TE	Tris EDTA
TGF-β	transformation growth factor beta
Th cell	T helper cell
THF	tetrahydrofuran
TIL	tumor infiltrating lymphocytes
TIR	Toll–interleukin-1 receptor
TIRAP	Toll–interleukin (IL)-1 receptor (TIR)- associated protein
TLC	thin layer chromatography
TLR	toll-like receptor
TMB	3,3',5,5' tetramethylbenzidine
TNF-α	tumor necrosis factor alpha
TRAF	TNF-receptor associated factors
TRAM	TRIF related adaptor molecule
T_{reg}	regulatory T cells
TRIF	Toll receptor-associated activator of interferon
VEGF	vascular endothelial growth factor
w/o/w	water-in-oil-in-water
Y	tyrosine

Chapter 1

Introduction

1.1 Introduction: an overview

The immune system can recognize malignant cells as foreign agents and develop anticancer immune responses resulting in the destruction of a developing cancer [1]. The existence of an immune response to cancer supports the idea that a therapeutic strategy which can boost anticancer immune responses and keep the immune system effective and functional, would guarantee complete cancer remission and keep the cancer in check [1]. During the last two decades several cancer immunotherapy strategies including cancer vaccines have been successfully developed [2-4]. Although vaccine-based cancer immunotherapy strategies have shown great capability in breaking tolerance to cancer antigens and priming tumor-specific immune responses, they have shown poor therapeutic outcome in clinical cancer treatment [5-7]. More recent studies suggests that the immunosuppressive tumor environment, which is frequently found in many types of cancer and believed to limit the trafficking and function of anti-tumor immune effector cells, is partly to be blamed for the poor therapeutic efficacy of cancer vaccines. A major endeavor for research in tumor immunotherapy today is to figure out how to overcome immunosuppression in the tumor microenvironment and facilitate the effector phase of anti-tumor immune responses [8-10].

Cancer cells develop several mechanisms to induce immunosuppression in tumor microenvironment [7,9,11]. Accumulating evidence shows that cancer cells usurp the biological role of immune cells, in particular dendritic cells (DCs), to establish an immunosuppressive tumor environment. DCs are professional antigen presenting cells (APCs) of the immune system and play a key role in the induction

of tolerance versus immunity [12,13]. Cancer cells produce immunosuppressive factors and are defective in the production of pro-inflammatory cytokines. This promotes the activation of tolerogenic DCs which in turn can activate immunosuppressor regulatory T (T_{reg}) cells. Tolerogenic DCs and T_{reg} cells are important cellular effectors of tumor immunosuppression [7,14]. Constitutive activation of a key transcriptional factor, signal transducer and activator of transcription 3 (STAT3) in tumor and DCs has been identified as an important mechanism by which cancer induces activation of tolerogenic DCs and T_{reg} cells and establish an immunosuppressive network in tumor environment [11,15-17]. STAT3 is constitutively active in many types of cancer and plays an important role in tumor progression through the modulation of the genes involved in tumor growth, survival, angiogenesis, metastasis, and cancer immune evasion [18-20]. Therefore, blocking STAT3 in tumor has been suggested as a promising strategy for the inhibition of tumor growth and modulation tumor immunosuppression.

Cucurbitacin I (JSI-124) and cucurbitacin B are potent anticancer agents which selectively inhibit STAT3 pathway [21,22]. Previous studies have shown that JSI-124 can exert immunomodulatroy effects through inhibition of STAT3 in immunosuppressed DCs and enhance the therapeutic efficacy of a cancer vaccine [23,24]. The first part of this project has investigated the immunomodulatory effects of JSI-124 in combination with ligands of Toll-like receptors (TLRs) that activate DCs, in mice carrying B16 melanoma tumor with constitutively active STAT3. TLR ligands, in particular unmethylated cytosine-phosphate-guanine (CpG) (TLR9 ligand) and synthetic lipid A analogous (TLR4 ligands), have been

extensively studied as an adjuvant in vaccine-based cancer immunotherapy strategies [25,26]. Activation of DCs through their TLRs has been extensively investigated as an attractive strategy for the induction of T cell mediated anticancer immune responses, which is believed to be critical for effective anti-tumor immunity [27]. In addition to activating T cell mediated immune responses against cancer, ligation of TLR receptors can serve to reverse the suppressive effects of T_{reg} cells, which play an important role in the suppression of anti-tumor immune responses [28,29]. Clinical application of cucurbitacins is restricted because of their poor water solubility and non-specific toxicity. The second part of this project was; therefore, devoted to the development of two polymeric nano-carriers, i.e., polymeric micelles and nanoparticles, for the solubilization and controlled delivery of cucurbitacins to tumor and/or DCs. In light of the above mentioned research objectives, in this chapter, we will first provide an overview on cancer-immune system interaction and the role of STAT3 and TLR ligands in modulating anticancer immune responses and will describe the potential effects of selective STAT3 inhibition and TLR ligandation in tumor/dendrtic cells in cancer immunotherapy strategies. In the second part, polymeric nano-delivery systems used in this research for tumor and/or DC targeting of JSI-124 and TLR ligands, i.e, polymeric micelles and nanoparticles, will be briefly discussed.

1.2 Immune system and cancer

An increasing body of evidence supports the idea that the immune system plays an important role in fight against cancer [1,30,31]. The cancer-protective

role of immune system was first described as a concept termed 'immunosurveillance'. Based on this theory, immune system sees cancer as foreign and develops immune responses, which result in the destruction of transformed or malignant cells. Although this theory was able to describe the function of immune system in eliminating pre-clinical cancers, it couldn't provide convincing explanation of how pre-clinical cancers develop into clinically detectable tumor in the presence of a functioning immune system. The updated theory of 'Immunoediting' provides more comprehensive explanation for the role of immune system in cancer [1,32]. In this theory, selection pressures applied by the immune response to tumors are believed to modulate tumor immunogenicity and growth. Based on the concept of 'Immunoediting', the interaction of the immune system with cancer involves three phases including elimination, equilibrium, and escape (Figure 1-1. adopted from [32]). During the elimination phase which is equivalent to 'immunosurveillance', immune cells recognize and destroy a developing tumor, thus protecting host against cancer. After elimination phase, cancer cells and immune cells enter into a dynamic equilibrium as a result of which immune resistant cancer cells are selected. The equilibrium phase, which is believed to be as long as 20 years, is followed by the escape phase of tumor development. The immune resistant cells in escape phase have several mechanisms to evade anticancer immune responses and develop to clinically apparent tumors. Accumulating evidence, including the occurrence of spontaneous tumor remissions, epidemiological studies indicating high prevalence of cancer in immunosuppressed individuals, and the prognostic role of tumor-

infiltrating lymphocytes (TILs), supports a surveillance role for the immune system in the elimination of pre-clinical cancers. It also supports a powerful role for the immune system in modifying the immunogenicity and behavior of clinically evident cancers [33,34].

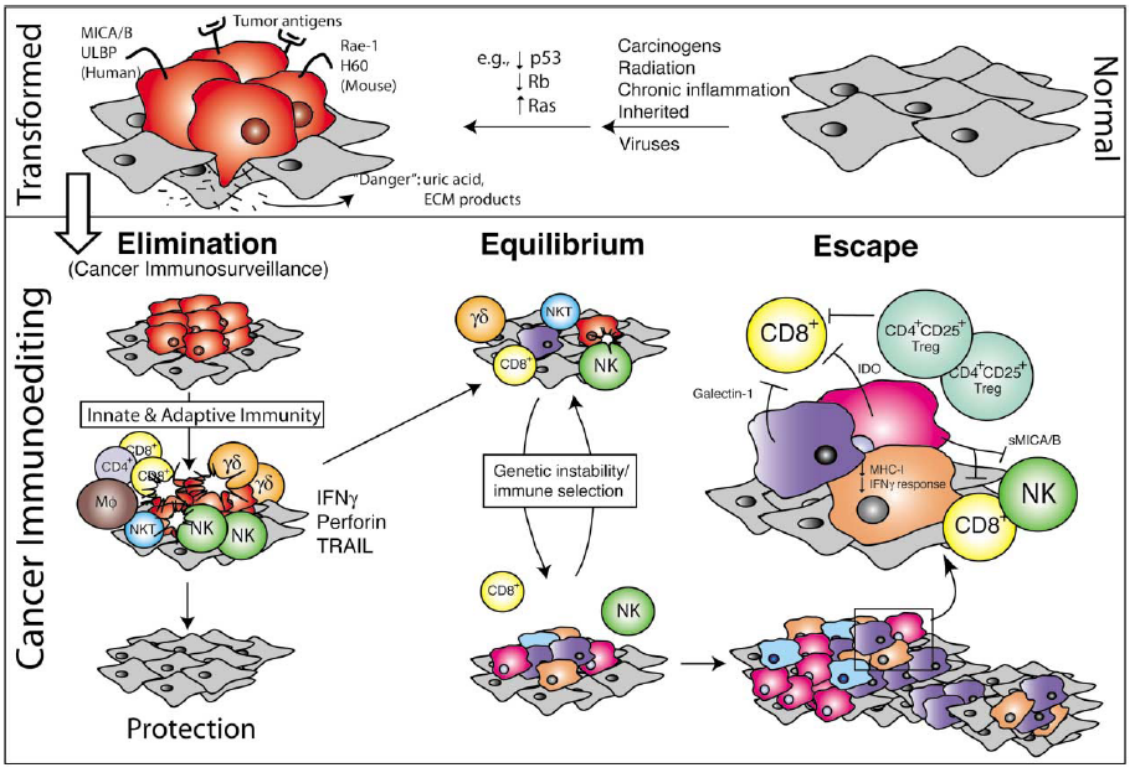

Figure 1-1. The three phases of the cancer immunoediting process (adopted from [32]). Normal cells (gray) subject to common oncogenic stimuli ultimately undergo transformation and become tumor cells (red) (top). Even at early stages of tumorigenesis, these cells may express distinct tumor-specific markers and generate proinflammatory "danger" signals that initiate the cancer immunoediting process (bottom). In the first phase of elimination, cells and molecules of innate and adaptive immunity, which comprise the cancer immunosurveillance network, may eradicate the developing tumor and protect the host from tumor formation. However, if this process is not successful, the tumor cells may enter the equilibrium phase where they may be either maintained chronically or immunologically sculpted by immune "editors" to produce new populations of tumor variants. These variants may eventually evade the immune system by a variety of mechanisms and become clinically detectable in the escape phase.

1.3 DCs, T cells, and anticancer immunity

DCs, the most professional APCs, play a central role in initiating and controlling adaptive immune responses [35-37]. DCs are a heterogeneous population of cells with a dendritic shape which originate from hemopoietic progenitors in the bone marrow either through myeloid or lymphoid pathways and serve as ‘sentries’ in most peripheral tissues. DCs can be subdivided into conventional DCs (cells having phenotypic and functional characteristics of DCs) and pre-DCs (cells which require a further step of development to gain phenotypic and functional DC features). Conventional DCs have been categorized into two major subsets including migratory and lymphoid tissue-resident DCs. Migratory DCs are the sentinels of non-lympoid tissues and migrate to the draining lymph nodes (LNs) after encounter with antigen and inflammatory stimuli. Migration to LNs can also occur at low rate in steady-state conditions. Lymphoid tissue-resident DCs do not migrate to the lymphoid organs through the lymphatics, but capture the antigen directly inside the lymphoid organ. Most of thymic, spleen and around half of lymph node DCs are lymphoid tissue-resident cells [38-40].

Functional maturation of DCs is a critical step in the induction of adaptive immunity. Before antigen encounter, DCs are in the immature state. As they encounter microbes, they engulf them through phagocytosis [41]. This results in the activation, maturation and migration of DCs to draining LNs, where they present the processed antigens in association with major histocompatibility complex (MHC) class I and class II molecules to the naïve T cells resulting in T cell activation. The microenvironment of antigen capture and antigen presentation

by DCs, control the direction and magnitude of immune responses [42,43]. DCs distinguish between 'non-self' and 'self' by recognition of pathogen-associated molecular patterns (PAMP) using pattern recognition receptors (PRR). TLRs are the most well characterized type of PRR. PAMPs are considered 'exogenous danger signals' for DCs and are critical for the functional maturation and efficient activation of DCs [44]. In addition to PAMP, recent studies have identified some endogenous danger signals called damage associated molecular pattern (DAMP) which are released by tissues undergoing stress, damage or abnormal death and can efficiently activate DCs through PRRs [45].

Development of immune responses against cancer can be divided into two distinguished phases including priming and effector phases (Figure 1-2. adopted from [10]). In priming phase of anticancer immunity, DCs take up cancer cell debris carrying cancer specific/associated antigens expressed by tumor cells and can become activated by endogenous danger signals (i.e. DAMP) released by stressed or damaged cells which are abundant in tumor. The activated DCs then induce T cell mediated immune responses, which is considered to be the main mechanism for immune system to fight against cancer. During the effector phase of anticancer immunity, activated T cells traffic in tumor microenvironment and fight against cancer cells [10]. Although spontaneous activation of tumor specific T cell responses has been reported in many types of human cancer [1], the development and function of anticancer immune effector cells are defective in most cases for the following reasons. First of all, cancer cells arise from the body's normal cells so they have same antigenic epitopes to which the immune

system is tolerant. Moreover, most tumors are poorly immunogenic and most importantly cancer cells develop several mechanisms to suppress both the priming phase and the effector phase of anticancer immune responses. Several cancer immunotherapy strategies have been developed to boost immune system function in cancer patients [7,46,47].

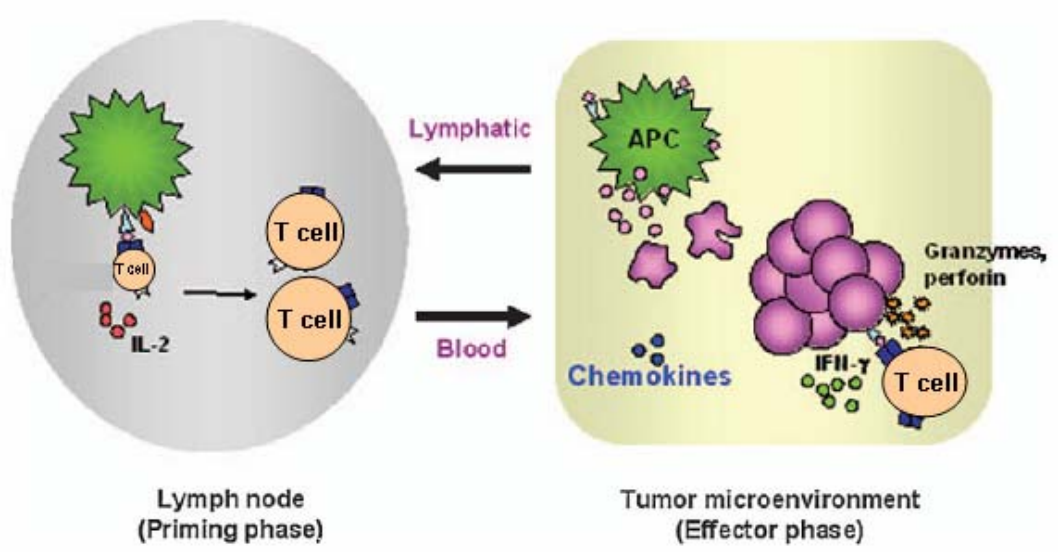

Figure 1-2. Model distinguishing between the priming phase and effector phase of an antitumor immune response (adopted from [10]). The steps believed to be required for the generating of an effective anti-tumor T-cell response have been divided into the priming phase (believed to occur in LNs) and the effector phase, which is focused on tumor sites.

1.4 Cancer immunotherapy

Immunotherapy for cancer attempts to harness the superb power and specificity of the immune system for the treatment of malignancy [46]. Immunotherapies of cancer have been investigated by two main methods including passive and active immunization against cancer. Passive immunotherapy strategies aim at supplying a component of the immune system to strengthen the anticancer immune responses. In this type of immunotherapy,

antibodies, cytokines, or other immune system components are made outside of the body (i.e. in the laboratory) and administered to patients to provide immunity against cancer. Monoclonal antibody (mAb) therapy is the most widely used form of passive immunotherapy. The therapeutic effects of mAb are exerted through various mechanisms [48]. The direct anticancer effects of mAb therapy is generated by blocking growth factor receptors resulting in arresting tumor cell proliferation and induction of apoptosis or programmed cell death. Indirect effects of mAb therapy include recruiting cytotoxic cells, such as monocytes and macrophages. This type of antibody-mediated cell killing is called antibody-dependent cell mediated cytotoxicity (ADCC). Monoclonal Abs also bind to complement, leading to direct cell toxicity, known as complement dependent cytotoxicity (CDC) [48]. While passive immunotherapies do not stimulate a patient's immune system to "actively" respond to cancer, active immunotherapy strategies seek to stimulate the immune system and activate tumor-specific immune responses (Figure 1-3. adopted from [49]). In active immunotherapy, cancer associated or specific antigens are delivered to APCs which then present antigenic epitope (peptide) of cancer cells in the context of major MHC molecules to T cells and activate adaptive immune responses against cancer. For cancer immunotherapy, generation of active immunity is believed to be a better option, since it induces an endogenous anti-tumor immune response, which has a potential to initiate long-term immunologic memory. In the field of cancer immunotherapy, most enthusiasm has been directed towards the design and application of cancer vaccines that are developed to generate active

immunizations against growing tumors**.** The ultimate goal of vaccine-based cancer immunotherapy is to elicit potent anticancer immune responses that will cause the eradication of the tumor, and at the same time, generate a long-term memory response that will lead to complete cancer remission and keep the cancer in check [46].

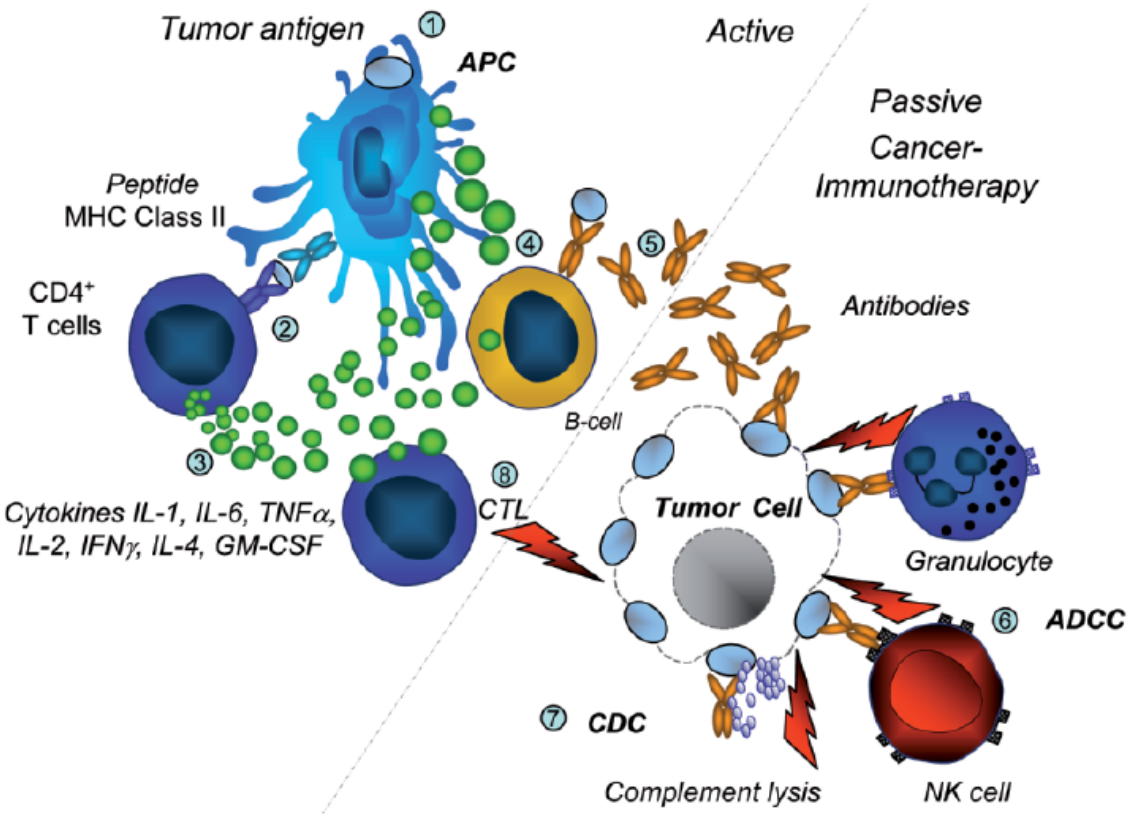

Figure 1-3. Active vs. passive immunotherapy of cancer (adopted from [49]). The whole spectrum of passive and active cancer immunotherapy is summarized. Active cancer immunotherapy comprises tumor antigen uptake by APCs (1), epitope (peptide) presentation to CD4+ T cells (2), cytokine release (3), B cell activation (4), and antibody production (5), leading to lysis of tumor cells including different (passive) alternatives like ADCC (6), CDC (7) or unspecific attack by cytotoxic T lymphocytes (8).

Despite major advancements in understanding the mechanisms of tumor immunity and successful development of several cancer vaccines that can break tolerance to cancer and induce potent anti-tumor immune responses, success of cancer vaccines in the clinic has been limited. This is mainly due to the ability of cancer to develop several strategies to thwart anti-tumor immune responses. Recent studies have shown that tumors can establish an immunosuppressive microenvironment by elaboration of immunosuppressive factors, activation of immunosuppressive immune cells, impairment of antigen presentation, and the activation of co-inhibitory signals [6,7,46,47].

1.5 Tumor immunosuppression: a major obstacle to cancer immunotherapy

One of the major obstacles to effective immunotherapy of cancer is the ability of tumors to promote an immunosuppressive microenvironment that limits the activation, tumor infiltration, and function of anti-tumor immune effector cells [9,10,47]. The immunosuppression by cancer cells is induced through production of immunosuppressive enzymes and cytokines, which in turn mediate the activation of immunosuppressive cells including tolerogenic DCs and T_{reg} cells [7,9]. The tolerogenic DCs and T_{reg} cells are the major cellular effectors of tumoral immunosuppression [7,9,14,43,50-53]. Tolerogenic DCs can be generated due to the expression of immunosuppressive factors by cancer cells and the lack of pro-inflammatory cytokines in tumor environment. Such tolerogenic DCs are incapable of inducing anti-tumor immune responses. Instead, they can activate T_{reg} cells [43,52,54]. T_{reg} cells have important physiological functions in the

induction of tolerance to self antigens and preventing autoimmunity diseases [55,56]. In cancer, T_{reg} cell activation has been identified as an important mechanism by which cancer suppress the activation and function of anti-tumor T cell responses. Activation of T_{reg} cells by tumor is a major obstacle against success in cancer immunotherapy [14]. Although convincing evidence indicates the critical role of T_{reg} cells in the suppression of anti-tumor immune responses, the mechanisms of their suppressive activity remains to be established [50,53,57-60]. The best characterized type of T_{reg} cells are naturally occurring $CD4^+$ T_{reg} cells which constitutively express CD25 (IL-2 receptor α chain) on their surface and constitute 5–6% of $CD4^+$ T cells in human [56,61]. In addition to naturally occurring $CD4^+$ $CD25^+$ T_{reg} cells, other $CD4^+$ T_{reg} cells include Tr-1 cells secreting IFN-γ, and IL-10, and Th3 cells secreting high levels of transforming growth factor-beta (TGF-β), interleukin (IL)-4 and IL-10 [43,62]. The expression of CD25 on T-cells has been used as a useful marker of T_{reg} cells, but since CD25 is also expressed on activated T cells; its expression is not necessarily associated with T_{reg} cell function. Among the other molecules identified for T_{reg} cells, forked-head transcription factor 3 (Foxp3) may be a specific marker of $CD4^+$ T_{reg} cells in mice and human [63-65].

The indoleamine 2,3-dioxygenase (IDO) and cyclooxygenase 2 (COX2) are two important enzymes which are produced by tumors and tolerogenic DCs [7]. IDO catabolizes the essential amino acid tryptophan and contributes to tumoral immune tolerance by blocking the activation of effector T cells. IDO has also been shown to limit the trafficking of immune effector cells to tumors [9,66-

68]. On the other hand, COX2 has been shown to play an important role in the generation of T_{reg} cells [9,69-71]. The most important immunosuppressive cytokines involved in cancer immune evasion, are vascular endothelial growth factor (VEGF), IL-10 and TGF-β [9]. VEGF which is abundantly expressed by a large percentage of solid tumors and originally thought to be only involved in tumor angiogenesis, has emerged as a significant agent mediating immune tolerance in the tumor microenvironment. Compelling evidence has shown that VEGF inhibits DC activation and induces T_{reg} cell generation in cancer [72-76]. IL-10 and TGF-β have been shown to be expressed by many types of tumors as well as tolerogenic DCs and T_{reg} cells and suppress the activation and function of anti-tumor immune responses [9,77-79].

The molecular mechanisms by which cancer produce immunosuppressive factors, inhibit pro-inflammatory cytokines, and induce activation of tolerogenic DCs and T_{reg} cells are not completely understood. Nevertheless, recent studies of host-tumor interaction have identified important molecules involved in tumor-induced immunosuppression. One of these molecules is an important oncogenic protein called STAT3 which is believed to be a key mediator of tumor-induced immunosuppression [11].

1.6 The role of STAT3 in cancer

1.6.1 STAT proteins

STAT3 belongs to STATs family of proteins which is one of the recently recognized oncogenic signaling pathways. This family of proteins comprises

seven known members including STAT1 to STAT4, STAT6, and the closely related STAT5a and STAT5b proteins [18,80,81]. These proteins have dual roles as cytoplasmic signaling proteins and as nuclear transcription factors that activate a diverse set of genes involved in cellular fundamental processes including cell development, differentiation, proliferation and survival. Structurally, STAT proteins have distinct domains including the N-terminal, coiled-coil, (deoxyribonucleic acid) DNA binding, the Linker, Src-homology 2 (SH2) and C-terminal transactivation domains (Figure 1-4. adopted from [20]). Each of these domains has been associated with a distinct function of STAT protein. For instance, the N-terminal domain is important in STAT dimer-dimer interactions; the DNA binding domain forms complexes between STAT proteins and DNA; the SH2 domain engages in dimerization between two activated STAT monomers through reciprocal phospho-tyrosine (pTyr)-SH2 domain interactions; and the C-terminal portion of the protein functions as the transcriptional activation domain [18].

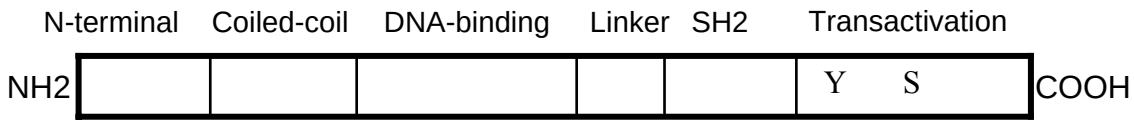

Figure 1-4. A schematic representation of STAT protein structure (Figure adopted from [20]). Linear representation of the domain structures of the STAT proteins. The critical tyrosyl residue (Y) is shown, the phosphorylation of which initiates STAT activation and the dimerization between two STAT monomers through a reciprocal pTyr-SH2 domain interactions. A serine (S) residue is present in the C-terminal transactivation domain of some STAT proteins and is phosphorylated to enhance transcriptional activity. NH2, amino (N) terminus; COOH, carboxyl (C) terminus.

In normal cells, STAT proteins transmit cytoplasmic signals from cytokines and growth factors that have receptors with intrinsic or associated tyrosine-kinase activity. Upon the binding of growth factors or cytokines to their cognate receptors on the cell surface, STATs are recruited to the cytoplasmic portions of the receptors, where they become phosphorylated on a critical tyrosyl residue (Y) in the C-terminus by Tyr kinases of growth factor receptors, or by cytoplasmic non-receptor Tyr kinases, including Src, Janus kinases (Jaks) or Abelson (ABL) kinase. Transactivation domain of some STAT proteins has serine residue (S) the phosphorylation of which has been shown to maximize the transcriptional activity of these proteins. Tyrosine-phosphorylated STATs then dimerize through reciprocal pTyr-SH2 domain interactions, translocate into the nucleus where they bind to specific STAT-response elements in the promoters of target genes and regulate their transcription [18,82] (Figure 1-5. adopted from [18]).

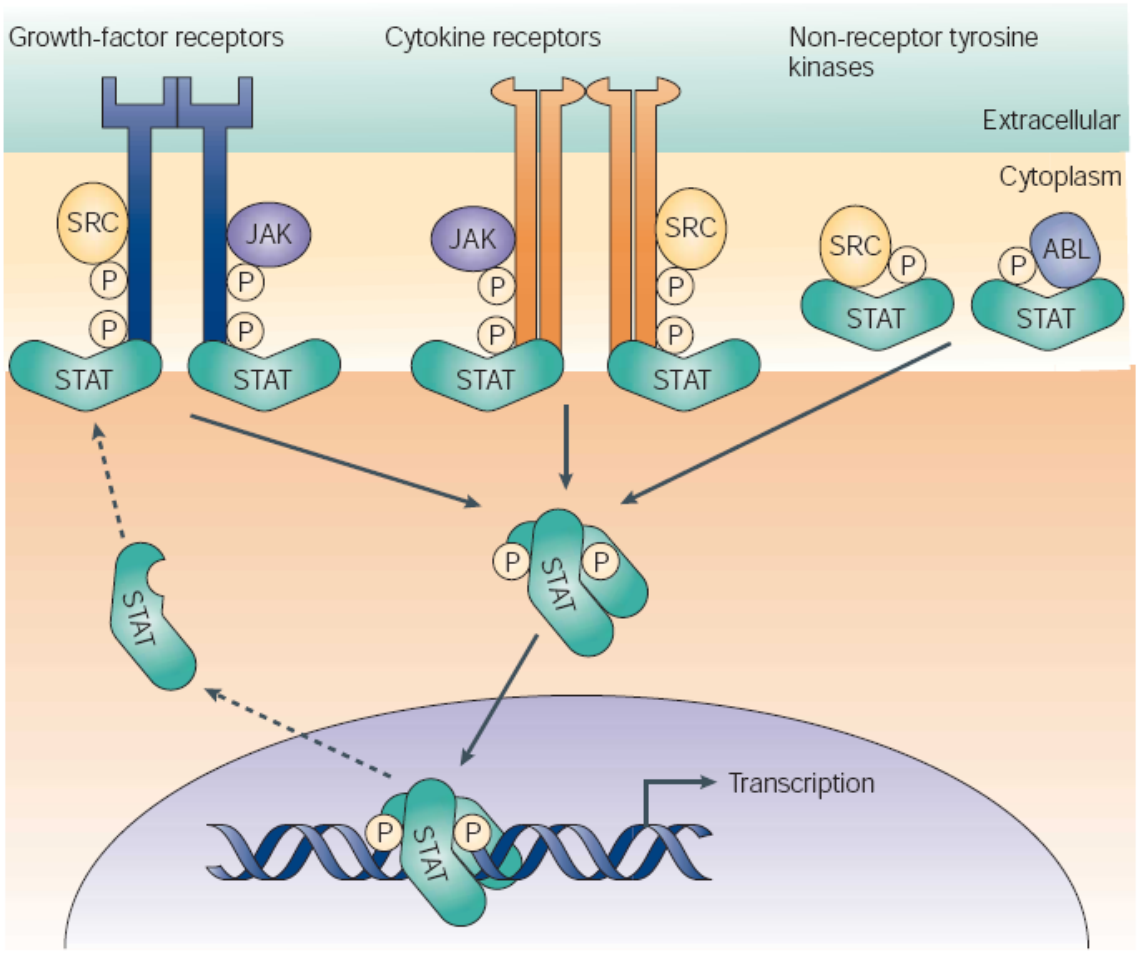

Figure 1-5. Signaling pathways that converge on STATs (Figure adopted from [18]). Binding of growth factors or cytokines to their receptors results in the activation of intrinsic receptor tyrosine-kinase activity or of receptor-associated kinases, such as the JAK or SRC tyrosine kinases. These tyrosine kinases subsequently phosphorylate the cytoplasmic tails of the receptor to provide docking sites for the recruitment of monomeric STATs. Once they have been recruited, STATs themselves become substrates for tyrosine phosphorylation. Non-receptor tyrosine kinases, such as the oncoproteins SRC and BCR–ABL (a fusion of the breakpoint-cluster region (BCR) and Abelson leukaemia (ABL) proteins), can phosphorylate STATs independently of receptor engagement. Phosphorylated STATs dimerize and translocate to the nucleus, where the dimers directly regulate gene expression. Whereas STAT activation is tightly regulated in normal cells, the persistent activation of tyrosine kinases in cancer causes constitutive activation of STATs in particular STAT3 and STAT5. This leads to permanent changes in the expression of genes that control fundamental cellular processes, which are subverted in cancer cells. Dashed arrows indicate the 'recycling' of STAT proteins from the nucleus to the cytoplasm.

STAT proteins can cross-talk with other central signaling pathways, such as the mitogen-activated protein kinase (MAPK) family of proteins and the nuclear receptor signaling pathways. Phoshorylated tyrosine on intracellular domain of activated receptors which provide docking site for STATs, can recruit other SH2 containing adaptor proteins from other signaling pathways. This includes SHP-2 and Shc which recruit growth factor receptor-bound protein 2 (GRB2) adaptor protein which in turn stimulate Ras pathway. Ras pathway stimulation activates MAPK which phosphorylate STATs in serin 727 near c-terminus of most STATs, which is believed to be important for STAT DNA binding and its transcriptional activity [83]. STAT3 has been reported to have an important cross talk with nuclear factor kappa beta (NF-κβ) transcription factors. It has been shown that phosphorylated form of STAT3 can bind to NF-κβ subunits and inhibit their transcriptional activity. Since NF-κβ pathway activation is critical for the maturation and activation of DCs, this type of cross talk in immunosuppressed DCs with constitutively active STAT3 is believed to be responsible for their impaired maturation [23]. Other proteins known to interact with and modulate STAT signaling pathways are the protein inhibitor of activated STAT (PIAS) family of protein. PIAS function as negative regulator of STAT proteins [83].

From STAT family of cell signaling proteins, STAT3 is implicated in human malignancies. STAT3 is found to be constitutively activated in many types of cancers [18,20], including 82% of prostate cancers [84], 70% of breast cancers [85], more than 82% of the carcinomas of the head and neck [86], and 71% of

nasopharyngeal carcinoma [87]. Compelling evidence has established that aberrant STAT3 is a molecular abnormality that has a critical role in the development and progression of human tumors [18,88].

1.6.2 The oncogenic effects of STAT3 on tumor growth

Constitutively activated STAT3 contributes to cancer development and progression by regulating the expression of genes that are involved in cell proliferation, survival, angiogenesis, metastasis, and cancer immune evasion [18] (Figure 1-6 adopted from [20]). Initial work showed that conditional knockout of the STAT3 gene or inhibition of STAT3 function blocks v-Src-induced transformation in cancer model systems, indicating a pivotal role for STAT3 in malignant transformation [89-91]. An important proof for the oncogenic potential of STAT3 come from studies showing artificially engineered, constitutively dimerized STAT3C alone is sufficient to induce malignant transformation and tumor formation in mice [92]. For many of the human tumors, evidence indicates a strong correlation between persistent STAT3 activity and the maintenance of the malignant phenotype [18,19,93-96]. Although the exact mechanisms by which constitutively active STAT3 mediates malignant transformation and human tumor formation, has not been completely understood, there is convincing evidence for the conclusion that persistent STAT3 activation mediates critical gene expression changes that favor tumorigenesis.

STAT3 has been shown to upregulate the expression of the genes involved in uncontrolled cell proliferation and survival. These include genes that encode

cell cycle regulators, c-MYC, cyclin D1 and cyclin D2 [92,97,98], the survival factors, Bcl-2, Bcl-X_L, Mcl-1 [99-103], and the inhibitors of apoptosis, survivin and the cellular inhibitor of apoptosis 2 (c-IAP2), [104,105]. In addition, constitutively activated STAT3 promotes the induction of Akt [106] and repress the expression of p53 which is the most potent inhibitor of cell proliferation and inducer of apoptosis [107]. As a key regulator of VEGF expression, which is critical for neovascularization, STAT3 signaling also stimulates tumor angiogenesis [108,109]. STAT3 has been also shown to promote metastasis by inducing expression of the metastatic gene, matrix metalloproteinas (MMP)-2 [110]. Consistent with the identified molecular events mediated by STAT3, several studies have shown that pharmacological or genetic disruption of STAT3 signaling pathways leads to the inhibition of the expression of Bcl-xL, Mcl-1, Bcl-2 [99,101,102,111] and Survivin [104], induce the expression of the pro-apoptotic protein BAX [112,113], and induces apoptosis of tumor cells in many cancer cell lines and xenograft models [18,94-96,114]. Other studies have provided more evidence for the role of STAT3 in cancer resistance to apoptosis by showing that the combination of STAT3 inhibitors and chemotherapy sensitizes cancer cells to apoptosis [115-118].

Altogether, numerous studies have provided compelling evidence in support of the critical role of constitutive STAT3 activation in the development and progression of human cancers. Thus blocking constitutively activated STAT3 has been suggested as a novel approach for inducing cancer cell apoptosis and hence treating cancer patients.

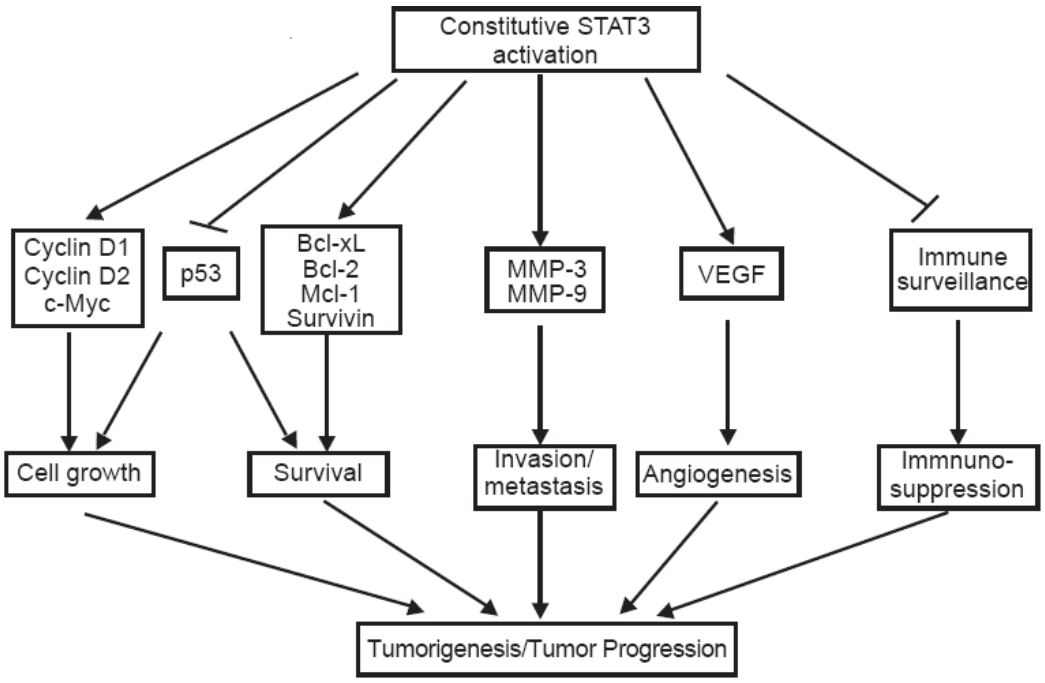

Figure 1-6. The role of constitutively activated STAT3 in cancer (Figure adopted from [20]). Constitutive STAT3 activation results in dysregulation of cell cycle control and apoptosis genes, and genes that promote invasion, metastasis, and angiogenesis, and also leads to the suppression of host immune surveillance. These molecular changes together contribute to oncogenesis.

1.6.3 The role of STAT3 in tumor-induced immunosuppression

In addition to the oncogenic effects of STAT3 in cancer, constitutively activated STAT3 has been implicated in the manipulation of anticancer immune responses at three levels. First, tumor cells in which STAT3 is constitutively active are impaired in the secretion of the pro-inflammatory cytokines. Consequently, tumors with hyperactive STAT3 had impaired infiltration of diverse type of immune cells including neutrophils, macrophages, effector T cells and natural killer (NK) cells [119]. Secondly, constitutive activation of STAT3 in tumor results in the upregulation of several immunosuppressive factors including VEGF and IL-10, which negatively influence the function and tumor infiltration

of various immune cell types [11,17]. Finally, tumor-derived immunosuppressive factors activate STAT3 in diverse types of immune cells in particular DCs and render them either immunosuppressive or dysfunctional [11,17,120,121]. It has been postulated that the lack of pro-inflammatory factors results in the activation of tolerogenic DCs incapable of maturation to effective DCs [52]. This is believed to be a result of the up-regulation of STAT3 in DCs induced by tumor-secreted immunosuppressive factors [9,54]. Tolerogenic DCs can induce activation of T_{reg} cells, which further inhibit the function of DCs and effector T cells leading to a vicious cycle of immunosuppression in tumor [9,11,43,54]. In view of these concepts, blockade of STAT3 activation in tumor and DCs has been suggested as a promising strategy for enhancing the effectiveness of cancer immunotherapy.

1.7 Strategies for the inhibition of STAT3

With respect to the high prevalence of STAT3 hyperactivation in human cancers and its key role in cancer progression, several research groups have investigated the possible mechanisms of STAT3 hyperactivation in cancer and developed a number of strategies for the inhibition of STAT3 activity [20,122]. The exact mechanisms by which STAT3 become constitutively activated in tumor or immune cells have not been completely understood. However, recent studies have suggested that STAT3 can become constitutively activated in cancer through two main mechanisms including dysregulation of upstream kinases and the loss of the proteins which negatively regulate the function of STAT3 [20].

STAT3 is phosphorylated and activated by non-receptor Tyr kinases (NRTKs) such as src and receptor Tyr kinases (RTK) including receptor associated kinases mainly JAKs and growth factor receptors with intrinsic kinase activity [89,123-125]. Overexpression or aberrant expression of growth factor receptors and their ligands have been found in several types of human cancers. Therefore, targeting growth factor receptors may be one of the important strategies for the inhibition of STAT3 [126,127]. STAT3 is downstream target of RTKs and NRTKs which are important oncogenic proteins and found constitutively activated in cancer due to genetic alterations. Thus RTKs and NRTKs including Src and JAKs have been targets of choice for the development of small-molecules inhibitors as novel cancer therapeutic agents. Studies have shown that the small-molecule Src inhibitors such as PD166285, SU6656, and PD180970, induced cell cycle arrest and apoptosis of tumor cells, including melanoma, lung and breast cancers, by mechanisms involving the inhibition of aberrant STAT3 and down-regulation of STAT3 target genes, including those for Bcl-xL and Mcl-1 anti-apoptotic proteins [128,129]. JAK kinase inhibitor, AG940, have been found to be effective in suppressing the level of p-STAT3 and inducing apoptosis in malignant cells [99,130]. Cucurbitacin I (also called JSI-124 due to its inhibitory effects on JAK/STAT pathway) and cucurbitacin B are small molecules which selectively inhibit JAK/STAT3 pathway, induce apoptosis and inhibit tumor growth in several types of malignancies [21,22,130-133]. NPM-ALK (nucleophosmin-anaplastic lymphoma kinase), a tumor specific NRTK expressed in anaplastic large cell lymphoma (ALCL), has been shown to be

important in hyperactivation of STAT3 in this type of cancer. JSI-124 has been shown to suppress the level of NPM-ALK and inhibit STAT3 in ALCL [132].

The downregulation of negative physiological regulators of STAT3 has been suggested as another mechanism for STAT3 hyperactivation and small molecules mimicking the function of STAT3 negative regulator are being developed as novel inhibitors of STAT3. The function of activated STAT3 is terminated by different regulators including suppressor of cytokine signaling proteins (SOCS-1 and SOC-S), PIAS, and Tyr phosphatase (PIPase). Transcriptional silencing of SOCS-1 by hypermethylation has been reported in human hepatocellular carcinoma in which STAT3 is constitutively active [134]. There are initial indications that small molecules which mimic SOCS-1 and SOCS-3 might be useful in suppressing the level of STAT3. A recent work shows that a cell-permeable SOCS-1-mimic peptide inhibits STAT3 activation and inhibit prostate cancer cell growth [135]. SHP-1 and SHP-2 from PIPase proteins control STAT3 activity [136] so modulation of PIPase activity might be another effective approach for inhibition of STAT3 activity in cancer.

Another important and promising approach for the suppression of STAT3 is direct inference with constitutively active STAT3. Phosphorylated STAT3 (p-STAT3) dimerize through pTyr-SH2 interactions which is essential for its transcriptional activity. Phosphopeptide and peptidomimetic analogs of the STAT3 SH2 domains have been developed and shown STAT3 inhibitory and anticancer activity in cancer cells [137-139]. Small molecules which inhibit STAT3 dimerization such as STA-21 have been also identified and evaluated for

their anti-cancer activity [140]. Blocking interaction of STAT3 with DNA is another approach to inhibit STAT3 activity. Studies have reported the development of STAT3 decoy oligonucleotides which block the binding of STAT3 to DNA and inhibit its function. Abrogation of STAT3 function using a decoy oligonucleotide have shown to suppress STAT3 target genes (VEGF, Bcl-xL, and cyclin D1), induce apoptosis and inhibit tumor growth [114,141]. Platinum (IV) complexes are another important category of STAT3 inhibitors which are believed to interact with the DNA-binding domain of the protein and inhibit its DNA-binding activity [142,143].

1.7.1 JSI-124 (Cucurbitacin I) and cucurbitacin B

JSI-124 and Cucurbitacin B (Figure1-7) are potent anti-cancer agents with selective inhibitory effect on STAT3 pathway [21,22,131]. JSI-124 and cucurbitacin B belong to a group of natural products called cucurbitacins, tetracyclic triterpinoid substances which have been isolated from various plant families such as *Cucurbitaceae*. Cucurbitacins, possess a broad range of potent biological activity derived largely from their cytotoxic properties [144]. A number of compounds of this group have been investigated for their hepatoprotective, anti-inflammatory, antimicrobial, and most importantly anticancer properties [131,144-146]. The molecular mechanism of the various biological activities of cucurbitacins has not been fully investigated. Various functions of cucurbitacins have been related to their polarity and chemical structure [22,147]. For instance, it has been demonstrated that cytotoxic effects of cucurbitacins increase linearly

with their hydrophobicity [148]. For this family of plants, JSI-124 and cucurbitacin B have been shown to have potent anticancer activity in several cancer cell lines *in vitro* and there are some reports on their anti-tumor activity, *in vivo* [21,131-133]. Furthermore, JSI-124 and cucurbitacin B have been shown to have selective STAT3 inhibitory activity in several cancer cell lines, *in vitro* [21,22,132,149]. The anticancer activity of JSI-124 and cucurbitacin B is believed to be related to their STAT3 inhibitory effects since these compounds don't show significant anticancer activity against cancers in which STAT3 is not constitutively active [21,22]. The STAT3 mediated anticancer effects of JSI-124 and cucurbitacin B is expected to be more selective on cancer cells over normal cells because previous studies have shown that unlike cancer cells, normal cells are not dependent on STAT3 activity for their growth and survival [150]. The exact mechanism by which JSI-124 and cucurbitacin B suppress the level of p-STAT3 is not known. Nevertheless previous studies suggest that cucurbitaicns may suppress the level of p-STAT3 by direct dephosphorylation of STAT3 or upstream kinase (e.i JAK3 and JAK2) through the activation of phosphotases or by facilitation of their degradation via the proteosome pathway [21,132].

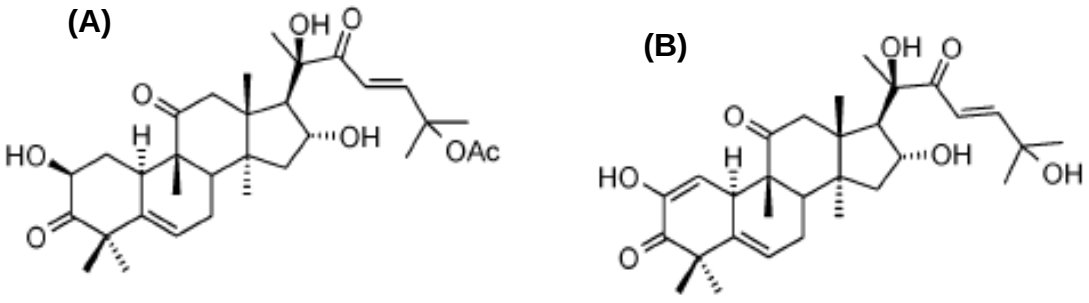

Figure 1-7 Chemical Structure of A) cucurbitacin B; B) JSI-124

1.8 Targeting TLRs in cancer immunotherapy

1.8.1 Characterization of TLRs

TLRs are a family of PRR which are evolutionarily conserved to recognize PAMP on invading pathogens including conserved molecules from bacteria, DNA and ribonucleic acid (RNA) viruses, fungi and protozoa. TLRs are predominantly expressed on APCs including macrophages, DCs, and B cells as well as on tissues that are directly exposed to microorganisms (lungs, gastrointestinal tract, and skin). At least 11 types of TLRs and some of their corresponding ligands have been identified. Examples of TLRs ligands include lipopolysaccharides (LPS; recognized by TLR4), lipopeptides (by cooperation of TLR2 with TLR1 or TLR6), viral single- or double-stranded RNA (by TLR7 with TLR8 and by TLR3, respectively), bacterial or viral DNA containing CpG motifs (by TLR9) and flagellin (by TLR5) [151,152].

In addition to exogenous (microbial) ligands, a growing number of endogenous ligands are being explored as stimulators of TLRs. These include heat shock proteins (HSP60, HSP70, endoplasmin, HSPB8 and α-crystallin A chain), high mobility group box 1 (HMGB1), uric acid crystals, surfactant protein A, and various products of the extracellular matrix such as fibronectin, heparan sulphate, biglycan, fibrinogen, oligosaccharides of hyaluronan23 and hyaluronan breakdown fragments [45,152-154] (Figure 1-8. adopted from [152]).

Activation of TLRs by the corresponding ligands results in the initiation of a signaling cascade involving several signaling intermediates, including myeloid differentiation factor-88 (MyD88), Toll–IL-1 receptor (TIR)- associated protein

(TIRAP, also known as MAL); Toll receptor-associated activator of interferon (TRIF), Toll receptor-associated molecule (TRAM), IL-1 receptor associated kinases (IRAK) and tumor necrosis factor (TNF) receptor-associated factor 6 (TRAF6) (Figure 1- 8. adopted from [152]). Activation of these signaling events leads to the induction of host immune responses.

The regulation of antimicrobial responses by epithelial cells, which are the first line of defense at the mucosal sites, might be the most evolutionarily conserved role of TLRs. In addition, TLRs play a crucial role in the recruitment of leukocytes to the inflamed or infected tissue by the induction of the expression of chemokines and their corresponding receptors in the endothelium. In addition to the role of TLRs in the innate immune responses, adaptive immune responses are controlled by TLRs at multiple checkpoints. This dictates the initiation of an immune response, its type, magnitude, duration and also the generation of long-term memory. TLRs are considered to be central to the regulation of host adaptive immune response since they play a key role in the induction of DC maturation, which is a key event in the induction of adaptive immune responses [44,152].

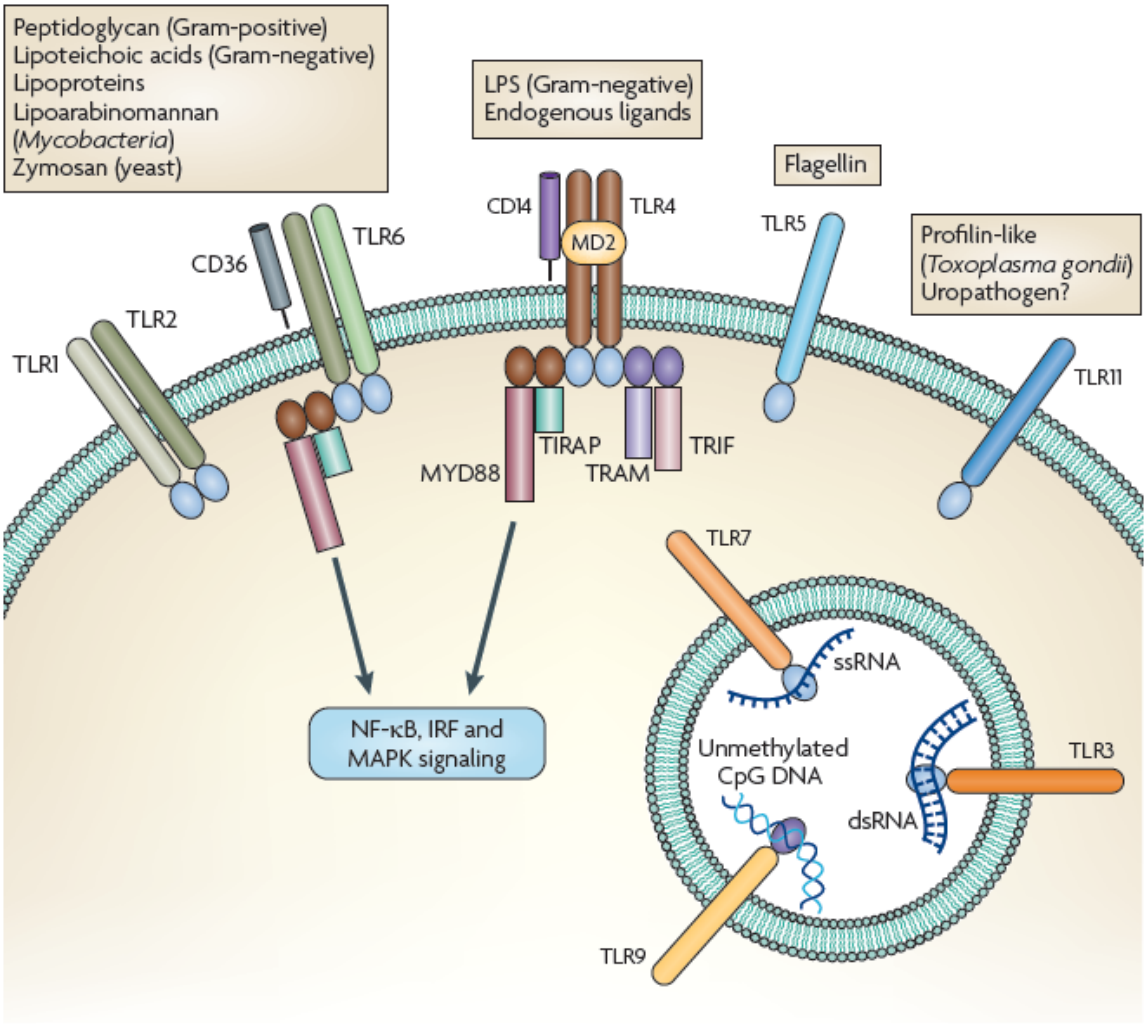

Figure 1-8. Physiological functions of TLRs (Figure adopted from [152]). TLRs are involved in the recognition of microbial and endogenously derived molecular patterns. This occurs both at the plasma membrane and at intracellular compartments. After ligation of TLR ligands either directly or with the help of accessory molecules such as cD14, MD2 (also known as LY96) and cD36, TLRs dimerize and transmit signals throughout the cell by means of adaptor molecules such as MYD88 and TRIF. This leads to the activation of multiple cellular phenomena, the best-described of which being the activation of signal transduction to the nucleus (for instance through activation of NF-κβ, MAPKs and interferon regulatory factors (IRFs)). TLR activation leads to the regulation of innate and adaptive immune responses, inflammation and tissue repair.

1.8.2 TLRs, DC functional maturation, and T cell activation

TLR-mediated activation of DCs is a critical step in the process of the activation of the adaptive immunity against pathogens and cancer [44,155,156]. Recognition of ligands by the corresponding TLRs on DCs triggers NF-κβ, type-1 interferon, and MAPK pathways leading to the functional maturation of DCs. DCs reside in tissues in immature status and exhibit active phagocytosis but they lack sufficient cell surface MHC class II and co-stimulatory molecules (CD83, CD86) for efficient antigen presentation to T lymphocytes. Upon ligation of TLRs on DCs, the expression of MHC class II and co-stimulatory molecule are increased and their capacity of phagocytosis is decreased. This phenomenon turns DCs from 'antigen capture mode' into 'antigen presenting mode'. Ligation of TLRs on DCs also results in the production of pro-inflammatory cytokines that are essential in stimulating T cells to differentiate to T helper [157].

Functionally mature DCs prime $CD4^+$ T cells and skew the immune responses either towards Th1, Th2, Th17 or T_{reg} cell subsets. Commitment of T cells to a particular Th cell type is highly dependent on the cytokine milieu surrounding the activated T cells, which can be influenced by the type of TLR ligand used for DC maturation. For instance, LPS which is a TLR4 ligand, induces secretion of IL-12 by DCs leading to the generation of Th1 responses. Th1 immune responses are elicited following secretion of IFN-γ by activated $CD4^+$ T cells that support generation of $CD8^+$ T cells responses. Th2 immune responses are generated following secretion of IL-4, IL-5, and IL-13 by the activated $CD4^+$ T cells and support induction of humoral immune responses. Th17

cells, a recently discovered type of T helper cells, are generated in the presence of the high level of TGF-β, IL-6, IL-23, and IL-21 which serve to positively regulate Th17 differentiation. T_{reg} cells are believed to be activated when TGF-β and IL-10 are present at high level and there is a lack of pro-inflammatory cytokines. T_{reg} cells have been shown to be critical for the induction and maintenance of peripheral tolerance [27,155,156,158,159].

1.8.3 TLRs for the regulation of T_{reg} cell function

In addition to the effect of TLRs ligation on DCs activation, TLRs signaling have been shown to directly or indirectly modulate the immunosuppressive function of T_{reg} cells [29]. Indirect effects of TLR activation on the function of T_{reg} cells are believed to be mediated by DCs. It has been shown that the ligation of TLR4 or TLR9 on DCs results in the activation of DCs and production of pro-inflammatory cytokines, which in turn decrease the suppressive effects of T_{reg} cells on T cell proliferation, *in vitro* [28]. The effects of TLR ligands on T_{reg} cells can also be mediated by TLRs expressed on T_{reg} cells. Among TLR ligands with direct effect on T_{reg} cell function, TLR8 ligands have recently been of particular interest because of their potential in reversing the suppressive function of human T_{reg} cells. TLR8 has been found to be expressed in both human DCs and T_{reg} cells. Interestingly, the ligation of TLR8 expressed in human DCs results in the functional maturation of DCs whereas engagement of TLR8 on human T_{reg} cells efficiently inhibits the suppressive function of T_{reg} cells [160].

1.8.4 TLR ligands and anticancer immunotherapy

TLR ligands have attracted a great deal of interest as adjuvants in cancer immunotherapy due to their potential to efficiently activate DCs and modulate the immunosuppressive function of T_{reg} cells. Among TLR ligands, TLR9 and TLR4 agonists have been extensively investigated as adjuvants in vaccine-based cancer immunotherapy strategies [25,26,161]. TLR7/8 ligands have recently been of particular interest because of their potent inhibitory effect on the suppressive function of T_{reg} cells and they are under investigation as potent adjuvants for cancer vaccines [162].

TLR9 is expressed in endosomal compartments of APCs and recognizes CpG dinucleotides, which are relatively common in bacterial and viral DNA, but not in vertebrate since they methylate 70%-80% of CpG in their DNA. While in mice B cells, monocytes, and probably all DC subsets express TLR9, the expression of TLR9 in human is limited to B cells and only plasmacytoid subset of DCs (pDCs). pDCs originate from lymphoid DC lineage and play a very important role in host defense, as they produce IFNs and induce the activation of myeloid DCs (mDCs) and NK cells. TLR9 ligands have been shown to efficiently activate NK cells and DCs of innate immunity and polarize adaptive immune responses toward Th1 responses and CTL activation, which is the main mechanism of anti-tumor immunity [25,156,163,164] (Figure 1-9. adopted from [164]). TLR 9 signaling cascade begins when CpG is localized in endosomal compartment of the cells by the aid of Class III phosphatidylinositol 3-kinase (PI3K). The interaction between CpG DNA and TLR9 transduces an

intracytoplasmic activation signal leading to the recruitment of MYD88 to the TIR domain of TLR9, followed by the activation of the IRAK–TRAF6 complex. This leads to the activation of both MAPK pathway and inhibitor of NF-κβ kinase (IKK) complexes, culminating in the upregulation of transcription factors, including NF-κβ and activating protein 1 (AP1). TLR9 signaling has been illustrated in Figure 1-10. adopted from [164].

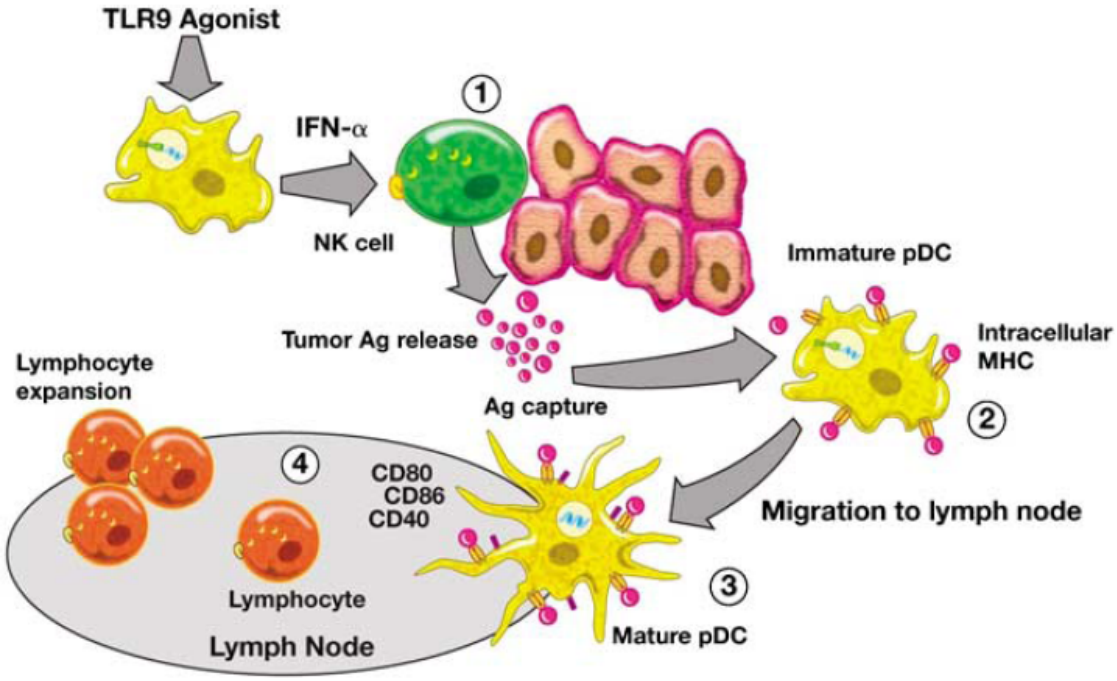

Figure 1-9. TLR9 in cancer immunotherapy (Figure adopted from [164]). (1) TLR9 agonists stimulate innate and adaptive antitumor immune responses. TLR9 agonists induce secretion of interferon-α (IFN-α) from immature pDCs, which may activate NK cell lysis of tumor cells and release tumor antigens (Ags). (2) DCs activated directly or indirectly by the TLR9 agonist therapy can capture and process tumor-associated antigens, increase surface expression of MHC and co-stimulatory receptors, and (3) migrate to the LNs where antigens can be presented to lymphocytes, inducing (4) the expansion of lymphocytes that recognize the tumor antigen. Because the response occurs in a Th1-like cytokine milieu, the lymphocyte response tends to be Th1-like, including cytotoxic T lymphocytes (CTLs).

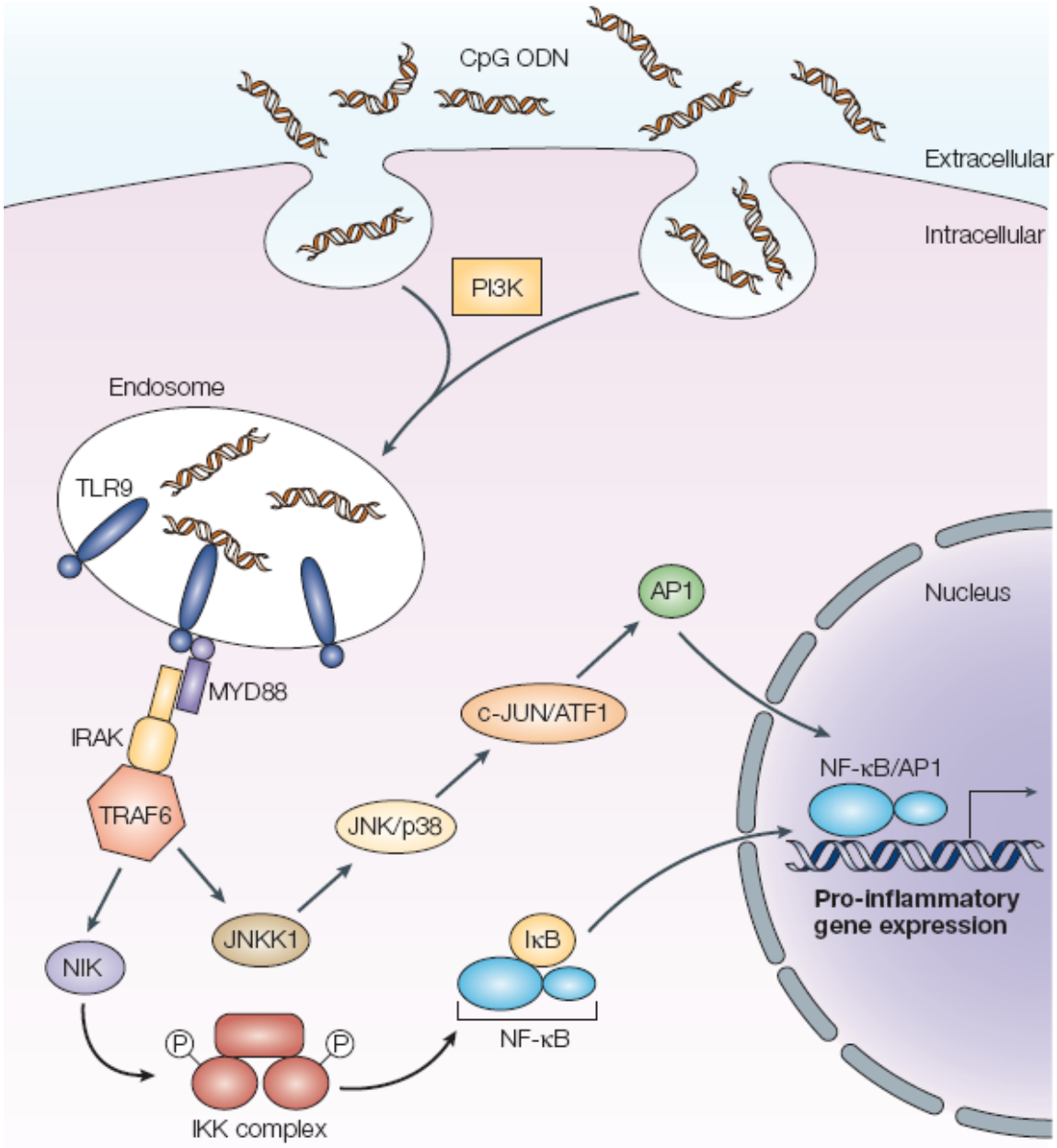

Figure 1-10. CpG-DNA–TLR9-mediated cell signaling (Figure adopted from [165]). PI3K facilitates the internalization of CpG ODNs into endosomal vesicles that contain TLR9. The interaction between CpG DNA and TLR9 transduces an intracytoplasmic activation signal. The signal initiates with the recruitment of MYD88 to the TIR domain of TLR9, followed by the activation of the IRAK–TRAF6 complex. This leads to the activation of both MAPKs: JNK1/2 and p38 and IKK complexes, culminating in the upregulation of transcription factors, including NF-κβ and AP1. ATF1, activating transcription factor 1; JNKK1, c-JUN N-terminal kinase (JNK) kinase 1; NIK, NF-κβ-inducing kinase; TRAF6, tumour-necrosis factor receptor-associated factor 6.

In addition to Th1 adjuvant activity of CpG, ligation of TLR9 by CpG ODN has been shown to reverse the suppressive effects of T_{reg} cells on T cells proliferation, *in vitro* [28]. It has been also shown that CpG ODN therapy inhibits the generation of T_{reg} cells in B16 melanoma tumor-bearing mice and melanoma patients [25,166,167]. These studies indicate the capability of TLR9 ligands as an efficient adjuvant to cancer immunotherapy strategies aiming at reversing tumor-induced immunosuppression and induction of effective anticancer immune responses. Thus, during the last decade several types of synthetic oligodeoxynucleotides containing one or more unmethylated CpG dinucleotides have been developed and are being evaluated in human clinical trials as adjuvants to cancer vaccines or in combination with other therapies with promising results [25].

TLR4 ligands are another important category of adjuvants which have been studied for the development of cancer vaccines [168]. Similar to TLR9 ligands, TLR4 induced activation of DCs leads to the activation of Th1 responses. In addition, ligation of TLR4 on DCs has been investigated as a strategy to reverse the suppressive activity of T_{reg} cells on T cell activation [28]. Monophosphoryl lipid A (MPLA) is one of the most promising TLR4 ligands investigated for cancer immunotherapy. MPLA is a chemically modified derivative of LPS that exhibits potent adjuvant activity but is 100–10,000 fold less toxic than LPS [169]. A series of preclinical safety investigations in various animal models have been performed to support clinical use of MPLA as an adjuvant [170]. Following clinical success of MPLA containing vaccines, several

other synthetic lipid A analogues are being developed and shown to efficiently activate DCs and induce CTL responses [171]. [172,173].

TLR7/8 ligands have been recently identified and are under investigations as adjuvants in cancer immunotherapy [162]. TLR7 and TLR8 recognize single-stranded viral RNAs or guanosine-related analogues (loxoribine and imidazoquinoline) [174,175]. TLR8 is expressed in both human DCs and T_{reg} cells. As mentioned before, the ligation of TLR8 on human T_{reg} cell results in the inhibition of T_{reg} cell function while TLR8 ligands efficiently activate human DCs and induce Th1 immune responses. These finding suggest TLR8 ligands as potential target for reversal of anti-tumor immunity [160,162].

1.8.5 Expression of TLRs by cancer cells

Recent studies have shown that TLRs are also expressed on cancer cells, but their signaling pathway and biological function in cancer cells are not completely understood. While ligation of TLRs in some cancer cells have been shown to support cancer cell growth, the ligation of TLRs in other types of cancer leads to cancer cells apoptosis. This indicates that the signaling pathways and function of TLRs expressed by cancer cells may be different from what is reported for APCs. Since TLR ligation on cancer cells may result in undesirable cancer supportive effects of TLRs ligands, delivery systems are needed to be developed to support the selective and efficient delivery of TLR ligands to DCs [151,176].

1.9 Targeting TLR ligands and other therapeutic agents to DCs

Several strategies have being developed for targeting antigens and DC stimulatory adjuvants to DCs. The receptors expressed on DCs and their corresponding ligands have been explored and investigated for targeting antigens to DCs. This includes Fc receptors (which binds to the Fcγ portion of immunoglobulin (Ig)) Manan, DEC-205, CD 11c, and the HSP receptors [177-181]. Targeted delivery of antigens to DCs using ligands specific to DC cell surface receptors have shown great promise. However, further studies are needed to fully characterize DC surface receptors, corresponding ligands, their function and the downstream signaling pathways activated by each receptor.

Another approach to target antigens and drugs to DCs is to use particulate drug delivery system. It has been shown that DCs take up antigens as particles 1000 times more efficiently than soluble antigens. Among several different kinds of particles investigated to introduce antigens and adjuvants into DCs, poly (D,L-lactic-co-glycolic acid) (PLGA) micro- and nanoparticles have shown great promise for targeted delivery of therapeutic agents to DCs [182-184]. The potential application of PLGA nanoparticles (NPs) in targeting therapeutic agents to DCs is described in the following section.

1.10 Polymeric nano-carriers

Therapeutic use of a variety of polymeric drug nano-carriers has significant impact on the treatment and potential cure of many chronic diseases, including cancer. Nanoscopic polymeric systems can deliver therapeutic agents to

the intended site of action and improve efficacy while minimizing unwanted side effects elsewhere in the body. PLGA nanoparticles and poly (ethylene oxide)-*block* (PEO-*b*)-poly(ester)s-based micelles are biodegradable and biocompatible nano-carriers which have been extensively investigated for targeted delivery of a variety of therapeutic agents.

1.10.1 PLGA polymer-based delivery system

PLGA micro- and NPs have been extensively used as delivery system for various therapeutic agents owing to their biodegradability and biocompatibility. PLGA is a polyester which is synthesized by means of random ring-opening co-polymerization of two different monomers, the cyclic dimers (1,4-dioxane-2,5-diones) of glycolic acid and lactic acid. This polyester undergoes non-enzymatic hydrolysis in the body to produce the original monomers, i.e., lactic acid and glycolic acid (Figure 1-11). These two monomers are by-products of various metabolic pathways in the body and the body effectively deals with them. Therefore, PLGA is considered as a biocompatible polymer and has been approved by the food & drug administration (FDA) and Health Canada for human administration [185,186].

PLGA is also a suitable polymer for the encapsulation and controlled delivery of a broad range of biologically active compounds with different physicochemical properties. Previous studies have established that hydrophobic molecules such as lipopeptides and glycolipids are formulated into PLGA particles as single emulsion (oil/water) formulation, whereas hydrophilic

molecules are prepared as double emulsion (water/oil/water) formulations [187-189].

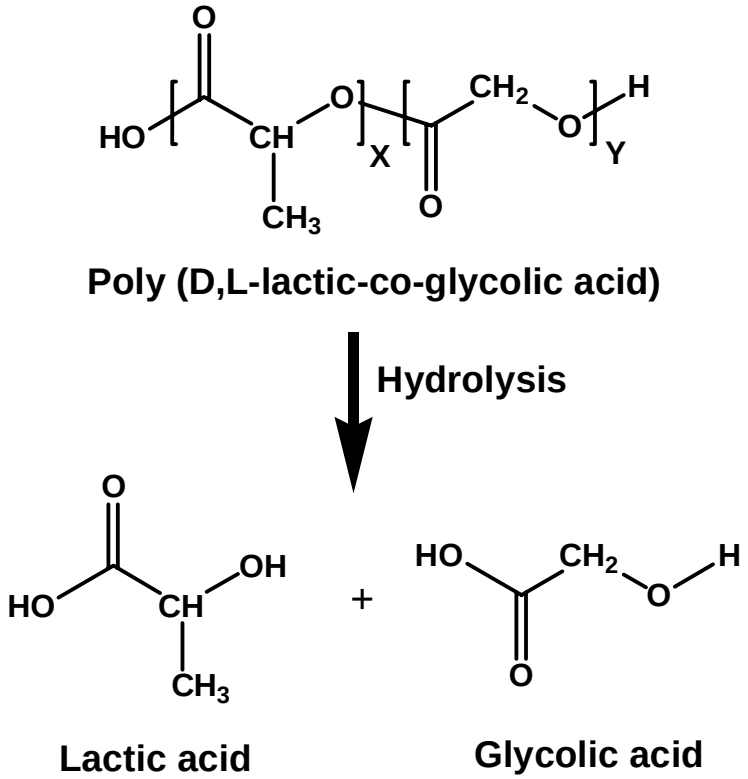

Figure 1-11. Chemical Structure and biodegradation products of PLGA- PLGA is aliphatic polyester composed of varying proportions of lactic and glycolic acid. X and Y represent number of units of lactic and glycolic acid, respectively.

The release of encapsulated materials from PLGA carriers can be controlled by several parameters including the ratio of lactic to glycolic acid, molecular weight of the components, and particle size [190-192]. The lactic to glycolic acid composition of the co-polymer also affects the crystallinity, hydrophobicity, and the degree of polymer hydration. It has been shown that 50:50 ratio of the lactic to glycolic acid gives a higher rate of degradation than polymers fabricated with higher proportions of either of the monomers (Figure 1-12. adopted from [191]). The reason for this is the amorphous nature of PLGA

with 50:50 ratios of PLA and PGA. Since the hydrophobicity of the lactic acid is higher than that of glycolic acid, an increase in the composition of the lactic acid above 50%, results in PLGA co-polymers with slower lower degradation characteristics. Also, the D,L lactic acid is preferred over L-lactic acid because it forms an amorphous polymer where the antigen or the drug is homogeneously dispersed within the polymeric matrix [193]. The release profile of drug from PLGA NPs has been shown to be triphasic with an initial quick burst release followed by a lag phase and then continued zero-order release due to bulk erosion of the polymer. Several PLGA NPs-based pharmaceutical products have been successfully developed and moved to the clinic [194,195].

PLGA micro- and NPs have been shown to be excellent delivery systems for targeting numerous molecules (e.g., peptides, proteins, TLR ligands, DNA, oligonucleotides) to DCs, *in vitro* and *in vivo* [184,188,196,197]. PLGA micro and NPs containing an antigen have been shown to be efficiently internalized by macrophages and DCs and prolong the MHC-I presentation of the encapsulated antigen by DCs, *in vitro* [183,198]. The uptake of PLGA particles by DCs is affected by size, surface charge, and hydrophobicity. It has been shown that co-delivery of antigens and TLR ligands to DCs induces antigen-specific T cell responses *in vitro* and *in vivo* that is 100 to 1000 fold greater in potency than what is achievable by soluble formulations. In this research project, we have proposed to use PLGA NPs for delivery of 7-acylipid A (TLR4 ligand) and CpG (TLR9 ligand) to DCs.

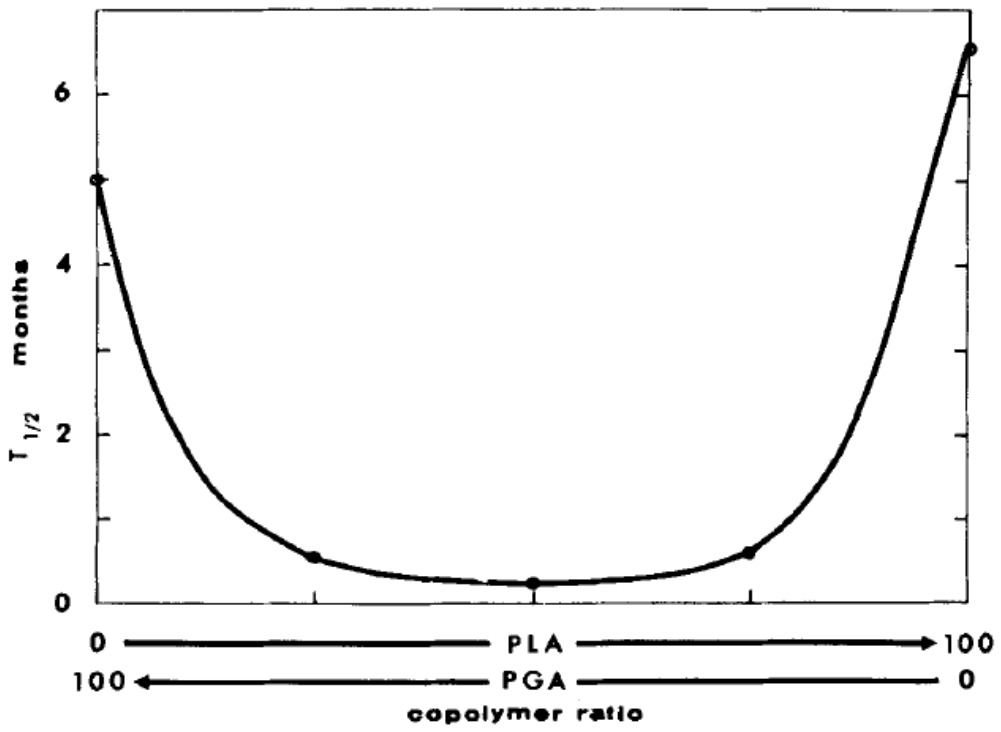

Figure 1-12. Half-life of PLGA polymers with various ratios of PLA and PGA (Figure adopted from [191])

PLGA NPs-based drug delivery systems have been also investigated for delivery of several anticancer agents to tumors [185,199-204]. One approach of drug delivery by polymeric nano-carriers is the chemical conjugation of drug to the polymer by a hydrolysable bond which can be easily cleaved under the physiological conditions leading to the release of functional drug. The conjugation approach of drugs to natural and synthetic polymers has been widely used to prolong the circulation of drugs in blood stream, targeting to a specific organ, and sustained release at the injection site [205]. In the sixth chapter of this thesis chemical conjugation of JSI-124 to acid terminated PLGA polymer has been investigated as a strategy for sustained delivery of this compound to tumor and it selective delivery to DCs.

1.10.2 Polymeirc micellar-based drug delivery systems

Amphiphilic copolymer micellar-based drug delivery system have been extensively studied for tumor-targeted delivery of anticancer agents [206]. Co-polymeric micelles are nanoscopic in diameter (20 to 100 nm) and characterized with an unique core-shell architecture, where hydrophobic blocks are segregated from the aqueous exterior to form an inner core surrounded by a palisade of hydrophilic segments (Figure1-13).

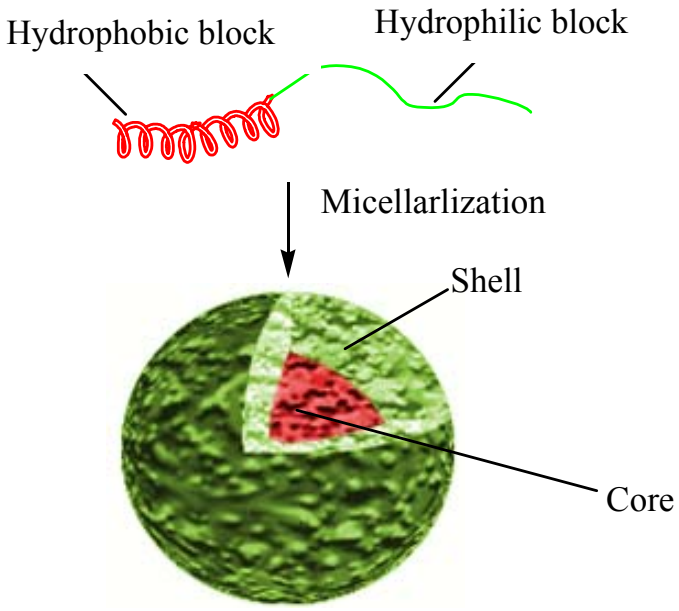

Figure 1-13. Schematic illustration of formation of polymeric micelles from amphiphilic copolymers

A self-assembled polymeric micelle is thermodynamically stable, prefers assembly to micellar structure relative to disassembly to single chains, if the concentration of the copolymer exceeds the critical micelle concentration (CMC). In this respect, amphiphilic copolymer micelles have a distinct advantage over those formed from conventional surfactants such as Cremophor EL™ or

polysorbates, since amphiphilic copolymer not only display lower CMCs, but also in some cases resist disassembly upon dilution due to physical interactions among chains in the micelle core [207,208].

The widespread application of polymeric micelles in drug delivery is linked to their unique core-shell architecture in which the hydrophobic core of micelles creates a cargo space for the encapsulation of hydrophobic drugs, proteins or DNA; and the hydrophilic shell is a brush-like corona masking the hydrophobic core from the biological milieu. Since hydrophilic shell minimizes protein adsorption on micelles and cellular adhesion of micelles, polymeric micelles have the ability to evade non-specific capture by the reticuloendothelial system (RES), and expect to demonstrate prolonged circulation time in blood [207-210]. With these propensities, polymeric micelles not only have shown a great potential for solubilization and controlled delivery of poorly soluble drugs, but they have demonstrated a promise in targeted drug delivery especially in cancer therapy. This is due to their promoted accumulation in the solid tumors as a result of the enhanced permeability and retention (EPR) effect (induced by the presence of leaky blood vessels and poorly developed lymphatics at solid tumors). Micelles have the potential to lodge several types of anti-tumor molecules and accumulate extensively at solid tumors, increasing the range of therapeutic options for cancer therapy [207,208]. Polymeric micelles consisting of PEO-*b*-polypropylene oxide (PPO), PEO-*b*-poly(ester)s and PEO-*b*-poly(amino acid)s have been extensively investigated for drug solubilization, controlled drug release and drug targeting [207,208,211] (Figure 1-14. adopted from [207] .

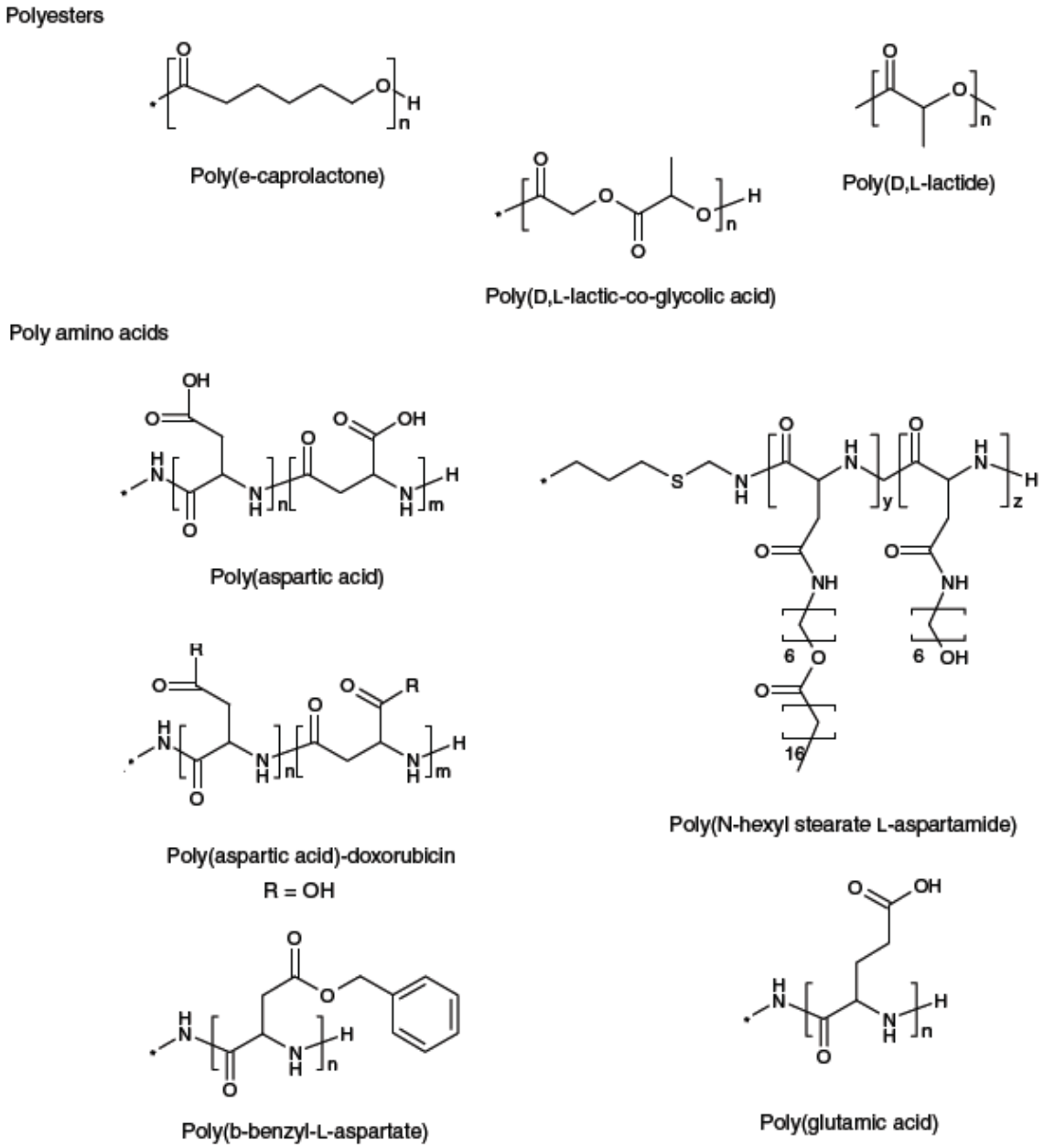

Figure 1-14. Chemical structure of the most commonly used poly(ester) and poly(amino acid) core-forming blocks in polymeric micelles (Figure adopted from [207])

Polymeric micelles-based drug delivery systems developed so far, can be categorized to three classes including micelle-forming polymer-drug conjugates, polymeric micellar nano-containers, and polyion complex micelles.

In micelle-forming polymer-drug conjugates, drug is incorporated and stabilized within the micellar carrier through formation of hydrolysable chemical bonds between the functional group(s) of the polymeric backbone and the drug. PEO-*b*-poly(ester) and PEO-*b*-poly(amino acid) block copolymers have been investigated for the development of different micelle-forming drug conjugates [207].

When solubilization and stabilization of water insoluble drugs in the polymeric micelles is achieved via formation of hydrophobic interactions or hydrogen bonds between the micelle forming block copolymer and drug, the resulting system is called a polymeric micellar nano-container. The method chosen for the preparation of polymeric micellar nano-containers is dependent on the solubility of the polymer being used. If the polymer is relatively water soluble, two methods may be employed for the formation of drug incorporated micelles. The first is the direct dissolution method, in which the copolymer is simply added to the aqueous media at a concentration above the CMC and drug is allowed to partition into the core of the micelles. The method, however, is not very efficient in terms of drug loading levels and not feasible for most block copolymer/drug structures. The second method is solvent evaporation method which involves the dissolution of the copolymer and drug in a volatile solvent which is then evaporated to leave a film in the bottom of a vial. This film is then reconstituted in

an aqueous phase by vigorous shaking. If the polymer is not readily soluble in water, drug encapsulated polymeric micelles can be prepared by a dialysis, or co-solvent evaporation, or oil in water emulsion method. In the dialysis method, the polymer and drug are solubilized in a water-miscible organic solvent followed by dialysis against aqueous media. In this method, organic solvent is gradually replaced with water resulting in self-association of copolymers and entrapment of drug in the assembled structure. In co-solvent evaporation method the drug and polymer are dissolved in a volatile water miscible organic solvent (co-solvent). Self assembly and drug entrapment is then triggered by the addition of aqueous phase (non-solvent for the core-forming block) to the organic phase (or vise versa) followed by the evaporation of the organic co-solvent. The oil in water emulsion procedure involves the addition of a solution of drug in a volatile, water immiscible organic solvent (such as chloroform or methylene chloride) into rapidly stirring aqueous media, with or without a surfactant, and the evaporation of the solvent. The polymer may be dissolved in either organic or aqueous phase. The organic solvent is then removed by evaporation [207].

The third class of polymeric micelles are polyion complex micelles in which drug incorporation is promoted through electrostatic interactions between oppositely charged polymer/drug combinations. Neutralization of the charge on the core-forming block the copolymer will then trigger self assembly of the polyion complex and stabilization of the complex within the hydrophobic environment of the micellar core. Polyion complex micelles have been

investigated for delivery of different therapeutic moieties that carry charge (e.g., small drugs [212,213], peptides [214] and DNA [214-217].

Several examples of copolymeric micelles-based delivery systems demonstrate their potential for the solubilization, controlled and targeted delivery of several clinically important drugs which are poorly water soluble and possess dose-limiting toxicity [207]. In this context, polymeric micelles have been successfully used in the solubilization of doxorubicin (DOX), paclitaxel (PXT), amphotericin B, cyclosporine A, and rapamycin without the inclusion of potentially harmful surfactants and excipients such as Cremephor® EL and ethanol. In addition polymeric micelles have shown promise in tumor-targeted delivery of several anticancer drugs including DOX and PXT [207]. To date, seven polymeric micellar formulations, all designed for solubilization and controlled delivery of anticancer drugs, are currently under assessments in preclinical and clinical trials (Table 1-1)

PEO-*b*-poly(ε-caprolactone) (PCL) is a biocompatible copolymer which have been successfully used for the solubilization and controlled delivery of a number of hydrophobic drugs [218-221]. PEO-*b*-PCL micelles were also shown to cause a favorable shift in the pharmacokinetics and biodistribution of cyclosporine A and Hydroxylcampthotecin after intravenous (i.v.) administration [222,223]. PEO-*b*-poly(α-benzyl carboxylate ε-caprolactone) (PBCL) is a newly synthesized block co-polymer with lower CMC compared to PEO-*b*-PCL [224]. In the chapter 5 of this thesis, PEO-*b*-PCL and PEO-*b*-PBCL micelles have been investigated for solubilization and controlled delivery JSI-124 and cucurbitacin B.

Table 1-1 Polymeric micellar delivery systems in clinical trials

Trade Name	Polymer Category	Incorporated drug	Progress	Most significant outcome	Ref
K911	PEO-*b*- poly(L-amino acid) (PLAA)	DOX/chemically conjugated and physically loaded	Phase II	Significant pharmacokinetic improvement and tumor accumulation	[225]
K105	PEO-*b*-PLAA	Paclitaxel/ physically loaded	Phase I	Improved tumor accumulation and anti-tumor activity in mice (preclinical)	[226]
C-6004	PEO-*b*-PLAA	Cisplatine/to form complex	Phase I	Reduced nephrotoxicity and neurotoxicity in rats (preclinical)	[227]
SP1049C	Pluronic	DOX/physically loaded	Phase II	Partial response in some patients	[228]
PAXCEED®	PEO-*b*-poly(ester)	Paclitaxel/ physically loaded	Phase I/ II	Lower toxicity (mice) and increase in solubility (no pharmacokinetic improvement)	http:// www.angiotech.com/
Genexol®-PM	PEO-*b*-poly(ester)	Paclitaxel/ physically loaded	Phase II	Increased MTD (no pharmacokinetic improvement)	[229]
NK012	PEG-*b*-poly glutamate	SN-38/ chemically conjugated	Phase I	Increased MTD and Lower toxicity	[230, 231]

1.11 Research Proposal

1.11.1 Central Hypothesis and Objectives

The central hypothesis of this project is that selective delivery of STAT3 inhibitor cucurbitacins, to tumor and immunosuppressed DCs can reverse the immunosuppressive environment inside tumor resulting in the induction of potent anticancer immune responses by a cancer vaccine. Two main objectives were set to test this central hypothesis: 1. to assess the effects of STAT3 inhibition by cucurbitacins in tumor on overcoming cancer immunosuppression and boosting anticancer immune responses induced by TLR ligands; and 2. to develop polymeric nano-carriers for solubilization and targeted delivery of cucurbitacins to tumor and immunosuppressed DCs.

1.11.2 Rational

TLR-induced activation of DCs offers an important strategy for immunotherapy of cancer. Previous studies suggest that inhibition of STAT3 in tumors can modulate tumor induced immunosuppression and enhance the therapeutic efficacy of cancer immunotherapy [11]. Thus we purposed to evaluate the anticancer and immunomodulatory effects of TLR4/TLR9–based cancer immunotherapy in combination with JSI-124 induced inhibition of STAT3 in mice carrying B16 tumor with constitutively active STAT3.

STAT3 inhibitor cucurbitacins are poorly water soluble compound with non-specific toxicity, which limit their clinical application. Therefore, in an attempt to overcome theses limitations and enhance the therapeutic benefits of this

important category of anticancer agents, PEO-*b*-PCL-based micelles containing physically encapsulated cucurbitacins was developed. For quantitative analysis of STAT3 inhibitor cucurbitacins in different studies, a sensitive and reproducible liquid chromatography-mass spectrometry (LC-MS) method was also developed and validated.

Tumor-affected immunosuppressed DCs with constitutively active STAT3 are believed to be crucial in the establishment of tumor immunosuppressive microenvironment which is a major obstacle to effective immunotherapy of cancer. Blocking STAT3 in immunosuppressed DCs is suggested as a promising strategy for overcoming tumor-induced immunosuppression. Thus, we purpose to target STAT3 inhibitor JSI-124 to DCs by chemical attachment of this compound to PLGA NPs which is the nano-carrier of choice for delivery of therapeutic agents (e.g adjuvants) to DCs.

1.11.3 Working Hypotheses

1- Intra-tumoral co-delivery of STAT3 inhibitor JSI-124 and TLR9 ligand, (CpG oligodeoxynucleotide) or TLR4 ligand (7-acyl lipid A), would decrease cancer immunosuppression and enhance anti-tumor immune responses resulting in superior anticancer effects compared to monotherapy with each agent alone.

2- LC-MS provide a sensitive, specific, reproducible and reliable method for quantitative analysis of STAT3 inhibitor cucurbitacins.

3- PEO-*b*-PCL-based polymeric micelles efficiently encapsulate cucurbitacins and provide enhanced delivery of functional drug to tumor.
4- Chemical conjugation of JSI-124 to PLGA NPs would provide a useful platform for delivery of JSI-124 to tumor and its targeted delivery to DCs.

1.11.4 Specific objectives

1) To investigate the effects of intra-tumoral injection of STAT3 inhibitor JSI-124 in combination with 7-acyl lipid A or CpG on the inhibition of tumor growth and modulation of anti-tumor immune responses in a B16 mouse melanoma model
2) To develop and validate a sensitive and reproducible LC-MS method for quantitative analysis of STAT3 inhibitor cucurbitacins
3) To evaluate the potential of PEO-*b*-PCL-based micelles for solubilizaiton and controlled delivery of STAT3 inhibitor cucurbitacins to tumor
4) To investigate the chemical conjugation of JSI-124 to carboxyl ended PLGA NPs as a strategy for preparation of a drug platform for JSI-124 delivery to tumor and its targeted delivery to DCs

1.11.5 Significance

Our observations on the superior anticancer effects of CpG-based immunotherapy in combination with JSI-124 induced inhibition of STAT3 prove the principle of STAT3 inhibition for enhancing the efficacy of cancer immunotherapy. The LC-MS method developed in this research is a sensitive and

specific method which can be used for quantitative analysis of STAT3 inhibitor cucurbitacins in various *in vitro* and *in vivo* studies. Our findings showed that PEO-*b*-PCL-based micelles can potentially solubilize STAT3 inhibitor cucurbitacins and overcome the problem of poor water solubility which is one the major limitation for clinical application of these important anticancer agents. PLGA-JSI-124 NPs developed in this research can potentially provide useful platforms for sustained delivery of JSI-124 in tumor and also for targeted co-delivery of cancer antigens, adjuvants and JSI-124 to DCs paving the way toward development of efficient cancer therapeutic vaccines.

1.12 References

1. Dunn GP, Old LJ, Schreiber RD: The three Es of cancer immunoediting. Annu Rev Immunol 2004;22:329-360.
2. Samuel J, Budzynski WA, Reddish MA, Ding L, Zimmermann GL, Krantz MJ, Koganty RR, Longenecker BM: Immunogenicity and antitumor activity of a liposomal MUC1 peptide-based vaccine. Int J Cancer 1998;75:295-302.
3. Slingluff CL, Speiser DE: Progress and controversies in developing cancer vaccines. J Transl Med 2005;3:18-27.
4. Morse MA, Chui S, Hobeika A, Lyerly HK, Clay T: Recent developments in therapeutic cancer vaccines. Nat Clin Pract Oncol 2005;2:108-113.
5. Rosenberg SA, Yang JC, Restifo NP: Cancer immunotherapy: moving beyond current vaccines. Nat Med 2004;10:909-915.
6. Pejawar-Gaddy S, Finn OJ: Cancer vaccines: Accomplishments and challenges. Crit Rev Oncol Hematol 2008.
7. Bronte V, Mocellin S: Suppressive influences in the immune response to cancer. J Immunother 2009;32:1-11.
8. Kaufman HL, Disis ML: Immune system versus tumor: shifting the balance in favor of DCs and effective immunity. J Clin Invest 2004;113:664-667.
9. Zou W: Immunosuppressive networks in the tumour environment and their therapeutic relevance. Nat Rev Cancer 2005;5:263-274.

10. Gajewski TF, Meng Y, Blank C, Brown I, Kacha A, Kline J, Harlin H: Immune resistance orchestrated by the tumor microenvironment. Immunol Rev 2006;213:131-145.

11. Yu H, Kortylewski M, Pardoll D: Crosstalk between cancer and immune cells: role of STAT3 in the tumour microenvironment. Nat Rev Immunol 2007;7:41-51.

12. Novak N, Bieber T: 2. Dendritic cells as regulators of immunity and tolerance. J Allergy Clin Immunol 2008;121:S370-374; quiz S413.

13. Cools N, Ponsaerts P, Van Tendeloo VF, Berneman ZN: Balancing between immunity and tolerance: an interplay between dendritic cells, regulatory T cells, and effector T cells. J Leukoc Biol 2007;82:1365-1374.

14. Nizar S, Copier J, Meyer B, Bodman-Smith M, Galustian C, Kumar D, Dalgleish A: T-regulatory cell modulation: the future of cancer immunotherapy? Br J Cancer 2009;100:1697-1703.

15. Kortylewski M, Xin H, Kujawski M, Lee H, Liu Y, Harris T, Drake C, Pardoll D, Yu H: Regulation of the IL-23 and IL-12 balance by Stat3 signaling in the tumor microenvironment. Cancer Cell 2009;15:114-123.

16. Stewart CA, Trinchieri G: Reinforcing suppression using regulators: a new link between STAT3, IL-23, and Tregs in tumor immunosuppression. Cancer Cell 2009;15:81-83.

17. Nefedova Y, Gabrilovich DI: Targeting of Jak/STAT pathway in antigen presenting cells in cancer. Curr Cancer Drug Targets 2007;7:71-77.

18. Yu H, Jove R: The STATs of cancer--new molecular targets come of age. Nat Rev Cancer 2004;4:97-105.

19. Darnell JE: Validating Stat3 in cancer therapy. Nat Med 2005;11:595-596.

20. Al Zaid Siddiquee K, Turkson J: STAT3 as a target for inducing apoptosis in solid and hematological tumors. Cell Res 2008;18:254-267.

21. Blaskovich MA, Sun J, Cantor A, Turkson J, Jove R, Sebti SM: Discovery of JSI-124 (cucurbitacin I), a selective Janus kinase/signal transducer and activator of transcription 3 signaling pathway inhibitor with potent antitumor activity against human and murine cancer cells in mice. Cancer Res 2003;63:1270-1279.

22. Sun J, Blaskovich MA, Jove R, Livingston SK, Coppola D, Sebti SM: Cucurbitacin Q: a selective STAT3 activation inhibitor with potent antitumor activity. Oncogene 2005;24:3236-3245.

23. Nefedova Y, Cheng P, Gilkes D, Blaskovich M, Beg AA, Sebti SM, Gabrilovich DI: Activation of Dendritic Cells via Inhibition of Jak2/STAT3 Signaling. J Immunol 2005;175:4338-4346.

24. Nefedova Y, Nagaraj S, Rosenbauer A, Muro-Cacho C, Sebti SM, Gabrilovich DI: Regulation of dendritic cell differentiation and antitumor immune response in cancer by pharmacologic-selective inhibition of the janus-activated kinase 2/signal transducers and activators of transcription 3 pathway. Cancer Res 2005;65:9525-9535.

25. Krieg AM: Development of TLR9 agonists for cancer therapy. J Clin Invest 2007;117:1184-1194.

26. Melief CJ, Van Der Burg SH, Toes RE, Ossendorp F, Offringa R: Effective therapeutic anticancer vaccines based on precision guiding of cytolytic T lymphocytes. Immunol Rev 2002;188:177-182.

27. Trinchieri G: Interleukin-12 and the regulation of innate resistance and adaptive immunity. Nat Rev Immunol 2003;3:133-146.

28. Pasare C, Medzhitov R: Toll pathway-dependent blockade of CD4+CD25+ T cell-mediated suppression by dendritic cells. Science 2003;299:1033-1036.

29. Liu G, Zhao Y: Toll-like receptors and immune regulation: their direct and indirect modulation on regulatory CD4+ CD25+ T cells. Immunology 2007;122:149-156.

30. Pardoll D: Does the immune system see tumors as foreign or self? Annu Rev Immunol 2003;21:807-839.

31. Kim R, Emi M, Tanabe K: Cancer immunoediting from immune surveillance to immune escape. Immunology 2007;121:1-14.

32. Dunn GP, Old LJ, Schreiber RD: The immunobiology of cancer immunosurveillance and immunoediting. Immunity 2004;21:137-148.

33. Dunn GP, Bruce AT, Ikeda H, Old LJ, Schreiber RD: Cancer immunoediting: from immunosurveillance to tumor escape. Nat Immunol 2002;3:991-998.

34. Swann JB, Smyth MJ: Immune surveillance of tumors. J Clin Invest 2007;117:1137-1146.

35. Lanzavecchia A, Sallusto F: Regulation of T cell immunity by dendritic cells. Cell. 2001;106:263-266.

36. Banchereau J, Steinman RM: Dendritic cells and the control of immunity. Nature 1998;392:245-252.

37. Stockwin LH, McGonagle D, Martin IG, Blair GE: Dendritic cells: immunological sentinels with a central role in health and disease. Immunol & Cell Biol. 2000;78:91-102.

38. Naik SH, Sathe P, Park HY, Metcalf D, Proietto AI, Dakic A, Carotta S, O'Keeffe M, Bahlo M, Papenfuss A, Kwak JY, Wu L, Shortman K: Development of plasmacytoid and conventional dendritic cell subtypes from single precursor cells derived in vitro and in vivo. Nat Immunol 2007;8:1217-1226.

39. Shortman K, Liu YJ: Mouse and human dendritic cell subtypes. Nature Reviews. Immunology. 2002;2:151-161.

40. Shortman K, Naik SH: Steady-state and inflammatory dendritic-cell development. Nat Rev Immunol 2007;7:19-30.

41. Underhill DM, Ozinsky A: Phagocytosis of microbes: complexity in action. Annu Rev Immunol 2002;20:825-852.

42. Kim R, Emi M, Tanabe K, Arihiro K: Potential functional role of plasmacytoid dendritic cells in cancer immunity. Immunology 2007;121:149-157.

43. Hubert P, Jacobs N, Caberg JH, Boniver J, Delvenne P: The cross-talk between dendritic and regulatory T cells: good or evil? J Leukoc Biol 2007;82:781-794.

44. Palm NW, Medzhitov R: Pattern recognition receptors and control of adaptive immunity. Immunol Rev 2009;227:221-233.

45. Gallucci S, Matzinger P: Danger signals: SOS to the immune system. Curr Opin Immunol 2001;13:114-119.

46. Dougan M, Dranoff G: Immune therapy for cancer. Annu Rev Immunol 2009;27:83-117.

47. Rabinovich GA, Gabrilovich D, Sotomayor EM: Immunosuppressive strategies that are mediated by tumor cells. Annu Rev Immunol 2007;25:267-296.

48. Weiner GJ: Monoclonal antibody mechanisms of action in cancer. Immunol Res 2007;39:271-278.

49. Schuster M, Nechansky A, Kircheis R: Cancer immunotherapy. Biotechnol J 2006;1:138-147.

50. Vieweg J, Su Z, Dahm P, Kusmartsev S: Reversal of tumor-mediated immunosuppression. Clin Cancer Res 2007;13:727s-732s.

51. Kuang DM, Zhao Q, Xu J, Yun JP, Wu C, Zheng L: Tumor-educated tolerogenic dendritic cells induce CD3epsilon down-regulation and apoptosis of T cells through oxygen-dependent pathways. J Immunol 2008;181:3089-3098.

52. Steinman RM, Hawiger D, Nussenzweig MC: Tolerogenic dendritic cells. Annu Rev Immunol 2003;21:685-711.

53. Qin FX: Dynamic behavior and function of Foxp3+ regulatory T cells in tumor bearing host. Cell Mol Immunol 2009;6:3-13.

54. Gabrilovich D: Mechanisms and functional significance of tumour-induced dendritic-cell defects. Nat Rev Immunol 2004;4:941-952.

55. Piccirillo CA: Regulatory T cells in health and disease. Cytokine 2008;43:395-401.

56. Raimondi G, Turner MS, Thomson AW, Morel PA: Naturally occurring regulatory T cells: recent insights in health and disease. Crit Rev Immunol 2007;27:61-95.

57. Gallimore AM, Simon AK: Positive and negative influences of regulatory T cells on tumour immunity. Oncogene 2008;27:5886-5893.

58. Wang RF: Immune suppression by tumor-specific CD4+ regulatory T-cells in cancer. Semin Cancer Biol 2006;16:73-79.

59. Antony PA, Restifo NP: Do CD4+ CD25+ immunoregulatory T cells hinder tumor immunotherapy? J Immunother 2002;25:202-206.

60. Sojka DK, Huang YH, Fowell DJ: Mechanisms of regulatory T-cell suppression - a diverse arsenal for a moving target. Immunology 2008;124:13-22.

61. Wing K, Ekmark A, Karlsson H, Rudin A, Suri-Payer E: Characterization of human CD25+ CD4+ T cells in thymus, cord and adult blood. Immunology 2002;106:190-199.

62. Shevach EM: From vanilla to 28 flavors: multiple varieties of T regulatory cells. Immunity 2006;25:195-201.

63. Walker MR, Kasprowicz DJ, Gersuk VH, Benard A, Van Landeghen M, Buckner JH, Ziegler SF: Induction of FoxP3 and acquisition of T regulatory activity by stimulated human CD4+CD25- T cells. J Clin Invest 2003;112:1437-1443.

64. Fontenot JD, Gavin MA, Rudensky AY: Foxp3 programs the development and function of CD4+CD25+ regulatory T cells. Nat Immunol 2003;4:330-336.

65. Khattri R, Cox T, Yasayko SA, Ramsdell F: An essential role for Scurfin in CD4+CD25+ T regulatory cells. Nat Immunol 2003;4:337-342.

66. Katz JB, Muller AJ, Prendergast GC: Indoleamine 2,3-dioxygenase in T-cell tolerance and tumoral immune escape. Immunol Rev 2008;222:206-221.

67. Ino K, Yamamoto E, Shibata K, Kajiyama H, Yoshida N, Terauchi M, Nawa A, Nagasaka T, Takikawa O, Kikkawa F: Inverse correlation between tumoral indoleamine 2,3-dioxygenase expression and tumor-infiltrating lymphocytes in endometrial cancer: its association with disease progression and survival. Clin Cancer Res 2008;14:2310-2317.

68. Rutella S, Bonanno G, De Cristofaro R: Targeting indoleamine 2,3-dioxygenase (IDO) to counteract tumour-induced immune dysfunction: from biochemistry to clinical development. Endocr Metab Immune Disord Drug Targets 2009;9:151-177.

69. Bergmann C, Strauss L, Zeidler R, Lang S, Whiteside TL: Expansion of human T regulatory type 1 cells in the microenvironment of cyclooxygenase 2 overexpressing head and neck squamous cell carcinoma. Cancer Res 2007;67:8865-8873.

70. Akasaki Y, Liu G, Chung NH, Ehtesham M, Black KL, Yu JS: Induction of a CD4+ T regulatory type 1 response by cyclooxygenase-2-overexpressing glioma. J Immunol 2004;173:4352-4359.

71. Li JF, Chu YW, Wang GM, Zhu TY, Rong RM, Hou J, Xu M: The prognostic value of peritumoral regulatory T cells and its correlation with intratumoral cyclooxygenase-2 expression in clear cell renal cell carcinoma. BJU Int 2009;103:399-405.

72. Ohm JE, Carbone DP: VEGF as a mediator of tumor-associated immunodeficiency. Immunol Res 2001;23:263-272.

73. Mimura K, Kono K, Takahashi A, Kawaguchi Y, Fujii H: Vascular endothelial growth factor inhibits the function of human mature dendritic cells mediated by VEGF receptor-2. Cancer Immunol Immunother 2007;56:761-770.

74. Li B, Lalani AS, Harding TC, Luan B, Koprivnikar K, Huan Tu G, Prell R, VanRoey MJ, Simmons AD, Jooss K: Vascular endothelial growth factor blockade reduces intratumoral regulatory T cells and enhances the efficacy of a GM-CSF-secreting cancer immunotherapy. Clin Cancer Res 2006;12:6808-6816.

75. Johnson BF, Clay TM, Hobeika AC, Lyerly HK, Morse MA: Vascular endothelial growth factor and immunosuppression in cancer: current knowledge and potential for new therapy. Expert Opin Biol Ther 2007;7:449-460.

76. Ohm JE, Carbone DP: Immune dysfunction in cancer patients. Oncology (Williston Park) 2002;16:11-18.

77. Derynck R, Akhurst RJ, Balmain A: TGF-beta signaling in tumor suppression and cancer progression. Nat Genet 2001;29:117-129.

78. Becker C, Fantini MC, Schramm C, Lehr HA, Wirtz S, Nikolaev A, Burg J, Strand S, Kiesslich R, Huber S, Ito H, Nishimoto N, Yoshizaki K, Kishimoto T, Galle PR, Blessing M, Rose-John S, Neurath MF: TGF-beta suppresses tumor progression in colon cancer by inhibition of IL-6 trans-signaling. Immunity 2004;21:491-501.

79. Kirkbride KC, Blobe GC: Inhibiting the TGF-beta signalling pathway as a means of cancer immunotherapy. Expert Opin Biol Ther 2003;3:251-261.

80. Darnell JE, Jr., Kerr IM, Stark GR: Jak-STAT pathways and transcriptional activation in response to IFNs and other extracellular signaling proteins. Science 1994;264:1415-1421.

81. Darnell JE, Jr.: STATs and gene regulation. Science 1997;277:1630-1635.

82. Wen Z, Zhong Z, Darnell JE, Jr.: Maximal activation of transcription by Stat1 and Stat3 requires both tyrosine and serine phosphorylation. Cell 1995;82:241-250.

83. Rawlings JS, Rosler KM, Harrison DA: The JAK/STAT signaling pathway. J Cell Sci 2004;117:1281-1283.

84. Mora LB, Buettner R, Seigne J, Diaz J, Ahmad N, Garcia R, Bowman T, Falcone R, Fairclough R, Cantor A, Muro-Cacho C, Livingston S, Karras J, Pow-Sang J, Jove R: Constitutive activation of Stat3 in human prostate tumors and cell lines: direct inhibition of Stat3 signaling induces apoptosis of prostate cancer cells. Cancer Res 2002;62:6659-6666.

85. Dolled-Filhart M, Camp RL, Kowalski DP, Smith BL, Rimm DL: Tissue microarray analysis of signal transducers and activators of transcription 3 (Stat3) and phospho-Stat3 (Tyr705) in node-negative breast cancer shows nuclear localization is associated with a better prognosis. Clin Cancer Res 2003;9:594-600.

86. Nagpal JK, Mishra R, Das BR: Activation of Stat-3 as one of the early events in tobacco chewing-mediated oral carcinogenesis. Cancer 2002;94:2393-2400.

87. Hsiao JR, Jin YT, Tsai ST, Shiau AL, Wu CL, Su WC: Constitutive activation of STAT3 and STAT5 is present in the majority of nasopharyngeal carcinoma and correlates with better prognosis. Br J Cancer 2003;89:344-349.

88. Groner B, Lucks P, Borghouts C: The function of Stat3 in tumor cells and their microenvironment. Semin Cell Dev Biol 2008;19:341-350.

89. Turkson J, Bowman T, Garcia R, Caldenhoven E, De Groot RP, Jove R: Stat3 activation by Src induces specific gene regulation and is required for cell transformation. Mol Cell Biol 1998;18:2545-2552.

90. Bromberg JF, Horvath CM, Besser D, Lathem WW, Darnell JE, Jr.: Stat3 activation is required for cellular transformation by v-src. Mol Cell Biol 1998;18:2553-2558.

91. Schlessinger K, Levy DE: Malignant transformation but not normal cell growth depends on signal transducer and activator of transcription 3. Cancer Res 2005;65:5828-5834.

92. Bromberg JF, Wrzeszczynska MH, Devgan G, Zhao Y, Pestell RG, Albanese C, Darnell JE, Jr.: Stat3 as an oncogene. Cell 1999;98:295-303.

93. Bowman T, Garcia R, Turkson J, Jove R: STATs in oncogenesis. Oncogene 2000;19:2474-2488.

94. Buettner R, Mora LB, Jove R: Activated STAT signaling in human tumors provides novel molecular targets for therapeutic intervention. Clin Cancer Res 2002;8:945-954.

95. Turkson J, Jove R: STAT proteins: novel molecular targets for cancer drug discovery. Oncogene 2000;19:6613-6626.

96. Turkson J: STAT proteins as novel targets for cancer drug discovery. Expert Opin Ther Targets 2004;8:409-422.

97. Sinibaldi D, Wharton W, Turkson J, Bowman T, Pledger WJ, Jove R: Induction of p21WAF1/CIP1 and cyclin D1 expression by the Src

oncoprotein in mouse fibroblasts: role of activated STAT3 signaling. Oncogene 2000;19:5419-5427.

98. Bowman T, Broome MA, Sinibaldi D, Wharton W, Pledger WJ, Sedivy JM, Irby R, Yeatman T, Courtneidge SA, Jove R: Stat3-mediated Myc expression is required for Src transformation and PDGF-induced mitogenesis. Proc Natl Acad Sci U S A 2001;98:7319-7324.

99. Catlett-Falcone R, Landowski TH, Oshiro MM, Turkson J, Levitzki A, Savino R, Ciliberto G, Moscinski L, Fernandez-Luna JL, Nunez G, Dalton WS, Jove R: Constitutive activation of Stat3 signaling confers resistance to apoptosis in human U266 myeloma cells. Immunity 1999;10:105-115.

100. Niu G, Bowman T, Huang M, Shivers S, Reintgen D, Daud A, Chang A, Kraker A, Jove R, Yu H: Roles of activated Src and Stat3 signaling in melanoma tumor cell growth. Oncogene 2002;21:7001-7010.

101. Epling-Burnette PK, Liu JH, Catlett-Falcone R, Turkson J, Oshiro M, Kothapalli R, Li Y, Wang JM, Yang-Yen HF, Karras J, Jove R, Loughran TP, Jr.: Inhibition of STAT3 signaling leads to apoptosis of leukemic large granular lymphocytes and decreased Mcl-1 expression. J Clin Invest 2001;107:351-362.

102. Iwamaru A, Szymanski S, Iwado E, Aoki H, Yokoyama T, Fokt I, Hess K, Conrad C, Madden T, Sawaya R, Kondo S, Priebe W, Kondo Y: A novel inhibitor of the STAT3 pathway induces apoptosis in malignant glioma cells both in vitro and in vivo. Oncogene 2007;26:2435-2444.

103. Bhattacharya S, Ray RM, Johnson LR: STAT3-mediated transcription of Bcl-2, Mcl-1 and c-IAP2 prevents apoptosis in polyamine-depleted cells. Biochem J 2005;392:335-344.

104. Gritsko T, Williams A, Turkson J, Kaneko S, Bowman T, Huang M, Nam S, Eweis I, Diaz N, Sullivan D, Yoder S, Enkemann S, Eschrich S, Lee JH, Beam CA, Cheng J, Minton S, Muro-Cacho CA, Jove R: Persistent activation of stat3 signaling induces survivin gene expression and confers resistance to apoptosis in human breast cancer cells. Clin Cancer Res 2006;12:11-19.

105. Diaz N, Minton S, Cox C, Bowman T, Gritsko T, Garcia R, Eweis I, Wloch M, Livingston S, Seijo E, Cantor A, Lee JH, Beam CA, Sullivan D, Jove R, Muro-Cacho CA: Activation of stat3 in primary tumors from high-risk breast cancer patients is associated with elevated levels of activated SRC and survivin expression. Clin Cancer Res 2006;12:20-28.

106. Park S, Kim D, Kaneko S, Szewczyk KM, Nicosia SV, Yu H, Jove R, Cheng JQ: Molecular cloning and characterization of the human AKT1 promoter uncovers its up-regulation by the Src/Stat3 pathway. J Biol Chem 2005;280:38932-38941.

107. Niu G, Wright KL, Ma Y, Wright GM, Huang M, Irby R, Briggs J, Karras J, Cress WD, Pardoll D, Jove R, Chen J, Yu H: Role of Stat3 in regulating p53 expression and function. Mol Cell Biol 2005;25:7432-7440.

108. Xu Q, Briggs J, Park S, Niu G, Kortylewski M, Zhang S, Gritsko T, Turkson J, Kay H, Semenza GL, Cheng JQ, Jove R, Yu H: Targeting Stat3

blocks both HIF-1 and VEGF expression induced by multiple oncogenic growth signaling pathways. Oncogene 2005;24:5552-5560.

109. Niu G, Wright KL, Huang M, Song L, Haura E, Turkson J, Zhang S, Wang T, Sinibaldi D, Coppola D, Heller R, Ellis LM, Karras J, Bromberg J, Pardoll D, Jove R, Yu H: Constitutive Stat3 activity up-regulates VEGF expression and tumor angiogenesis. Oncogene 2002;21:2000-2008.

110. Kortylewski M, Jove R, Yu H: Targeting STAT3 affects melanoma on multiple fronts. Cancer Metastasis Rev 2005;24:315-327.

111. Siddiquee K, Zhang S, Guida WC, Blaskovich MA, Greedy B, Lawrence HR, Yip ML, Jove R, McLaughlin MM, Lawrence NJ, Sebti SM, Turkson J: Selective chemical probe inhibitor of Stat3, identified through structure-based virtual screening, induces antitumor activity. Proc Natl Acad Sci U S A 2007;104:7391-7396.

112. Alas S, Bonavida B: Inhibition of constitutive STAT3 activity sensitizes resistant non-Hodgkin's lymphoma and multiple myeloma to chemotherapeutic drug-mediated apoptosis. Clin Cancer Res 2003;9:316-326.

113. Nielsen M, Kaestel CG, Eriksen KW, Woetmann A, Stokkedal T, Kaltoft K, Geisler C, Ropke C, Odum N: Inhibition of constitutively activated Stat3 correlates with altered Bcl-2/Bax expression and induction of apoptosis in mycosis fungoides tumor cells. Leukemia 1999;13:735-738.

114. Xi S, Gooding WE, Grandis JR: In vivo antitumor efficacy of STAT3 blockade using a transcription factor decoy approach: implications for cancer therapy. Oncogene 2005;24:970-979.

115. Real PJ, Sierra A, De Juan A, Segovia JC, Lopez-Vega JM, Fernandez-Luna JL: Resistance to chemotherapy via Stat3-dependent overexpression of Bcl-2 in metastatic breast cancer cells. Oncogene 2002;21:7611-7618.

116. Lee YK, Isham CR, Kaufman SH, Bible KC: Flavopiridol disrupts STAT3/DNA interactions, attenuates STAT3-directed transcription, and combines with the Jak kinase inhibitor AG490 to achieve cytotoxic synergy. Mol Cancer Ther 2006;5:138-148.

117. Yau CY, Wheeler JJ, Sutton KL, Hedley DW: Inhibition of integrin-linked kinase by a selective small molecule inhibitor, QLT0254, inhibits the PI3K/PKB/mTOR, Stat3, and FKHR pathways and tumor growth, and enhances gemcitabine-induced apoptosis in human orthotopic primary pancreatic cancer xenografts. Cancer Res 2005;65:1497-1504.

118. Gariboldi MB, Ravizza R, Molteni R, Osella D, Gabano E, Monti E: Inhibition of Stat3 increases doxorubicin sensitivity in a human metastatic breast cancer cell line. Cancer Lett 2007;258:181-188.

119. Burdelya L, Kujawski M, Niu G, Zhong B, Wang T, Zhang S, Kortylewski M, Shain K, Kay H, Djeu J, Dalton W, Pardoll D, Wei S, Yu H: Stat3 activity in melanoma cells affects migration of immune effector cells and nitric oxide-mediated antitumor effects. J Immunol 2005;174:3925-3931.

120. Kortylewski M, Kujawski M, Wang T, Wei S, Zhang S, Pilon-Thomas S, Niu G, Kay H, Mule J, Kerr WG, Jove R, Pardoll D, Yu H: Inhibiting Stat3 signaling in the hematopoietic system elicits multicomponent antitumor immunity. Nat Med 2005;11:1314-1321.

121. Wang T, Niu G, Kortylewski M, Burdelya L, Shain K, Zhang S, Bhattacharya R, Gabrilovich D, Heller R, Coppola D, Dalton W, Jove R, Pardoll D, Yu H: Regulation of the innate and adaptive immune responses by Stat-3 signaling in tumor cells. Nat Med 2004;10:48-54.

122. Jing N, Tweardy DJ: Targeting Stat3 in cancer therapy. Anticancer Drugs 2005;16:601-607.

123. Darnell JE, Jr.: Studies of IFN-induced transcriptional activation uncover the Jak-Stat pathway. J Interferon Cytokine Res 1998;18:549-554.

124. Stark GR, Kerr IM, Williams BR, Silverman RH, Schreiber RD: How cells respond to interferons. Annu Rev Biochem 1998;67:227-264.

125. Park OK, Schaefer TS, Nathans D: In vitro activation of Stat3 by epidermal growth factor receptor kinase. Proc Natl Acad Sci U S A 1996;93:13704-13708.

126. Thomas SM, Grandis JR: Pharmacokinetic and pharmacodynamic properties of EGFR inhibitors under clinical investigation. Cancer Treat Rev 2004;30:255-268.

127. Baselga J: Why the epidermal growth factor receptor? The rationale for cancer therapy. Oncologist 2002;7 Suppl 4:2-8.

128. Garcia R, Bowman TL, Niu G, Yu H, Minton S, Muro-Cacho CA, Cox CE, Falcone R, Fairclough R, Parsons S, Laudano A, Gazit A, Levitzki A, Kraker A, Jove R: Constitutive activation of Stat3 by the Src and JAK tyrosine kinases participates in growth regulation of human breast carcinoma cells. Oncogene 2001;20:2499-2513.

129. Song L, Turkson J, Karras JG, Jove R, Haura EB: Activation of Stat3 by receptor tyrosine kinases and cytokines regulates survival in human non-small cell carcinoma cells. Oncogene 2003;22:4150-4165.

130. Sriuranpong V, Park JI, Amornphimoltham P, Patel V, Nelkin BD, Gutkind JS: Epidermal growth factor receptor-independent constitutive activation of STAT3 in head and neck squamous cell carcinoma is mediated by the autocrine/paracrine stimulation of the interleukin 6/gp130 cytokine system. Cancer Res 2003;63:2948-2956.

131. Jayaprakasam B, Seeram NP, Nair MG: Anticancer and antiinflammatory activities of cucurbitacins from Cucurbita andreana. Cancer Lett 2003;189:11-16.

132. Shi X, Franko B, Frantz C, Amin HM, Lai R: JSI-124 (cucurbitacin I) inhibits Janus kinase-3/signal transducer and activator of transcription-3 signalling, downregulates nucleophosmin-anaplastic lymphoma kinase (ALK), and induces apoptosis in ALK-positive anaplastic large cell lymphoma cells. Br J Haematol 2006;135:26-32.

133. Tannin-Spitz T, Grossman S, Dovrat S, Gottlieb HE, Bergman M: Growth inhibitory activity of cucurbitacin glucosides isolated from Citrullus

colocynthis on human breast cancer cells. Biochem Pharmacol 2007;73:56-67.

134. Nagai H, Kim YS, Konishi N, Baba M, Kubota T, Yoshimura A, Emi M: Combined hypermethylation and chromosome loss associated with inactivation of SSI-1/SOCS-1/JAB gene in human hepatocellular carcinomas. Cancer Lett 2002;186:59-65.

135. Flowers LO, Subramaniam PS, Johnson HM: A SOCS-1 peptide mimetic inhibits both constitutive and IL-6 induced activation of STAT3 in prostate cancer cells. Oncogene 2005;24:2114-2120.

136. Carpenter LR, Farruggella TJ, Symes A, Karow ML, Yancopoulos GD, Stahl N: Enhancing leptin response by preventing SH2-containing phosphatase 2 interaction with Ob receptor. Proc Natl Acad Sci U S A 1998;95:6061-6066.

137. Turkson J, Ryan D, Kim JS, Zhang Y, Chen Z, Haura E, Laudano A, Sebti S, Hamilton AD, Jove R: Phosphotyrosyl peptides block Stat3-mediated DNA binding activity, gene regulation, and cell transformation. J Biol Chem 2001;276:45443-45455.

138. Turkson J, Kim JS, Zhang S, Yuan J, Huang M, Glenn M, Haura E, Sebti S, Hamilton AD, Jove R: Novel peptidomimetic inhibitors of signal transducer and activator of transcription 3 dimerization and biological activity. Mol Cancer Ther 2004;3:261-269.

139. Costantino L, Barlocco D: STAT 3 as a target for cancer drug discovery. Curr Med Chem 2008;15:834-843.

140. Bhasin D, Cisek K, Pandharkar T, Regan N, Li C, Pandit B, Lin J, Li PK: Design, synthesis, and studies of small molecule STAT3 inhibitors. Bioorg Med Chem Lett 2008;18:391-395.

141. Leong PL, Andrews GA, Johnson DE, Dyer KF, Xi S, Mai JC, Robbins PD, Gadiparthi S, Burke NA, Watkins SF, Grandis JR: Targeted inhibition of Stat3 with a decoy oligonucleotide abrogates head and neck cancer cell growth. Proc Natl Acad Sci U S A 2003;100:4138-4143.

142. Turkson J, Zhang S, Mora LB, Burns A, Sebti S, Jove R: A novel platinum compound inhibits constitutive Stat3 signaling and induces cell cycle arrest and apoptosis of malignant cells. J Biol Chem 2005;280:32979-32988.

143. Turkson J, Zhang S, Palmer J, Kay H, Stanko J, Mora LB, Sebti S, Yu H, Jove R: Inhibition of constitutive signal transducer and activator of transcription 3 activation by novel platinum complexes with potent antitumor activity. Mol Cancer Ther 2004;3:1533-1542.

144. Chen JC, Chiu MH, Nie RL, Cordell GA, Qiu SX: Cucurbitacins and cucurbitane glycosides: structures and biological activities. Nat Prod Rep 2005;22:386-399.

145. Miro M: cucurbitacins and their pharmacological effects. phytother res 1995;9:159-168.

146. Duncan MD, Duncan KL: Cucurbitacin E targets proliferating endothelia. J Surg Res 1997;69:55-60.

147. Dinan L, Whiting P, Girault JP, Lafont R, Dhadialla TS, Cress DE, Mugat B, Antoniewski C, Lepesant JA: Cucurbitacins are insect steroid hormone antagonists acting at the ecdysteroid receptor. Biochem J 1997;327 (Pt 3):643-650.

148. Bartalis J, Halaweish FT: Relationship between cucurbitacins reversed-phase high-performance liquid chromatography hydrophobicity index and basal cytotoxicity on HepG2 cells. J Chromatogr B Analyt Technol Biomed Life Sci 2005;818:159-166.

149. Van Kester MS, Out-Luiting JJ, von dem Borne PA, Willemze R, Tensen CP, Vermeer MH: Cucurbitacin I Inhibits Stat3 and Induces Apoptosis in Sezary Cells. J Invest Dermatol 2008.

150. Niu G, Heller R, Catlett-Falcone R, Coppola D, Jaroszeski M, Dalton W, Jove R, Yu H: Gene therapy with dominant-negative Stat3 suppresses growth of the murine melanoma B16 tumor in vivo. Cancer Res 1999;59:5059-5063.

151. Chen K, Huang J, Gong W, Iribarren P, Dunlop NM, Wang JM: Toll-like receptors in inflammation, infection and cancer. Int Immunopharmacol 2007;7:1271-1285.

152. Rakoff-Nahoum S, Medzhitov R: Toll-like receptors and cancer. Nat Rev Cancer 2009;9:57-63.

153. Vabulas RM, Ahmad-Nejad P, Ghose S, Kirschning CJ, Issels RD, Wagner H: HSP70 as endogenous stimulus of the Toll/interleukin-1 receptor signal pathway. J Biol Chem 2002;277:15107-15112.

154. Beg AA: Endogenous ligands of Toll-like receptors: implications for regulating inflammatory and immune responses. Trends Immunol 2002;23:509-512.

155. Pasare C, Medzhitov R: Toll-like receptors: linking innate and adaptive immunity. Adv Exp Med Biol 2005;560:11-18.

156. Iwasaki A, Medzhitov R: Toll-like receptor control of the adaptive immune responses. Nat Immunol 2004;5:987-995.

157. van Duin D, Medzhitov R, Shaw AC: Triggering TLR signaling in vaccination. Trends Immunol 2006;27:49-55.

158. Agrawal S, Agrawal A, Doughty B, Gerwitz A, Blenis J, Van Dyke T, Pulendran B: Cutting edge: different Toll-like receptor agonists instruct dendritic cells to induce distinct Th responses via differential modulation of extracellular signal-regulated kinase-mitogen-activated protein kinase and c-Fos. J Immunol 2003;171:4984-4989.

159. Stumhofer JS, Silver J, Hunter CA: Negative regulation of Th17 responses. Semin Immunol 2007;19:394-399.

160. Wang RF, Miyahara Y, Wang HY: Toll-like receptors and immune regulation: implications for cancer therapy. Oncogene 2008;27:181-189.

161. Elamanchili P, Lutsiak CM, Hamdy S, Diwan M, Samuel J: "Pathogen-mimicking" nanoparticles for vaccine delivery to dendritic cells. J Immunother 2007;30:378-395.

162. Schon MP, Schon M: TLR7 and TLR8 as targets in cancer therapy. Oncogene 2008;27:190-199.

163. Liu YJ: IPC: professional type 1 interferon-producing cells and plasmacytoid dendritic cell precursors. Annu Rev Immunol 2005;23:275-306.

164. Krieg AM: Toll-like receptor 9 (TLR9) agonists in the treatment of cancer. Oncogene 2008;27:161-167.

165. Klinman DM: Immunotherapeutic uses of CpG oligodeoxynucleotides. Nat Rev Immunol 2004;4:249-258.

166. Molavi O, Ma Z, Hamdy S, Lai R, Lavasanifar A, Samuel J: Synergistic antitumor effects of CpG oligodeoxynucleotide and STAT3 inhibitory agent JSI-124 in a mouse melanoma tumor model. Immunol Cell Biol 2008.

167. Molenkamp BG, van Leeuwen PA, Meijer S, Sluijter BJ, Wijnands PG, Baars A, van den Eertwegh AJ, Scheper RJ, de Gruijl TD: Intradermal CpG-B activates both plasmacytoid and myeloid dendritic cells in the sentinel lymph node of melanoma patients. Clin Cancer Res 2007;13:2961-2969.

168. Baldridge JR, McGowan P, Evans JT, Cluff C, Mossman S, Johnson D, Persing D: Taking a Toll on human disease: Toll-like receptor 4 agonists as vaccine adjuvants and monotherapeutic agents. Expert Opin Biol Ther 2004;4:1129-1138.

169. Takayama K, Ribi E, Cantrell JL: Isolation of a nontoxic lipid A fraction containing tumor regression activity. Cancer Res 1981;41:2654-2657.

170. Baldrick P, Richardson D, Elliott G, Wheeler AW: Safety evaluation of monophosphoryl lipid A (MPL): an immunostimulatory adjuvant. Regul Toxicol Pharmacol 2002;35:398-413.

171. Jiang ZH, Budzynski WA, Qiu D, Yalamati D, Koganty RR: Monophosphoryl lipid A analogues with varying 3-O-substitution: synthesis and potent adjuvant activity. Carbohydr Res 2007;342:784-796.

172. Hamdy S, Elamanchili P, Alshamsan A, Molavi O, Satou T, Samuel J: Enhanced antigen-specific primary CD4+ and CD8+ responses by codelivery of ovalbumin and toll-like receptor ligand monophosphoryl lipid A in poly(D,L-lactic-co-glycolic acid) nanoparticles. J Biomed Mater Res A 2007;81:652-662.

173. Hamdy S, Haddadi A, Somayaji V, Ruan D, Samuel J: Pharmaceutical analysis of synthetic lipid A-based vaccine adjuvants in poly (D,L-lactic-co-glycolic acid) nanoparticle formulations. J Pharm Biomed Anal 2007;44:914-923.

174. Heil F, Hemmi H, Hochrein H, Ampenberger F, Kirschning C, Akira S, Lipford G, Wagner H, Bauer S: Species-specific recognition of single-stranded RNA via toll-like receptor 7 and 8. Science 2004;303:1526-1529.

175. Diebold SS, Kaisho T, Hemmi H, Akira S, Reis e Sousa C: Innate antiviral responses by means of TLR7-mediated recognition of single-stranded RNA. Science 2004;303:1529-1531.

176. Huang B, Zhao J, Unkeless JC, Feng ZH, Xiong H: TLR signaling by tumor and immune cells: a double-edged sword. Oncogene 2008;27:218-224.

177. Rodriguez A, Regnault A, Kleijmeer M, Ricciardi-Castagnoli P, Amigorena S: Selective transport of internalized antigens to the cytosol for MHC class I presentation in dendritic cells. Nat Cell Biol 1999;1:362-368.

178. Guyre CA, Barreda ME, Swink SL, Fanger MW: Colocalization of Fc gamma RI-targeted antigen with class I MHC: implications for antigen processing. J Immunol 2001;166:2469-2478.

179. Binder RJ, Han DK, Srivastava PK: CD91: a receptor for heat shock protein gp96. Nat Immunol 2000;1:151-155.

180. Engering AJ, Cella M, Fluitsma D, Brockhaus M, Hoefsmit EC, Lanzavecchia A, Pieters J: The mannose receptor functions as a high capacity and broad specificity antigen receptor in human dendritic cells. Eur J Immunol 1997;27:2417-2425.

181. Wei H, Wang S, Zhang D, Hou S, Qian W, Li B, Guo H, Kou G, He J, Wang H, Guo Y: Targeted Delivery of Tumor Antigens to Activated Dendritic Cells via CD11c Molecules Induces Potent Antitumor Immunity in Mice. Clin Cancer Res 2009.

182. Langer R, Cleland JL, Hanes J: New advances in microsphere-based single-dose vaccines. Adv Drug Deliv Rev 1997;28:97-119.

183. Lutsiak ME, Robinson DR, Coester C, Kwon GS, Samuel J: Analysis of poly(D,L-lactic-co-glycolic acid) nanosphere uptake by human dendritic cells and macrophages in vitro. Pharm Res 2002;19:1480-1487.

184. Newman KD, Elamanchili P, Kwon GS, Samuel J: Uptake of poly(D,L-lactic-co-glycolic acid) microspheres by antigen-presenting cells in vivo. J Biomed Mater Res 2002;60:480-486.

185. Bala I, Hariharan S, Kumar MN: PLGA nanoparticles in drug delivery: the state of the art. Crit Rev Ther Drug Carrier Syst 2004;21:387-422.

186. Jiang W, Gupta RK, Deshpande MC, Schwendeman SP: Biodegradable poly(lactic-co-glycolic acid) microparticles for injectable delivery of vaccine antigens. Adv Drug Deliv Rev 2005;57:391-410.

187. Ogawa Y, Yamamoto M, Okada H, Yashiki T, Shimamoto T: A new technique to efficiently entrap leuprolide acetate into microcapsules of polylactic acid or copoly(lactic/glycolic) acid. Chem Pharm Bull (Tokyo) 1988;36:1095-1103.

188. Elamanchili P, Diwan M, Cao M, Samuel J: Characterization of poly(D,L-lactic-co-glycolic acid) based nanoparticulate system for enhanced delivery of antigens to dendritic cells. Vaccine 2004;22:2406-2412.

189. Samuel J, Kwon GK: Polymeric Nanoparticle Delivery of Cancer Vaccines. USA, Informa Healthcare, 2005.

190. Eldridge JH, Staas JK, Meulbroek JA, McGhee JR, Tice TR, Gilley RM: Biodegradable microspheres as a vaccine delivery system. Mol Immunol 1991;28:287-294.

191. Miller RA, Brady JM, Cutright DE: Degradation rates of oral resorbable implants (polylactates and polyglycolates): rate modification with changes in PLA/PGA copolymer ratios. J Biomed Mater Res 1977;11:711-719.

192. Cutright DE, Perez B, Beasley JD, 3rd, Larson WJ, Posey WR: Degradation rates of polymers and copolymers of polylactic and polyglycolic acids. Oral Surg Oral Med Oral Pathol 1974;37:142-152.

193. Cohen S, Alonso MJ, Langer R: Novel approaches to controlled-release antigen delivery. Int J Technol Assess Health Care 1994;10:121-130.

194. Hutchinson FG, Furr BJ: Biodegradable polymers for the sustained release of peptides. Biochem Soc Trans 1985;13:520-523.

195. Gombotz WR, Pettit DK: Biodegradable polymers for protein and peptide drug delivery. Bioconjug Chem 1995;6:332-351.

196. Diwan M, Elamanchili P, Lane H, Gainer A, Samuel J: Biodegradable nanoparticle mediated antigen delivery to human cord blood derived dendritic cells for induction of primary T cell responses. J Drug Target 2003;11:495-507.

197. Wang D, Robinson DR, Kwon GS, Samuel J: Encapsulation of plasmid DNA in biodegradable poly(D, L-lactic-co-glycolic acid) microspheres as a novel approach for immunogene delivery. J Control Release 1999;57:9-18.

198. Audran R, Peter K, Dannull J, Men Y, Scandella E, Groettrup M, Gander B, Corradin G: Encapsulation of peptides in biodegradable microspheres

prolongs their MHC class-I presentation by dendritic cells and macrophages in vitro. Vaccine 2003;21:1250-1255.

199. Kalaria DR, Sharma G, Beniwal V, Ravi Kumar MN: Design of Biodegradable Nanoparticles for Oral Delivery of Doxorubicin: In vivo Pharmacokinetics and Toxicity Studies in Rats. Pharm Res 2009;26:492-501.

200. Tong W, Wang L, D'Souza MJ: Evaluation of PLGA microspheres as delivery system for antitumor agent-camptothecin. Drug Dev Ind Pharm 2003;29:745-756.

201. Hussain M, Beale G, Hughes M, Akhtar S: Co-delivery of an antisense oligonucleotide and 5-fluorouracil using sustained release poly (lactide-co-glycolide) microsphere formulations for potential combination therapy in cancer. Int J Pharm 2002;234:129-138.

202. Wang YM, Sato H, Adachi I, Horikoshi I: Preparation and characterization of poly(lactic-co-glycolic acid) microspheres for targeted delivery of a novel anticancer agent, taxol. Chem Pharm Bull (Tokyo) 1996;44:1935-1940.

203. Danhier F, Lecouturier N, Vroman B, Jerome C, Marchand-Brynaert J, Feron O, Preat V: Paclitaxel-loaded PEGylated PLGA-based nanoparticles: in vitro and in vivo evaluation. J Control Release 2009;133:11-17.

204. Yoo HS, Lee KH, Oh JE, Park TG: In vitro and in vivo anti-tumor activities of nanoparticles based on doxorubicin-PLGA conjugates. J Control Release 2000;68:419-431.

205. Elvira C, Gallardo A, Roman JS, Cifuentes A: Covalent polymer-drug conjugates. Molecules 2005;10:114-125.

206. Matsumura Y: Preclinical and clinical studies of anticancer drug-incorporated polymeric micelles. J Drug Target 2007;15:507-517.

207. Aliabadi HM, Lavasanifar A: Polymeric micelles for drug delivery. Expert Opin Drug Deliv 2006;3:139-162.

208. Kwon GK, Forrest ML: Amphiphilic block copolymer micelles for nanoscale drug delivery. Drug Development Research 2006;67:15-22.

209. Stolnik S, Illum L, Davis S: Long circulating microparticulate drug carriers. Adv. Drug Deliv. Rev 1995;16:195-214.

210. Kataoka K, Kwon GS, Yokoyama M, Okano T, Sakurai Y: Block copolymer micelles as vehicles for drug delivery. J. Control. Release 1993;24:119-132.

211. Sutton D, Nasongkla N, Blanco E, Gao J: Functionalized micellar systems for cancer targeted drug delivery. Pharm Res 2007;24:1029-1046.

212. Nishiyama N, Yokoyama M, Aoyaga T, Okano T, Sakurai Y, Kataoka K: Preparation and characterization of self-assembled polymer-metal complex micelle from cis-dichlorodiammineplatinium (II) and poly(ethylene glycole)-poly(aspartic acid) block copolymer in an aqueous medium. Langmuir 1999;15:377-383.

213. Nishiyama N, Okazaki S, Cabral H, Miyamoto M, Kato Y, Sugiyama Y, Nishio K, Matsumura Y, Kataoka K: Novel cisplatin-incorporated polymeric micelles can eradicate solid tumors in mice. Cancer Res 2003;63:8977-8983.

214. Yuan X, Harada A, Yamasaki Y, Kataoka K: Stabilization of lysozyme-incorporated polyion complex micelles by the omega-end derivatization of poly(ethylene glycol)-poly(alpha,beta-aspartic acid) block copolymers with hydrophobic groups. Langmuir 2005;21:2668-2674.

215. Wakebayashi D, Nishiyama N, Itaka K, Miyata K, Yamasaki Y, Harada A, Koyama H, Nagasaki Y, Kataoka K: Polyion complex micelles of pDNA with acetal-poly(ethylene glycol)-poly(2-(dimethylamino)ethyl methacrylate) block copolymer as the gene carrier system: physicochemical properties of micelles relevant to gene transfection efficacy. Biomacromolecules 2004;5:2128-2136.

216. Wakebayashi D, Nishiyama N, Yamasaki Y, Itaka K, Kanayama N, Harada A, Nagasaki Y, Kataoka K: Lactose-conjugated polyion complex micelles incorporating plasmid DNA as a targetable gene vector system: their preparation and gene transfecting efficiency against cultured HepG2 cells. J Control Release 2004;95:653-664.

217. Itaka K, Yamauchi K, Harada A, Nakamura K, Kawaguchi H, Kataoka K: Polyion complex micelles from plasmid DNA and poly(ethylene glycol)-poly(L-lysine) block copolymer as serum-tolerable polyplex system:

physicochemical properties of micelles relevant to gene transfection efficiency. Biomaterials 2003;24:4495-4506.

218. Allen C, Yu Y, Maysinger D, Eisenberg A: Polycaprolactone-b-poly(ethylene oxide) block copolymer micelles as a novel drug delivery vehicle for neurotrophic agents FK506 and L-685,818. Bioconjug Chem 1998;9:564-572.

219. Allen C, Han J, Yu Y, Maysinger D, Eisenberg A: Polycaprolactone-b-poly(ethylene oxide) copolymer micelles as a delivery vehicle for dihydrotestosterone. J Control Release 2000;63:275-286.

220. Kim SY, Shin IG, Lee YM, Cho CS, Sung YK: Methoxy poly(ethylene glycol) and epsilon-caprolactone amphiphilic block copolymeric micelle containing indomethacin. II. Micelle formation and drug release behaviours. J Control Release 1998;51:13-22.

221. Aliabadi HM, Mahmud A, Sharifabadi AD, Lavasanifar A: Micelles of methoxy poly(ethylene oxide)-b-poly(epsilon-caprolactone) as vehicles for the solubilization and controlled delivery of cyclosporine A. J Control Release 2005;104:301-311.

222. Aliabadi HM, Brocks DR, Lavasanifar A: Polymeric micelles for the solubilization and delivery of cyclosporine A: pharmacokinetics and biodistribution. Biomaterials 2005;26:7251-7259.

223. Shi B, Fang C, You XM, Zhang Y, Fu S, PEI YY: Stealth MePEG-PCL micelles: Effects of polymer composition on micelle physicochemical characteristics, in vivo drug release, in vivo pharmacokinetics in rats and

biodistribution in S180 tumor bearing mice. Coll. Polym. Sci 2005;283:954-967.

224. Mahmud A, Xiong X, Lavasanifar A: Novel poly(ethylene oxide)-*block*-poly(e-caprolactone) block copolymers with functional side groups on the polyester block for drug delivery. *Macromolecules* 2006;39:9419-9428.

225. Matsumura Y, Hamaguchi T, Ura T, Muro K, Yamada Y, Shimada Y, Shirao K, Okusaka T, Ueno H, Ikeda M, Watanabe N: Phase I clinical trial and pharmacokinetic evaluation of NK911, a micelle-encapsulated doxorubicin. Br J Cancer 2004;91:1775-1781.

226. Hamaguchi T, Matsumura Y, Suzuki M, Shimizu K, Goda R, Nakamura I, Nakatomi I, Yokoyama M, Kataoka K, Kakizoe T: NK105, a paclitaxel-incorporating micellar nanoparticle formulation, can extend in vivo antitumour activity and reduce the neurotoxicity of paclitaxel. Br J Cancer 2005;92:1240-1246.

227. Uchino H, Matsumura Y, Negishi T, Koizumi F, Hayashi T, Honda T, Nishiyama N, Kataoka K, Naito S, Kakizoe T: Cisplatin-incorporating polymeric micelles (NC-6004) can reduce nephrotoxicity and neurotoxicity of cisplatin in rats. Br J Cancer 2005;93:678-687.

228. Danson S, Ferry D, Alakhov V, Margison J, Kerr D, Jowle D, Brampton M, Halbert G, Ranson M: Phase I dose escalation and pharmacokinetic study of pluronic polymer-bound doxorubicin (SP1049C) in patients with advanced cancer. Br J Cancer 2004;90:2085-2091.

229. Kim TY, Kim DW, Chung JY, Shin SG, Kim SC, Heo DS, Kim NK, Bang YJ: Phase I and pharmacokinetic study of Genexol-PM, a cremophor-free, polymeric micelle-formulated paclitaxel, in patients with advanced malignancies. Clin Cancer Res 2004;10:3708-3716.

230. Kato K, Hamaguchi T, Shirao K, Shimada Y, Yamada Y, Doi T: Phase I study of NK012, polymer micelle SN-38, in patients with advanced cancer. Am Soc Clin Oncol GI 2008:(Abs#485).

231. Burris H, Infante J, Spigel D, Greco F, Thompson D, Matsumoto S: A phase I dose-escalation study of NK012. Am Soc Clin Oncol 2008:(Abs#2538).

Chapter 2

Immunomodulatory and Anticancer Effects of Intra-tumoral Co-Delivery of Synthetic Lipid A Adjuvant and STAT3 Inhibitor, JSI-124

A version of this chapter has been published: Molavi, O., Ma, Z., Hamdy, S., Samuel, J., Lavasanifar, A. Immunomodulatory and anticancer effects of intra-tumoral co-delivery of synthetic lipid A adjuvant and STAT3 inhibitory agent, JSI-124. *Immunopharmacology and Immunotoxicology* 2008 Sep 16: 1-14

2.1 Introduction

During the last decade, several cancer vaccines have shown success in breaking self tolerance and priming immune responses against cancer associated antigens in murine tumor models and in cancer patients [1-3]. However, development of functional anti-tumor immune responses that can lead to effective cancer treatment by vaccination has been hampered in clinical setting in most cases [4]. Defects in trafficking and function of effectors T cells in tumor caused by immunosuppressive environment of the tumor involving tolerogenic DCs and T_{reg} cells is implicated as a major reason behind shortcomings of therapeutic cancer vaccines [5-7]. In this regard, constitutive activation of STAT3 in tumor and immune cells has been identified as one the major mechanisms by which cancer induce the activation of tolerogenic DCs and T_{reg} cells [8].

STAT3 is constitutively active in many types of cancers and plays an important role in tumor progression through the modulation of the genes involved in tumor cell proliferation, survival, angiogenesis, metastasis, and cancer immune evasion [8-10]. Constitutive activation of STAT3 in tumor results in blockade of the production of pro-inflammatory cytokines and induction of immunosuppressive factors. This leads to the generation of p-STAT3 positive tolerogenic DCs which in turn can induce activation of immune suppressive T_{reg} cells. Both tolerogenic DCs and T_{reg} cells mediate the establishment of immunosuppression in tumor environment [8,11,12]. One of the most important immunosuppressive factors induced by constitutive activation of STAT3 in tumor is VEGF [8,13,14]. VEGF is a potent angiogenic factor which has been shown to

inhibit functional maturation of DCs and make a major contribution to tumor induced immunosuppression [8,15,16].

DCs have a determinant role in the induction of tolerance versus immunity [17]. DCs distinguish between self and non-self by recognition of PAMPs through their TLRs [18]. An example of PAMPs is LPS which activate DCs through TLR4 [19]. MPLA is a chemically modified less toxic derivative of LPS that exhibits potent adjuvant activity [20]. Clinical use of MPLA as an adjuvant is supported by a series of preclinical safety investigations in various animals [21]. Following clinical success of MPLA containing vaccine, several other lipid A analogues have been developed. Biomira Inc (now changed its name to Oncothyreon Inc) has developed several synthetic lipid A analogues. One of these compounds is BC1-005 which is called 7-acyl lipid A (Figure 2-1) and is comprised of β-(1 → 6) diglucosamine moiety bearing three identical (*R*)-tetradecanoyl-oxytetradecanoyl residues on the 2, 2′ and 3′ positions and one (*R*)-3-hydroxytetradecanoyl group on 3 position (Figure 2-1). Structurally, this analogue is closer to the natural MPLA [22].

Ligation of TLR4 on DCs has been investigated as a strategy for overcoming the suppressive activity of T_{reg} cells [23]. Blockage of STAT3 in tumor and DCs were subjects of other studies for overcoming immunosuppression involving tolerogenic DCs and T_{reg} cells [8,24]. It has been shown that the maturation of DCs in tumors can be restored with STAT3 inhibition, as evidenced by a decrease in $CD11c^{+}MHC\text{-}II^{low}CD86^{low}$ immature DCs [11]. Moreover inhibition of STAT3 in DCs using a small molecule inhibitor of STAT3, JSI-124

[25] leads to improved function and activation of impaired STAT3-active DCs [24,26]. A previous study from our lab showed that 7-acyl lipid A encapsulated in PLGA NPs stimulates DCs maturation and enhances their ability in activation of T cell [27]. In this study we purpose to test whether delivery of TLR4 ligand, 7-acyl lipid A, encapsulated in PLGA NPs to DCs can reverse the suppressive effects of T_{reg} cells on T cells *in vitro*. Next we investigated the effects of intra-tumoral co-administration of 7-acyl lipid A loaded PLGA NPs and STAT3 inhibitory agent, JSI-124 on the recruitment of T cells to tumor and inhibition of tumor growth in a B16-F10 mouse melanoma tumor model *in vivo*.

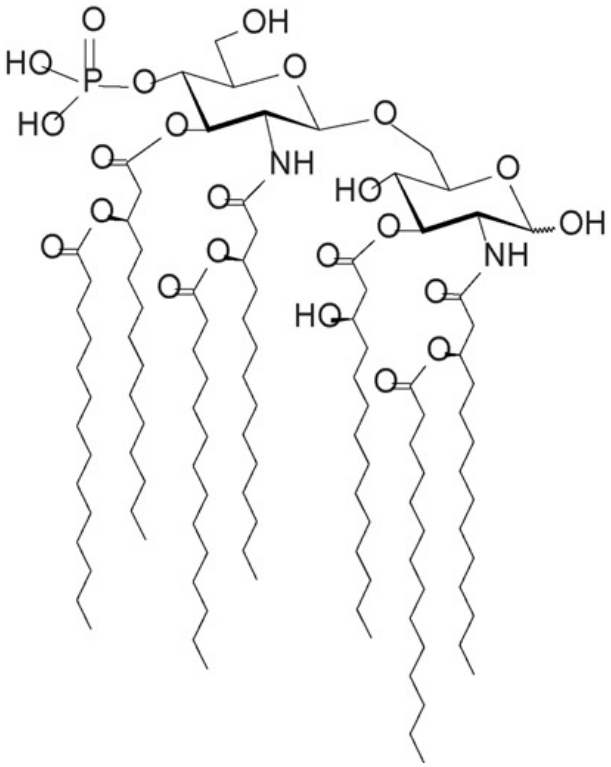

Figure 2-1. Chemical structure of 7-acyl lipid A

2.2 Materials and Methods

2.2.1 Reagents and antibodies

7-Acyl lipid A (BC1-005) was kindly provided by Biomira (now changed its name to Oncothyreon Inc, Edmonton, AB, Canada). Polyvinyl alcohol (PVA), MW. 31–50 KDa and PLGA co-polymer, monomer ratio 50:50, MW. 7 KDa, were purchased from Absorbable Polymers International (Pelham, AL, USA). Recombinant murine Granulocyte Monocyte Colony Stimulating Factor (GM-CSF) was purchased from Peprotech (Rocky Hill, NJ, USA). Murine CD4 and CD25 isolation kits were purchased from StemCell Technologies (Vancouver, BC, Canada). RPMI-1640, L-glutamine, and gentamicin were purchased from Gibco-BRL (Burlington, ON, Canada). Fetal calf serum (FCS) was obtained from Hyclone Laboratories (Logan, UT). JSI-124 was purchased from Calbiochem (San Diego, CA, USA). Fluorescene isothiocyanate (FITC) conjugated anti-mouse CD3 (145-2C11) and purified anti-mouse CD3 Abs, PE-Cy5-conjugated anti-mouse CD8 (53-6.7) and CD4 (H129.19) mAbs, and their respective isotype controls were purchased from E-Bioscience (San Diego, CA, USA).

2.2.2 Mice and tumor cells

C57BL/6 male mice, 6 to 10 weeks old, were purchased from the Jackson Laboratory (Bar Harbor, ME, USA) and maintained under standard conditions. Procedures involving animals and their care were conducted in conformity with the University of Alberta Health Sciences Animal Policy and Welfare Committee.

B16-F10, a melanoma of C57BL/6 origin was obtained from American Type Culture Collection, ATCC.

2.2.3 Preparation and characterization of 7-acyl lipid A loaded PLGA NPs

PLGA NPs containing 7-acyl lipid A were prepared as oil/water single emulsion formulation by the solvent evaporation method. Briefly, 200-2000 μg 7-acyl lipid A in 100 μL of 1:4 methanol:chloroform mixture (v/v) was added to the polymer solution in chloroform (100 mg polymer in 300 μL chloroform). The resulting solution was then emulsified in 2 mL of PVA solution (9%, w/v PVA in PBS) by sonication for 45 s at level 4, using a microtip sonicator (Heat systems Inc., Farmingdale, NY, USA). The emulsion was added into 8 mL of stirring PVA solution in a drop-wise manner. NPs were stirred for 3 h and then collected by centrifugation of the emulsion at 40,000 × g for 10 min at 4 °C. Nanoparticles were washed twice with cold deionized water and lyophilized. The volume mean diameter of the NPs was determined by dynamic light scattering technique using a Zetasizer 3000 (Malvern, UK). The level of 7-acyl lipid A in NPs was measured by a LC-MC method as described earlier [28]. Briefly 7-acyl lipid A was extracted from PLGA NPs by dispersing 10 mg of NPs in 400μL of acetonitrile followed by centrifugation at 15,000×g for 15 min. The supernatant was removed. The residue was then extracted by adding 500μL of 1:4 methanol–chloroform mixture. The sample was centrifuged at 15,000×g for 15 min and the supernatant was assayed for 7-acyl lipid A by LC-MS using aWaters Micromass ZQ 4000 spectrometer, coupled to a Waters 2795 separations module with an autosampler

(Milford, MA, USA). Chromatographic separation was achieved using an Agilent Technologies (Palo Alto, CA, USA) Zorbax eclipse XDB C8 3.5 μm (2.1 mm × 50 mm) as the stationary phase. The mobile phase was consisting of 2 solutions; *Solution A* is 0.1% glacial acetic acid, 0.1% triethylamine in methanol and *Solution B* is 0.1% glacial acetic acid, 0.1% triethylamine, 10% methanol in tetrahydrofuran (THF). The mobile phases were delivered at a constant flow rate of 0.2 ml/min. Asp-PET lipid A (another synthetic lipid A derivative) was used as an internal standard (I.S). The mass spectrometer was operated in negative ionization mode with selected ion recording (SIR) acquisition. SIR at *m*/*z* 1955.5 and 1698.2, related to M-H were selected for quantification of 7-acyl lipid A and the internal standard, respectively.

2.2.4 Preparation of murine bone marrow derived DCs

DC primary cultures were generated from murine bone marrow precursors from femurs of C57BL/6 mice in complete media in the presence of GM-CSF as described previously [29]. Briefly, femurs were removed and purified from the surrounding muscle tissue. Then intact bones were left in 70% ethanol for 2 min for disinfection, washed with PBS and both ends were cut with scissors, and the marrow flushed with PBS using a syringe with a 0.45-mm diameter needle. After one wash in PBS, about 1-1.5 × 10^7 leukocytes were obtained per femur. Cell culture medium was RPMI-1640 supplemented with gentamicin (80 μg/mL), L-glutamine (2 mM), and 10% heat-inactivated FCS. At day 0, bone marrow leukocytes were seeded at 2 × 10^6 per 100 mm dish in 10 mL complete medium

containing 20 ng/mL GM-CSF. At day 3, another 10 mL complete medium containing 20 ng/mL GM-CSF were added to the plates. At day 6, half of the culture supernatant was collected, centrifuged, and the cell pellet resuspended in 10 mL fresh medium containing 20 ng/mL GM-CSF, and given back into the original plate. At day 7 cells can be used. The purity of the DC population on day 7 was found to be between 70 and 75% based on the expression of CD11c on the semi-adherent and non-adherent cell populations.

2.2.5 T cell proliferation assays / T_{reg} cells suppression assays

$CD4^+$ T cells were purified from total splenocytes of C57BL/6 normal mice using mouse $CD4^+$ T cells enrichment cocktail (stem cell technologies), then $CD4^+CD25^+$ T_{reg} cells were isolated from $CD4^+$ T cell population by PE positive selection cocktail (stem cell technologies) according to the instructions of the manufacturer. Both $CD4^+CD25^-$ and $CD4^+CD25^+$ subsets of T cells were characterized with respect to cell surface markers using flow cytometry. To establish T cell proliferation/T_{reg} suppression assay, 100,000 $CD4^+CD25^-$ was stimulated with anti-CD3 mAb (20 ng/mL) in the presence of different numbers of $CD4^+CD25^+$ T_{reg} cells (25,000, 50,000, and 100,000). To evaluate the effect of PLGA NPs delivery of 7-acyl lipid A on the suppressive effects of T_{reg} cells on T cell proliferation *in vitro*, mouse bone marrow originated DCs on day 6 were treated with 0.1 μg/mL LPS or 7-acyl lipid A either soluble or encapsulated in 1 mg of PLGA NPs and incubated for 24 hours at 37°C . Then untreated and treated DCs were irradiated with 3000 rads X-ray, washed and resuspended in their own

culture media (collected from the culture of DCs on day 7) and co-cultured with $CD4^+CD25^-$ T cells (5000 DCs with 100,000 T cells, 1:20 ratio) in the presence and absence 100,000 $CD4^+CD25^+$ T_{reg} cells (1:1) in flat-bottom 96-well plates for 60 hours. Anti CD3 Ab was added to the culture at the concentration of 20 ng/mL. Proliferation of T cells was determined by incorporation of ^3H for the last 24 hours of the culture.

2.2.6 Tumor cell implantation and treatment

C57BL/6 mice were injected subcutaneously (s.c) at their left flank with 1×10^6 B16-F10 melanoma cells. Tumors were allowed to grow until they became palpable (7 days after tumor implantation), then animals were randomly assigned to four groups and received daily intra-tumoral injection of either of the followings for 8 days; 50 μL phosphate buffered saline (PBS), 154 mM NaCl, 1.9 mM NaH_2PO_4, 8.1 mM Na_2HPO_4, pH 7.3) containing 20% ethanol (PBS group) and 7-acyl lipid A encapsulated in PLGA NPs (10 mg NPs containing ~ 15 μg 7-acyl lipid A was suspended in 50 μL) and/or 1 mg/kg JSI-124 (soluble in PBS containing 20% ethanol). Tumor size was measured during treatment twice a week by vernier caliper and tumor volume (mm^3) was calculated using the following equation: Tumor volume = (longer diameter) x $(\text{shorter diameter})^2/2$.

T2.2.7 FTlow cytometric analysis

After 8 days treatment (on day 15 after tumor implantation) tumor-bearing animals were sacrificed, tumors were collected, weighed and an equal amount of

tumor from each group was homogenized by mechanical dispersion using frosted slides to a cell suspension in a flow cytometry buffer (PBS with 5% fetal bovine serum (FBS)). The supernatant of the tumor cells after filtering through 70 μm cell strainers (BD Biosceinces, Mississauga, Ontario, Canada) were stained with appropriate fluorescence conjugated Abs or their respective isotype controls and incubated for 30 min at 4°C. All samples were acquired on a Becton-Dickinson TFlow cytometer and analyzed by Cell-Quest software. For analysis of immune cells in tumors, forward scatter gain was set at E00, and the mononuclear population was gated. The percentage of the immune cells which were expressing the markers of interest in the gated population of the whole cell suspension was acquired from flow cytometry.

2.2.8 Statistical analysis

The significance of differences among groups was analyzed by one-way analysis of variance (ANOVA) followed by the Student-Newman-Keuls post hoc test for multiple comparisons. Before executing the ANOVA, data were tested for normality and equal variance. If neither of the latter criteria were met, data were compared using a Kruskal-Wallis one-way ANOVA on ranks. A P value of ≤ 0.05 was set for the significance of difference among groups. The statistical analysis was performed with SigmaStat software (Systat Software Inc. San Jose, California, USA).

2.3 Results

2.3.1 The effects of PLGA-NP delivery of 7-acyl lipid A to DCs on suppressive effects of T_{reg} cells on T cells *in vitro*

T cell proliferation/T_{reg} suppression assay was established by co-culturing DCs with $CD4^+CD25^-$ naïve T cells in the presence of 20 ng/mL anti-CD3 Ab, and indicated number of $CD4^+CD25^+$ T_{reg} (Figure 2-2A). DCs were either left untreated or treated with soluble or PLGA-NP loaded 7-acyl lipid A for 24 h, and then co-cultured with $CD4^+CD25^-$ naïve T cells in the presence and absence of $CD4^+CD25^+$ T_{reg} cells. As it has been shown in Figure 2-2B, in comparison with untreated DCs and DCs treated with soluble 7-acyl lipid A, DCs loaded with PLGA NPs containing 7-acyl lipid A strongly stimulated the proliferation of $CD4^+CD25^-$ naïve T cells in the absence of CD4+CD25+ T_{reg} cells. In the presence of T_{reg} cells, although the proliferation of T cells stimulated by DCs treated with 7-acyl lipid A encapsulated in PLGA NPs was lower than that in the absence of T_{reg} cells; the level of T cell proliferation was still significantly higher than what observed with untreated DCs or DCs treated with soluble 7-acyl lipid A in the presence of T_{reg} cells ($P<0.01$) (Figure 2-2B). Our *in vitro* findings showed a potential for 7-acyl lipid A encapsulated in PLGA NPs in strong stimulation of T cell proliferation. However PLGA NPs delivery of 7-acyl lipid A to DCs was unable to reduce the suppressive effects of T_{reg} cells on T cell proliferation *in vitro.*

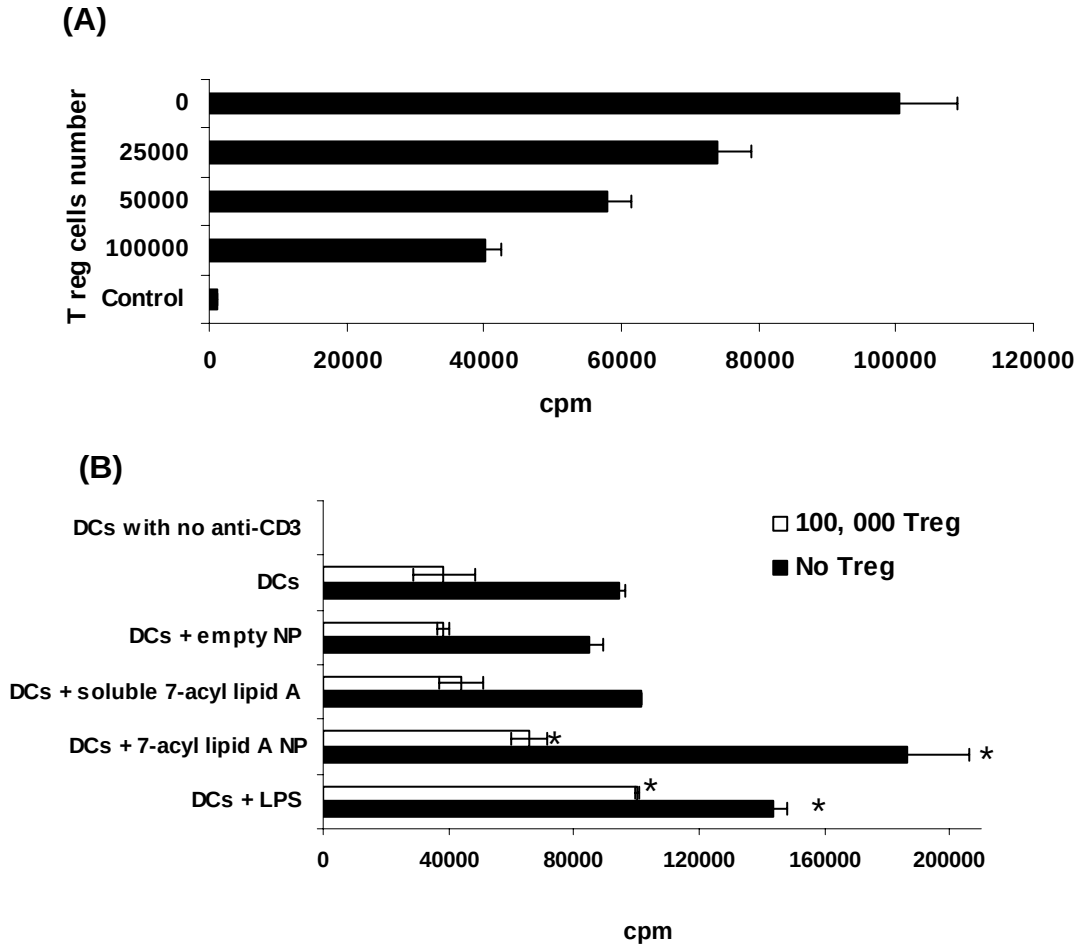

Figure 2-2. The effect of PLGA-NP delivery of 7-acyl lipid A to DCs on suppressive effects of T_{reg} cells on T cell proliferation, *in vitro*. $CD4^+CD25^-$ and $CD4^+CD25^+$ subsets of T cells were purified from total splenocytes of C57BL/6 normal mice and co-cultured with mouse bone marrow originated DCs A) treated with 20 ng/mL anti-CD3 Ab; B) treated with 20 ng/mL anti-CD3 Ab in combination with either of the following; empty PLGA NPs, 0.1 μg/ml LPS, 20 μg 7-acyl lipid A either soluble or encapsulated in 1 mg of PLGA NPs (for 24 h at 37°C) in flat-bottom 96-well plates for 60 hours. Proliferation of T cells was determined by incorporation of ^3H for the last 24 hours of the culture. *Significantly different from T cells stimulated with anit-CD3 Ab and untreated or empty NPs treated DCs in the presence of T_{reg} cells (n=3)

2.3.2 The effects of intra-tumoral delivery of JSI-124 and 7-acyl lipid A on the recruitment of T cells to B16-F10 tumors *in vivo*

Next we purpose to test whether intra-tumoral PLGA-NP delivery of 7-acyl lipid A alone or in combination with a STAT3 inhibitory agent, JSI-124, can induce the activation and recruitment of T cells to B16-F10 tumor harboring hyperactive STAT3, *in vivo*. Intra-tumoral delivery of either 7-acyl lipid A NPs or JSI-124 resulted in only 3-9 fold increases in the percentage of $CD4^+$ T cells, co-administration of 7-acyl lipid A NPs and JSI-124 resulted in a 58 fold increase in the percentage of these cells (Figure 2-3). Intra-tumoral delivery of 7-acyil lipid A encapsulated in PLGA NPs in combination with JSI-124 also resulted in a remarkable increase (31 fold) in the percentage of $CD8^+$ T cells in B16-F10 tumors whereas only 3-8 fold increases in the percentage of $CD8^+$ T cells was observed in tumors injected with either 7-acyl lipid A loaded PLGA NPs or JSI-124 alone (Figure 2-3).

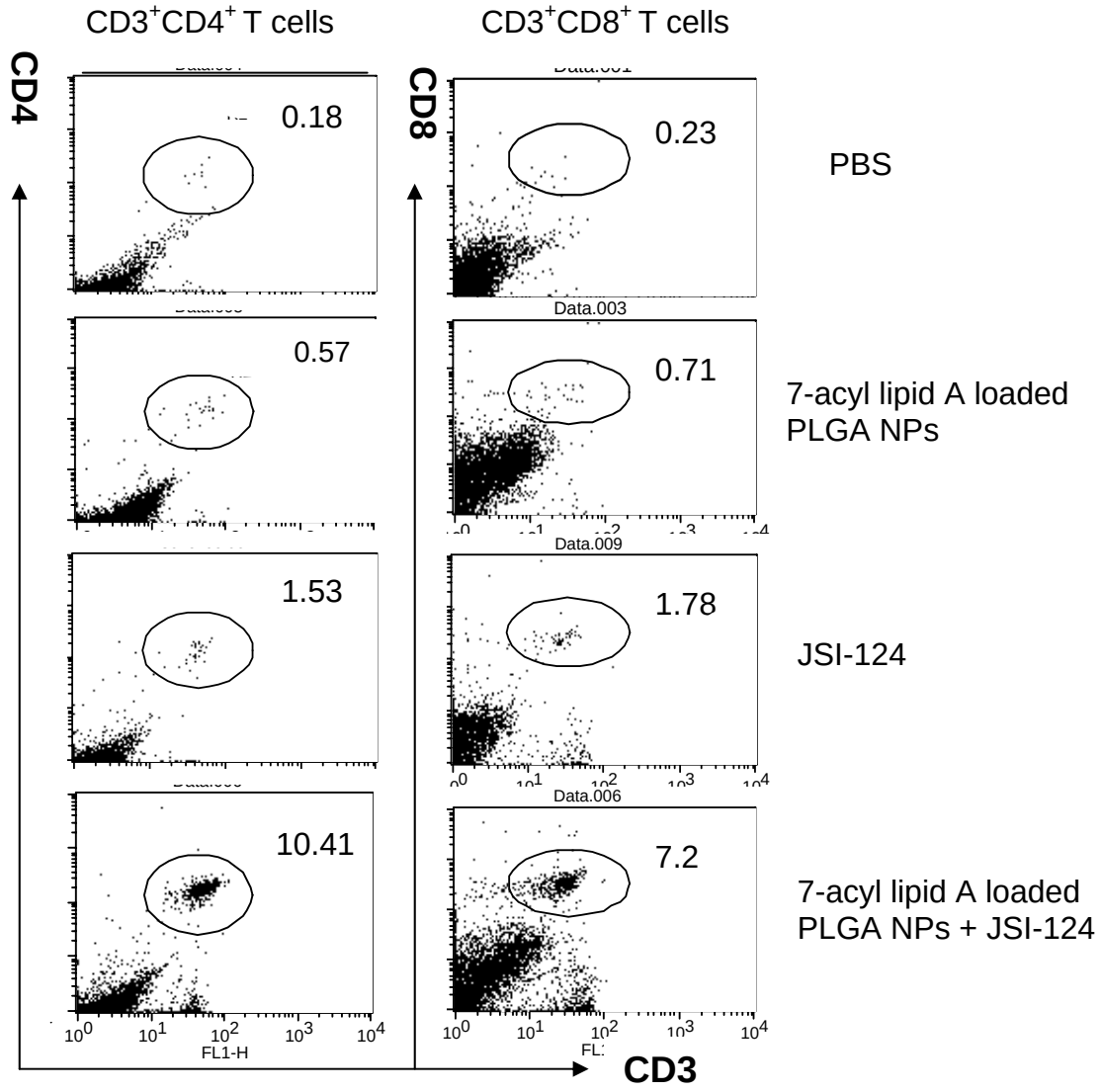

Figure 2-3. Recruitment of $CD4^+$ and $CD8^+$ T cells into tumors following treatment with 7-acyl lipid A loaded PLGA NPs and/or JSI-124. Following 8 days intra-tumoral injection of either of PBS containing 20 % ethanol (PBS group); 7-acyl lipid A loaded PLGA NPs; JSI-124; or JSI-124 + 7-acyl lipid A loaded PLGA NPs; tumors were isolated and analyzed for T cell surface markers using flow cytometry. The percentage $CD3^+$ $CD4^+$ and $CD3^+$ $CD8^+$ T cells in 0.4 g of tumors collected from the mice were acquired from flow cytometry. The data represent one out of two independent experiments which showed similar results (n=5 per group in each experiment).

2.3.3 Anti-tumor effects of 7-acyl lipid A loaded PLGA NPs and JSI-124 in a B16-F10 mouse melanoma tumor model *in vivo*

The anticancer activity of 7-acyl lipid A NPs + JSI-124 combination therapy in comparison with 7-acyl lipid A NPs and JSI-124 monotherapy groups in B16-F10 tumor-bearing mice was then evaluated. As shown in Figure 2-4A, the average tumor size increased rapidly in the PBS group and the mice that received 7-acyl lipid A loaded PLGA NPs. Tumor volume reached over 1,400 mm^3 after 15 days of tumor implantation in these groups. However, daily intra-tumoral injection of 1 mg/kg JSI-124 alone or in combination with 20 μg 7-acyl lipid A encapsulated in PLGA NPs efficiently inhibited tumor growth as compared to the PBS group or 7-acyl lipid A loaded PLGA NPs injected tumors ($P<0.001$) (Figure 2-4A). The average tumor volume on day 10-15 after tumor implantation in the mice that received combination therapy was found to be significantly lower than that in JSI-124 group at the same period (63-103 mm^3 in 7-acyl lipid A + JSI-124 versus 160-300 mm^3 in JSI-124 group) ($P<0.05$) (Figure 2-4A). Consistent with these data, the average tumor weight after 8 days of treatment with either JSI-124 (0.26 gram) or 7-acyl lipid A loaded PLGA NPs + JSI-124 (0.13 gram) was significantly lower than that of the PBS group (0.97 gram) and 7-acyl lipid A NP-injected tumors (0.93 gram) ($P<0.001$) (Figure 2-4B).

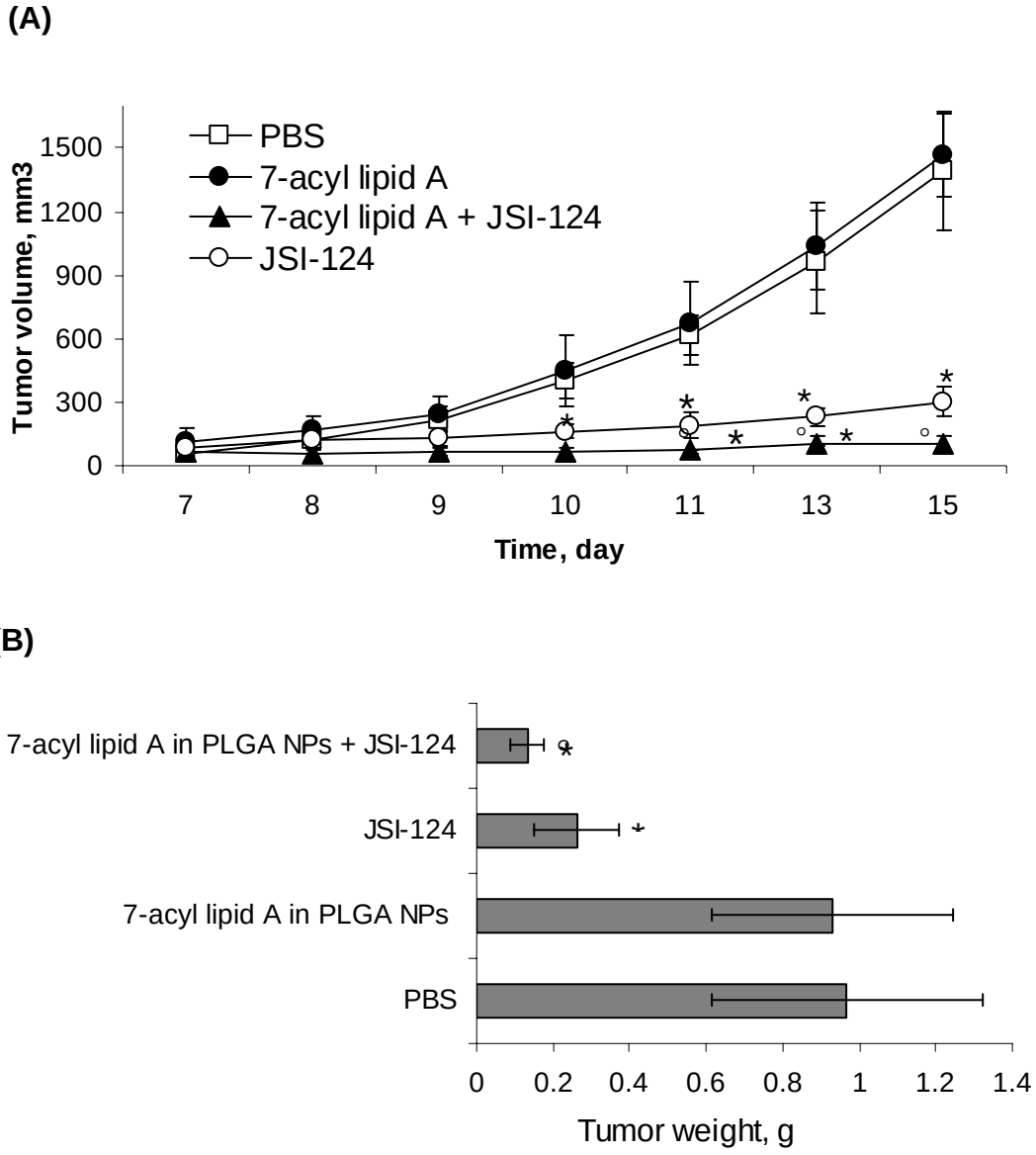

Figure 2-4. Anticancer activity of 7-acyl lipid A loaded PLGA NPs + JSI-124 combination therapy *in vivo*. On day 7 after tumor implantation, the mice were assigned to four groups, treated intra-tumorally with either PBS containing 20 % ethanol (PBS group); 20 μg 7-acyl lipid A encapsulated in 1 mg PLGA NPs, 1 mg/kg JSI-124 or the same doses of 7-acyl lipid A loaded PLGA NPs + JSI-124, and monitored for tumor growth. A) Average tumor volume in animals (n=5-8, mean ± SE); B) Average tumor weight on day 15 after tumor cell injection (n=5, mean ± SD); *significantly different from PBS and 7-acyl lipid A groups ($P<0.001$), °significantly different from tumors injected with JSI-124 ($P<0.05$).

2.4 Discussion

Ligation of DCs through their TLR4 receptor has been investigated as a strategy for the reversal of the suppressive effects of T_{reg} cells on T cell proliferation [23]. Previous studies have shown that PLGA-NP delivery of 7-acyl lipid A induces maturation and activation of DCs, characterized by the up-regulation of CD40, CD86 and pro-inflammatory cytokines, and enhances their capability to stimulate T cells, *in vitro* [27,28]. Consistent with these results, we showed that the level of T cell proliferation stimulated by DCs treated with 7-acyl lipid A loaded PLGA NPs, was two times higher than that by DCs treated with soluble 7-acyl lipid A or empty PLGA NPs. Others have shown that activation of DCs through their TLR4 receptor by LPS can reverse the suppressive effects of T_{reg} cells on T cells [23]. Herein we have shown that DCs treated with PLGA NPs of 7-acyl lipid A strongly stimulate T cell proliferation *in vitro* but they were unable to significantly reduce the suppressive effects of T_{reg} cells on T cell proliferation when they were co-cultured with T cells in the presence of T_{reg} cells.

Accumulating evidence shows that the recruitment of immune cells in tumor is limited due to the existence of an immunosuppressive tumor environment [7,8]. STAT3 has been identified as one of the important mediators of tumor-induced immunosuppression [8]. Specifically, activation of STAT3 in DCs, often triggered by tumor cell-derived immunosuppressive factors (such as VEGF), inhibits the functional maturation of DCs [8,15,16]. Therefore we hypothesized that the activation of DCs through their TLR4 by 7-acyl lipid A encapsulated in PLGA NPs in an STAT3 inhibited environment (induced by JSI-124) can change

the tumor immunosuppressive environment and increase T cell trafficking and function in tumor. In support of our hypothesis, we found a significantly higher percentage of $CD4^+$ and $CD8^+$ T cells in tumors that received 7-acyl lipid A loaded PLGA NPs + JSI-124 as compared with tumors receiving PBS or monotherapy (either 7-acyl lipid A loaded PLGA NPs or JSI-124 alone). Treatment of tumors with JSI-124 alone also significantly enhanced the trafficking of T cells in tumor as compared with control group that received PBS. These observations are in line with the results of previous studies that have shown blocking STAT3 in STAT3-active tumor cells leads to the secretion of soluble factors stimulating lymphocyte migration *in vitro* [30]. By immunohistochemistry, it also has been shown that STAT3 inhibition in B16-F10 tumors results in an increase in tumor infiltration by T cells, *in vivo*, although the immunophenotype of these T-cells was not further characterized [11]. These observations are of great significance since inadequate trafficking of immune effector cells in tumors is considered as one of the major barriers to effective cancer immunotherapy [7].

Several studies have shown that increased tumor infiltration by immune effector cells is associated with an improved therapeutic outcome in cancer patients [31-34]. The synergistic anti-tumor effects of the combination therapy, as observed in the current set of data, may also stem from significant increase in the percentage of tumor infiltrated $CD4^+$ and $CD8^+$ T cells. However, further studies are required to explain the exact mechanisms by which combination therapy generates synergistic anti-tumor effects. Consistent with previous studies, we observed a significant anticancer activity after JSI-124 monotherapy. This can be

related to direct inhibitory effects of JSI-124 on tumor growth as well as its indirect effects, which are associated with immune-mediated mechanisms [25,35]. With respect to the well-documented role of VEGF in tumor angiogenesis and cancer immune evasion, an important part of JSI-124 anticancer effects can be generated by inhibition of cancer angiogenesis and restoring the function of DCs as reported in the previous studies [24,26]. Intra-tumoral injection of 7-acyl lipid A loaded PLGA NPs appear not to have any anticancer activity. More recent studies have found that TLR4 is also expressed on some type of cancer cells including mouse B16-F10 melanoma and their ligation can induce anti-apoptotic pathways in cancer cells [36]. Based on these findings, the concomitant anti-apoptotic effects of 7-acyl lipid A on tumor cells through their TLR4 receptor could mask the anti-tumor effects of 7-acyl lipid A resulting from its immunomodulatory effects. Thus further studies are needed to improve the ability PLGA NPs for specific and selective delivery of 7-acyl lipid A to DCs thus avoiding its undesirable direct effects on tumor cells.

In conclusion, we have shown that DCs activated through their TLR4 by 7-acyl lipid A loaded PLGA NPs strongly stimulate T cell proliferation *in vitro*. Importantly, we found that intra-tumoral delivery of 7-acyl lipid A encapsulated in PLGA NPs in combination with a STAT3 inhibitor, JSI-124, significantly induces the trafficking/proliferation of T cell in tumors and results in superior anti-tumor effects, *in vivo*.

2.5 References

1. Morse MA, Chui S, Hobeika A, Lyerly HK, Clay T: Recent developments in therapeutic cancer vaccines. Nat Clin Pract Oncol 2005;2:108-113.
2. Samuel J, Budzynski WA, Reddish MA, Ding L, Zimmermann GL, Krantz MJ, Koganty RR, Longenecker BM: Immunogenicity and antitumor activity of a liposomal MUC1 peptide-based vaccine. Int J Cancer 1998;75:295-302.
3. Acres B, Paul S, Haegel-Kronenberger H, Calmels B, Squiban P: Therapeutic cancer vaccines. Curr Opin Mol Ther 2004;6:40-47.
4. Rosenberg SA, Yang JC, Restifo NP: Cancer immunotherapy: moving beyond current vaccines. Nat Med 2004;10:909-915.
5. Neeson P, Paterson Y: Effects of the tumor microenvironment on the efficacy of tumor immunotherapy. Immunol Invest 2006;35:359-394.
6. Muller AJ, Scherle PA: Targeting the mechanisms of tumoral immune tolerance with small-molecule inhibitors. Nat Rev Cancer 2006;6:613-625.
7. Chen Q, Wang WC, Evans SS: Tumor microvasculature as a barrier to antitumor immunity. Cancer Immunol Immunother 2003;52:670-679.
8. Yu H, Kortylewski M, Pardoll D: Crosstalk between cancer and immune cells: role of STAT3 in the tumour microenvironment. Nat Rev Immunol 2007;7:41-51.
9. Yu H, Jove R: The STATs of cancer--new molecular targets come of age. Nat Rev Cancer 2004;4:97-105.

10. Kortylewski M, Jove R, Yu H: Targeting STAT3 affects melanoma on multiple fronts. Cancer Metastasis Rev 2005;24:315-327.

11. Wang T, Niu G, Kortylewski M, Burdelya L, Shain K, Zhang S, Bhattacharya R, Gabrilovich D, Heller R, Coppola D, Dalton W, Jove R, Pardoll D, Yu H: Regulation of the innate and adaptive immune responses by Stat-3 signaling in tumor cells. Nat Med 2004;10:48-54.

12. Kortylewski M, Kujawski M, Wang T, Wei S, Zhang S, Pilon-Thomas S, Niu G, Kay H, Mule J, Kerr WG, Jove R, Pardoll D, Yu H: Inhibiting Stat3 signaling in the hematopoietic system elicits multicomponent antitumor immunity. Nat Med 2005;11:1314-1321.

13. Jung JE, Lee HG, Cho IH, Chung DH, Yoon SH, Yang YM, Lee JW, Choi S, Park JW, Ye SK, Chung MH: STAT3 is a potential modulator of HIF-1-mediated VEGF expression in human renal carcinoma cells. Faseb J 2005;19:1296-1298.

14. Srivastava K, Kundumani-Sridharan V, Zhang B, Bajpai AK, Rao GN: 15(S)-hydroxyeicosatetraenoic acid-induced angiogenesis requires STAT3-dependent expression of VEGF. Cancer Res 2007;67:4328-4336.

15. Laxmanan S, Robertson SW, Wang E, Lau JS, Briscoe DM, Mukhopadhyay D: Vascular endothelial growth factor impairs the functional ability of dendritic cells through Id pathways. Biochem Biophys Res Commun 2005;334:193-198.

16. Mimura K, Kono K, Takahashi A, Kawaguchi Y, Fujii H: Vascular endothelial growth factor inhibits the function of human mature dendritic

cells mediated by VEGF receptor-2. Cancer Immunol Immunother 2007;56:761-770.

17. Dhodapkar MV, Dhodapkar KM, Palucka AK: Interactions of tumor cells with dendritic cells: balancing immunity and tolerance. Cell Death Differ 2008;15:39-50.

18. van Duin D, Medzhitov R, Shaw AC: Triggering TLR signaling in vaccination. Trends Immunol 2006;27:49-55.

19. Lu YC, Yeh WC, Ohashi PS: LPS/TLR4 signal transduction pathway. Cytokine 2008;42:145-151.

20. Takayama K, Ribi E, Cantrell JL: Isolation of a nontoxic lipid A fraction containing tumor regression activity. Cancer Res 1981;41:2654-2657.

21. Baldrick P, Richardson D, Elliott G, Wheeler AW: Safety evaluation of monophosphoryl lipid A (MPL): an immunostimulatory adjuvant. Regul Toxicol Pharmacol 2002;35:398-413.

22. Jiang ZH, Budzynski WA, Qiu D, Yalamati D, Koganty RR: Monophosphoryl lipid A analogues with varying 3-O-substitution: synthesis and potent adjuvant activity. Carbohydr Res 2007;342:784-796.

23. Pasare C, Medzhitov R: Toll pathway-dependent blockade of CD4+CD25+ T cell-mediated suppression by dendritic cells. Science 2003;299:1033-1036.

24. Nefedova Y, Cheng P, Gilkes D, Blaskovich M, Beg AA, Sebti SM, Gabrilovich DI: Activation of dendritic cells via inhibition of Jak2/STAT3 signaling. J Immunol 2005;175:4338-4346.

25. Blaskovich MA, Sun J, Cantor A, Turkson J, Jove R, Sebti SM: Discovery of JSI-124 (cucurbitacin I), a selective Janus kinase/signal transducer and activator of transcription 3 signaling pathway inhibitor with potent antitumor activity against human and murine cancer cells in mice. Cancer Res 2003;63:1270-1279.

26. Nefedova Y, Nagaraj S, Rosenbauer A, Muro-Cacho C, Sebti SM, Gabrilovich DI: Regulation of dendritic cell differentiation and antitumor immune response in cancer by pharmacologic-selective inhibition of the janus-activated kinase 2/signal transducers and activators of transcription 3 pathway. Cancer Res 2005;65:9525-9535.

27. Hamdy S, Elamanchili P, Alshamsan A, Molavi O, Satou T, Samuel J: Enhanced antigen-specific primary CD4+ and CD8+ responses by codelivery of ovalbumin and toll-like receptor ligand monophosphoryl lipid A in poly(D,L-lactic-co-glycolic acid) nanoparticles. J Biomed Mater Res A 2007;81:652-662.

28. Hamdy S, Haddadi A, Somayaji V, Ruan D, Samuel J: Pharmaceutical analysis of synthetic lipid A-based vaccine adjuvants in poly (D,L-lactic-co-glycolic acid) nanoparticle formulations. J Pharm Biomed Anal 2007;44:914-923.

29. Lutz MB, Kukutsch N, Ogilvie AL, Rossner S, Koch F, Romani N, Schuler G: An advanced culture method for generating large quantities of highly pure dendritic cells from mouse bone marrow. J Immunol Methods 1999;223:77-92.

30. Burdelya L, Kujawski M, Niu G, Zhong B, Wang T, Zhang S, Kortylewski M, Shain K, Kay H, Djeu J, Dalton W, Pardoll D, Wei S, Yu H: Stat3 activity in melanoma cells affects migration of immune effector cells and nitric oxide-mediated antitumor effects. J Immunol 2005;174:3925-3931.

31. Blattman JN, Greenberg PD: Cancer immunotherapy: a treatment for the masses. Science 2004;305:200-205.

32. Naito Y, Saito K, Shiiba K, Ohuchi A, Saigenji K, Nagura H, Ohtani H: CD8+ T cells infiltrated within cancer cell nests as a prognostic factor in human colorectal cancer. Cancer Res 1998;58:3491-3494.

33. Zhang L, Conejo-Garcia JR, Katsaros D, Gimotty PA, Massobrio M, Regnani G, Makrigiannakis A, Gray H, Schlienger K, Liebman MN, Rubin SC, Coukos G: Intratumoral T cells, recurrence, and survival in epithelial ovarian cancer. N Engl J Med 2003;348:203-213.

34. Piersma SJ, Jordanova ES, van Poelgeest MI, Kwappenberg KM, van der Hulst JM, Drijfhout JW, Melief CJ, Kenter GG, Fleuren GJ, Offringa R, van der Burg SH: High number of intraepithelial CD8+ tumor-infiltrating lymphocytes is associated with the absence of lymph node metastases in patients with large early-stage cervical cancer. Cancer Res 2007;67:354-361.

35. Molavi O, Ma Z, Mahmud A, Alshamsan A, Samuel J, Lai R, Kwon GS, Lavasanifar A: Polymeric micelles for the solubilization and delivery of

STAT3 inhibitor cucurbitacins in solid tumors. Int J Pharm 2008;347:118-127.

36. Huang B, Zhao J, Unkeless JC, Feng ZH, Xiong H: TLR signaling by tumor and immune cells: a double-edged sword. Oncogene 2008;27:218-224.

Chapter 3

Synergistic anti-tumor effects of CpG oligodeoxynucleotide and STAT3 inhibitory agent JSI-124 in a mouse melanoma tumor model

---

A version of this chapter has been published: Molavi, O., Ma, Z., Hamdy, S., Samuel, J., Lai, R., Lavasanifar, A. Synergistic anti-tumor effects of CpG oligodeoxynucleotide and STAT3 inhibitory agent JSI-124 in a mouse melanoma tumor model. *Immunology & Cell Biology*, 86(6):506-14, 2008

3.1 Introduction

Active immunotherapy of cancer using cancer vaccines offers an attractive therapeutic approach for cancer treatment due to their capability in delivering treatment of high specificity, low toxicity, and prolonged activity [1,2]. While specific anti-tumor T cell responses often can be induced by vaccination, effective eradication of established tumors in murine models or patients is rarely seen [3]. Accumulating evidence suggests that the limited success of this approach may be linked to the frequent existence of an immunosuppressive microenvironment within tumors, as evidenced by the presence of dysfunctional tumor-infiltrating immune effector cells [4]. Recent studies of tumor–host interactions have led to the identification of important molecules that contribute to this tumor-induced immunosuppression and dominant tolerogenic state. One of these molecules is STAT3. In addition to its oncogenic effects on cell proliferation, angiogenesis and metastasis, STAT3 plays an important role in establishing the intra-tumoral immunosuppressive state by blocking the secretion of various pro-inflammatory mediators and increasing that of immunosuppressive factors [5]. These changes are believed to inhibit the recruitment and functions of various immune cell types. Much attention has been given recently to DCs which play key roles in the initiation of anti-tumor immune responses. It has been postulated that several tumor-derived immunosuppressive factors, including VEGF and IL-10, activate STAT3 in DCs and other immune cells, rendering them immunosuppressive or dysfunctional [5-8]. Moreover, the lack of pro-inflammatory factors results in the activation of tolerogenic DCs [9] which can be further inhibited from becoming

mature effective DCs through up-regulation of STAT3 induced by tumor-secreted immunosuppressive factors [10,11]. Tolerogenic DCs not only are unable to initiate anti-tumor immunity, but they induce activation of T_{reg} cells which further inhibit the function of DCs and effector T cells [5,10,11].

In view of these concepts, blockade of STAT3 activation in DCs has been suggested as a strategy for enhancing the effectiveness of cancer immunotherapy. It has been shown that the maturation of DCs in tumors can be restored with STAT3 inhibition, as evidenced by a decrease in $CD11c^{+}MHC\text{-}II^{low}CD86^{low}$ immature DCs [8]. Moreover inhibition of STAT3 in DCs using a small molecule inhibitor of STAT3, JSI-124, [12] leads to improved function and activation of impaired STAT3-active DCs [13,14]. Another approach for enhancing the efficacy of cancer immunotherapy is to stimulate DCs through TLRs. Among 10 different TLRs, TLR9 of plasmacytoid DCs and B cells recognize ODNs with unmethylated CpG motifs (CpG) [15]. Although TLR9 has been also shown to be expressed in mouse but not human myeloid DCs [16,17], recent studies suggest CpG ODNs as a potential immunostimulatory agent of human myeloid DCs [18-20]. CpG ODNs are potent stimulators of both innate (i.e. NK cells and macrophages) and adaptive immunologic responses [21]. CpG ODNs are well recognized for the induction of Th1 responses [21] and accumulating evidence in experimental animals shows their anti-tumor activity against different types of tumors in both preventive and therapeutic settings [22]. Given the potent Th1 adjuvant properties and anticancer activity of CpG ODNs, they have been introduced into various clinical trials and are currently being tested in phase II and

phase III human clinical trials as adjuvants to cancer vaccines and in combination with other therapies [23].

Considering the importance of DCs in mounting effective anti-tumor effects, and the role of STAT3 activation in rendering DCs ineffective, we hypothesized that the combination of DC activation induced by CpG and STAT3 inhibition induced by JSI-124 may result in synergistic anti-tumor effects. To test this hypothesis, we compared the tumor suppressive effects achieved by CpG alone, JSI-124 alone and the combination of CpG + JSI-124, in a mouse melanoma model. We believe that our findings provide the proof-of-principle of employing the combination of CpG-induced DC activation and STAT3 inhibition in cancer immunotherapy.

3.2 Material and Methods

3.2.1 Materials

JSI-124 was purchased from Calbiochem (San Diego, CA, USA). CpG (unmethylated CpG dinucleotides, ODN#1826) was obtained from InvivoGen (San Diego, CA, USA). Murine IL-2, IFN-γ, TGF-β and TNF-α, ELISA (enzyme-linked immunosorbent assay) kits, FITC conjugated anti-mouse CD3 (145-2C11) and CD86 (B7-2)(GL7) mAbs, Phycoerythrin (PE) conjugated anti-mouse NK1.1 (PK136), CD11a (M17/4), CD69 (H1.2F3) and MHC II (M5/114.15.2) mAbs, PE-Cy5-conjugated anti-mouse CD8 (53-6.7), CD4 (H129.19) and CD11c (N418) mAbs, their respective isotype controls, and a mouse T_{reg} cell staining kit were purchased from E-Bioscience (San Diego, CA, USA). Murine IL-12 ELISA and

AnnexinV-FITC/PI apoptosis kits were purchased from BD Biosciences (Mississauga, ON, Canada). Mouse VEGF ELISA kit was from R&D systems, Inc (Minneapolis, USA). Anti-p-STAT3 antibody was purchased from Cell Signaling technology, Inc. (Danvers, MA, USA). Protease inhibitor and Sigma 104 phosphatase substrate were obtained from Sigma-Aldrich (Ontario-Canada).

3.2.2 Mice and tumor cells

C57BL/6 male mice, 6 to 10 weeks old, were purchased from the Jackson Laboratory (Bar Harbor, ME, USA) and maintained under standard conditions. Procedures involving animals and their care were conducted in conformity with the University of Alberta Health Sciences Animal Policy and Welfare Committee. B16-F10, a melanoma of C57BL/6 origin was obtained from ATCC.

3.2.3 Tumor cell implantation and treatment

A total of 80 C57BL/6 mice were injected subcutaneously (s.c) at their left flank with 1×10^6 B16-F10 melanoma cells. Tumors were allowed to grow until they became palpable (7 days after tumor implantation) then animals were randomly assigned to four groups (20 mice per group) and received daily intra-tumoral treatments for 8 days as following. Control mice received 50 μL PBS containing 20% ethanol (PBS group) and experimental groups received 1 mg/Kg JSI-124 (soluble in 50 μL PBS with 20% ethanol) and/or 10 μg CpG (suspended in 50 μL PBS). Tumor size was measured during treatment twice a week by vernier caliper and tumor volume (mm^3) was calculated using the following

equation: Tumor volume = (longer diameter) x (shorter diameter)^2/2. In the survival study the tumor-bearing mice were sacrificed when the tumor volume was approximately 2000 mm^3.

3.2.4 Flow cytometric analysis

At selected time-points after tumor inoculation, tumor bearing animals were sacrificed and tumors and LNs were collected. Tumors were weighed and an equal amount of tumor from each group was homogenized by mechanical dispersion using frosted slides to a cell suspension in flow cytometry buffer (PBS with 5% FBS. LNs were also dissociated and suspended in flow cytometry buffer. The supernatant of the tumour cells after filtering through 70 μm cell strainers (BD Falcon) were stained with appropriate fluorescence conjugated antibodies or their respective isotype controls and incubated for 30 min at 4°C. Intracellular Foxp3 (FJK-16s) staining was done according to the manufacturer's instructions. Cell suspensions of tumors isolated from animals were stained with Annexin V-FITC PI following the manufacturer's instructions. All samples were acquired on a Becton-Dickinson Facsort and analyzed by Cell-Quest software. For analysis of immune cells in tumors, forward scatter gain was set at E00, and the mononuclear population was gated. The percentage of the immune cells which were expressing the markers of interest in the gated population of the whole cell suspension was acquired from flow cytometry. To measure apoptosis, the detector gain was set at E-1 and all the cells were gated for analysis.

3.2.5 ELISA

The supernatant of cell suspension from harvested tumors were collected, filtered sequentially through 70 μm cell strainers and analyzed for the level of IL-12, IFN-γ, IL-2, TNF-α, VEGF and TGF-β by ELISA using the commercially available ELISA kits in a 96 well microplate using a microplate reader (Powerwave with KC Junior software; Bio-Tek, Winooski, VT) at OD of 450 nm according to the manufacturer's directions. The minimum detection levels of the cytokines were: IL-12, 62 pg/mL; TNF-α, 7 pg/mL; IFN-γ, 15 pg/mL; VEGF, 7.8 pg/mL; IL-2, 2 pg/mL and TGF-β, 62 pg/mL.

3.2.6 Immunohistochemistry and Western blot analysis for p-STAT3

Immunohistochemical staining was performed using standard techniques as previously described [24]. Briefly, formalin-fixed, paraffin-embedded tissue sections of 4 μm thickness were deparaffinized and hydrated. Heat-induced epitope retrieval was performed using citrate buffer (pH 6.0), a pressure cooker and microwave for 20 min. After cooling down, endogenous peroxidase activity was blocked by incubation with 3% H_2O_2 for 10 min. Tissue sections were incubated with anti-p-STAT3 antibody overnight in a humidified chamber at 4°C. They were then reacted with biotinylated MultiLink antibodies and labelled with a streptavidin horseradish peroxidase complex. The reaction was visualized using 3-3 diaminobenzidene (DAB) chromagen solution (Dako) resulting in a brown precipitate. Slides were counter-stained in hematoxylin, rinsed in water and dehydrated with increasing concentrations of ethanol and then xylene. For western

blotting tumor tissues were homogenized and lysed in a buffer containing 30 mM HEPES (4-(2-hydroxyethyl)-1-piperazineethanesulfonic acid)) (pH 7.5), 2 mM Na_3VO_4 (sodium orthovanadate), 25 mM NaF (Sodium Fluoride), 2 mM EGTA (ethyleneglycotetraacetic acid), 1:100 protease inhibitor mixture, 0.5 mM DTT (dithiothreitol) and 6.4 mg/mL Sigma 104 Phosphatase Substrate. Cell lysates were centrifuged for 20 seconds at 16000 × g. Total protein extract was determined by Micro BCA Protein Assay. Equal amounts of protein (20 μg) were loaded in 8% SDS-PAGE (sodium dodecyl sulfate polyacrylamide gel electrophoresis). SK-MEL-28+IFN-γ Cell Lysate (Santa Cruz Biotech) was used as positive control**.** Proteins were transferred into polyvinylidene fluoride (PVDF) membrane and were probed with anti-p-STAT3 antibody (Santa Cruz Biotech). To confirm equal loading, membranes were stripped and re-probed with anti-Glyseraldehyde-3-phosphate dehydrogenase (GAPDH) (Santa Cruz Biotech). Membranes were developed using ECL plus detection kit (Amersham).

3.2.7 Statistical analysis

The significance of differences among groups was analyzed by one-way ANOVA followed by the Student-Newman-Keuls post hoc test for multiple comparisons. Before executing the ANOVA, data were tested for normality and equal variance. If neither of the latter criteria were met, data were compared using a Kruskal-Wallis one-way ANOVA on ranks. A P value of ≤ 0.05 was set for the significance of difference among groups. The statistical analysis was performed with SigmaStat software (Systat Software Inc. San Jose, California, USA).

3.3 Results

3.3.1 Intra-tumoral injection of CpG + JSI-124 suppresses p-STAT3 level and induces apoptosis in B16-F10 tumor *in vivo*

JSI-124 is a selective inhibitor of the JAK/STAT3 pathway and it has been shown to induce anti-tumor effects in a variety of human cancer cell lines [12]. Western blots analysis has confirmed high expression of , p-STAT3 in B16-F10 cells (chapter 5, section 5.3.4) [25]. In this study, we assessed the expression of p-STAT3 in B16-F10 tumor grafted to C57BL/6 mice using immunohistochemistry and Western blots. As shown in Figure 3-1A and B, tumors isolated from the mice treated with PBS or CpG showed strong nuclear expression of p-STAT3. By contrast, there was a marked decrease in the level of p-STAT3 in tumors injected with JSI-124 alone or CpG + JSI-124.

FITC-Annexin V/PI flow cytometric analysis of cell suspensions prepared from isolated tumor cells following 8 days of treatment revealed a significant increase in the percentage of late apoptotic cells ($AnnV^+/PI^+$) in tumors injected with JSI-124 + CpG as compared to the PBS group ($P<0.05$) (Figure 3-1C). However we didn't find any statistically significant increase in the percentage of late apoptotic cells in tumors treated with either CpG or JSI-124 alone as compared to PBS group (Figure 3-1C) ($P>0.05$). The percent of early apoptotic cells ($AnnV^+/PI^-$) was small in all groups and the total apoptotic cells were significantly different between CpG + JSI-124 and PBS groups ($P<0.05$).

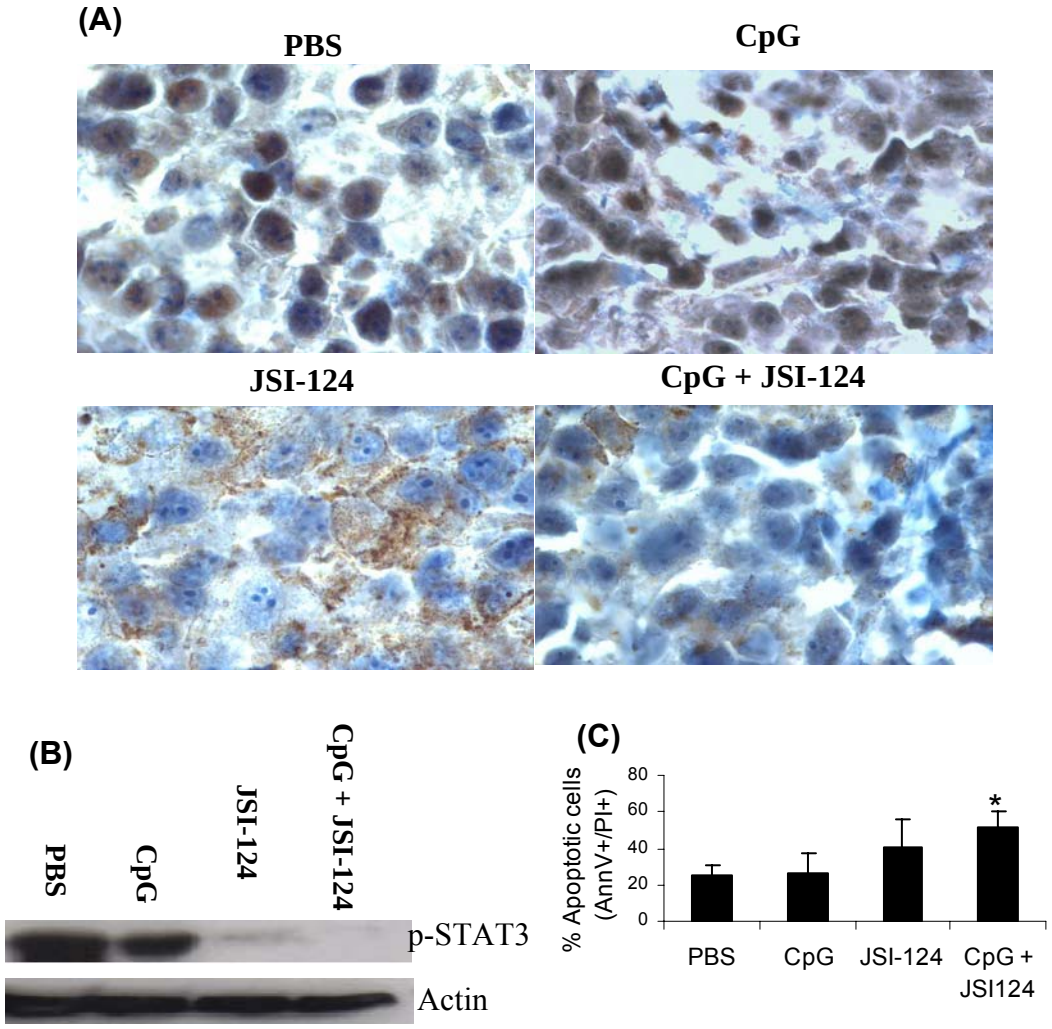

Figure 3-1. Analysis of B16-F10 tumors for p-STAT3 levels *in vivo*. B16-F10 tumor cells were implanted in C57BL/6 mice and tumors that formed were treated intra-tumorally with either PBS containing 20 % ethanol (PBS group), CpG (10 μg), JSI-124 (1 mg/kg) or CpG + JSI-124 at the same doses daily for 8 days. Tumors were then isolated and analyzed for: A) p-STAT3 by immunohistochemistry (p-STAT3 positive cells are stained brown); B) p-STAT3 level by Western blot; and C) Apoptosis by flow cytometry (Annexin V-FITC PI staining of tumor cells suspension). Images (1000X magnified) and blots are representative of two independent experiments. Apoptosis data represent the mean ± SD of three independent experiments (n=2 for each experiment) (*significantly different from PBS group, $P<0.05$)

3.3.2 Intra-tumoral injection of CpG + JSI-124 has superior effects on tumor growth and significantly improves the survival time of tumor-bearing mice

As shown in Figure 3-2A, the average tumor size increased rapidly in the PBS group and it reached above 1,500 mm^3 after 15 days of tumor implantation, whereas daily intra-tumoral injection of 10 μg CpG resulted in significantly slower tumor growth; the average tumor volume was below 500 mm^3 during the same period of time ($P<0.01$). Daily intra-tumoral injection of 1 mg/kg JSI-124 alone or in combination with 10 μg CpG efficiently inhibited tumor growth as compared to the PBS group or CpG injected tumors ($P<0.001$) (Figure 3-2A). The average tumor volume on day 11-14 after tumor implantation in the mice that received combination therapy was found to be significantly lower than that in JSI-124 group at the same period (13-19 mm^3 in CpG + JSI-124 versus 43-106 mm^3 in JSI-124 group) ($P<0.05$). Consistent with these data, the average tumor weight after 8 days of treatment with either JSI-124 (0.2 gram) or CpG + JSI-124 (0.09 gram) was significantly lower than that of the PBS group (1.15 gram) and CpG-injected tumors (0.63 gram) ($P<0.001$). The average tumor weight of CpG-injected tumors following 8 days treatment was also found to be significantly less than that of the PBS group ($P<0.05$)(Figure 3-2B). It should be noted that during 8 days of treatment, the treated animals did not show any commonly observed sign of toxicity such as weight loss.

To further compare the effects of the CpG + JSI-124 combination therapy to those of JSI-124 and CpG monotherapy, animals in all treatment groups were monitored for tumor growth and survival after stopping drug injection on day 15.

As shown in Figure 3-2 A and C, tumors rapidly grew in animals that received JSI-124 after stopping the treatment, survival dropped from 100% on day 17 to 11% on day 24 after tumor implantation, and none of the mice were tumor-free. However, at the same time point (day 24), 45 % of the mice that received CpG + JSI-124 combination therapy were tumor-free and the survival was 100% (Figure 3-2C and D). For mice that received CpG alone, survival gradually went down from 78% on day 15 to 22% on day 24 (Figure 3-2C). Among animals that received CPG + JSI-124, 1 of 9 mice remained tumor-free and did not develop tumor when it was re-challenged with 1×10^6 B16 tumor cells on day 40 after the initial tumor implantation. As a control group for tumor re-challenging study, the same number of tumor cells was grafted in 3 mice which had never been injected with tumor before. While mice in the control group developed palpable tumors on day 8 after implantation, the mouse that survived due to CpG + JSI-124 combination didn't develop any tumor during 24 days monitoring after it was re-challenged with tumor.

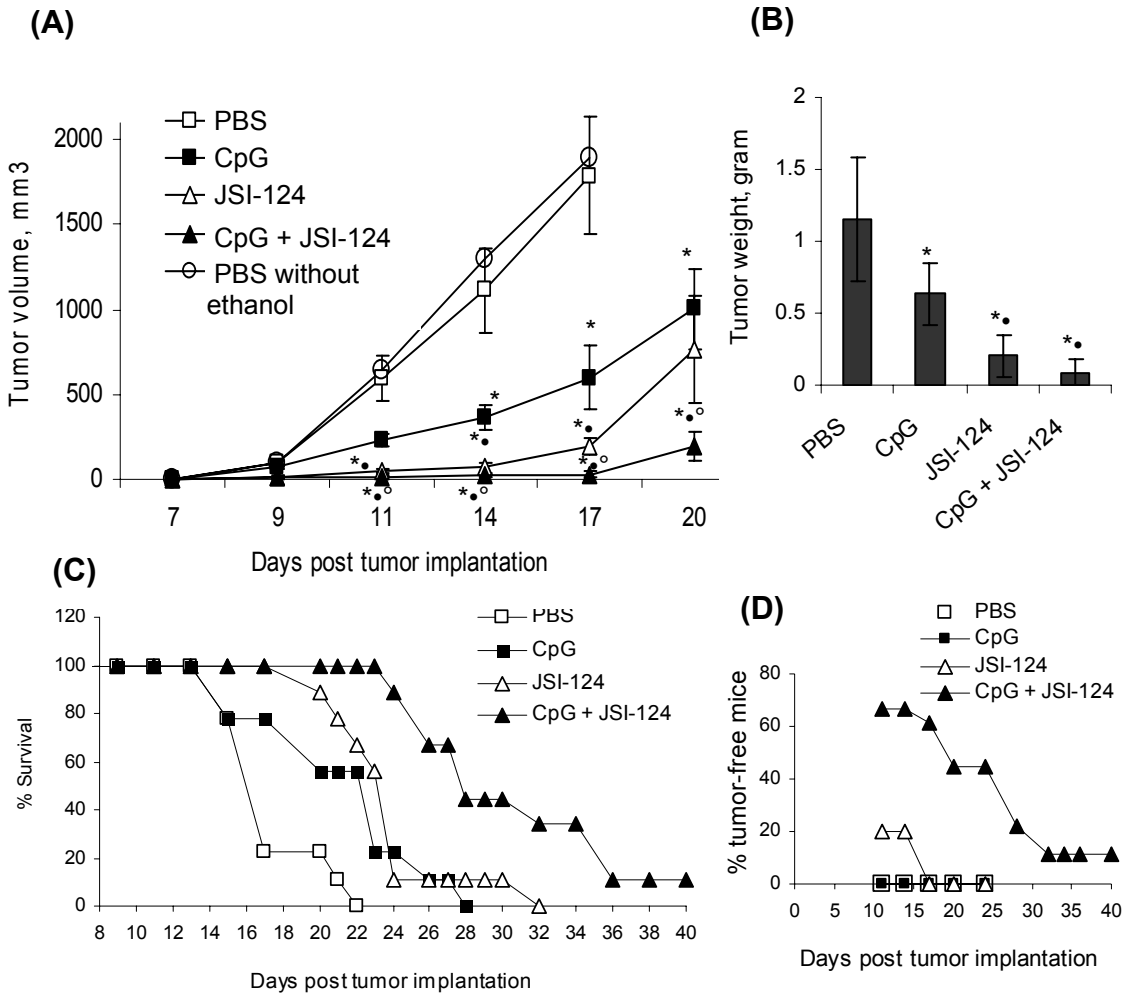

Figure 3-2. Anticancer activity of CpG + JSI-124 combination therapy *in vivo*. On day 7 after tumor implantation, the mice were assigned to four groups (20 per group), treated intra-tumorally with either PBS containing 20 % ethanol (PBS group) or 10 μg CpG or 1 mg/kg JSI-124 or the same doses of CpG + JSI-124, and monitored for tumor growth and survival. A) Average tumor volume in animals (n=13-15, mean ± SE); B) Average tumor weight on day 15 after tumor cells injection (n=7, mean ± SD); C) % survival in a period of 40 days after tumor implantation (n=9); and D) % tumor-free mice (n=9). *significantly different from PBS group ($P<0.01$ for CpG group and $P<0.001$ for JSI-124 and CpG + JSI-124 groups), •significantly different form tumors that received only CpG ($P<0.01$), °significantly different from tumors injected with JSI-124 ($P<0.05$).

3.3.3 Primary tumors are infiltrated by NK cells and $CD8^+$ and $CD4^+$ T cells following intra-tumoral injection of JSI-124 + CpG

In an attempt to provide a biological explanation for the superior anti-tumor effects of JSI-124 + CpG, we analyzed the intra-tumoral lymphocyte infiltrates following 8 days of treatment. In comparison to the PBS group, intra-tumoral treatment with CpG + JSI-124 resulted in 75, 50 and 125-fold increases in the percentage of NK cells, $CD8^+$ and $CD4^+$ T cells in the tumors, respectively (Figure 3-3A). On the other hand, only 2 to 5 fold increases in the percentage of NK cells and T cells were observed in the tumors that received either CpG or JSI-124 (Figure 3-3A). The increase in the percentage of T cells and NK cells in the CpG + JSI-124 group was significantly different from the PBS, CpG or JSI-124 group alone ($P < 0.01$).

The $CD3^+/CD4^+$ and $CD3^+/CD8^+$ T cells were further analyzed for the expression of activation/memory markers using flow cytometry. In the CpG + JSI-124 group, CD11a, CD69 and CD44 were expressed in 31 %, 15 % and 92 % of $CD3^+/CD4^+$ T cells and 24 %, 27 % and 88 % of $CD3^+/CD8^+$ T cells, respectively (Figure 3-3B). The proportions of cells showing these activation/memory markers were not significantly different from those in the monotherapy groups. The expression of these activation/memory markers was not detectable in the PBS group.

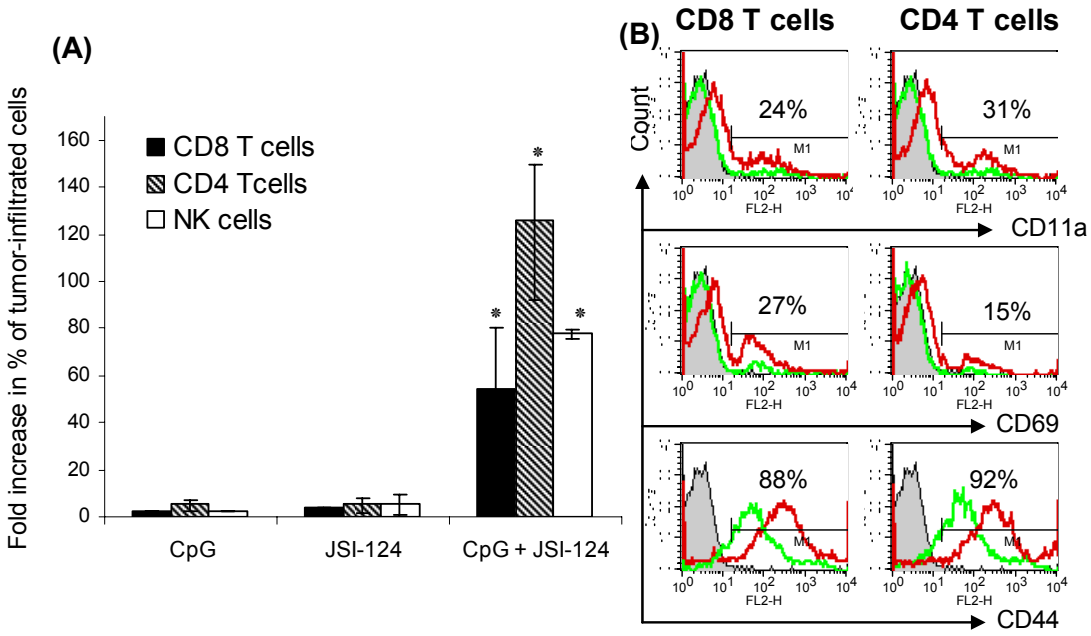

Figure 3-3. Recruitment of T cells expressing activation/memory markers and NK cells into tumors following treatment with CpG and/or JSI-124. Following 8 days intra-tumoral injection of either of the followings; PBS containing 20 % ethanol (PBS group), CpG, JSI-124, or JSI-124 + CpG, tumor were isolated and analyzed for T cell and NK cell surface markers using flow cytometry. The percentage of $NK1.1^+$ NK cells and $CD3^+$ $CD4^+$ an $CD3^+$ $CD8^+$ T cells in 0.4 gram of tumors collected from the mice were acquired from flow cytometry and fold increases in the percentage of these cells in the test groups were calculated based on the percentage of the cells in the PBS group A) Fold increase in the percentage of NK cells and T cells which infiltrated tumors that received CpG and/or JSI-124 as compared with tumors injected with PBS. The data is shown as mean ± SD of three independent experiments. *significantly different from either PBS, CpG or JSI-124 group ($P<0.01$); B) CD11a, CD69 and CD44 expression (Red lines) in the gated tumor infiltrating $CD3^+$ $CD4^+$ and $CD3^+$ $CD8^+$ T cells from the mice that received CpG + JSI-124 combination therapy. Filled histograms and green lines represent isotype controls and the expression of memory markers by naïve T cells, respectively. The data is the representative of three independent experiments.

3.3.4 Intra-tumoral injection of CpG + JSI-124 results in a significant increase in the proportion of activated DCs in tumor and regional LNs

DCs play a key role in the activation of effector T cells, but they have been shown to be dysfunctional or tolerogenic in the tumor immunosuppressive microenvironment. Recruitment of a higher number of T cells with activation/memory phenotype in tumors injected with CpG + JSI-124 (as shown above) may reflect improved function of DCs in tumors and LNs in this group. To test this hypothesis, we evaluated the activation status of DCs in the tumors and regional LNs following 6 days of intra-tumoral injections. To minimize the activation of DCs during isolation that may artificially activate DCs, [26] DCs were not purified from the tumors or LNs, but stained directly for the expression of DC maturation markers. The gating strategy for DCs using the $CD11c^{+}MHC\text{-}II^{high}$ immunophenotype has been previously reported [6]. $CD11c^{+}MHC\text{-}II^{high}$ DCs were gated and analyzed for CD86 expression, a marker known to be associated with activated DC [27]. The percentage of $CD11c^{+}MHC\ II^{high}$ DCs in tumors was found to be 2.6 %, 7 %, 9 %, and 15.7 % in the PBS, CpG, JSI-124, and CpG + JSI-124 groups, respectively (Figure 3-4A). Statistical analysis of the data revealed no significant difference in the percentage of $CD11c^{+}MHC\ II^{high}$ DCs among the PBS group and tumors injected with either CpG or JSI-124 alone ($P>0.05$). However, the proportion of $CD11c^{+}MHC\ II^{high}$ DCs in the CpG + JSI-124 group was significantly higher than that in the PBS group as well as that of the CpG and JSI-124 ($P<0.05$) monotherapy groups (Figure 3-4A). While $CD11c^{+}MHC\ II^{high}$ DCs from the PBS group were found to be negative for CD86

expression, CD86 was expressed on 3.7 %, 10.7 %, and 13.3 % of $CD11c^{+}MHC\ II^{high}$ DCs in the CpG, JSI-124, and CpG + JSI-124 groups, respectively (Figure 3-4B). The percentage of $CD11c^{+}MHC\ II^{high}$ DCs in LNs of the PBS, CpG and JSI-124 treatment groups was not statistically different from each other (P>0.05), but the percentage of $CD11c^{+}MHC\ II^{high}$ DCs significantly increased from 4.5-7 % in the PBS, CpG, and JSI-124 experimental groups to 12 % in the mice that received JSI-124 + CpG (Figure 3-4A) (P < 0.05). CD86 was expressed in only 8-10 % of $CD11c^{+}MHC\ II^{high}$ DCs from the LNs in either the PBS, CpG alone or JSI-124 alone groups. However a significantly higher portion of $CD11c^{+}MHC\ II^{high}$ DCs (22.5 %) exhibited CD86 expression in the CpG + JSI-124 group (Figure 3-4B).

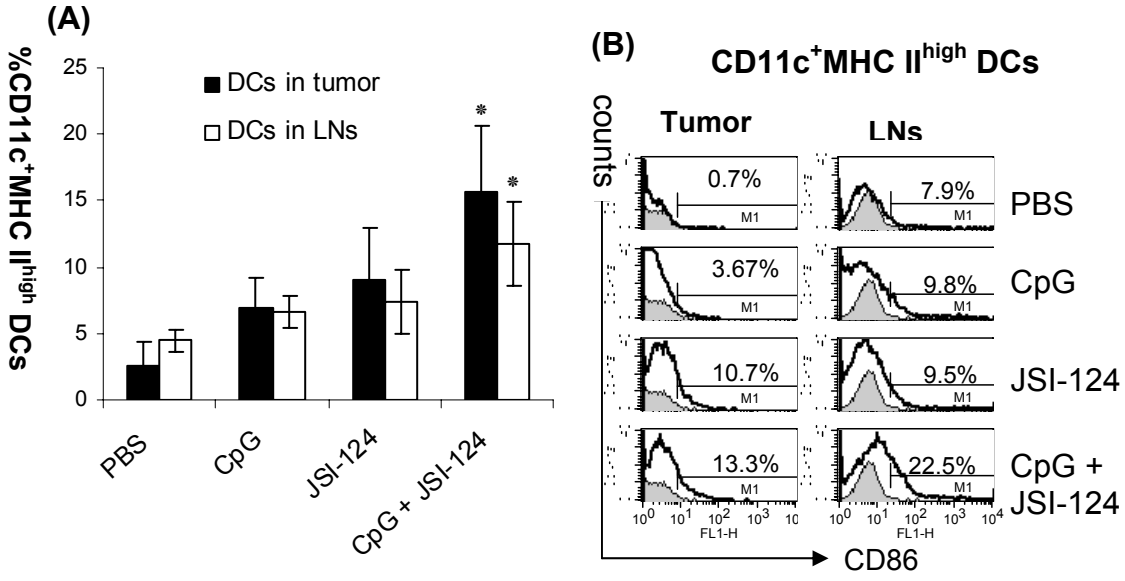

Figure 3-4. Phenotypic analysis of DCs in tumor and regional LNs. Tumor-bearing mice received daily intra-tumoral injection of either PBS containing 20 % ethanol or CpG or JSI-124, or CpG + JSI-124. After 6 days treatment tumors and LNs were isolated and analyzed for the presence of activated DCs. The percentage of $CD11c^{+}MHC\ II^{high}$ DCs expressing CD86 was acquired from flow cytometry. A) % $CD11c^{+}MHC\ II^{high}$ DCs in tumors (black bars) and regional LNs (white bars); The data represent the mean ± SD of three independent experiments. *significantly different from tumors treated with PBS or CpG or JSI-124 (P<0.05). B) CD86 expression (solid lines) in the gated $CD11c^{+}MHC\ II^{high}$ DCs. Filled histograms represents isotype controls. The data is the representative of three independent experiments (n=5 per group).

3.3.5 CpG + JSI-124 therapy enhanced the level of pro-inflammatory cytokines and reduced the level of immunosuppressive factors in the tumors

To further analyze the mechanisms by which the CpG + JSI-124 combination therapy induces DC activation and intra-tumoral recruitment of T cells, tumors were evaluated for the level of a panel of effector and immunosuppressive cytokines. IL-12, IFN-γ, IL-2 (cytokines involved in Th1-immune responses) and TNF-α have been shown to be capable of eliciting beneficial anti-tumor effects through their dual function as pro-inflammatory and anti-angiogenic factors in a variety of experimental tumor models [28-31]. VEGF and TGF-β are potent immunosuppressive factors which promote and sustain non-responsiveness of the immune system to growing tumors through negative regulation of DC maturation and induction of T_{reg} cell activation [5,32-36]. As shown in Figure 3-5, intra-tumoral injection of CpG + JSI-124 resulted in a significant increase in the intra-tumoral level of IL-12, TNF-α, IL-2 ($P<0.05$), and IFN-γ ($P<0.001$), as compared to that in the PBS group, CpG or JSI-124 monotherapy group. Intra-tumoral injection of JSI-124 alone or in combination with CpG significantly reduced VEGF level in tumors as compared with the PBS or CpG group (Figure 3-5) ($P<0.001$). The level of VEGF in the CpG group was not significantly different from that in the PBS group ($P>0.05$). Compared to the PBS group, treatment with either CpG or JSI-124 did not result in any significant change in the level of TGF-β ($P>0.05$); however, CpG + JSI-124 therapy significantly reduced the TGF-β level in tumors as compared with PBS group and the mice that received CpG or JSI-124 monotherapy ($P<0.01$)(Figure 3-5).

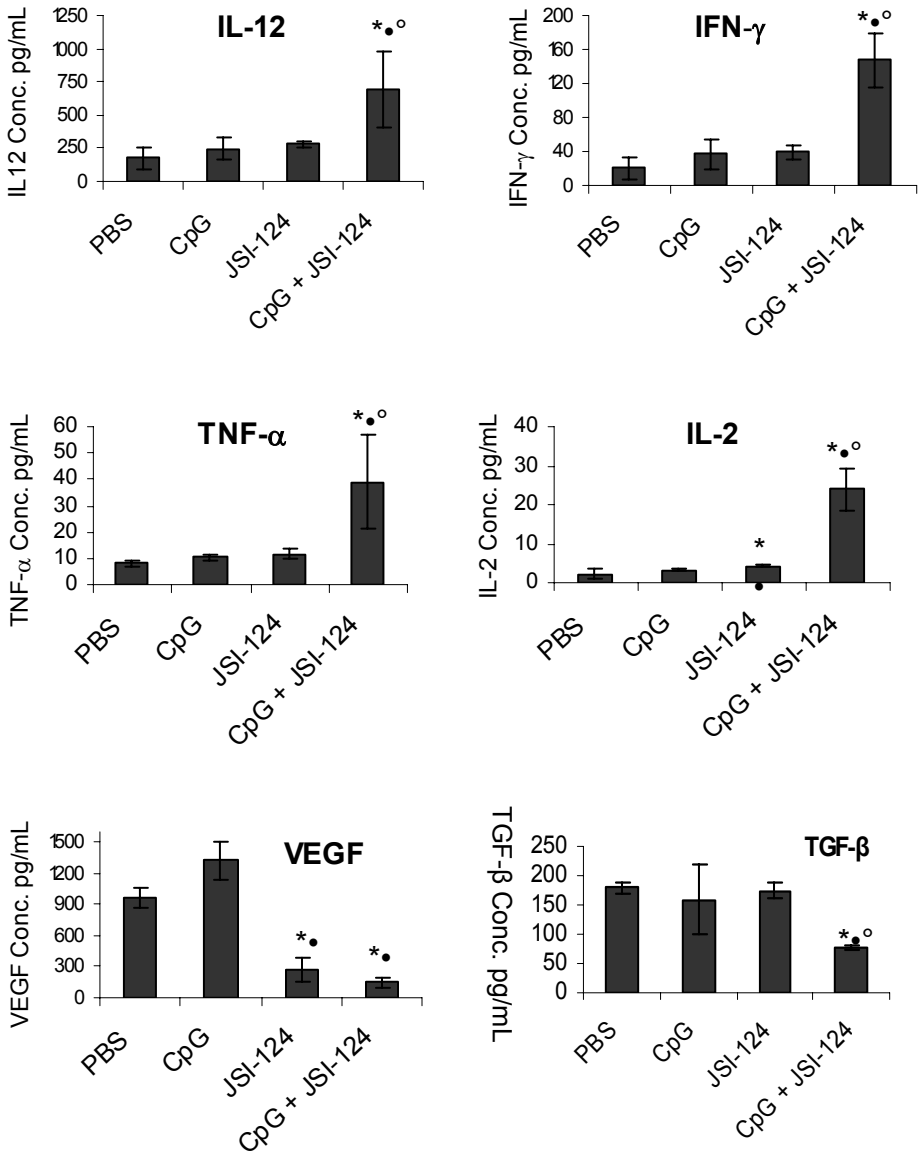

Figure 3-5. Evaluation of the level of pro-inflammatory cytokines and immunosuppressive factors in the tumors. Supernatant of tumors isolated from the mice, 8 days after intra-tumoral injection of either PBS containing 20 % ethanol (PBS group) or CpG or JSI-124 or CpG + JSI-124 was analyzed for the level of IL-12, TNF-α, IFN-γ, IL-2, VEGF and TGF-β by ELISA. Each bar represents the mean ± SD of three independent experiments (n=3 for each experiment). *significantly different from tumors injected with PBS ($P<0.05$ for IL-12, TNF-α, IL-2, $P<0.01$ for TGF-β, and $P<0.001$ for IFN-γ and VEGF), •significantly different from tumors injected with CpG ($P<0.05$ for IL-12 and $P<0.001$ for VEGF), °significantly different from JSI-124 group ($P<0.05$).

3.3.6 The population of $CD4^+CD25^+$ $Foxp3^+$ T cells decreases in regional LNs following intra-tumoral injection of CpG and JSI-124

Previous studies indicate that $CD4^+CD25^+$ T_{reg} characterized by the expression of Foxp3 play a significant role in suppressing anti-tumor immunity [37,38]. Thus, we tested whether treatment with JSI-124 and/or CpG inhibits induction of $CD4^+CD25^+Foxp3^+$ T_{reg} cells in the regional LNs. Because regulatory $CD4^+$ T cell activity has been identified in the $CD4^+CD25^+$T-cell population, we first estimated the proportion of such $CD4^+CD25^+$ T cells in LNs. However, it is difficult to distinguish T_{reg} cells based on CD25 expression, especially in LNs where T cell priming is going on. CD25 is also up-regulated on effector T cells upon T cell receptor engagement before clonal expansion. Therefore, we analyzed $CD4^+CD25^+$ T cells population for Foxp3 expression. As Figure 3-6 shows, there was no significant difference among frequencies of $CD4^+CD25^+$ T cells in LNs from different treatment groups ($P>0.05$). However, 40% of $CD4^+CD25^+$ T cells from the PBS group were positive for Foxp3, consistent with T_{reg} cell phenotype. On the other hand, only 3-7 % of $CD4^+CD25^+$ T cell from the groups that received CpG and/or JSI-124 expressed Foxp3 (Figure 3-6).

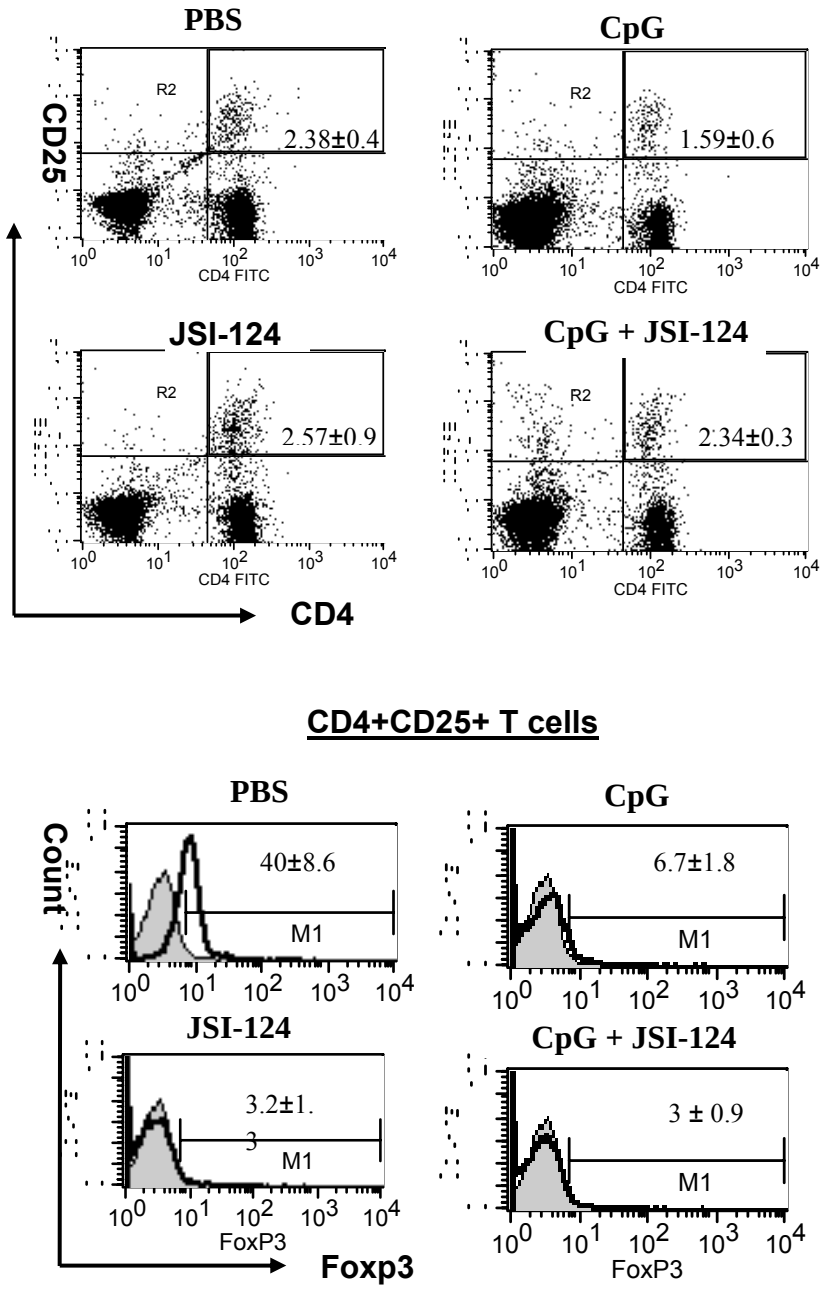

Figure 3-6. Phenotypic analysis of T_{reg} cells in regional LNs. Cell suspensions of LNs, isolated from the tumor-bearing mice 6 days after daily treatment with either PBS containing 20 % ethanol (PBS group) or CpG or JSI-124 or CpG + JSI-124, were stained with antibodies against CD4, CD25 surface markers and intracellular Foxp3 and analyzed by flow cytometry. $CD4^+CD25^+$ T cells were gated and analyzed for Foxp3 expression (solid lines). Filled histograms represent isotype controls. The data represent the mean ± SD of three independent experiments.

3.4 Discussion

The induction and efficacy of the anti-tumor immune responses are often limited by the presence of immunosuppressive factors in the tumor microenvironment. STAT3 has been identified as one of the important mediators of tumor-induced immunosuppression [5]. Specifically, activation of STAT3 in DCs, often triggered by tumor cell-derived immunosuppressive factors (such as VEGF), inhibits the functional maturation of DCs [5,39-41]. In support of this concept, a previous study shows that tumor-infiltrating DCs in hematopoietically STAT3-ablated mice ($STAT^{-/-}$) express a higher level of CD86 and MHC II as compared to those in $STAT3^{+/+}$ mice [6]. DCs that fail to mature properly can turn into tolerogenic DCs, known to induce the production of immunosuppressive factors (such as TGF-β) as well as T_{reg} cells, which further dampen the anti-tumor immune response [5,11,35]. Previous attempts have been made to disrupt this vicious cycle of immunosuppression, with a focus on restoring the functions of DCs. One approach is to inhibit STAT3 activation in DCs and the other approach is to activate DCs using CpG. Both of these approaches have shown to be effective. For instance, JSI-124 has been shown to significantly inhibit tumor growth in the B16 mouse melanoma tumor model [12,25]. Intra-tumoral injection of CpG has been also shown to inhibit tumor growth and increase the survival of mice bearing B16 melanoma tumors [42]. In this study, we demonstrated that the CpG + JSI-124 combination therapy exhibits synergistic anti-tumor cancer activity characterized by significantly lower tumor size and improved survival, as

compared with the negative control group, and the JSI-124 or CpG monotherapy groups.

Our data showed that intra-tumoral injection of CpG + JSI-124 resulted in tumor regression, associated with decreases in immunosuppresion within the tumors. Importantly, when we assessed the anti-tumor effects of the combination of CpG + JSI-124, we found profound and synergistic anti-tumor activity compared to the other experimental groups. These synergistic anti-tumor effects appear to stem from fundamental changes in the anti-tumor response, as reflected by significant changes in several parameters, including increases in the recruitment of T cells expressing activation/memory markers and NK cells, enhanced activation and maturation of DCs, increases in the levels of several Th1-related pro-inflammatory cytokines, and decreases in intra-tumoral levels of TGF-β and VEGF. The number of T_{reg} cells was also found to be decreased in the regional LNs. While treatment with CpG alone or JSI-124 alone also resulted in a similar pattern of changes in the anti-tumor responses, the magnitudes observed were significantly less than those of the combination treatment.

While the exact mechanisms to explain the synergistic anti-tumor effects of the combination therapy require further studies, we made the following speculation based on the current concept and our findings regarding changes in the anti-tumor immune response. We believe that the combination of JSI-124 and CpG effectively disrupts the vicious cycle of immunosuppression, as described above. Since STAT3 is known to upregulate VEGF expression, [43] it is expected that suppression of p-STAT3 in tumor results in a substantial decrease in VEGF, a

potent immunsuppressive factor. Consequently, immune effectors cells are recruited and their anti-tumor functions can be somewhat restored. For DCs, the decrease in the tumor-derived suppressive factors (which can activate STAT3 in DCs), in conjunction with direct STAT3 inhibition by JSI-124 and CpG-induced activation, can greatly restore their maturation and anti-tumor functions, which in turn promotes an effective anti-tumor immune response. Both T_{reg} cells and TGF-β, known to be upregulated by immature and tolerogenic DCs [5,11], are also greatly decreased. Thus, as a result of the combination treatment, the vicious cycle of immunosuppression is turned into a circuit of effective anti-tumor responses which is sustained by a positive feedback loop between the immune effector cells and DCs. This scenario likely explains the observed superior anticancer effects and the magnitude of changes in the immune response induced by JSI-124 + CpG.

With regard to the recruitment of effector immune cells, we found that treatment using JSI-124 alone resulted in 2-5 fold increment in the number of T cells and NK cells within the tumors. These observations are in keeping with the results of previous studies that have shown that blocking STAT3 in STAT3-active tumor cells leads to the secretion of soluble factors stimulating lymphocyte migration, *in vitro* [44]. By immunohistochemistry, it also has been shown that STAT3 inhibition in B16 tumors results in an increase in tumor infiltration by T cells, *in vivo*, although the immunophenotype of these T-cells was not further characterized [8]. In our study, CpG alone also induced a 2-5 fold increase in the number of infiltrating T-cells. By contrast, CpG + JSI-124 combination therapy resulted in a dramatic increase (75-150 fold) in the percentage of T cells and NK

cells in the tumor. We believe that these observations are of great significance since inadequate trafficking of effector cells in tumors is considered one of the major barriers to effective cancer immunotherapy [4]. Several studies also suggest that increased tumor infiltration by immune effector cells is associated with an improved therapeutic outcome in cancer patients [45-48].

The proportion of activated DCs significantly increased with the combination treatment. Intra-tumoral injection of CpG alone did not result in any significant change in the number of activated DCs. This is consistent with other studies showing that CpG on its own cannot activate impaired DCs in tumor [49]. Intra-tumoral injection of JSI-124 was also found unable to significantly increase DC maturation in tumor and regional LNs. Others have shown that intraperitoneal injection of JSI-124 increases the number of mature myeloid DCs in LNs of the mice bearing tumor without hyperactive STAT3 [13]. The differences between our observation and the previous study in terms of the ability of JSI-124 monotherapy for enhancing DC maturation, *in vivo,* may be related to the use of different cancer cell line and/or treatment schedule.

The induction of T cell mediated immune responses in the mice treated with CpG + JSI-124 correlates well with higher levels of Th1-related pro-inflammatory cytokines including IL-12, IL-2 and IFN-γ. Pro-inflammatory cytokines not only positively regulate the recruitment and function of immune effector cells, they also reduce immunosuppression in tumors by blocking the activation of tolerogenic DCs and T_{reg} cells [5,9].

To further support the hypothetical model, we also found a significantly lower number of $CD4^+CD25^+Foxp3^+$ T_{reg} cells in the tumor-draining LNs in all treated groups as compared to the PBS group. Our result showing that CpG can inhibit the production of activated T_{reg} cells is in line with the studies which have shown intradermal injection of CpG to melanoma patients results in lower frequencies of T_{reg} cells in sentinel LN [18]. The inhibitory effect of JSI-124 on the production of T_{reg} cells is likely via blocking VEGF which plays an important role in the activation of these cells [41].

One interesting observation in this study was that one mouse from the group that received combination therapy remained tumor free and did not show any sign of tumor development when it was re-challenged with tumor. This observation may suggest the development of long-lasting tumor-specific immunity, which may be related to the intensity of the immune responses found in this group. Further studies are needed to validate this hypothesis and characterize the mechanism of possible for long-lasting immune responses elicited by this immunomodulation approach.

In conclusion, we believe that our findings, for the first time, have provided the proof-of-principle of using DC activation and STAT3 inhibition for cancer immunotherapy. Our data support the concept that the combination therapy is superior to JSI-124 or CpG monotherapy by virtue of its effective disruption of the vicious cycle of immunosuppression within the tumors. As a result of these changes, the immune environment in the tumor favors effective recruitment and activation of anti-tumor effector cells. Since our experiments involved only in one

cell line, further studies are needed to test the efficacy of our immunomodulation approach in other STAT3-active tumors. It is also of great interest to determine whether CpG + JSI-124 combination therapy can be effective in tumors without constitutively active STAT3.

3.5 Referecnes

1. Slingluff CL, Speiser DE: Progress and controversies in developing cancer vaccines. J Transl Med 2005;3:18-27.
2. Morse MA, Chui S, Hobeika A, Lyerly HK, Clay T: Recent developments in therapeutic cancer vaccines. Nat Clin Pract Oncol 2005;2:108-113.
3. Rosenberg SA, Yang JC, Restifo NP: Cancer immunotherapy: moving beyond current vaccines. Nat Med 2004;10:909-915.
4. Chen Q, Wang WC, Evans SS: Tumor microvasculature as a barrier to antitumor immunity. Cancer Immunol Immunother 2003;52:670-679.
5. Yu H, Kortylewski M, Pardoll D: Crosstalk between cancer and immune cells: role of STAT3 in the tumour microenvironment. Nat Rev Immunol 2007;7:41-51.
6. Kortylewski M, Kujawski M, Wang T, Wei S, Zhang S, Pilon-Thomas S, Niu G, Kay H, Mule J, Kerr WG, Jove R, Pardoll D, Yu H: Inhibiting Stat3 signaling in the hematopoietic system elicits multicomponent antitumor immunity. Nat Med 2005;11:1314-1321.
7. Nefedova Y, Gabrilovich DI: Targeting of Jak/STAT pathway in antigen presenting cells in cancer. Curr Cancer Drug Targets 2007;7:71-77.
8. Wang T, Niu G, Kortylewski M, Burdelya L, Shain K, Zhang S, Bhattacharya R, Gabrilovich D, Heller R, Coppola D, Dalton W, Jove R, Pardoll D, Yu H: Regulation of the innate and adaptive immune responses by Stat-3 signaling in tumor cells. Nat Med 2004;10:48-54.

9. Steinman RM, Hawiger D, Nussenzweig MC: Tolerogenic dendritic cells. Annu Rev Immunol 2003;21:685-711.

10. Gabrilovich D: Mechanisms and functional significance of tumour-induced dendritic-cell defects. Nat Rev Immunol 2004;4:941-952.

11. Zou W: Immunosuppressive networks in the tumour environment and their therapeutic relevance. Nat Rev Cancer 2005;5:263-274.

12. Blaskovich MA, Sun J, Cantor A, Turkson J, Jove R, Sebti SM: Discovery of JSI-124 (cucurbitacin I), a selective Janus kinase/signal transducer and activator of transcription 3 signaling pathway inhibitor with potent antitumor activity against human and murine cancer cells in mice. Cancer Res 2003;63:1270-1279.

13. Nefedova Y, Nagaraj S, Rosenbauer A, Muro-Cacho C, Sebti SM, Gabrilovich DI: Regulation of dendritic cell differentiation and antitumor immune response in cancer by pharmacologic-selective inhibition of the janus-activated kinase 2/signal transducers and activators of transcription 3 pathway. Cancer Res 2005;65:9525-9535.

14. Nefedova Y, Cheng P, Gilkes D, Blaskovich M, Beg AA, Sebti SM, Gabrilovich DI: Activation of dendritic cells via inhibition of Jak2/STAT3 signaling. J Immunol 2005;175:4338-4346.

15. Hemmi H, Takeuchi O, Kawai T, Kaisho T, Sato S, Sanjo H, Matsumoto M, Hoshino K, Wagner H, Takeda K, Akira S: A Toll-like receptor recognizes bacterial DNA. Nature 2000;408:740-745.

16. Iwasaki A, Medzhitov R: Toll-like receptor control of the adaptive immune responses. Nat Immunol 2004;5:987-995.

17. Liu YJ: IPC: professional type 1 interferon-producing cells and plasmacytoid dendritic cell precursors. Annu Rev Immunol 2005;23:275-306.

18. Molenkamp BG, van Leeuwen PA, Meijer S, Sluijter BJ, Wijnands PG, Baars A, van den Eertwegh AJ, Scheper RJ, de Gruijl TD: Intradermal CpG-B activates both plasmacytoid and myeloid dendritic cells in the sentinel lymph node of melanoma patients. Clin Cancer Res 2007;13:2961-2969.

19. Hellman P, Eriksson H: Early activation markers of human peripheral dendritic cells. Hum Immunol 2007;68:324-333.

20. Brocks CP, Pries R, Frenzel H, Ernst M, Schlenke P, Wollenberg B: Functional alteration of myeloid dendritic cells through head and neck cancer. Anticancer Res 2007;27:817-824.

21. Carpentier AF: [Cancer immunotherapy with CpG-ODN]. Med Sci (Paris) 2005;21:73-77.

22. Krieg AM: Antitumor applications of stimulating toll-like receptor 9 with CpG oligodeoxynucleotides. Curr Oncol Rep 2004;6:88-95.

23. Krieg AM: Development of TLR9 agonists for cancer therapy. J Clin Invest 2007;117:1184-1194.

24. Hui D, Satkunam N, Al Kaptan M, Reiman T, Lai R: Pathway-specific apoptotic gene expression profiling in chronic lymphocytic leukemia and follicular lymphoma. Mod Pathol 2006;19:1192-1202.

25. Molavi O, Ma Z, Mahmud A, Alshamsan A, Samuel J, Lai R, Kwon GS, Lavasanifar A: Polymeric micelles for the solubilization and delivery of STAT3 inhibitor cucurbitacins in solid tumors. Int J Pharm 2008;347:118-127.

26. Gallucci S, Lolkema M, Matzinger P: Natural adjuvants: endogenous activators of dendritic cells. Nat Med 1999;5:1249-1255.

27. Reis e Sousa C: Dendritic cells in a mature age. Nat Rev Immunol 2006;6:476-483.

28. Qin Z, Schwartzkopff J, Pradera F, Kammertoens T, Seliger B, Pircher H, Blankenstein T: A critical requirement of interferon gamma-mediated angiostasis for tumor rejection by CD8+ T cells. Cancer Res 2003;63:4095-4100.

29. Wigginton JM, Park JW, Gruys ME, Young HA, Jorcyk CL, Back TC, Brunda MJ, Strieter RM, Ward J, Green JE, Wiltrout RH: Complete regression of established spontaneous mammary carcinoma and the therapeutic prevention of genetically programmed neoplastic transition by IL-12/pulse IL-2: induction of local T cell infiltration, Fas/Fas ligand gene expression, and mammary epithelial apoptosis. J Immunol 2001;166:1156-1168.

30. Nelson D, Ganss R: Tumor growth or regression: powered by inflammation. J Leukoc Biol 2006;80:685-690.

31. Crittenden MR, Thanarajasingam U, Vile RG, Gough MJ: Intratumoral immunotherapy: using the tumour against itself. Immunology 2005;114:11-22.

32. Ohm JE, Carbone DP: VEGF as a mediator of tumor-associated immunodeficiency. Immunol Res 2001;23:263-272.

33. Gabrilovich D, Ishida T, Oyama T, Ran S, Kravtsov V, Nadaf S, Carbone DP: Vascular endothelial growth factor inhibits the development of dendritic cells and dramatically affects the differentiation of multiple hematopoietic lineages in vivo. Blood 1998;92:4150-4166.

34. Oyama T, Ran S, Ishida T, Nadaf S, Kerr L, Carbone DP, Gabrilovich DI: Vascular endothelial growth factor affects dendritic cell maturation through the inhibition of nuclear factor-kappa B activation in hemopoietic progenitor cells. J Immunol 1998;160:1224-1232.

35. Powrie F, Carlino J, Leach MW, Mauze S, Coffman RL: A critical role for transforming growth factor-beta but not interleukin 4 in the suppression of T helper type 1-mediated colitis by CD45RB(low) CD4+ T cells. J Exp Med 1996;183:2669-2674.

36. Marie JC, Letterio JJ, Gavin M, Rudensky AY: TGF-beta1 maintains suppressor function and Foxp3 expression in CD4+CD25+ regulatory T cells. J Exp Med 2005;201:1061-1067.

37. Viguier M, Lemaitre F, Verola O, Cho MS, Gorochov G, Dubertret L, Bachelez H, Kourilsky P, Ferradini L: Foxp3 expressing CD4+CD25(high) regulatory T cells are overrepresented in human metastatic melanoma lymph nodes and inhibit the function of infiltrating T cells. J Immunol 2004;173:1444-1453.

38. Wang RF: Immune suppression by tumor-specific CD4+ regulatory T-cells in cancer. Semin Cancer Biol 2006;16:73-79.

39. Mimura K, Kono K, Takahashi A, Kawaguchi Y, Fujii H: Vascular endothelial growth factor inhibits the function of human mature dendritic cells mediated by VEGF receptor-2. Cancer Immunol Immunother 2007;56:761-770.

40. Johnson BF, Clay TM, Hobeika AC, Lyerly HK, Morse MA: Vascular endothelial growth factor and immunosuppression in cancer: current knowledge and potential for new therapy. Expert Opin Biol Ther 2007;7:449-460.

41. Li B, Lalani AS, Harding TC, Luan B, Koprivnikar K, Huan Tu G, Prell R, VanRoey MJ, Simmons AD, Jooss K: Vascular endothelial growth factor blockade reduces intratumoral regulatory T cells and enhances the efficacy of a GM-CSF-secreting cancer immunotherapy. Clin Cancer Res 2006;12:6808-6816.

42. Sharma S, Karakousis CP, Takita H, Shin K, Brooks SP: Intra-tumoral injection of CpG results in the inhibition of tumor growth in murine Colon-26 and B-16 tumors. Biotechnol Lett 2003;25:149-153.

43. Chen Z, Han ZC: STAT3: A critical transcription activator in angiogenesis. Med Res Rev 2007.

44. Burdelya L, Kujawski M, Niu G, Zhong B, Wang T, Zhang S, Kortylewski M, Shain K, Kay H, Djeu J, Dalton W, Pardoll D, Wei S, Yu H: Stat3 activity in melanoma cells affects migration of immune effector cells and nitric oxide-mediated antitumor effects. J Immunol 2005;174:3925-3931.

45. Blattman JN, Greenberg PD: Cancer immunotherapy: a treatment for the masses. Science 2004;305:200-205.

46. Naito Y, Saito K, Shiiba K, Ohuchi A, Saigenji K, Nagura H, Ohtani H: CD8+ T cells infiltrated within cancer cell nests as a prognostic factor in human colorectal cancer. Cancer Res 1998;58:3491-3494.

47. Zhang L, Conejo-Garcia JR, Katsaros D, Gimotty PA, Massobrio M, Regnani G, Makrigiannakis A, Gray H, Schlienger K, Liebman MN, Rubin SC, Coukos G: Intratumoral T cells, recurrence, and survival in epithelial ovarian cancer. N Engl J Med 2003;348:203-213.

48. Piersma SJ, Jordanova ES, van Poelgeest MI, Kwappenberg KM, van der Hulst JM, Drijfhout JW, Melief CJ, Kenter GG, Fleuren GJ, Offringa R, van der Burg SH: High number of intraepithelial CD8+ tumor-infiltrating lymphocytes is associated with the absence of lymph node metastases in patients with large early-stage cervical cancer. Cancer Res 2007;67:354-361.

49. Vicari AP, Chiodoni C, Vaure C, Ait-Yahia S, Dercamp C, Matsos F, Reynard O, Taverne C, Merle P, Colombo MP, O'Garra A, Trinchieri G, Caux C: Reversal of tumor-induced dendritic cell paralysis by CpG immunostimulatory oligonucleotide and anti-interleukin 10 receptor antibody. J Exp Med 2002;196:541-549.

Chapter 4

Development of a sensitive and specific LC-MS method for the quantification of JSI-124 in rat plasma

---

A version of this chapter has been published: Molavi, O., Shayeganpour, A., Somayaji, V., Hamdy, S., Brocks, D., Lavasanifar, A., Kwon, G.K., Samuel, J. Development of a sensitive and specific liquid chromatography/mass spectrometry method for the quantification of cucurbitacin I (JSI-124) in rat plasma. *Journal of Pharmacy and Pharmaceutical Sciences* 9:19-25, 2006**.**

4.1 Introduction

JSI-124 (Cucurbitacin I) is an anticancer agent with potent and selective inhibitory effects on JAK2/STAT3 signaling pathway [1]. An important procedural aspect of new drug development and research is the establishment and validation of a satisfactory analytical method for the conduction of pharmaceutical and pharmacokinetic studies. To our knowledge, a few analytical methods have been reported for the analysis of cucurbitacins in plants and organic solutions [2,3]. Since the concentration of a natural compound such as JSI-124 in the plasma and other biosamples after dosing is always much lower than that in its organic extracts from plants, the previously developed methods may not be suitable for pharmacokinetic studies. The main purpose of this study was to develop and validate a sensitive and reproducible LC-MS method for quantitative analysis of JSI-124 in non-biological samples and rat plasma. The assay has been validated in order to meet the accepted criteria for a bioanalytical method [4].

4.2 Materials and Methods

4.2.1 Materials

JSI-124 (Cucurbitacin I) was purchased from Calbiochem (San Diego, California, USA). 4-hydroxybenzophenone was used as an I.S. from Sigma, Aldrich chemical company (Milwaukee, USA). Methanol, acetonitrile, dichloromethane, water (all HPLC grades) and formic acid 88% were purchased from Fisher Scientific (Fair Lawn, NJ, USA).

4.2.2 LC-MS conditions

LC-MS analyses were performed using a Waters Micromass ZQ 4000 spectrometer, coupled to a Waters 2795 separations module with an autosampler (Milford, MA, USA). The mass spectrometer was operated in negative ionization mode with SIR acquisition. The nebulizer gas was obtained from an in house high purity nitrogen source. The temperature of the source was set at 150°C, and the voltages of the capillary and cone were 3.11 KV and 24 V, respectively. The gas flow of desolvation and the cone were set at 550 and 80 L/h, respectively. Chromatographic separation was achieved using a Waters (Milford, MA, USA) XT_{erra}MSC18 3.5 µm (2.1×50 mm) as the stationary phase. The mobile phase consisting of a mixture of acetonitrile : water containing 1% formic acid with initial ratio of 20:80, employing a linear gradient to a final ratio of 40:60 v/v over 13 minutes, was delivered at a constant flow rate of 0.2 mL/min. 4-hydroxybenzophenone was used as I.S. Selected ion recorder (SIR) at *m*/*z* 559.14 corresponding to deprotonated molecular ion of JSI-124 + formic acid ([M–H + formic acid]) and at *m/z* 196.8 related to deprotonated molecular ion of I.S [M-H] were selected for quantification of JSI-124 and I.S., respectively.

4.2.3 Standard and stock solutions

A stock solution of JSI-124 was prepared by dissolving 1 mg of JSI-124 in 1 mL methanol. The solution was stored at -20°C between experiments. The working solution of JSI-124 was prepared fresh each day by making a 100-fold dilution of the stock solution in methanol. The calibration standards were then

prepared by serial dilution of the working solution. The stock solution of the I.S. was prepared by dissolving 5 mg of 4-hydroxybenzohpenone in 5 mL methanol, followed by the preparation of a working solution of 10 µg/mL by a further 100-fold dilution of the stock solution. The stock solution of I.S. was stored at -20°C between experiments and working solution of I.S. was prepared monthly from stock solution and was stored at 4°C.

4.2.4 Extraction procedure

To extract JSI-124 from plasma samples, 0.3 mL acetonitrile and 0.05 mL of I.S solution were added to 0.1 mL of rat plasma in a 1.5 mL centrifuge tube, which was briefly vortex-mixed to precipitate plasma proteins. The supernatants were transferred to clean glass tubes containing 0.3 mL HPLC grade water and 3 mL dichloromethane, vortex-mixed for 30 seconds and centrifuged at 3000 × g for 3 min. The resultant organic solvent layer was transferred to new tubes and evaporated to dryness in vacuo. The dried samples were reconstituted with 0.2 mL of methanol and an aliquot of 10 µL was injected into the LC-MS system.

4.2.5 Recovery

The extraction efficiency was determined by comparing peak area ratios between JSI-124 and I.S. of known amounts of JSI-124 in methanol directly injected to LC-MS (unextracted) to that of plasma samples containing the same amounts of JSI-124 in plasma after extraction. The recoveries were assessed at concentration of 50 and 1000 ng/mL using 4 replicates at each concentration.

4.2.6 Calibration, accuracy and validation

Calibration curves were constructed over the quantification limit 5-10000 ng/mL for the solution of JSI-124 in methanol and 10-1000 ng/mL for plasma samples. The ratios of JSI-124 to I.S. peak areas were calculated and plotted vs. JSI-124 concentration. Due to the wide range of concentrations, data for calibration curves were weighted by a factor of 1/concentration for plasma samples.

The method was tested in a 3-day validation protocol for quantification of JSI-124 in plasma samples. Selectivity, linearity; precision and accuracy of quantification were assessed. A total of five replicates for each concentration were used for the determination of intra-day precision and accuracy. The inter-day precision and accuracy were determined for three independent experimental assays of the aforementioned replicates. Precision was assessed by coefficient of variation, which was calculated as:

$$CV\%_{\text{int}\,raday} = \frac{100 \times SD}{Mean\ measured\ concentration}$$

and

$$CV\%_{\text{int}\,erday} = \frac{CV\%_{run1} + CV\%_{run2} + CV\%_{run3}}{3}$$

Bias was assessed by determining percent error, which was calculated as:

$$Mean\,\%\,error_{\text{int}\,raday} = 100 \times \frac{measured\ concentration - \exp ected\ concentration}{\exp ected\ concentration}$$

and

$$Mean\,\%\,error_{\text{int}\,erday} = \frac{error\,\%_{run1} + error\,\%_{run2} + error\,\%_{run3}}{3}$$

4.2.7 Animal study

To test the applicability of the developed method *in vivo*, three Sprague-Dawley rats (0.3 kg), were cannulated the day before the experiment in right jugular vein with Micro-Renathane tubing (Braintree Scientific, Braintree, MA) under halothane anesthesia as previously described [5]. The protocol was approved by the University of Alberta Health Sciences Animal Policy and Welfare Committee. JSI-124 was solublized by the aid of 2.5 % dimethyl sulfoxide (DMSO) in 5% glucose isotonic solution and injected to the rats at the dose of either 1.5 mg/kg or 1 mg/kg. Moreover micellar formulation of JSI-124 was prepared by PEO-*b*-PCL and injected intravenously to the rat at a dose of 0.4 mg/kg. Blood samples (100-200 μL) were nominally collected from the cannula at 0.083, 0.25, 0.75, 1, 2 and 3.5 h after dosing. Blood samples were immediately centrifuged for 3 min and the plasma was separated and stored at -30°C until analysis which was performed shortly after the experiment. The plasma concentration of JSI-124 was analyzed by the developed and validated LC-MS method and the time versus plasma concentration curve was profiled.

4.3 Results

4.3.1 Chromatography and mass conditions

The mass spectra of JSI-124 and I.S. dissolved in methanol with 1% formic acid is shown in Figure 4-1. The molecular ion at m/z of 559 corresponding to [M-H + formic acid] and m/z of 196.8 related to [M-H] were selected for quantification of JSI-124 and I.S., respectively.

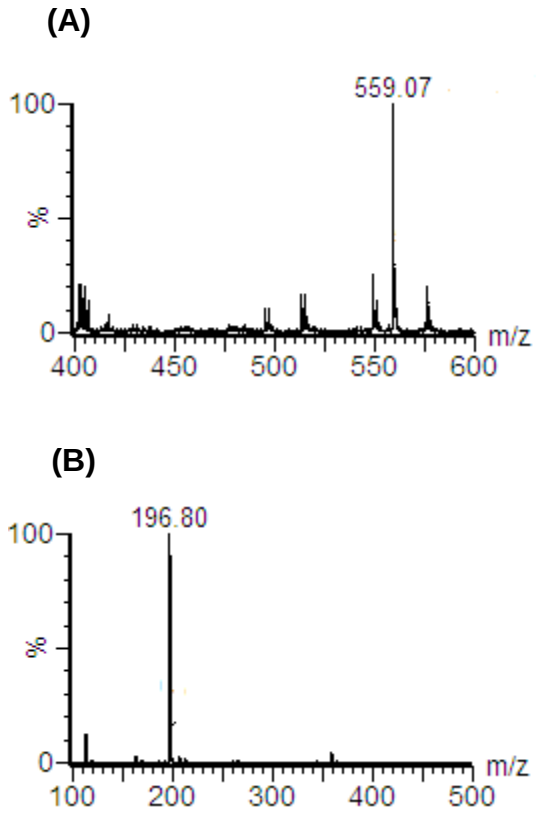

Figure 4-1. Mass spectra of A) JSI-124 and B) I.S. in methanol containing 1% formic acid.

Figure 4-2 shows the SIR chromatograms of JSI-124 and I.S in methanol. Peaks of JSI-124 and I.S. are well separated in the established chromatographic condition. The retention times of JSI-124 and I.S. were approximately 12 and 11 min, respectively, and the analytical run time was 15 min.

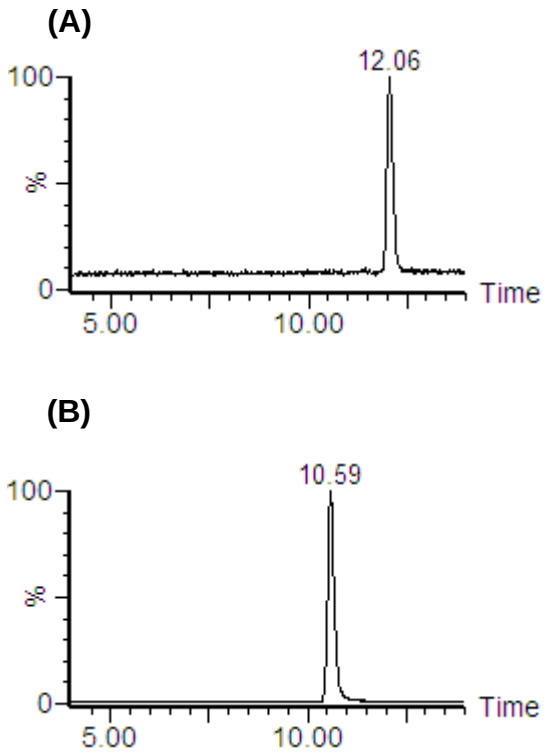

Figure 4-2. SIR chromatograms of A) JSI-124 and B) I.S in methanol monitored at 559 m/z for JSI-124 and 196.8 m/z for I.S.

SIR chromatograms of JSI-124 and I.S. in rat plasma are shown in Figure 4-3. The chromatogram of JSI-124 in the plasma sample from the rat received JSI-124 by i.v route showed that there was no endogenous plasma component interfering with this compound (Figure 4-3 C).

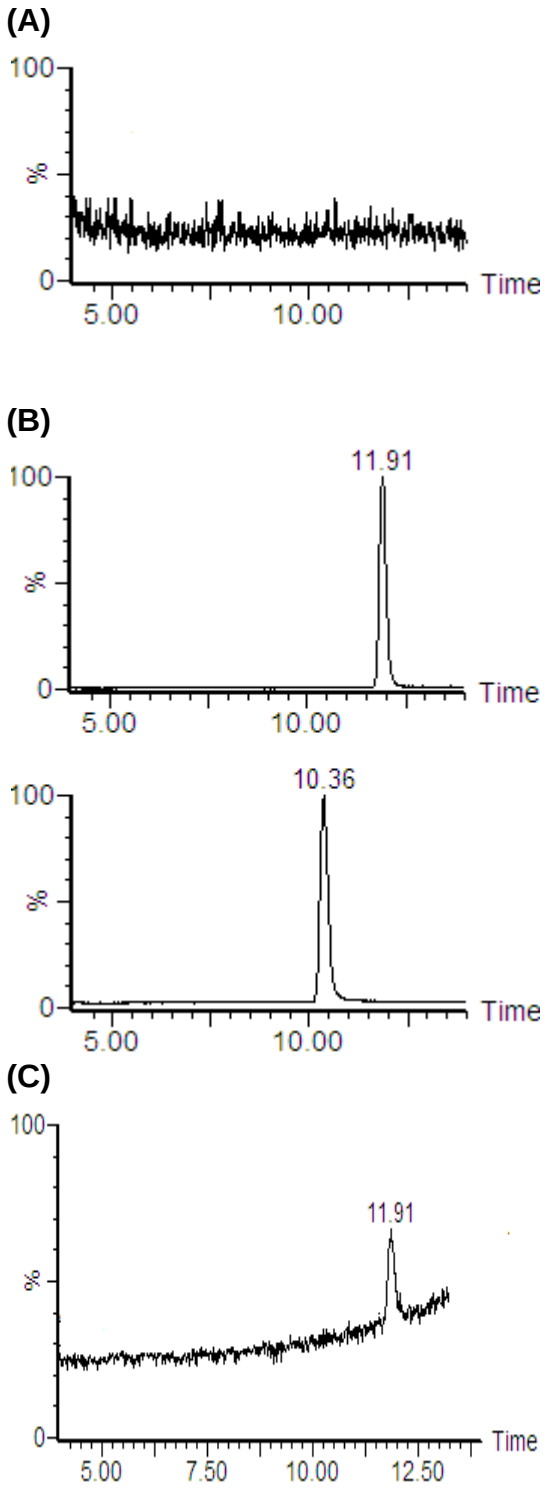

Figure 4-3. SIR Chromatograms of JSI-124 in rat plasma; A) blank rat plasma; B) blank plasma spiked with 100 ng/mL JSI-124 and I.S.; C) rat plasma after 3.5 h, i.v injection of 0.4 mg/kg JSI-124.

4.3.2 Linearity of calibration curves

The regression analysis of JSI-124 was constructed by plotting the peak-area ratio of JSI-124 to I.S. versus analyte concentration (ng/mL). The calibration curve was linear (r^2>0.999) within the range of 5-10000 ng/mL for the solution of JSI-124 in methanol as well as 10-1000 ng/mL of the compound extracted from rat plasma samples (Figure 4-4).

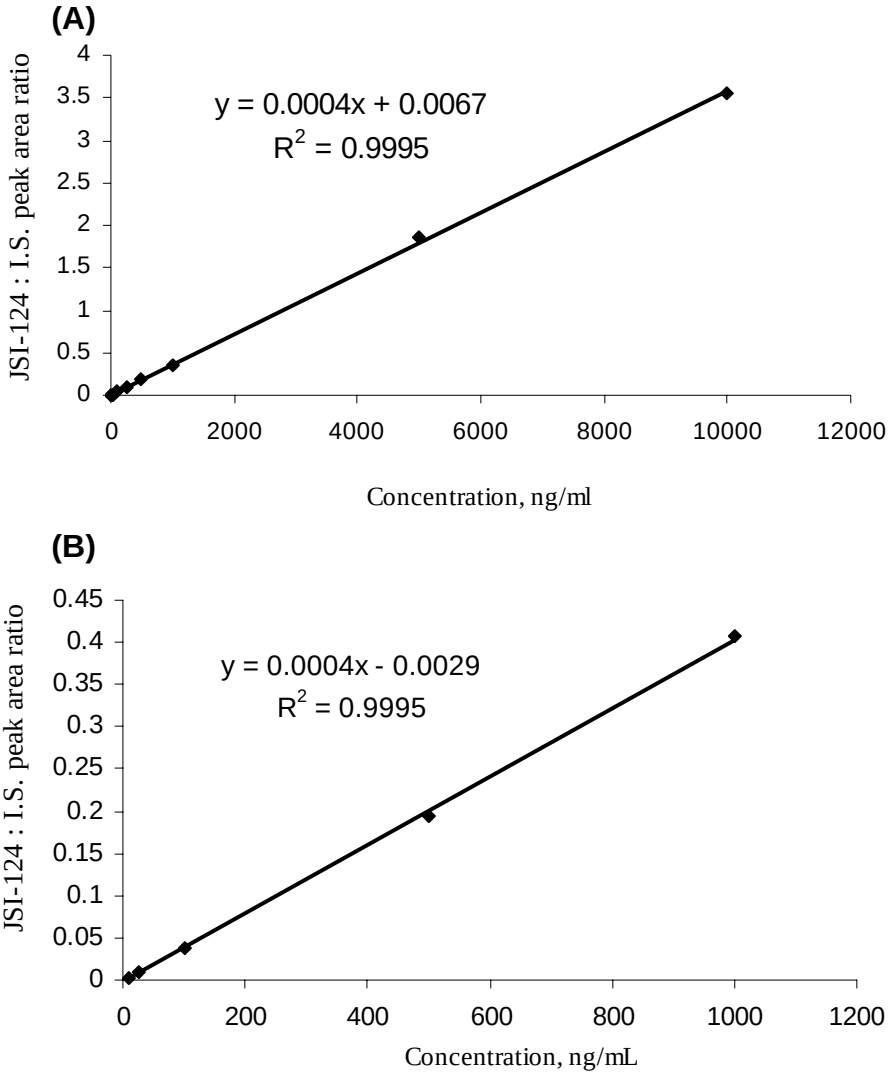

Figure 4-4. A representative standard curve for A) JSI-124 in methanol extending from 5-10000 ng/mL and B) in rat plasma extending from 10-1000 ng/mL.

4.3.3 Accuracy and precision

The average extraction recoveries were 86 and 98% at the concentration of 50 and 1000 ng/mL of JSI-124 in 0.1 mL plasma, respectively. The assay coefficient of variation at all of the intraday and interday assessment was less than 15%, and the mean intraday error in rat plasma was less than 10% (Table 4-1). The lower limit of quantification of the assay based on the mean error and CV% results was 10 ng/mL.

Table 4-1. Validation data for JSI-124 in rat plasma. Five replicates per concentration were included for each intraday run.

Expected concentration of JSI-124 (ng/mL)	Intraday mean± SD measured concentrations (intraday CV% in parenthesis), (ng/mL)			Interday mean±SD measured concentrations, (ng/mL)	Interday CV (%)	Interday mean error (%)
10	11.8±1.45 (12.3)	11.5±1.60 (13.9)	10.4±1.44 (13.8)	11.2±0.73	13.3	9.55
25	28.7±3.29 (11.5)	25.3±2.97 (11.7)	28.0±3.54 (12.7)	27.3±1.79	12.0	1.27
100	107±10.0 (9.33)	100±7.35 (7.32)	86.1±6.26 (7.27)	97.9±10.8	7.98	7.20
500	434±18.8 (4.34)	520±17.2 (3.31)	488±10.8 (2.22)	481±43.4	3.29	-2.26
1000	989±4.48 (0.453)	960±46.2 (4.82)	997±39.6 (3.97)	982±20.0	3.08	-1.63

4.3.4 Application of the method

In order to test whether this method can satisfy the needs of a pharmacokinetics study, three rats were injected through i.v route with either 1.5 mg/kg or 1 mg/kg single dose of JSI-124 solubilized in 5% glucose solution with 2.5% DMSO or 0.4 mg/kg single dose of a micellar formulation of JSI-124. The plasma concentration vs. time profile could be studied for up to 3.5 h after dosing with the micellar formulation and up to 2 h after i.v injection of drug solution in 5% glucose (Figure 4-5). The rat injected with the micellar formulation did not

experience any overt signs of toxicity with the drug, but the two other rats injected with either 1.5 mg/kg or 1 mg/kg of JSI-124 solubilized in isotonic glucose solution appeared to have labored breathing within 1 h after the dose was administered, and perished shortly after the 2 h blood sample was withdrawn.

The data using the administered micellar formulation appeared to fit well to a one compartment open model, although there was a suggestion of a distribution phase from time of dosing to 0.75 h postdose (Figure 4-5). The terminal half-life was estimated to be 1.4 h in the rat. The distribution phase was more apparent in the data of the rat given the non-micellar formulation, and within 2 h the concentrations fell to near to the lower limit of quantitation even with the higher dose compared to the rat given the micellar formulation.

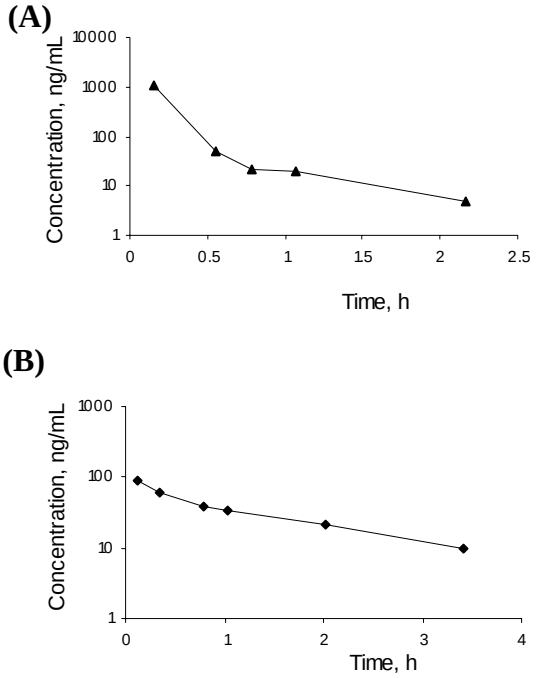

Figure 4-5. Plasma concentration vs. time profiles of A) JSI-124 solubilized in 5% glucose solution with 2.5% DMSO and given at a dose of 1.5 mg/kg by intravenous bolus injection B) JSI-124 given in micellar formulation at a dose of 0.4 mg/kg by intravenous bolus injection.

4.4 Discussion

The assay described in this study is highly specific, sensitive and reproducible for the quantitative analysis of JSI-124 in non-biological solvents as well as rat plasma samples. The calibration curves were highly linear over a wide range of concentrations (Figure 4-4). The extraction procedure used in this work yielded good recoveries as well as high repeatability. These two requisites are of great importance when an analytic method needs to be validated for providing reliable data. Another notable advantage of the current method is that it uses a stable and commercially available internal standard.

The specificity of the LC-MS method makes the determination of this compound in the presence of other endogenous and exogenous plasma components possible. The chromatographs of JSI-124 and I.S. in rat plasma (Figure 4-3) showed that no significant interfering peak was co-eluted with the JSI-124 and I.S. After administration of the drug to rat, there was no evidence in the chromatogram of chromatographic interference (Figure 4-3C).

The analytical precision data (Table 4-1) demonstrate the robustness and reproducibility of the developed method as well as its high sensitivity (50 Pg). The detection limit of the method is as low as 10 ng/mL in rat plasma allowing quantification of JSI-124 at low concentrations in body fluids. The application of the developed LC-MS method for a pharmacokinetic study was successful (Figure 4-5). Determination of drug levels in body fluids such as plasma is important in general unknown screening, toxicological evaluations, and in pharmacokinetic

studies to guide the tailoring of the dose for newly developed pharmaceutical components.

In conclusion, we have described the first LC–MS method for the quantitative analysis of JSI-124 in plasma. The reproducibility, specificity and high sensitivity of the method allows for the selective and reliable determination of JSI-124 in rat plasma.

4.5 References

1. Blaskovich MA, Sun J, Cantor A, Turkson J, Jove R, Sebti SM: Discovery of JSI-124 (cucurbitacin I), a selective Janus kinase/signal transducer and activator of transcription 3 signaling pathway inhibitor with potent antitumor activity against human and murine cancer cells in mice. Cancer Res 2003;63:1270-1279.
2. Seger C, Sturm S, Haslinger E, Stuppner H: A new cucurbitacin D related 16,23-epoxy derivative and its isomerization products. Org Lett 2004;6:633-636.
3. Halaweish FT, Tallamy DW: Quantitative determination of cucurbitacins by high performance liquid chromatography and high performance thin layer chromatography. *J. Liq. Chromatogr* 1993;16: 497-511.
4. FDA guidance C, US Department of Health and Human Services, Food and Drug, Administration CfDEaRaCfV, (CVM). M: Guidance for the Industry. Bioanalytical Method validation. 2001.
5. Brocks DR: Stereoselective pharmacokinetics of desbutylhalofantrine, a metabolite of halofantrine, in the rat after administration of the racemic metabolite or parent drug. Biopharm Drug Dispos 2000;21:365-371.

Chapter 5

Polymeric micelles for the solubilization and delivery of STAT3 inhibitor cucurbitacins in solid tumors

---

A version of this chapter has been published: Molavi, O., Ma, Z., Mahmud, A., Alshamsan, A., Lavasanifar, A., G S. Kwon and Samuel, J. Polymeric micelles for the solubilization and controlled delivery of STAT3 inhibitor cucurbitacins in solid tumors. *International Journal of Pharmaceutics* 347:118-127, 2008.

5.1 Introduction

JSI-124 (Cucurbitacin I) and cucurbitacin B (Figure 1-7) are potent anticancer agents with selective inhibitory effect on STAT3 pathway [1-3]. STAT3 is a common oncogenic signaling pathway which is constitutively activated in many types of cancers [4] and plays a major role in tumor cell growth, resistance to apoptosis and immune evasion by cancer. STAT3 inhibitory and potent anti-proliferative activity of JSI-124 and cucurbitacin B make them excellent and novel drug candidates in cancer therapy. However, problems of poor water solubility and non-specific toxicity have restricted their clinical benefit. Application of nanoscopic carriers such as polymeric micelles for the delivery of cucurbitacins is expected to overcome both limitations and enhance the therapeutic benefit of this important and emerging category of anticancer drugs.

Polymeric micelles, nanoscopic carriers with a hydrophilic shell/ hydrophobic core structure, have shown great promise in the solubilization and controlled delivery of hydrophobic drugs [5]. Polyethylene oxide block used as a hydrophilic shell of micelles, masks the hydrophobic block from biological milieu leading to their prolonged circulation following i.v. administration. Longevity in blood circulation is followed by improved tumor accumulation through EPR effect leading to enhanced drug delivery with reduced toxicity [6,7]. To date, only a limited number of polymeric micellar systems have shown positive results in tumor targeted delivery of poorly soluble drugs after systemic administration [8]. The key to success is to find the right drug-block copolymer combination that can withstand the destabilizing effect of biological environment and provide a proper

pattern of drug release in the biological system. PEO-*b*-PCL is a biocompatible copolymer which have been successfully used for the solubilization and controlled delivery of a number of hydrophobic drugs [9-12]. PEO-*b*-PCL micelles were also shown to cause a favorable shift in the pharmacokinetics and biodistribution of cyclosporine A and Hydroxylcampthotecin after i.v administration [13,14]. In this study, we have compared the potential of micelle-forming PEO-*b*-PCLs of different PCL molecular weights and the newly developed block copolymer, PEO-*b*-PBCL, as nanoscale drug delivery systems for the solubilization and controlled delivery of JSI-124 and cucurbitacin B. The anticancer activity of polymeric micellar formulations of cucurbitacins in a mouse melanoma tumor model has been also evaluated and compared to the activity of free drug both *in vitro* and *in vivo* after intra-tumoral administration.

5.2 Materials and methods

5.2.1 Materials

JSI-124 was purchased from Calbiochem (San Diego, CA 92121, USA). Cucurbitacin B was obtained from PhytoMyco Research Corporation (Greenville, North Carolina, USA). Methoxy PEO (average molecular weight of 5000 $g.mol^{-1}$), diisopropyl amine (99%), benzyl chloroformate (tech. 95%), sodium (in kerosin), butyl lithium (Bu-Li) in hexane (2.5 M solution), palladium coated charcoal, pyrene and thiazolyl blue tetrazolium bromide were purchased from Sigma (St. Louis, MO, USA). Caprolactone was purchased from Lancaster Synthesis, UK. Stannous octoate was purchased from MP Biomedicals Inc,

Germany. Fluorescent probe 1,3-(1,1′-dipyrenyl)propane was purchased from Molecular Probes, USA. All other chemicals were reagent grade.

5.2.2 Preparation and characterization of micellar formulations of JSI-124 and cucurbitacin B

PEO-*b*-PCL block copolymers having identical PEO chain molecular weight of 5000 g mol^{-1} and PCL molecular weights of 5000 or 24000 g mol^{-1} were synthesized by ring opening polymerization of ε-caprolactone using methoxy polyethylene oxide (MW ¼ 5000 g/mol) as initiator and stannous octoate (0.5% w/w) as catalyst [12]. Briefly Methoxy PEO (5 gram), ε-caprolactone (13 gram) and stannous octoate (92 mg) were added to a 10 mL previously flamed ampoule, nitrogen purged and sealed under reduced pressure. The reaction proceeded at 140 ◦C for 4 h. Synthesized block copolymer was dissolved in chloroform, collected by centrifuge after precipitation in an excess volume of cold methanol and dried under vacuum. To synthesize PEO-*b*-PBCL block copolymer, the functionalized monomer, i.e., α-benzylcarboxylate-ε-caprolactone, was synthesized according to the method reported previously [15]. Briefly Bu-Li (24 mL, 60 mmol) in hexane was slowly added to a solution of 60.0 mmol (8.4 ml) of dry diisopropylamine in 60 ml of dry THF in a three neck round bottom flask at −30°C under vigorous stirring with continuous argon supply. The solution was cooled to −78°C and kept stirring for additional 20 min. Freshly distilled ε-caprolactone (30 mmol or 3.42 gram) was dissolved in 8 mL of dry THF and added to the above mentioned mixture slowly, followed by the addition of benzyl chloroformate (30 mmol, 5.1

gram). The temperature was allowed to rise to 0°C after 1.5 h and the reaction was quenched with 5 ml of saturated ammonium chloride solution. The reaction mixture was diluted with water and extracted with ethyl acetate (3× 40 ml). The combined extracts were dried over Na_2SO_4 and purified by using silica gel. The purity of the monomer was confirmed with thin layer chromatography (TLC). PEO-*b*-PBCL copolymer was synthesized by the same method as described above for synthesis of PEO-*b*-PCL polymers. Synthesized block copolymers were characterized for their number average molecular weight using ^{1}H NMR and Gel Permeation Chromatography (GPC). A nomenclature , e.g., 5000-4700, 5000-5000 and 5000-24000, in which the left number corresponds to the theoretical molecular weight of the shell forming block and the right number corresponds to the molecular weight of the core forming block, is used throughout the manuscript to distinguish between prepared block copolymers. Encapsulation of cucurbitacins in PEO-*b*-PCL (5000-5000 and 5000-24000) and PEO-*b*-PBCL (5000-4700) micelles was achieved by a co-solvent evaporation method [12]. Briefly 20 mg of copolymer and 2 mg of either cucurbitacin B or JSI-124 were dissolved in 0.5 mL acetone. This solution was added to 2 mL distilled water (ddH_2O) in a drop-wise manner. After 4 h stirring at room temperature, the remaining acetone was removed by vacuum. The aqueous solution of the micellar formulation was then centrifuged at 14000 rpm for 5 min to remove free drug precipitates. Mean diameter and polydispersity of the micelles were defined by dynamic light scattering (DLS) technique using a Zetasizer 3000 (Malvern, UK).

5.2.3 Determination of encapsulation efficiency by LC-MS

To determine the level of encapsulated cucurbitacin in PEO-*b*-PCL and PEO-*b*-PBCL micelles, aqueous solution of polymeric micelles were placed in centrifugal filter tubes (MW. cut-off = 100,000 g mol $^{-1}$) and centrifuged at 3000 × *g* for 5 min to separate precipitated and micelle-incorporated drug. Then 50 μL aliquot of the micellar solution (the top layer) was diluted in 0.95 mL methanol to disrupt the micellar structure and release incorporated drug. Diluted solution (0.1 mL) was added to 0.1 mL of 4-hydrogybenzophenone solution (0.01mg/mL methanol), which was used as I.S. This solution (10 μL) was injected to Waters Micromass ZQ 4000 LC-MS spectrometer. Quantitative analysis of JSI-124 by LC-MS was performed as described in chapter 4 section 4.2.2 [16]. For quantification of cucurbitacin B by LC-MS, mass spectrometer was operated in negative ionization mode with selected ion recorder acquisition. Then the analytes were quantified with SIR at m/z 557 corresponding to [M-H] and m/z 539 corresponding to [M-H_2O-H] for cucurbitacin B and at *m/z* 196.8 for I.S. For chromatographic separation a mobile phase consisting of a mixture of acetonitrile: water containing 0.2% ammonium hydroxide (40:60) was employed for 3 min. This was followed by a non-linear gradient to a final ratio of 60:40 v/v over 8 min at a constant flow rate of 0.2 mL/min. Calibration curves were constructed over the quantification range of 5 to 10000 ng/mL for both JSI-124 and cucurbitacin B. The ratios of cucurbitacin to I.S. peak areas were calculated and plotted vs. cucurbitacin concentration. Cucurbitacin loading and encapsulation efficiency were calculated by the following equations:

$$Cucurbitacin\ loading\ (w/w) = \frac{amount\ of\ loaded\ cucurbitacin\ \ in\ mg}{amount\ of\ \ polymer\ in\ mg}$$

$$Cucurbitacin\ loading\ (M/M) = \frac{moles\ of\ \ loaded\ \ cucurbitacin}{moles\ of\ \ polymer}$$

$$Encapsulation\ Effeciency\ (\%) = 100 \times \frac{amount\ of\ cucurbitacin\ loaded\ \ in\ mg}{amount\ of\ cucurbitacin\ added\ \ in\ mg}$$

5.2.4 *In vitro* release study

Release study was preformed using dialysis method as reported previously [17]. As a control, free JSI-124 and cucurbitacin B were dissolved in water at a concentration of 1 mg/mL with the aid of methanol (2% v/v). Aqueous solution of polymeric micellar JSI-124 and cucurbitacin B were also prepared at a similar concentration. One mL of each sample was placed in a Spectra/Pore dialysis bag (M. wt. cut-off = 12000-14000 g mol $^{-1}$). The dialysis bag was located in 100 mL ddH_2O and whole system was placed in a rotating water bath where temperature was kept at 37 °C during the experiment. In order to maintain "perfect sink" conditions, the bath was overflowed with fresh ddH_2O so that the bath volume was refreshed every 1 h. Aliquots were taken at each time point from inside cassettes and drug concentrations were measured by LC-MS. Remaining drug in cassettes was determined and measurements were corrected for drug removed in the previous samples.

5.2.5 Cell viability assay

Anti-proliferative activity of free and PEO-*b*-PCL micellar cucurbitacin was assessed in B16-F10, a melanoma of C57/black origin (ATCC)**.** B16-F10 cells were grown in DMEM supplemented with 10% FBS, 2 mM L-glutamine and 100 IU/ml penicillin/streptomycin in 5% CO_2 atmosphere. Cell viability was monitored using the 3-(4,5-dimethylthiazole-2-yl)-2,5-biphenyl tetrazolium bromide (MTT) assay [18]. To evaluate cytotoxicity, B16-F10 cells were obtained from exponentially growing 90-95% confluent cultures and seeded at a density of 2000 cells/well in 96-well plates. After two days incubation the cells were washed twice in serum-free medium and treated with control vehicles (2% methanol and empty PEO-*b*-PCL micelles) or four different concentrations of either JSI-124 or cucurbitacin B, dissolved in methanol or encapsulated in 5000-24000 PEO-*b*-PCL micelles. After 24 or 48 h incubation at 37°C the medium was removed and cells were washed three times with the media followed by addition of 20 μL of 2 mg/mL solution of tetrazolium MTT dye. The plates were returned to the incubator for a period of 4 h. The residual MTT solutions were removed from wells then 0.2 mL of DMSO was added to each well and the plates were read at 570 nm using plate reader (PowerWave 340, Bio-Tek instruments Inc.). Concentrations required for 50% inhibition in cell growth (IC_{50}) were determined from log-linear dose-response curves for each agent.

5.2.6 Western blot analysis

To evaluate the effect of JSI-124 and cucurbitacin B formulations on STAT3 phosphorylation, B16 cells were plated into 6-well tissue culture plates (2x106 cells/well). Cells were then incubated with JSI-124 at a concentration of 10 μM or cucurbitacin B at concentration of 40 μM in either soluble form in 2% methanol or encapsulated in 5000-24000 PEO-*b*-PCL micelles for 24 h at 37°C. Cells were then collected and washed twice with ice-cold PBS and then lysed in a buffer containing 30 mM HEPES (pH 7.5), 2 mM Na_3VO_4, 25 mM NaF, 2 mM EGTA, 2% Nonidet P-40, 1:100 protease inhibitor mixture (Sigma-Aldrich), 0.5 mM DTT and 6.4 mg/mL Sigma 104 Phosphatase Substrate (Sigma-Aldrich). Then cells lysates were processed for Western blot analysis as described in chapter 3 section 3.2.6.

5.2.7 *In vivo* anti-tumor activity

The animal studies were carried out in accordance with procedures approved by the University of Alberta Health Sciences Animal Policy and Welfare Committee. A group of 16 C57Bl/6 mice were injected subcutaneously with 10^6 B16-F10 melanoma cells at their left flank. Tumors were allowed to grow until they reached approximately 110-130 mm^3 in size. Animals were then randomly assigned to four groups (4 mice per group). Control groups were kept untreated or received daily intra-tumoral injection of empty PEO-*b*-PBCL micelles. Test groups were treated with 1 mg /kg JSI-124 in either soluble form (in 20% ethanolic solution) or encapsulated in PEO-*b*-PBCL micelles daily

through intra-tumoral injection. Tumor size was measured during treatment three times a week by vernier caliper. Tumor volume (mm^3) was calculated using the following equation: Tumor volume = (longer diameter) x (shorter diameter)^2/2.

Tumor-bearing animals were sacrificed 8-10 days after treatment and blood and/or samples were collected. JSI-124 was extracted from mice serum and tumor samples and quantified by LC-MS as described in chapter 4 section 4.2.2 and 4.2.4.

5.2.8 Statistical analysis

The results are expressed as mean ± one standard deviation for each group. The significance of differences among groups was analyzed by one-way or two-way ANOVA followed by the Student-Newman-Keuls post hoc test for multiple comparisons. Before executing the ANOVA, data were tested for normality and equal variance. If any of those tests failed, data were compared using a Kruskal-Wallis one-way ANOVA on ranks. A P value of ≤ 0.05 was set for the significance of difference among groups. The statistical analysis was performed with SigmaStat software (Jandel Scientific, San Rafael, CA).

5. 3 Results

5.3.1 Encapsulation of JSI-124 and cucurbitacin B in polymeric micelles

Table 5-1 summarizes the characteristics of 5000-5000 and 5000-24000 PEO-*b*-PCL and 5000-4700 PEO-*b*-PBCL micelles loaded with cucurbitacin B and JSI-124. Polymeric micelles were able to increase the water solubility of cucurbitacins. The aqueous solubility of both derivatives increased from less than 0.05 mg/mL in the absence of the copolymer to around 0.30-0.44 and 0.65-0.68 mg/mL in the presence of 5000-5000 and 5000-24000 PEO-*b*-PCL micelles, respectively. Water solubility of JSI-124 in the presence of 5000-5000 PEO-*b*-PCL was found to be higher than that of B derivative (0.44 versus 0.30 mg/mL) ($P<0.05$, ANOVA). Between the two PEO-*b*-PCL micelles, those having longer PCL blocks were found to be more efficient in encapsulating both cucurbitacin derivatives. Maximum cucurbitacin solubilization was achieved with PEO-*b*-PBCL micelles for both derivatives (Table 5-1) despite a lower molecular weight of the PBCL block (4700 $g.mol^{-1}$). The difference in the solubilization of cucurbitacins by 5000-4700 PEO-*b*-PBCL in comparison to 5000-24000 PEO-*b*-PCL was more evident for the more hydrophobic derivative; i.e, cucurbitacin B. The aqueous solubility of cucurbitacin B and JSI-124 was found to be 0.92 and 0.74 mg/mL in the presence of PEO-*b*-PBCL micelles corresponding to an encapsulation efficiency of 92.9 and 74.1 %, respectively.

Table 5-1. Characteristics of cucurbitacin-loaded PEO-*b*-PCL and PEO-*b*-PBCL micelles (mean± S.D., n=3)

Compound	Copolymer /M.wt (g mol^{-1})	Cucurbitacin loading ± SD (mg/mg)	Cucurbitacin loading ± SD (M/M)	Encapsulation efficiency ± SD (%)	Micellar Size (nm)	Polydispersity Index
Cucurbitacin B	PEO-*b*-PCL 5000-5000	0.03±0.003	0.54±0.07	30.2±3.9	73.3±1.15	0.27±0.02
	PEO-*b*-PCL 5000-24000	0.065±0.003	3.38±0.19	65.1±3.8	78.2±1.11	0.26±0.01
	PEO-*b*-PBCL 5000-4700	0.092±0.005	1.65±0.09	92.9±4.6	76.3±7.12	0.26±0.02
JSI-124	PEO-*b*-PCL 5000-5000	0.044±0.01	0.86±0.2	44.1±10	72.2±2.01	0.27±0.026
	PEO-*b*-PCL 5000-24000	0.068±0.006	3.91±0.37	68.4±6.6	77.2±2.01	0.17±0.029
	PEO-*b*-PBCL 5000-4700	0.074±0.007	1.42±0.14	74.1±7.5	74.1±7.5	0.24±0.03

5.3.2 Release of cucurbitacin B and JSI-124 from polymeric micelles

The release profile of cucurbitacin B and JSI-124 from a methanolic solution and micellar formulations evaluated by dialysis method are shown in Figure 5-1A and B, respectively. The transfer of solubilized cucurbitacins from methanolic solution through the dialysis bag was found to be relatively rapid (> 60 and 90 % transfer in 1 and 4 h, respectively, for both derivatives). The 5000-5000 PEO-*b*-PCL micelles showed a burst release (42% release) for cucurbitacin B within 1 h followed by an accumulative 64% of encapsulated drug release within 8 h. An increase in the molecular weight of PCL block from 5000 to 24000 g mol^{-1} significantly reduced the burst release of cucurbitacin B in the first hour of experiment from 42 to 23% and resulted in a significant decrease in accumulative drug release ($P<0.0001$, ANOVA). This system released 40 % of its drug content

within 8 h (Figure 5-1A). The release profile of cucurbitacin B from PEO-*b*-PBCL micelles was similar to that for 5000-5000 PEO-*b*-PCL micelles, i.e., a burst release (around 45 %) within 1 h followed by an accumulative 64 % of encapsulated drug release within 8 h. In the case of JSI-124, 5000-5000 PEO-*b*-PCL showed a burst release of 55 % in the first hour followed by 90 % drug release within 8 h (Figure 5-1B). PEO-*b*-PCL micelles having 24000 $g.mol^{-1}$ of PCL significantly reduced the burst release of JSI-124 as well as accumulative drug release percent in 8 h ($P<0.0001$, ANOVA). This system showed a burst release of 30 % within 1 h followed by an accumulative release of 80 % for incorporated JSI-124 in 8 h. Micelles of PEO-*b*-PBCL showed a similar release profile for JSI-124 to that of 5000-5000 PEO-*b*-PCL micelles in initial time points (50% drug release at 1 h), but a decreased rate of JSI-124 release at later times (80% drug release at 8 h) (Figure 5-1B).

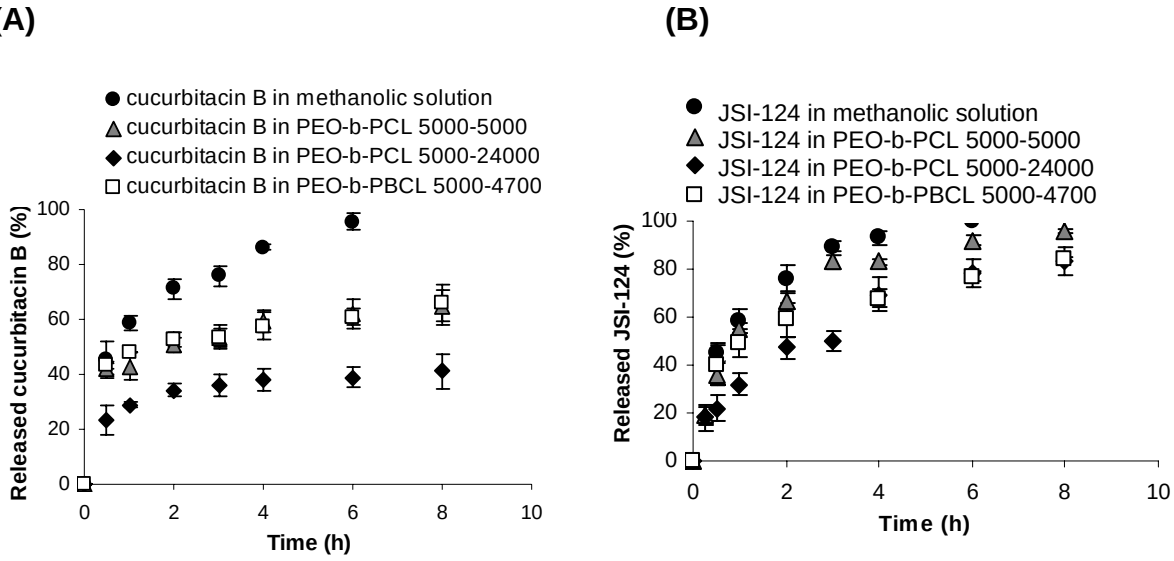

Figure 5-1. The effect of solubilizing vehicle on the *in vitro* release rate of A) cucurbitacin B; and B) JSI-124. Data shown are representative of three independent experiments and the values for each time point are mean of triplicates ± SD

5.3.3 Anticancer activity of free and polymeric micellar cucurbitacin B and JSI-124 in B16-F10 cell line *in vitro*

Figure 5-2 A and B depict the anticancer activity of methanolic solution or polymeric micellar formulation of JSI-124 and cucurbitacin B against B16-F10 cells after 24 and 48 h incubation. Treatment of B16 melanoma cells with increasing concentrations of JSI-124 or cucurbitacin B as free or encapsulated in 5000-24000 PEO-*b*-PCL micelles resulted in a significant loss of cell viability assessed by MTT assay. JSI-124 exerted more potent anti-proliferative activity than cucurbitacin B against the B16-F10 melanoma cells. Treatment of B16-F10 cells with JSI-124 in methanolic solution for 24 h at concentrations of 1, 5, 10 and 20 μM reduced the cell viability of treated cells to 81, 51, 43 and 22 % of untreated cells, respectively (Figure 5-2B), whereas cucurbitacin B incubation with B16-F10 melanoma cells for the same incubation period at concentrations of 1 and 5 μM didn't result in any significant loss of the cell viability and the presence of B derivative at concentrations of 10 and 20 μM left 64 and 47 % of B16-F10 cells viable, respectively (Figure 5-2A). As it has been shown in Table 5-2 the IC_{50} values for JSI-124 against the B16-F10 melanoma cells after 24 and 48 h incubation were significantly lower than those for cucurbitacin B at the same incubation time ($P<0.0001$, ANOVA). The IC_{50} values of free cucurbitacin B and JSI-124 after 24 h incubation were 18.9 and 4.7 μM. After 48 h incubation, the IC_{50} was calculated at 16.1 and 4.6 μM for cucurbitacin B and JSI-124, respectively.

Similar difference between the anti-proliferative activity of encapsulated cucurbitacin B and JSI-124 was observed. Treatment of B16-F10 cell with polymeric micellar cucurbitacin B at concentrations of 10, 20, 30 and 50 μM for 24 h reduced the cell viability to 83, 63, 61 and 58 %, which were significantly higher than the viability of the cells treated with free drug at identical concentrations ($P<0.0001$, ANOVA). However, when the incubation time was increased to 48 h, the viability of B16-F10 cells treated with polymeric micellar cucurbitacin B was not significantly different from that of free cucurbitacin B (Figure 5-2A) ($P>0.05$, ANOVA). When B16-F10 cells were treated with polymeric micelles of JSI-124, at concentrations of 1, 5, 10 and 20 μM, the viability of B16-F10 cells was 91, 60, 56 and 32 % of untreated cells after 24 h incubation, respectively. As Figure 5-2B indicates, the viability of B16-F10 cells treated with free JSI-124 at the same concentrations for the same period of time were significantly lower than what was observed with polymeric micellar JSI-124 ($P<0.0001$, ANOVA). Treatment of B16-F10 cell with polymeric micellar JSI-124 at the same concentrations for 48 h left 84, 53, 40 and 24 % of the cells viable, which were not significantly different from what was observed with free JSI-124 ($P>0.05$, ANOVA). As illustrated in Table 5-2, IC_{50} values for free form of both derivatives are significantly different from those for their polymeric micellar formulation after 24 h incubation ($P<0.05$, ANOVA). However, there is no significant differences in IC_{50} values between free and encapsulated forms of both derivatives after 48 h incubation ($P>0.05$, ANOVA). PEO-*b*-PCL and PEO-

b-PBCL block copolymers did not show any cytoxicity against B16-F10 cells when incubated at concentrations as high as 500 μg/mL or below for 24 h.

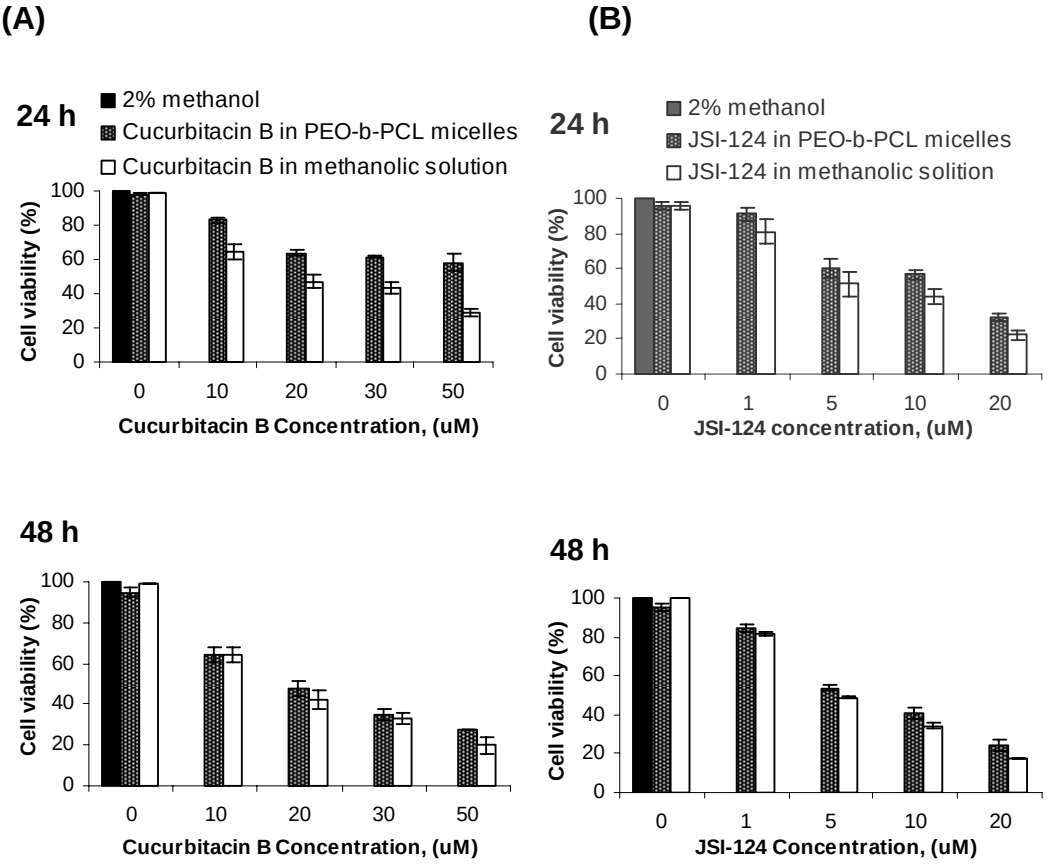

Figure 5-2. Anticancer activity of free and polymeric micellar (A) cucurbitacin B; (B) JSI-124 formulations against B16-F10 melanoma cell line after 24 and 48 h incubation, *in vitro*. B16-F10 cells were treated with 5 different concentrations of either cucurbitacin B or JSI-124 formulations in free or polymeric micellar form. After 24 or 48 h incubation, cell viability was estimated by MTT assay and expressed as percentage of untreated controls. The data represent the mean ± SD of three independent experiments

Table 5-2. The IC_{50} values of free and polymeric micellar cucurbitacins against B16-F10 cells (n=3)

Drug	Vehicle	IC_{50} ± SD(μM)	
		24 h	48h
Cucurbitacin B	2% Methanol	18.9 ± 2.1	16.1 ± 2.1
	5000-24000 PEO-*b*-PCL micelles	[a]52.9 ± 2.8	17.1 ± 0.3
JSI-124	2% Methanol	[b]4.7± 1.6	[b] 4.6 ± 0.1
	5000-24000 PEO-*b*-PCL micelles	[a,b] 9.7 ± 1.1	[a,b] 5.9 ± 0.5

[a] significantly different from free drug ($p<0.05$)
[b] significantly different from cucurbitacin B ($p<0.05$)

5.3.4 STAT3 inhibitory activity of free and polymeric micellar formulation of cucurbitacin B and JSI-124 in B16-F10 cell lines *in vitro*

Cucurbitacin B and JSI-124 are selective inhibitors of Janus kinase (JAK)/STAT3 pathway and block STAT3 activation through reduction in the phosphotyrosine STAT3 level in tumor cells. Measuring the level of p-STAT3 in B16-F10 using Western blot analysis provided means to evaluate the anit-STAT3 activity of cucurbitacin formulations in this study. As it is shown in Figure 5-3A, treatment of B16-F10 cells with free or in 5000-24000 PEO-*b*-PCL micellar cucurbitacin B at concentration of 40 μM for 24 h resulted in the suppression of p-STAT3 level. Free and 5000-24000 PEO-*b*-PCL micellar JSI-124 were found to reduce the level of p-STAT3 at a concentration of 10 μM (Figure 5-3B).

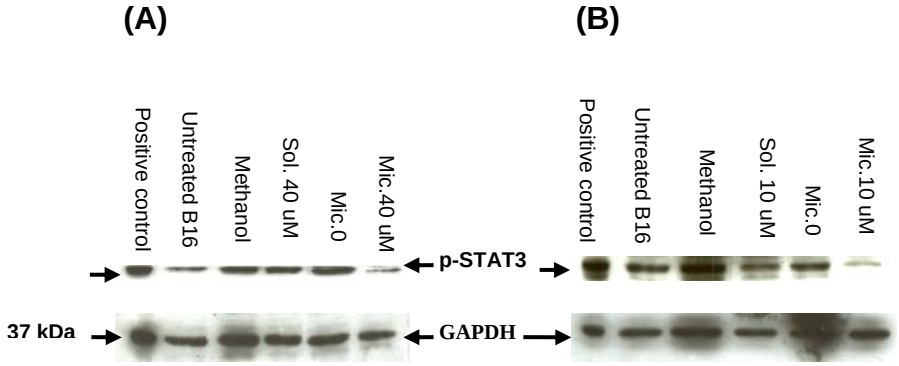

Figure 5-3. Inhibition of p-STAT3 in B16-F10 melanoma cells by soluble (Sol) and polymeric micellar (Mic) A) cucurbitacin B at concentration of 40 μM and B) JSI-124 at concentration of 10 μM. Methanol-treated group (Methanol) or empty-micelle treated group (Mic.0) were controls. SK-MEL-28 + IFN-γ cell lysate was used as positive control. p-STAT3 was detected by Western blot analysis. GAPDH levels were also detected and served as a loading control.

5.3.5 Anticancer activity of JSI-124 and its micellar formulation in a B16-F10 melanoma mouse model after intra-tumoral injection

Based on the result of *in vitro* anticancer and STAT3 inhibitory activity, between two cucurbitacins, JSI-124 (derivative I) was more efficient in the inhibition of B16-F10 cell growth as well as reduction of p-STAT3 level in this cell line. Therefore, JSI-124 was chosen for *in vivo* efficacy study in a B16-F10 melanoma tumor model. Among all the micellar formulations evaluated for the encapsulation of JSI-124, PEO-*b*-PBCL micelles was the most efficient one in the solubilization of this compound and the level of drug release from this polymeric micellar system was also relatively slow and except for the initial burst effect, was comparable to that of 5000-24000 PEO-*b*-PCL micelles. Thus, this block copolymer was selected to form the micellar structure of choice for JSI-124

during *in vivo* studies. As it has been shown in Figure 5-4A, B16-F10 tumors from the mice in control groups, either untreated or treated with empty micelles, grew to about 3200 mm^3 14 days after tumor implantation, whereas the tumor growth was efficiently inhibited in both test groups that received 1 mg/kg/day of intra-tumoral JSI-124 (~ 25 μg/ mouse) as free or encapsulated in PEO-*b*-PBCL micelles. Average tumor size in mice treated with JSI-124 was below 150 mm^3 at day 17 after tumor cell injection. The average weight of tumors in control animals that were untreated or received empty PEO-*b*-PBCL micelles was 5 times higher than that in the test groups treated with free or polymeric micellar JSI-124 (Figure 5-4B and C). Quantification of JSI-124 in the serum samples obtained from mice in test groups 24 h after the last treatment revealed detectable level of JSI-124 in the serum of mice treated with free drug (58 ± 24 ng/mL), but JSI-124 was below detectable level in the serum of animals receiving the micellar formulation of this drug (<10 ng/mL). Tumor samples harvested from mice in test group were also analyzed for drug concentration 24 h after the last treatment. JSI-124 was present at a concentration of 0.9 μg/g tumor tissue isolated from animals receiving free drug. The level of drug in tumor sample isolated from animals treated with PEO-*b*-PBCL micellar JSI-124 was 2.0 μg/g tumor. Daily intra-tumoral injection of 1 mg/kg/day JSI-124, free or encapsulated in micellar formulations had no effects activity or food intake of animals as compared with control groups, untreated animals or animals that received empty micelles.

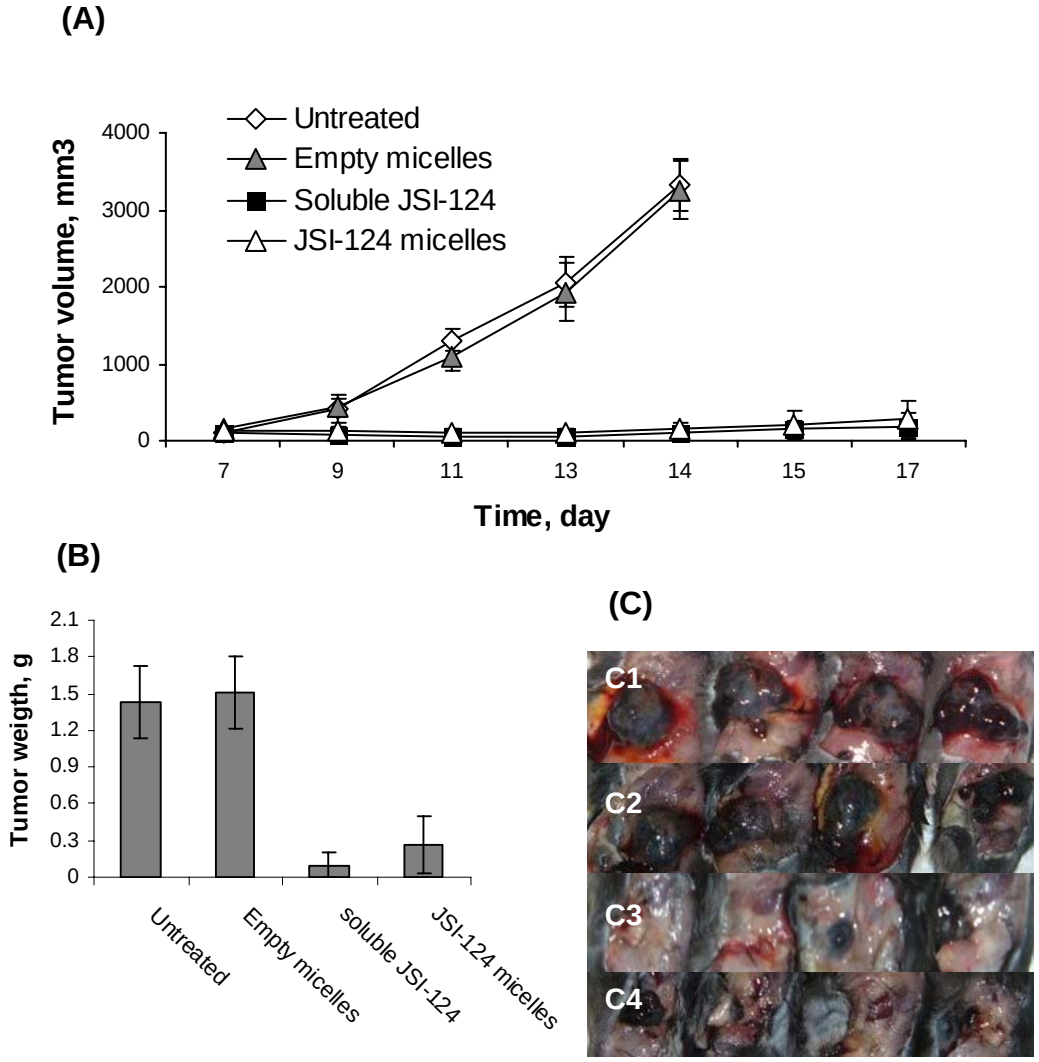

Figure 5-4. Anticancer activity of JSI-124 and its PEO-*b*-PBCL micellar formulation in B16-F10 melanoma tumor-bearing mice. Mice bearing B16-F10 melanoma tumor at their left flank received intra-tumoral injection of 1 mg/kg/day JSI-124, solubilized in 20 % ethanolic solution or encapsulated in polymeric micelles for 10 days. (A) average tumor volume in animals during treatment; (B) average tumor weight in each group at the end point of the experiment (day 15 and 17 after tumor implantation in control and test groups, respectively); and (C) photographs of tumor-bearing animals at the end of experiment: (C1) untreated, (C2) treated with empty micelles, (C3) soluble JSI-124, and (C4) polymeric micellar JSI-124

5.4 Discussion

JSI-124 and Cucurbitacin B are of great interest due to their selective STAT3 inhibitory activity and strong anti-proliferative function against a number of human carcinoma cell lines [1-3]. The IC_{50} values of cucurbitacins against several cancer cells are comparable with doxorubicin, a widely used anti-cancer drug [1]. Moreover selective STAT3 inhibitory activity of cucurbitacins makes them excellent drug candidates for delivery to tumor microenvironment to overcome tumor-induced immunosuppression, which may eventually lead to potent anti-tumor immune responses through inhibition of STAT3 [19]. The main limitations to the clinical application of cucurbitacins are their poor water solubility and non-specific toxicity. Development of a polymeric micellar carrier that can solubilize cucurbitacins effectively and control their rate of release was purposed to overcome both limitations. For this purpose micelle-forming PEO-*b*-poly(ester)s having identical PEO block and different poly(ester) blocks (PCL molecular weights of 5000 or 24000 g mol $^{-1}$ and PBCL molecular weight of 4700) were utilized.

Between two PEO-*b*-PCL copolymers with PCL molecular weights of 5000 or 24000 g mol $^{-1}$, micelles having longer hydrophobic block showed better efficiency for the solubilization of both drugs (Table 5-1). This is predictable since longer PCL block provide more hydrophobic core in the micellar structure leading to better incorporation of hydrophobic molecules in the micelles. PEO-*b*-PBCL micelles were found to be the most efficient vehicle for the solubilization of both cucurbitacins. The presence of aromatic ring on PCL block increases the

hydrophobicity of core forming block, therefore, PEO-*b*-PBCL is expected to be more efficient in encapsulating hydrophobic compounds when compared to PCL. More effective solubilization of cucurbitacin B (the more hydrophobic derivative) in PEO-*b*-PBCL micelles provides further evidence for this explanation.

PEO-*b*-PCL micelles having longer PCL blocks were found to be more efficient in sustaining the rate of release for both drugs, *in vitro* (Figure 5-1). The rate of cucurbitacin B release from PEO-*b*-PBCL micelles was comparable to that of 5000-5000 PEO-*b*-PCL thought the release study period. For JSI-124, the rate of drug release from PEO-*b*-PBCL was similar to 5000-5000 PEO-*b*-PCL micelles at the initial time point (<1 h) but it became slow and similar to that of 5000-24000 PEO-*b*-PCL micelles afterwards. A better control over the rate of drug release for cucurbitacin B over I by PEO-*b*-PCL and PEO-*b*-PBCL micelles is in line with higher hydrophobicity of chemical structure for the B derivative.

In the next step, we assessed the *in vitro* anti-cancer and STAT3 inhibitory activity of free and 5000-24000 PEO-*b*-PCL micellar cucurbitacin B and JSI-124 in B16-F10 melanoma cells in which STAT3 has been shown to be constitutively activated [20]. Our results indicated that both cucurbitacin B and JSI-124 have strong anti-proliferative activity in B16 cell line. The JSI-124 (derivative I) can exert more potent anti-proliferative activity characterized by a significantly lower IC_{50} value for JSI-124 in comparison to cucurbitacin B (Table 5-2). Treatment of B16 cell with 5000-24000 PEO-*b*-PCL micelles of JSI-124 for 48 h resulted in the loss of cell viability which was comparable with what was observed with free drug at equal concentrations. However, in shorter incubation time (24 h), free JSI-

124 was found to have better anti-proliferative activity than encapsulated drug (Table 5-2). Similarly, cucurbitacin B micelles showed higher IC_{50} value in comparison to free drug when they were incubated for 24 h with B16 cell. When incubation time was increased to 48 h, there was no significant difference between IC_{50} values of free and encapsulated B derivative (Table 5-2). The higher IC_{50} values of polymeric micellar cucurbitacins in shorter incubation times (24 h) may reflect slow release of incorporated drug from the micellar formulation (Figure 5-1). Investigation of anit-STAT3 activity of cucurbitacin B and JSI-124 formulations in B16 cell line, revealed that encapsulation of cucurbitacins in polymeric micelles doesn't have any significant negative effect on their ability to reduce the level of p-STAT3 (Figure 5-3). Taken together, the results of anticancer and STAT3 inhibitory activity show the ability of micellar formulations in the delivery of functional cucurbitacins to tumor cells.

The *in vivo* anti-cancer activity of more potent derivate, JSI-124, and its PEO-*b*-PBCL micellar formulation was also assessed in a mouse melanoma tumor model following antitumoral injection of free and encapsulated drug. The selection of PEO-*b*-PBCL formulation for *in vivo* studies was made based on the higher efficiency of PEO-*b*-PBCL micelles in the solubilization of JSI-124. The mouse melanoma tumor model was selected based on the results of our *in vitro* study that showed a potent anticancer activity for JSI-124 in this cell line. Our results indicated that intra-tumoral injection of 1 mg/kg/day JSI-124 free or encapsulated in PEO-*b*-PBCL micelles efficiently inhibits the growth of B16 tumor, *in vivo* (Figure 5-4). This is consistent with a pervious study that show

intra-peritoneal injection of 1 mg/kg/day of JSI-124 inhibits tumor growth in a mouse melanoma tumor model [2]. Quantitative analysis of JSI-124 in the serum samples of the animals treated with JSI-124 revealed detectable drug level in the serum of the mice treated with free drug but drug level was below detectable level in the serum of mice treated with JSI-124 micelles. On the other hand, the level of JSI-124 in tumors isolated from the mice treated with JSI-124 micelles was found to be higher than that in those received free drug. This points to the retention of micellar JSI-124 within the tumor tissue and a lower dissemination of drug encapsulated in micelles to the organs following its intra-tumoral administration which may lead to a lower systemic toxicity for the polymeric micellar formulation of JSI-124.

Although polymeric micelles of JSI-124 were found to give a high initial drug burst as well as a relatively rapid release profile *in vitro*, limited *in vivo* studies from our laboratory implied a potential for PEO-*b*-PCL micelles in causing a favorable change the pharmacokinetic profile of JSI-124 and reduction in its *in vivo* toxicity after systemic administration [16]. These findings are consistent with the recent reports on the *in vitro* release and pharmacokinetics of PEO-*b*-PCL micellar formulation of cyclosporine A and hydroxycompthotecin [13,14]. It is; however, not clear whether this degree of change in normal pharmacokinetics of JSI-124 by its polymeric micellar formulation will be sufficient to increase drug accumulation in solid tumor and reduce its toxicity after systemic administration. Further studies are underway to assess the potential

of PEO-*b*-PCL and PEO-*b*-PBCL micellar formulations in enhancing the therapeutic index of JSI-124 after intravenous administration.

Our results reveals a potential for PEO-*b*-PCL based micelles, especially PEO-*b*-PBCL and PEO-*b*-PCL having longer PCL blocks, as suitable vehicles for the solubilization and controlled delivery of cucurbitacin B and JSI-124. PEO-*b*-PCL micelles were shown superiority in controlling the rate of drug release for the more hydrophobic derivative, i.e., cucurbitacin B, but the I derivative (JSI-124) was found to be more potent in suppression of p-STAT3 level and inhibition of cell proliferation in a STAT3 over expressing murine cancer cell line. Finally, in comparison to free drug, PEO-*b*-PBCL micellar JSI-124 was found to provide comparable anticancer effects against B16 tumors in mice, limit drug levels in animal serum while increasing drug levels in tumor tissue.

5.5 References:

1. Jayaprakasam B, Seeram NP, Nair MG: Anticancer and antiinflammatory activities of cucurbitacins from Cucurbita andreana. Cancer Lett 2003;189:11-16.
2. Blaskovich MA, Sun J, Cantor A, Turkson J, Jove R, Sebti SM: Discovery of JSI-124 (cucurbitacin I), a selective Janus kinase/signal transducer and activator of transcription 3 signaling pathway inhibitor with potent antitumor activity against human and murine cancer cells in mice. Cancer Res 2003;63:1270-1279.
3. Sun J, Blaskovich MA, Jove R, Livingston SK, Coppola D, Sebti SM: Cucurbitacin Q: a selective STAT3 activation inhibitor with potent antitumor activity. Oncogene 2005;24:3236-3245.
4. Yu H, Jove R: The STATs of cancer--new molecular targets come of age. Nat Rev Cancer 2004;4:97-105.
5. Aliabadi HM, Lavasanifar A: Polymeric micelles for drug delivery. Expert Opin Drug Deliv 2006;3:139-162.
6. Nishiyama N, Okazaki S, Cabral H, Miyamoto M, Kato Y, Sugiyama Y, Nishio K, Matsumura Y, Kataoka K: Novel cisplatin-incorporated polymeric micelles can eradicate solid tumors in mice. Cancer Res 2003;63:8977-8983.
7. Hamaguchi T, Matsumura Y, Suzuki M, Shimizu K, Goda R, Nakamura I, Nakatomi I, Yokoyama M, Kataoka K, Kakizoe T: NK105, a paclitaxel-incorporating micellar nanoparticle formulation, can extend in vivo

antitumour activity and reduce the neurotoxicity of paclitaxel. Br J Cancer 2005;92:1240-1246.

8. Kwon GK, Forrest ML: Amphiphilic block copolymer micelles for nanoscale drug delivery. Drug Develop Res 2006;67:15-22.

9. Allen C, Yu Y, Maysinger D, Eisenberg A: Polycaprolactone-b-poly(ethylene oxide) block copolymer micelles as a novel drug delivery vehicle for neurotrophic agents FK506 and L-685,818. Bioconjug Chem 1998;9:564-572.

10. Allen C, Han J, Yu Y, Maysinger D, Eisenberg A: Polycaprolactone-b-poly(ethylene oxide) copolymer micelles as a delivery vehicle for dihydrotestosterone. J Control Release 2000;63:275-286.

11. Kim SY, Shin IG, Lee YM, Cho CS, Sung YK: Methoxy poly(ethylene glycol) and epsilon-caprolactone amphiphilic block copolymeric micelle containing indomethacin. II. Micelle formation and drug release behaviours. J Control Release 1998;51:13-22.

12. Aliabadi HM, Mahmud A, Sharifabadi AD, Lavasanifar A: Micelles of methoxy poly(ethylene oxide)-b-poly(epsilon-caprolactone) as vehicles for the solubilization and controlled delivery of cyclosporine A. J Control Release 2005;104:301-311.

13. Aliabadi HM, Brocks DR, Lavasanifar A: Polymeric micelles for the solubilization and delivery of cyclosporine A: pharmacokinetics and biodistribution. Biomaterials 2005;26:7251-7259.

14. Shi B, Fang C, You XM, Zhang Y, Fu S, PEI YY: Stealth MePEG-PCL micelles: Effects of polymer composition on micelle physicochemical characteristics, in vivo drug release, in vivo pharmacokinetics in rats and biodistribution in S180 tumor bearing mice. Coll. Polym. Sci 2005;283:954-967.

15. Mahmud A, Xiong X, Lavasanifar A: Novel poly(ethylene oxide)-*block*-poly(e-caprolactone) block copolymers with functional side groups on the polyester block for drug delivery. *Macromolecules* 2006;39:9419-9428.

16. Molavi O, Shayeganpour A, Somayaji V, Hamdy S, Brocks DR, Lavasanifar A, Kwon GS, Samuel J: Development of a sensitive and specific liquid chromatography/mass spectrometry method for the quantification of cucurbitacin I (JSI-124) in rat plasma. J Pharm Pharmaceut Sci 2006;9:158-164.

17. Forrest ML, Won CY, Malick AW, Kwon GS: In vitro release of the mTOR inhibitor rapamycin from poly(ethylene glycol)-b-poly(epsilon-caprolactone) micelles. J Control Release 2006;110:370-377.

18. Mosmann T: Rapid colorimetric assay for cellular growth and survival: application to proliferation and cytotoxicity assays. J Immunol Methods 1983;65:55-63.

19. Yu H, Kortylewski M, Pardoll D: Crosstalk between cancer and immune cells: role of STAT3 in the tumour microenvironment. Nat Rev Immunol 2007;7:41-51.

20. Niu G, Heller R, Catlett-Falcone R, Coppola D, Jaroszeski M, Dalton W, Jove R, Yu H: Gene therapy with dominant-negative Stat3 suppresses growth of the murine melanoma B16 tumor in vivo. Cancer Res 1999;59:5059-5063.

Chapter 6

Development of a PLGA nanoparticle formulation of STAT3 inhibitor JSI-124: Implication for cancer immunotherapy

---

A version of this chapter has been submitted to Molecular Pharmaceutics: Molavi, O., Mahmud, A., Hamdy, S., Hung, W. R., Lai, R., Samuel, J., Lavasanifar, A. Development of a poly(D,L-lactic-co-glycolic acid) (PLGA) nanoparticle formulation of STAT3 inhibitor JSI-124: Implication for cancer immunotherapy. *Molecular Pharmaceutics*, *Submitted June 2009*.

6.1 Introduction

Over the past few decades, several vaccines for cancer immunotherapy have been developed and advanced to clinical trials. Although most of the developed vaccination strategies have shown great potential for the induction of anti-tumor immune responses and breaking of tolerance to cancer antigens in animal tumor models and cancer patients, their therapeutic efficacy in clinical trials has been poor [1-3]. Recent studies suggest the immunosuppressive environment within tumor is a major factor responsible for the poor therapeutic outcome of cancer vaccines [4,5].

Constitutive activation of STAT3 in tumor results in diminished production of pro-inflammatory mediators and increased expression of immunosuppressive factors. These in turn leads to the activation of STAT3 in diverse subsets of immune cells rendering them either dysfunctional or immunosuppressive [6-8]. Among the affected immune cells, immunosuppressed DCs (so-called tolerogenic DCs) play a crucial role in the establishment of the immunosuppressive network in the tumor environment [5,7,8]. Immunosuppression of DCs by cancer leads to the generation of tolerogenic DCs, which are not only incapable of inducing anticancer immune responses but also are shown to activate suppressor cells such as T_{reg} cells. Tolerogenic DCs and other activated immune suppressor cells produce additional immunosuppressive factors and induce activation of more immune suppressor cells, resulting in a vicious cycle of immunosuppression in the tumor environment [5,8].

Since constitutively activated STAT3 in tumor and consequently in DCs is an important mediator in the induction of immunosuppressed DCs, blocking STAT3 in tumor and DCs represents a promising strategy for restoring the function of DCs and breaking the vicious cycle of immunosuppression in tumor environment [5,8,9]. Studies have shown that JSI-124, an anticancer inhibitor of STAT3 [10], reduces the level of p-STAT3 in dysfunctional p-STAT3^{high}DCs generated by culture in the presence of conditional medium (CM) from p-STAT3 hyperactive tumors, and restores their function *in vitro* [9,11,12]. Furthermore, we and others have shown that treatment of tumor-bearing mice with JSI-124 modulate immunosuppression in the tumor environment leading to increased infiltration of immune effector cells [9,13-15]. Our findings presented in chapter 3 showed that simultaneous inhibition of STAT3 by JSI-124 and activation of DCs by CpG, modulate tumor-induced immunosuppression and generate synergistic anti-tumor effects compared to CpG or JSI-124 alone in a B16 mouse melanoma model [15]. Kortylewski *et al* have reported a similar effect while studying the anticancer effects of a CpG-based cancer immunotherapy approach in combination with STAT3 inhibition induced by a small molecule inhibitor of STAT3 (CPA7) in a B16 tumor model [16].

In this chapter, development of PLGA NPs containing chemically conjugated JSI-124 has been pursued as a strategy for efficient delivery of JSI-124 to tumor and DCs. PLGA NPs are considered as the nano-carriers of choice for targeted delivery of therapeutic agents to DCs since they mimics pathogens in terms of size and are naturally targeted to these cells by phagocytosis. They have

been extensively studied for delivery of antigens, adjuvants and several small therapeutic molecules to DCs [17-21]. PLGA NPs have also been used for sustained delivery of several anticancer agents to tumor [22-26]. Therefore, PLGA nanopartculate formulations of JSI-124 are not only expected to provide sustained delivery of JSI-124 to cancer cells, but also to target JSI-124 to immunosuppressed DCs. Finally, PLGA NPs can provide a platform for co-delivery of cancer antigens, adjuvants and STAT3-inhibitor JSI-124 to DCs paving the way toward development of efficient cancer therapeutic vaccines.

6.2 Materials and methods

6.2.1 Materials

PVA, MW 31–50 KDa, carboxylic acid and ester terminated PLGA polymers, monomer ratio 50:50, MW 4-7 KDa, were purchased from Absorbable Polymers International (Pelham, AL, USA). N,N- dicyclohexylcarbodiimide (DCC) and dimethylaminopyridine (DMAP) were purchased from Sigma (St. Louis, MO, USA). Recombinant murine GM-CSF was purchased from Peprotech (Rocky Hill, NJ, USA). RPMI-1640, L-glutamine, and gentamicin were purchased from Invitrogen Canada, Inc. (Burlington, ON, Canada). FBS was obtained from Hyclone Laboratories (Logan, UT). JSI-124 was purchased from Indofine Chemicals, Inc. (Hillsborough, NJ, USA). Anti-p-STAT3 antibody and its respective isotype control were purchased from Santa Cruz Biotechnology. CpG, ODN#1826) was obtained from InvivoGen (San Diego, CA, USA).

6.2.2 Chemical Conjugation of JSI-124 to PLGA

For the conjugation of JSI-124 to COOH- terminated PLGA polymer, DMAP (52.41 mg , 0.429 mM) and DCC (88.5 mg, 0.429 mM) were added to a stirring solution of PLGA (300 mg, 0.0429 mM) in THF (25 mL) under argon gas. The reaction mixture was stirred for 1 h at room temperature. A solution of JSI-124 (22 mg, 0.0429 mM) in anhydrous THF (10 mL) was then added to the reaction mixture and the reaction was continued for an additional 96 h. Evaporation of the reaction mixture gave a residue that was dissolved in a 1:5 ratio of HPLC grade THF and methanol (10 mL). The solution of PLGA-JSI-124 polymer was then added to 20 mL water in a drop-wise manner while stirring. The resulting solution was dialyzed against water for 48 h to remove the unreacted JSI-124 and any other by-product. PLGA-JSI-124 conjugate was lyophilized to a bright yellow solid form for further use. TLC analysis of the conjugate compared to free drug using ethylacetate as the mobile phase and vanillin/phosphoric acid as a JSI-124 indicator confirmed the conjugation of JSI-124 to PLGA and the absence of free JSI-124 in the purified product [27]. Prepared drug-polymer conjugate was characterized by ^{1}H NMR (Bruker Unity-300 spectrometer) using deuterated chloroform ($CDCl_3$) as the solvent and tetramethylsilane as an internal reference.

6.2.3 Preparation and characterization of PLGA NPs containing JSI-124 or CpG

PLGA-JSI-124 conjugate was formulated into NPs by the single emulsion solvent evaporation method. Briefly, 60 mg of PLGA-JSI-124 polymer was dissolved in 450 μL of chloroform and the resulting solution was emulsified in 2 mL of PVA solution (9%, w/v PVA in PBS) by sonication for 45 s at level 4, using a microtip sonicator (Heat systems Inc., Farmingdale, NY, USA). The emulsion was added into 8 mL of stirring PVA solution in a drop-wise manner. The final emulsion was further stirred for 3 h and then collected by centrifugation of the emulsion at 40,000 × g for 10 min at 4 °C. The NPs were washed twice with cold deionized water and lyophilized. The volume mean diameter and polydispersity index of the nanoparticles were determined by DLS technique using a Zetasizer 3000 (Malvern, UK). PLGA-JSI-124 conjugate was further characterized for the level of conjugated JSI-124 by LC-MS. A Waters Micromass ZQ 4000 spectrometer, coupled to a Waters 2795 separations module with an autosampler (Milford, MA, USA) was used for LC-MS analysis. To measure the degree of JSI-124 conjugation, NPs were suspended in a formic acid solution at pH=2, then incubated in the water bath at 37°C for 4 h. After incubation the suspension was centrifuged and the level of JSI-124 in the supernatant was measured by the LC-MS method as described in chapter 4, section 4.2.2 [28]. To assess the release profile of JSI-124 from the formulation, NPs (3 mg) were suspended in 15 mL ddH_2O, then aliquated into 15 samples of 1 mL in microcentrifuge tubes. The samples were shaken in a water bath at 37°C.

At predetermined time intervals, the supernatant of one sample was collected by centrifugation (12,000 × g for 10 min) and analyzed for the level of released JSI-124 by LC-MS.

Physical encapsulation of CpG in PLGA NPs was achieved by the double emulsion solvent evaporation method. Briefly, CpG ODN (200 μg in 60 μL Tris EDTA (TE) buffer at pH 8) was emulsified with ester-terminated PLGA solubilized in chloroform (600 μL, 30% w/v) for 20s using the microtip sonicator. The resulting primary (w/o) emulsion was then combined with PVA solution (4 mL, 7.5% w/v in TE buffer) and sonicated for 40 s at level 4 to form a secondary (w/o/w) emulsion. This secondary emulsion was then added in a drop-wise manner to a beaker containing PVA solution (16 ml, 7.5% w/v in TE buffer) under constant stirring. The final emulsion was stirred for 3 h at room temperature and collected by centrifugation at 40,000 × g for 10 min at 4 °C. The NPs were washed twice with cold deionized water and lyophilized. The level of encapsulated CpG was estimated based on 50 % encapsulation efficiency of PLGA NPs for physically loaded CpG as reported previously [29].

6.2.4 Cell viability assay

Anticancer activity of free and PLGA NP-conjugated JSI-124 was assessed in B16-F10, a melanoma cell of C57BL/6 origin (ATCC)**.** B16-F10 cells were grown in RPMI-1640 supplemented with 10% FBS, 2 mM L-glutamine and 100 IU/mL penicillin/streptomycin at 37°C in 5% CO_2 atmosphere. Cell viability was monitored using MTT assay as described in chapter 5, section 5.2.5 [30].

6.2.5 Generation of tumor-induced immunosuppressed DCs

DC primary cultures were generated from murine bone marrow precursors of C57BL/6 mice in complete media in the presence of GM-CSF as described in chapter 2, section 2.2.4 [31]. To generate immunosuppressed p-STAT3^{high}DCs CM from B16-F10 cells was added to the culture of bone marrow originated DCs (~0.2 million DCs per mL) on day 7 and then DCs were incubated for 8-12 h before treatment with different formulations. To make B16 CM, B16 cells were kept in RPMI-1640 media with reduced (2%) FBS concentration for 48 h then the supernatants were collected, filtered and used in the experiments.

6.2.6 Analysis of p-STAT3 level by flow cytometry

Intracellular staining of p-STAT3 was done using PE labeled-anti-p-STAT3 antibody or isotype control according to the manufacturer's instructions. Briefly, DCs or B16 cells were collected, washed twice with PBS and then fixed with PBS/paraformaldehyde fixation solution (Santa Cruz Biotechnology) at 4°C for 30 min. After two washes, the cells were permeabilized by a saponin solution (Santa Cruz Biotechnology) at room temperature for 15 min, and then stained with PE labeled-anti-pSTAT3 antibody or isotype control (2 μg/10^6 cells) for 60 min at room temperature. After three washes with flow cytometry wash buffer (Santa Cruz Biotechnology), samples were acquired on a Becton-Dickinson FACSort and analyzed with Cell-Quest software.

6.2.7 Assessment of the functional characteristics of tumor-induced immunosuppressed DCs by mixed lymphocyte reaction (MLR)

DCs derived from C57BL/6 mice (on day 7 of their culture) were incubated with CM from B16-F10 cells, for 8-12 h, and then treated with different formulations. After 18 h incubation with the formulations, cells were harvested, washed, and irradiated (2000 rads). T cells were isolated from the spleen of Balb/c mice using the EasySep mouse T cell enrichment kit (Stem Cell Technologies). The irradiated DCs were co-cultured with T cells (1:10 ratio) for 60 h and the proliferation of T cells was determined by incorporation of ^{3}H-thymidine for the last 18 hours of the culture.

6.2.8 Statistical analysis

The significance of differences among groups was analyzed by ANOVA for parametric data, followed by the Student-Newman-Keuls post-hoc test for multiple comparisons, or by the Kruskal-Wallis one-way ANOVA for non-parametric data. A p-value of ≤ 0.05 was set for the significance of difference among groups. The statistical analysis was performed with SigmaStat software (Systat Software Inc. San Jose, California, USA).

6.3 Results

6.3.1 Synthesis and characterization of PLGA-JSI-124 conjugate

PLGA-JSI-124 conjugate was synthesized by forming an ester bond between a hydroxyl group from JSI-124 and the terminal carboxyl group of PLGA polymer using DMAP and DCC as the coupling agent and catalyst (Figure 6-1).

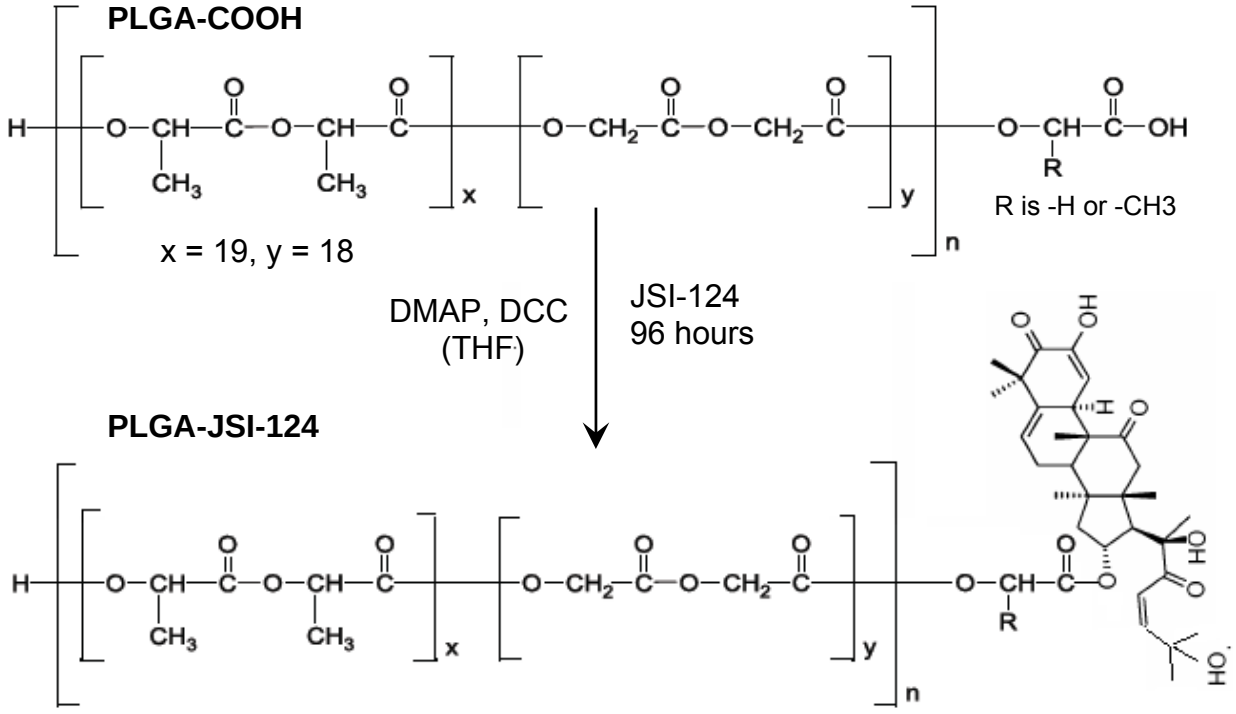

Figure 6-1. Synthetic scheme for the preparation of PLGA-JSI-124 conjugate

The conjugation of the JSI-124 to PLGA polymer was confirmed by the ^{1}H NMR spectrum of PLGA-JSI-124 (Figure 6-2A), free JSI-124 (Figure 6-2B), and PLGA polymer (Figure 6-2C). ^{1}H NMR spectrum of PLGA-JSI-124 in $CDCl_3$ (Figure 6-2A) demonstrated characteristic JSI-124 peaks at 1.35, 3.2, 3.5, and 6.8 ppm. Similar peaks were also present in the ^{1}H NMR spectrum of the free JSI-124 (Figure 6-2B). Further evidence for the conjugation of JSI-124 to PLGA polymer was provided by TLC and LC-MS analysis. TLC analysis of PLGA-JSI-124 conjugate showed the absence of free form of JSI-124 in PLGA-JSI-124 conjugate (Figure 6-2D). On the other hand, NPs of PLGA-JSI-124 conjugates showed the presence of a molecular ion peak at 559 m/z corresponding to MW of [JSI-124 + formic acid-H] when they were incubated in formic acid solution at pH=2 for 4 h and analyzed by LC-MS as described in chapter 4 (Figure 6-2E).

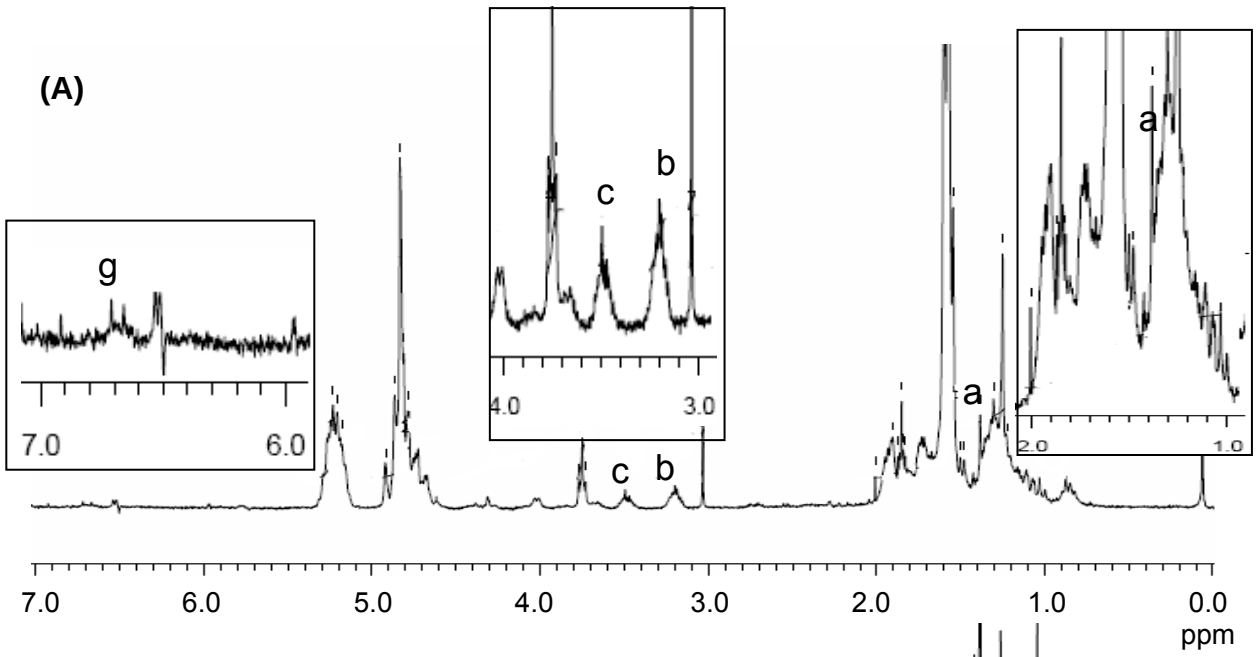
(A)
g
7.0
6.0
c
b
4.0
3.0
a
2.0
1.0
7.0
6.0
5.0
4.0
3.0
2.0
1.0
0.0
ppm

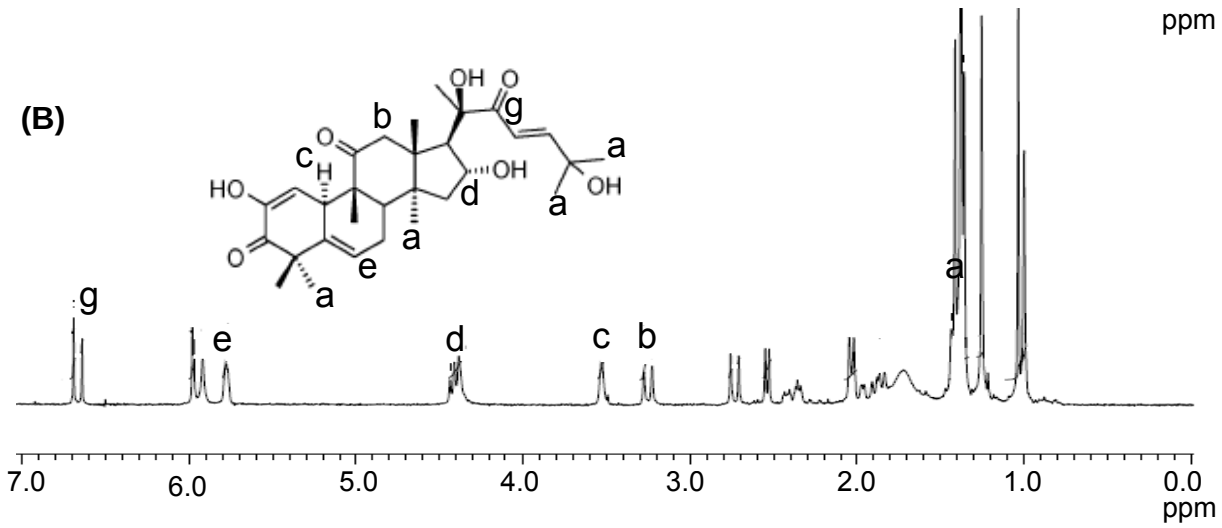
(B)
OH
O
g
b
c
H
O
HO
OH
d
a
OH
a
a
e
O
a
g
e
d
c
b
a
7.0
6.0
5.0
4.0
3.0
2.0
1.0
0.0
ppm

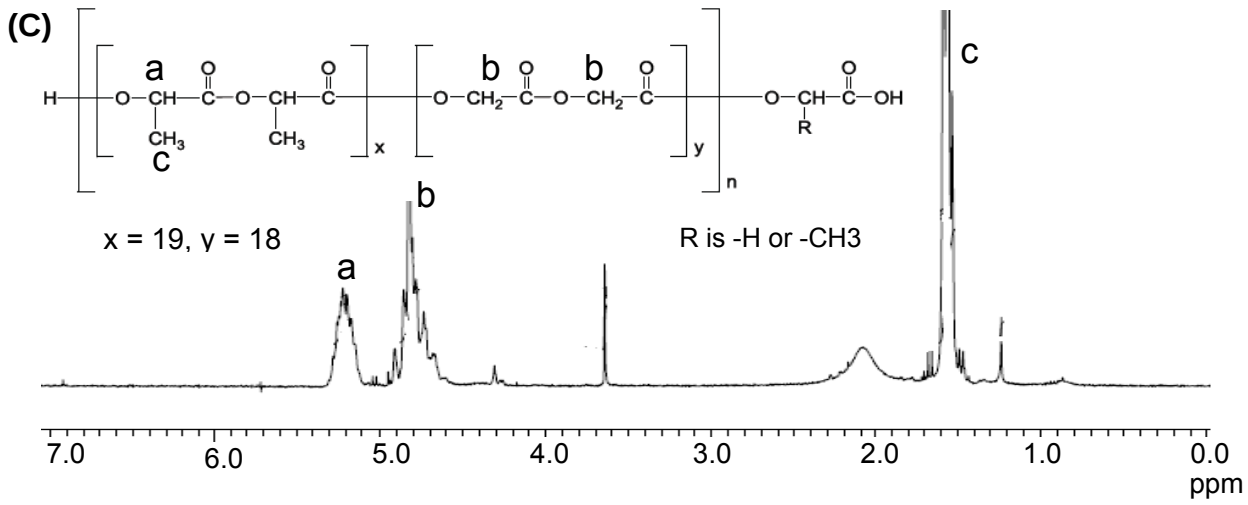
(C)
H
O
CH
C
O
CH
C
a
CH3
c
x
O
CH2
C
O
CH2
C
b
b
y
n
O
CH
C
OH
R
c
x = 19, y = 18
R is -H or -CH3
a
b
7.0
6.0
5.0
4.0
3.0
2.0
1.0
0.0
ppm

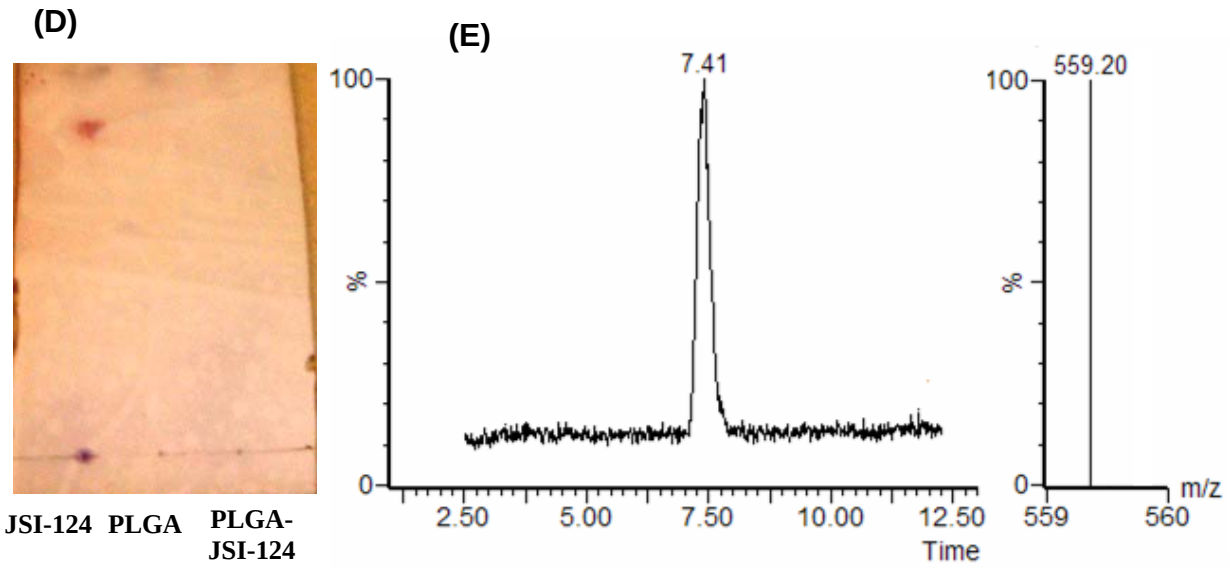

Figure 6-2. Characterization of PLGA-JSI-124 conjugate. ^{1}H NMR spectrum of A) PLGA-JSI-124 conjugate in CDCl3, B) free JSI-124 in CDCL3, C) PLGA polymer CDCl3; D) TLC analysis of PLGA-JSI-124, PLGA and free JSI-124 E) SIR chromatogram and mass spectra of PLGA-JSI-124 NPs after incubation in formic acid (pH=2) for 4h and monitored at 559 m/z.

6.3.2 Characterization of PLGA-JSI-124 NPs

The PLGA-JSI-124 NPs were 329 ± 44 nm in diameter with a polydispersity less than 0.1 as determined by DLS (Table 6-1). The level of conjugated JSI-124 was found to be 1.7± 0.3 µg per mg of PLGA polymer as assessed by the LC-MS method of quantification. This corresponds to 0.023 mol JSI-124 /mol PLGA.

Table 6-1. Characteristics of PLGA-JSI-124 NPs (n=3)

Size (nm)	329 ± 44
Polydispersity Index	0.09 ± 0.05
JSI-124 conjugated (µg per mg of PLGA)	1.7 ± 0.3

6.3.3 *In vitro* release profile of JSI-124 from NPs

PLGA-JSI-124 NPs showed a burst release (30%) of JSI-124 within the first 2 days followed by the establishment of a plateau phase in the next 21 days. PLGA NPs released 58% of conjugated JSI-124 to the receiving media within 21 days (Figure 6-3). The cumulative release of JSI-124 from the PLGA NPs over a period of 34 days was 86%. The triphasic release of JSI-124 from the PLGA NPs suggests a bulk erosion and biodegradation dependent release profile for this drug from PLGA NPs (Figure 6-3).

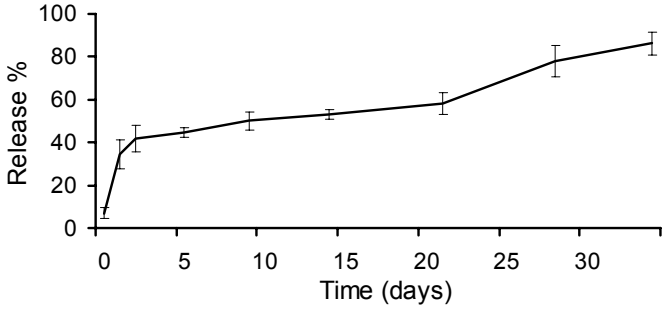

Figure 6-3. JSI-124 release profile from PLGA NPs *in vitro*. Each point represents mean ± SD (n=3).

6.3.4 Anticancer and STAT3 inhibitory activity of PLGA-JSI-124 NPs in B16-F10 cell line

Figure 6-4A depicts the anticancer activity of JSI-124 either free or conjugated to PLGA NPs against B16-F10 melanoma cells after 24 h incubation. Treatment of the murine B16 melanoma cells with increasing concentrations of free or PLGA-conjugated JSI-124 resulted in a significant loss of cell viability (ANOVA, $p<0.001$). Treatment of B16 cells with PLGA-JSI-124 NPs at concentrations of 1.25, 2.5, 5 and 10 μM for 24 h reduced the cell viability to 37, 25, 11 and 4 %, which were not significantly different from the viability of the

cells treated with free drug at identical concentrations (P>0.05, ANOVA). As shown in Figure 6-4A, JSI-124 either free or conjugated to PLGA NPs inhibited B16 cell growth in a dose-dependent manner. PLGA-JSI-124 NPs were able to efficiently suppress the level of p-STAT3 in B16 melanoma cell line at a concentration of 2 μM after 24 h incubation (Figure 6-4B).

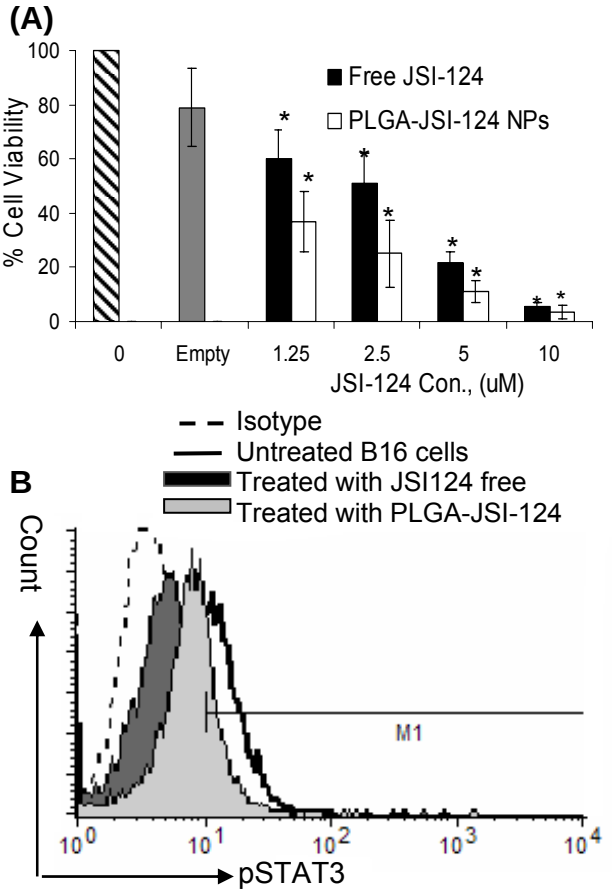

Figure 6-4. Assessment of the anticancer and STAT3 inhibitory activity of PLGA-JSI-124 NPs in B16-F10 cell line. A) Anticancer activity of free and chemically conjugated JSI-124 to PLGA NPs against B16 melanoma cell line after 24 h incubation, *in vitro*. B16 cells were treated with four different concentrations of JSI-124 either free or conjugated to PLGA NPs. After 24 h incubation, cell viability was estimated by MTT assay and expressed as percentage of untreated controls. The data represent the mean ± S.D. of three independent experiments; *significantly different from untreated B16 cells (P<0.05); B) p-STAT3 inhibitory activity of JSI-124 and JSI-124-PLGA NPs in B16 cells after 24 h incubation. The data represent one out of three independent experiments which showed similar results.

6.3.5 STAT3 inhibitory effects of PLGA-JSI-124 NPs on DCs

To evaluate the STAT3 inhibitory effects of the NPs on DCs, p-STAT3^{+}DCs were generated from C57BL/6 mouse bone marrow cells in the presence of B16 CM. As shown on Figure 6-5A, treatment of DCs with B16 CM results in a higher level of p-STAT3 in treated DCs as compared to untreated DCs. B16 CM-treated DCs characterized by higher level of p-STAT3, are referred to as B16CM-DCs. Treatment of B16CM-DCs with JSI-124 conjugated to PLGA NPs at concentrations of 100, 200, and 400 nM for 24 h reduced the percentage of p-STAT3^{+}DCs to 18, 7, and 5 %, which were significantly different from the percentage of p-STAT3^{+}DCs in untreated group or the cells treated with empty NPs (Figure 6-5B, $p<0.01$ ANOVA). The percentage of p-STAT3^{+}DCs treated with free JSI-124 at identical concentrations for the same period of time was not significantly different from what was observed with PLGA-JSI-124 NPs (ANOVA, $p>0.05$).

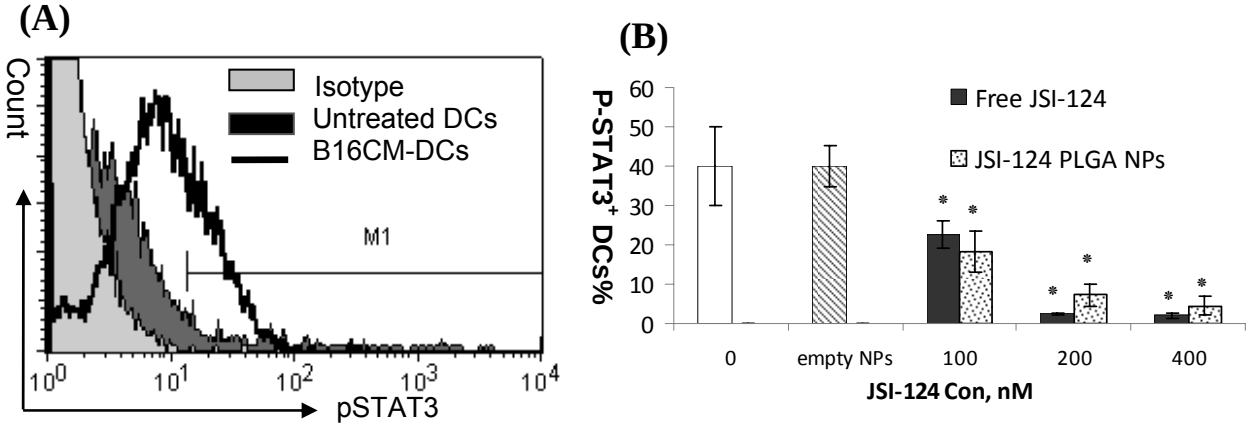

Figure 6-5. Assessment of the STAT3 inhibitory activity of PLGA-JSI-124 NPs in DCs. A) p-STAT3 expression in DCs treated with CM of B16 cell (B16CM-DCs), The data represent one out of three independent experiments which showed the similar results; B) p-STAT3 inhibitory activity of JSI-124 and PLGA-JSI-124 NPs in B16CM-DCs after 24 h incubation. The data represent the mean ± S.D. of three independent experiments; *significantly different from untreated B16CM-DCs or empty NP treated B16CM-DCs ($P<0.01$).

6.3.6 Immunomodulatory effects of PLGA NPs delivering JSI-124 and CpG on DCs

DCs treated with CM from B16 cells (B16CM-DCs) expressed higher level of p-STAT3 (Figure 6-5A) and were found to be dysfunctional in stimulating T cells in an MLR reaction (Figure 6-6). Treatment of B16CM-DCs with CpG NPs resulted in significant**,** albeit modest**,** increase in the level of T cell proliferation induced by treated B16CM-DCs, but it could not completely restore their function. This was indicated by significantly lower level of T cell proliferation in CpG treated group as compared to control untreated DCs ($p<0.05$). However, when B16CM-DCs were treated with 200 nM of JSI-124 either free or conjugated to the PLGA NPS for 24 h, the impaired DCs regained their ability to induce T cell proliferation in an MLR assay. The level of T cell proliferation induced by B16CM-DCs treated with either soluble or PLGA-JSI-124 NPs for 24 h was significantly higher than that induced with untreated B16CM-DCs or empty NP or CpG NP B16CM-DCs ($p<0.001$, ANOVA). There was no statistically significant difference in the level of T cell proliferation between the groups of B16CM-DCs treated with soluble and nanoparticulate formulation of JSI-124 (Figure 6-6, $p>0.05$ ANOVA).

Co-treatment of B16CM-DCs with CpG NPs and JSI-124, either free or nanoparticulate resulted in higher level of T cell proliferation as compared with the DCs treated with either CpG NPs or JSI-124 formulation alone (Figure 6-6 $p<0.01$ ANOVA). The level of T cell proliferation in the group of DCs treated

with CpG +JSI-124 free was not significantly different from that in DCs treated with CpG + JSI-124 PLGA NPs (P>0.05).

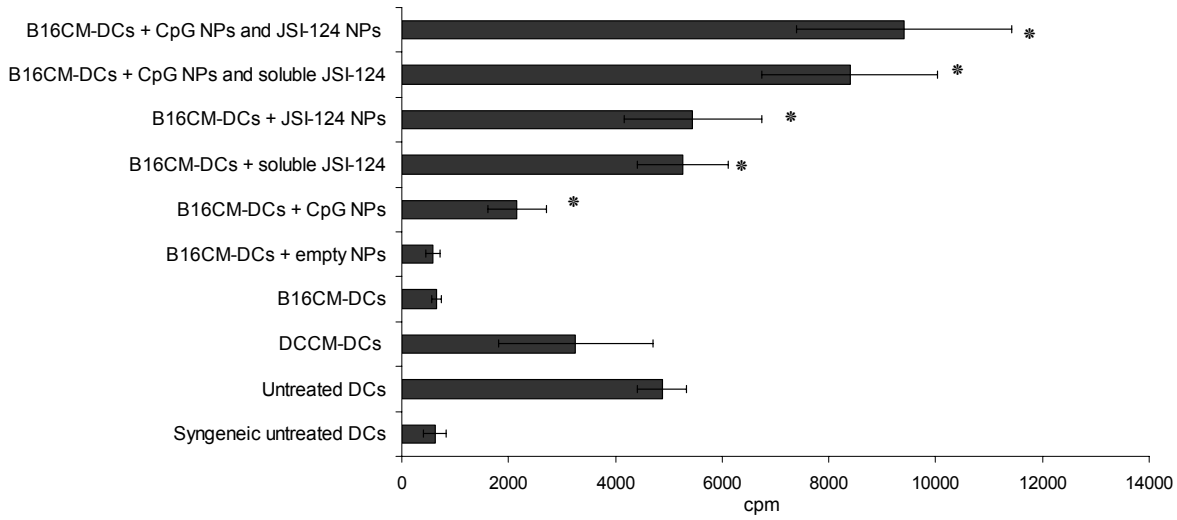

Figure 6-6. The effects of PLGA-NP delivery of JSI-124 on the function of DCs. DCs treated with B16CM (B16CM-DCs) were incubated with different formulations for 24 h then co-cultured with T cells isolated from the spleen of Balb/c mice for a MLR reaction. Proliferation of T cells was determined by incorporation of ^{3}H-thymidine for the last 24 hours of the culture. *significantly higher from B16CM-DC group (P<0.01).

6.4 Discussion

Activation of STAT3 is shown to play a major role in tumor growth, survival and invasion in several types of cancer. In addition, STAT3 activation in tumor is also known to provoke STAT3 activation in several tumor infiltrating immune cells, leading to the formation of an immunosuppressive network in the tumor milieu characterized by the accumulation of tolerogenic DCs and regulatory T cells as well as reduced level of mature DCs and Th1 cytokines [6-8,32]. Moreover, recent observations document an important role for STAT3 activation in restraining the immunostimulatory effect of TLR ligands that are regularly used as adjuvants to boost the effect of prophylactic or therapeutic cancer vaccines [16]. Therefore, inhibition of STAT3 in the tumor microenvironment and in tolerogenic DCs is an attractive approach not only to reduce tumor proliferation and metastasis, but also to break the vicious cycle of tumor-induced immunosuppression and increase the therapeutic efficacy of cancer immunotherapy strategies.

JSI-124, has been extensively studied for its STAT3 and anticancer activity in several human and murine cancers [10,14,15,33-37]. In addition, the immunomodulatory effects of JSI-124 mediated through inhibition of STAT3 have been illustrated in numerous *in vitro* and *in vivo* models [11-15]. In the previous chapter we reported on the development of polymeric micellar formulations that can increase the water solubility of JSI-124, sustain its release rate *in vitro*, and maintain the cytotoxic and immunomoulatory activity of JSI-124 while limiting the exposure of drug to non-target tissues after intratumoral

administration in a murine B16 melanoma model [34,38]. Although polymeric micellar formulations are promising nano-delivery systems for sustained JSI-124 delivery to the tumor microenvironment, their small size (< 100 nm) and the dense hydrophilic coating of PEO may limit their interaction with DCs. The purpose of this study was to achieve an optimal nano-carrier for selective delivery of JSI-124 to immunosuppressed DCs. Unlike polymeric micelles, PLGA-NPs are naturally targeted to DCs through phagocytosis, as their size is comparable to that of pathogens [39] and their surface is not protected by a hydrophilic palisade. The successful delivery of several antigens, adjuvants and small molecules to DCs by PLGA NPs has been well documented by our group and others [18,40-43]. Besides, PLGA NPs may provide a promising platform for co-delivery of cancer vaccines and STAT3 inhibitors to the same population of DCs. In addition to DCs, cancer cells have also shown to be able to take up PLGA NPs [44].

Development of the PLGA NP formulations of JSI-124 were accomplished through chemical conjugation of JSI-124 to COOH-terminated PLGA and further assembly of polymer conjugates to NPs as the physical encapsulation efficiency of JSI-124 in PLGA-NPs was found to be very low. Chemical conjugation of JSI-124 to PLGA NPs resulted in the generation of nano-carriers, which are able not only to carry a high load of drug (0.023 drug/polymer on molar basis), but also to control the release of JSI-124 from NPs over a 1-month period, *in vitro* (Figure 6-3). The triphasic release suggested a degradation-dependent mode of drug release, which is expected to favor the release of JSI-124 following endocytosis in the acidic environment of endosomes,

where hydrolysis of the ester linkage between JSI-124 and PLGA would be catalyzed, and bulk erosion of the PLGA NPs would be accelerated [45]. At the same time, the degradation-dependent delivery of free JSI-124 is expected to limit the release of conjugated JSI-124 at physiological pH before NP uptake by DCs or tumor cells restricting drug distribution into non-target tissues after *in vivo* administration. Our *in vitro* studies found comparable cytotoxicity in B16 melanoma cells (Figure 6-4), as well as a similar STAT3 inhibitory effects in B16 cells and DCs for PLGA-JSI-124 NPs as compared to free JSI-124 (Figure 6-4 and 6-5), indicating efficient uptake of PLGA-NPs and release of conjugated JSI-124 within cancer cells and DCs.

It has been shown that p-STAT3^{high}DCs generated in the presence of CM from STAT3 hyperactive tumor cells are dysfunctional and unable to efficiently stimulate T cells proliferation *in vitro* [12]. Consistent with these results, DCs treated with CM from B16 cells (B16CM-DCs) generated here were unable of stimulating T cell proliferation (Figure 6-6). Our research group have previously reported successful development of PLGA NP formulations of CpG, a potent adjuvant which activates untreated DCs through TLR9 and induces Th1 immune responses. The PLGA delivery of CpG to DCs strongly stimulates DC activation and induces Th1 type immune responses [29,46]. However, PLGA NP delivery of CpG to DCs pretreated with B16CM was found to be ineffective in restoring the function of impaired DCs in terms of stimulating T cell proliferation in the MLR reaction. This is consistent with other studies showing that CpG on its own cannot activate impaired DCs in tumor [47]. On the other hand, treatment of B16CM-

DCs with JSI-124 (either soluble or conjugated to PLGA NPs) significantly improved their T cell mitogenic activity when compared with untreated B16CM-DCs or B16CM-DCs treated with empty NPs. This is consistent with previous reports where inhibition of STAT3 by JSI-124 in CM-DCs has shown to improve DC function, *in vitro* [11]. Consistent with our observation on the similar effect of free and conjugated JSI-124 on STAT3 activation, restoration of DC activity in terms of T cell proliferation by free and conjugated JSI-124 was comparable.

We also found that PLGA NP delivery of CpG along with JSI-124 (soluble or conjugated) to B16CM-DCs results in an increased level of T cell proliferation as compared with B16CM-DCs treated with either JSI-124 or CpG alone. This is consistent with the result of our previously published data showing that intratumoral co-administration of JSI-124 and CpG in B16 tumor-bearing mice resulted in an increased percentage of activated DCs in tumor-draining lymph nodes and in the tumor itself [15].

It has been recently shown that activation of STAT3 in DCs can limit the efficacy of CpG for the induction of DC maturation and activation [16]. This study suggests a mechanism by which co-delivery of JSI-124 and CpG to immunosuppressed B16CM-DCs improves the function of B16CM-DCs and results in a significant increase in T cell proliferation as compared with the groups of B16CM-DCs treated with CpG alone. In other words, STAT3 activation in DCs might act like a ‘brake’ on TLR9 induced activation of DCs, while JSI-124 can release this ‘brake’ and restore efficient activation of DCs by CpG. The results of this study showed that JSI-124 either free or conjugated to PLGA NPs

enhanced the stimulatory effects of CpG NPs on immunosuppressed p-STAT3^{high}DCs. The statistically insignificant difference in the level of T cell proliferation between the group stimulated with CpG NP +free JSI-124 and with CpG NP+ PLGA-JSI-124 NPs indicates that functional JSI-124 is efficiently delivered by these newly developed nano-carriers to DCs.

In summary, chemical conjugation of JSI-124 to PLGA NPs generates an efficient drug delivery system for JSI-124 with degradation-controlled release properties. The developed PLGA-JSI-124 NP was found to provide comparable anticancer and STAT3 inhibitory activity against B16 melanoma cells with free JSI-124, *in vitro*. Furthermore, JSI-124 conjugated to PLGA NPs was able to suppress the level of p-STAT3 in B16CM-DCs and to significantly improve their function in stimulating T cell proliferation in an MLR reaction. These findings show the potential of PLGA-JSI-124 NPs for the delivery of functional JSI-124 to tumor and DCs. The results also demonstrate the ability of PLGA NP formulation of JSI-124 to restore the function of tumor suppressed DCs. Our present *in vitro* findings also points to the potential of PLGA NPs as efficient carriers for co-delivery of a small molecule inhibitor of STAT3 (e.g JSI-124) and a TLR ligand (i.e. CpG) to DCs, leading to improved responses in cancer immunotherapy.

6.5 References:

1. Slingluff CL, Speiser DE: Progress and controversies in developing cancer vaccines. J Transl Med 2005;3:18-27.
2. Morse MA, Chui S, Hobeika A, Lyerly HK, Clay T: Recent developments in therapeutic cancer vaccines. Nat Clin Pract Oncol 2005;2:108-113.
3. Rosenberg SA, Yang JC, Restifo NP: Cancer immunotherapy: moving beyond current vaccines. Nat Med 2004;10:909-915.
4. Chen Q, Wang WC, Evans SS: Tumor microvasculature as a barrier to antitumor immunity. Cancer Immunol Immunother 2003;52:670-679.
5. Zou W: Immunosuppressive networks in the tumour environment and their therapeutic relevance. Nat Rev Cancer 2005;5:263-274.
6. Wang T, Niu G, Kortylewski M, Burdelya L, Shain K, Zhang S, Bhattacharya R, Gabrilovich D, Heller R, Coppola D, Dalton W, Jove R, Pardoll D, Yu H: Regulation of the innate and adaptive immune responses by Stat-3 signaling in tumor cells. Nat Med 2004;10:48-54.
7. Kortylewski M, Kujawski M, Wang T, Wei S, Zhang S, Pilon-Thomas S, Niu G, Kay H, Mule J, Kerr WG, Jove R, Pardoll D, Yu H: Inhibiting Stat3 signaling in the hematopoietic system elicits multicomponent antitumor immunity. Nat Med 2005;11:1314-1321.
8. Yu H, Kortylewski M, Pardoll D: Crosstalk between cancer and immune cells: role of STAT3 in the tumour microenvironment. Nat Rev Immunol 2007;7:41-51.

9. Nefedova Y, Gabrilovich DI: Targeting of Jak/STAT pathway in antigen presenting cells in cancer. Curr Cancer Drug Targets 2007;7:71-77.

10. Blaskovich MA, Sun J, Cantor A, Turkson J, Jove R, Sebti SM: Discovery of JSI-124 (cucurbitacin I), a selective Janus kinase/signal transducer and activator of transcription 3 signaling pathway inhibitor with potent antitumor activity against human and murine cancer cells in mice. Cancer Res 2003;63:1270-1279.

11. Nefedova Y, Cheng P, Gilkes D, Blaskovich M, Beg AA, Sebti SM, Gabrilovich DI: Activation of Dendritic Cells via Inhibition of Jak2/STAT3 Signaling. J Immunol 2005;175:4338-4346.

12. Nefedova Y, Nagaraj S, Rosenbauer A, Muro-Cacho C, Sebti SM, Gabrilovich DI: Regulation of dendritic cell differentiation and antitumor immune response in cancer by pharmacologic-selective inhibition of the janus-activated kinase 2/signal transducers and activators of transcription 3 pathway. Cancer Res 2005;65:9525-9535.

13. Fujita M, Zhu X, Sasaki K, Ueda R, Low KL, Pollack IF, Okada H: Inhibition of STAT3 promotes the efficacy of adoptive transfer therapy using type-1 CTLs by modulation of the immunological microenvironment in a murine intracranial glioma. J Immunol 2008;180:2089-2098.

14. Molavi O, Ma Z, Hamdy S, Lavasanifar A, Samuel J: Immunomodulatory and Anticancer Effects of Intra-Tumoral Co-Delivery of Synthetic Lipid A

Adjuvant and STAT3 Inhibitor JSI-124. Immunopharmacol Immunotoxicol 2008:1-14.

15. Molavi O, Ma Z, Hamdy S, Lai R, Lavasanifar A, Samuel J: Synergistic antitumor effects of CpG oligodeoxynucleotide and STAT3 inhibitory agent JSI-124 in a mouse melanoma tumor model. Immunol Cell Biol 2008;86:506-514.

16. Kortylewski M, Kujawski M, Herrmann A, Yang C, Wang L, Liu Y, Salcedo R, Yu H: Toll-like receptor 9 activation of signal transducer and activator of transcription 3 constrains its agonist-based immunotherapy. Cancer Res 2009;69:2497-2505.

17. Waeckerle-Men Y, Gander B, Groettrup M: Delivery of tumor antigens to dendritic cells using biodegradable microspheres. Methods Mol Med 2005;109:35-46.

18. Elamanchili P, Lutsiak CM, Hamdy S, Diwan M, Samuel J: "Pathogen-mimicking" nanoparticles for vaccine delivery to dendritic cells. J Immunother 2007;30:378-395.

19. Schlosser E, Mueller M, Fischer S, Basta S, Busch DH, Gander B, Groettrup M: TLR ligands and antigen need to be coencapsulated into the same biodegradable microsphere for the generation of potent cytotoxic T lymphocyte responses. Vaccine 2008;26:1626-1637.

20. Jiang W, Gupta RK, Deshpande MC, Schwendeman SP: Biodegradable poly(lactic-co-glycolic acid) microparticles for injectable delivery of vaccine antigens. Adv Drug Deliv Rev 2005;57:391-410.

21. Waeckerle-Men Y, Groettrup M: PLGA microspheres for improved antigen delivery to dendritic cells as cellular vaccines. Adv Drug Deliv Rev 2005;57:475-482.

22. Bala I, Hariharan S, Kumar MN: PLGA nanoparticles in drug delivery: the state of the art. Crit Rev Ther Drug Carrier Syst 2004;21:387-422.

23. Tong W, Wang L, D'Souza MJ: Evaluation of PLGA microspheres as delivery system for antitumor agent-camptothecin. Drug Dev Ind Pharm 2003;29:745-756.

24. Hussain M, Beale G, Hughes M, Akhtar S: Co-delivery of an antisense oligonucleotide and 5-fluorouracil using sustained release poly (lactide-co-glycolide) microsphere formulations for potential combination therapy in cancer. Int J Pharm 2002;234:129-138.

25. Danhier F, Lecouturier N, Vroman B, Jerome C, Marchand-Brynaert J, Feron O, Preat V: Paclitaxel-loaded PEGylated PLGA-based nanoparticles: in vitro and in vivo evaluation. J Control Release 2009;133:11-17.

26. Yoo HS, Lee KH, Oh JE, Park TG: In vitro and in vivo anti-tumor activities of nanoparticles based on doxorubicin-PLGA conjugates. J Control Release 2000;68:419-431.

27. Afifi MS, Ross SA, El-Sohly MA, Naeem ZE, Halaweish FT: Cucurbitacins of Cucumis prophetarum and Cucumis prophetarum. J Chem Ecol 1999;25:847-859.

28. Molavi O, Shayeganpour A, Somayaji V, Hamdy S, Brocks DR, Lavasanifar A, Kwon GS, Samuel J: Development of a sensitive and specific liquid chromatography/mass spectrometry method for the quantification of cucurbitacin I (JSI-124) in rat plasma. J Pharm Pharm Sci 2006;9:158-164.

29. Diwan M, Elamanchili P, Cao M, Samuel J: Dose sparing of CpG oligodeoxynucleotide vaccine adjuvants by nanoparticle delivery. Curr Drug Deliv 2004;1:405-412.

30. Mosmann T: Rapid colorimetric assay for cellular growth and survival: application to proliferation and cytotoxicity assays. J Immunol Methods 1983;65:55-63.

31. Lutz MB, Kukutsch N, Ogilvie AL, Rossner S, Koch F, Romani N, Schuler G: An advanced culture method for generating large quantities of highly pure dendritic cells from mouse bone marrow. J Immunol Methods 1999;223:77-92.

32. Kortylewski M, Xin H, Kujawski M, Lee H, Liu Y, Harris T, Drake C, Pardoll D, Yu H: Regulation of the IL-23 and IL-12 balance by Stat3 signaling in the tumor microenvironment. Cancer Cell 2009;15:114-123.

33. Jayaprakasam B, Seeram NP, Nair MG: Anticancer and antiinflammatory activities of cucurbitacins from Cucurbita andreana. Cancer Lett 2003;189:11-16.

34. Molavi O, Ma Z, Mahmud A, Alshamsan A, Samuel J, Lai R, Kwon GS, Lavasanifar A: Polymeric micelles for the solubilization and delivery of

STAT3 inhibitor cucurbitacins in solid tumors. Int J Pharm 2008;347:118-127.

35. Shi X, Franko B, Frantz C, Amin HM, Lai R: JSI-124 (cucurbitacin I) inhibits Janus kinase-3/signal transducer and activator of transcription-3 signalling, downregulates nucleophosmin-anaplastic lymphoma kinase (ALK), and induces apoptosis in ALK-positive anaplastic large cell lymphoma cells. Br J Haematol 2006;135:26-32.

36. Van Kester MS, Out-Luiting JJ, von dem Borne PA, Willemze R, Tensen CP, Vermeer MH: Cucurbitacin I Inhibits Stat3 and Induces Apoptosis in Sezary Cells. J Invest Dermatol 2008.

37. Chen JC, Chiu MH, Nie RL, Cordell GA, Qiu SX: Cucurbitacins and cucurbitane glycosides: structures and biological activities. Nat Prod Rep 2005;22:386-399.

38. Mahmud A, Patel S, Molavi O, Choi P, Samuel J, Lavasanifar A: Self-Associating Poly(ethylene oxide)-b-poly(alpha-cholesteryl carboxylate-epsilon-caprolactone) Block Copolymer for the Solubilization of STAT-3 Inhibitor Cucurbitacin I. Biomacromolecules 2009.

39. Foged C, Sundblad A, Hovgaard L: Targeting vaccines to dendritic cells. Pharm Res 2002;19:229-238.

40. Elamanchili P, Diwan M, Cao M, Samuel J: Characterization of poly(D,L-lactic-co-glycolic acid) based nanoparticulate system for enhanced delivery of antigens to dendritic cells. Vaccine 2004;22:2406-2412.

41. Samuel J, Kwon GK: Polymeric Nanoparticle Delivery of Cancer Vaccines. USA, Informa Healthcare, 2005.

42. Hamdy S, Elamanchili P, Alshamsan A, Molavi O, Satou T, Samuel J: Enhanced antigen-specific primary CD4+ and CD8+ responses by codelivery of ovalbumin and toll-like receptor ligand monophosphoryl lipid A in poly(D,L-lactic-co-glycolic acid) nanoparticles. J Biomed Mater Res A 2007;81:652-662.

43. Gerelchuluun T, Lee YH, Lee YR, Im SA, Song S, Park JS, Han K, Kim K, Lee CK: Dendritic cells process antigens encapsulated in a biodegradable polymer, poly(D,L-lactide-co-glycolide), via an alternate class I MHC processing pathway. Arch Pharm Res 2007;30:1440-1446.

44. Feng SS, Mu L, Win KY, Huang G: Nanoparticles of biodegradable polymers for clinical administration of paclitaxel. Curr Med Chem 2004;11:413-424.

45. Yoo JY, Kim JM, Seo KS, Jeong YK, Lee HB, Khang G: Characterization of degradation behavior for PLGA in various pH condition by simple liquid chromatography method. Biomed Mater Eng 2005;15:279-288.

46. Diwan M, Elamanchili P, Lane H, Gainer A, Samuel J: Biodegradable nanoparticle mediated antigen delivery to human cord blood derived dendritic cells for induction of primary T cell responses. J Drug Target 2003;11:495-507.

47. Vicari AP, Chiodoni C, Vaure C, Ait-Yahia S, Dercamp C, Matsos F, Reynard O, Taverne C, Merle P, Colombo MP, O'Garra A, Trinchieri G,

Caux C: Reversal of tumor-induced dendritic cell paralysis by CpG immunostimulatory oligonucleotide and anti-interleukin 10 receptor antibody. J Exp Med 2002;196:541-549.

Chapter 7

General Discussion and Conclusions

7.1 Discussion

Over the past decade, the poor therapeutic outcome of vaccine-based cancer immunotherapy has sparked studies to find the reasons behind this breakdown and develop strategies to overcome the barriers against optimal anti-tumor immunity [1-3]. Recent studies consistently suggest that one of the obstacles to the effectiveness of cancer vaccines is the tumor immunosuppressive environment which suppresses the tumor infiltration and function of immune effector cells [4,5]. In recent years, the search for finding responsible mediators of immunosuppression in cancer at the molecular level, has identified STAT3 as an important protein in this regard [6-8]. In addition to the importance of constitutively active STAT3 in cancer-induced immunosuppression, STAT3 plays a key role in tumor progression through the modulation of genes involved in tumor growth, resistance to apoptosis, angiogenesis, and metastasis [9,10]. Because of the high incidence of constitutively active STAT3 in many types of cancer and its crucial role in cancer progression and immunosuppression, blocking STAT3 in tumors is considered a promising strategy for improving the efficacy of both cancer chemo and immunotherapy. Despite the cumulative evidence supporting STAT3 as a valid therapeutic target in cancer therapy and identification of several potent STAT3 inhibitors [9], no STAT3 inhibitor has moved into clinical trials yet. Insufficient characterization, poor water solubility, and non-specific toxicity of the STAT3 inhibitors are the main reasons for the absence of any clinically used STAT3 inhibitor to date.

JSI-124, discovered in 2003, is one of the most potent STAT3 inhibitors with a potential for clinical application. In comparison to other STAT3 inhibitory strategies investigated to date [11], JSI-124 is a fairly well characterized STAT3 inhibitor agent which has been also studied for its immunomodulatory effects. JSI-124 is highly selective for the inhibition of STAT3 pathway on which cancer cells are very dependent for their growth and survival. Therefore it has selective effects on killing of malignant cells over normal cells. Moreover JSI-124 is a small molecular weight compound, making it easier for delivery to tumor and immune cells using nano-carriers as compared with other peptides and oligonucleotide inhibitor of STAT3. While the potent anticancer and STAT3 inhibitory effects of JSI-124 has been well described previously [12-14], only a few studies have investigated immunomodulatory effects of this important therapeutic agent in cancer immunotherapy settings [15]. Therefore, we purposed to evaluate the effects of JSI-124 induced STAT3 inhibition on therapeutic efficacy of TLR4 and TLR9-based cancer immunotherapy. 7-acyl lipid A and CpG were used as TLR4 and TLR9 ligand, respectively. 7-acyl lipid A is a newly developed ligand for TLR4 and a few studies have shown its potential in the induction of T cell mediated immune responses [16,17]. On the other hand, CpG is a well characterized TLR ligand and it has been widely used as an adjuvant in cancer immunotherapy. CpG is a potent inducer of both innate and adaptive immunity and it is currently being tested in phase II and phase III human clinical trials as adjuvants to cancer vaccines and in combination with conventional chemotherapy and other therapies [18].

Superior anticancer effects of CpG or 7-acyl lipid A + JSI-124 combination therapy in comparison to monotherapy with either TLR9 or TLR4 ligand pointed to the STAT3 activation to restrict the therapeutic efficacy of TLR4 or TLR9-based cancer immunotherapy. JSI-124 induced inhibition of STAT3 in tumors receiving either CpG or 7-acyl lipid A resulted in increased recruitment of effector immune cells to tumor compared with those treated with each TLR ligand alone. Further analysis of anticancer immune responses in the mice that received CpG with or without JSI-124 showed significantly higher intra-tumoral levels of several Th1-related cytokines, increases in intra-tumoral $CD8^+$ and $CD4^+$ T cells expressing activation/memory markers and NK cells, and increases in activated DCs in the tumors and regional LNs of the mice treated with CpG + JSI-124 combination therapy. Concomitantly, the combination therapy led to a significantly decreased level of immunosuppression, as evidenced by lower intra-tumoral levels of VEGF and TGF-β, and decreased number of T_{reg} cells in the regional LNs. These observations suggested that immune-mediated mechanisms are involved in the superior anticancer effects generated by CpG + JSI-124 combination therapy. Kortylewski *et al* have recently used a different approach to demonstrate the immune-mediated mechanisms through which STAT3 inhibition enhances the therapeutic efficacy of CpG-based cancer immunotherapy [19]. The results of this study, published in 2009, show that anti-tumor immune responses induced by CpG-based immunotherapy is significantly enhanced in mice lacking STAT3 in their hematopoietic cells ($STAT3^{-/-}$). These observations go well with our observations (presented in chapter 3 of current

thesis and published as a paper in 2008) on the superior anticancer effects of CpG + JSI-124 combination therapy and provide further evidence for the immune-mediated mechanisms behind the synergistic anticancer effect between CpG and JSI-124 [20].

Since immune-mediated mechanisms seem to be involved in the superior anticancer activity of CpG + JSI-124 combination, such a combination therapy approach is expected to show the similar potent anticancer effects in tumors without STAT3. Many type of human cancers with or without constitutively active STAT3 produce immunosuppressive factors (such as IL10 and VEGF), which can potentially activate STAT3 in immune cells rendering them immunosuppressed [6,21,22]. Moreover, some of these immunosuppressive factors (i.e VEGF) have other oncogenic effects, which are mainly mediated through STAT3 pathway [23]. Therefore, co-delivery of STAT3 inhibitors and CpG to tumor without hyperactive STAT3 is expected to modulate anticancer immune responses and inhibit tumor growth through the following postulated mechanisms. First of all delivery of STAT3 inhibitor to the tumor environment will result in the suppression of STAT3 activity in immunosuppressed immune cells including DCs, effector NK and T cells leading to better functionality of these cells in fight against cancer [6,24]. Moreover, by STAT3 inhibition in immune cells, the population of immunosuppressive immune cells will be reduced inside tumor which subsequently can change the immunosuppressive milieu of tumor to an immunosupportive environment leading to better tumor infiltration and function of immune effector cells [6]. Lastly blocking STAT3 activity

negatively regulates the immunosuppressive and oncogenic effects of the tumor derived factors (such as VEGF) whose function is dependent on STAT3 activity [21,23].

The effect of JSI-124 on enhancing the anticancer and immunomodulatory effects of CpG-based cancer immunotherapy suggest that JSI-124 can, potentially, be an excellent candidate for the modulation of anticancer immune responses and enhancing the efficacy of cancer immunotherapy. However, the clinical application of this important STAT3 inhibitor is dependent on the development of nano-carriers which can solubilize this poorly soluble drug and at the same time provide enhanced delivery of this drug to tumors while reducing its side effects in non-target tissues.

Back in 2005 when this research started, one important limitation for conducting pharmaceutical studies on the development of nano-carriers for delivery of STAT3 inhibitor cucurbitacins and their pharmacokinetic characterization *in vivo* was the absence of a specific and highly sensitive method for the quantification of these compounds. Therefore, a highly sensitive LC-MS method (with sensitivity about 50 Pg) was established for quantitative analysis of cucurbitacin B and JSI-124 and used in different pharmaceutical and pharmacokinetic studies presented in this thesis.

In order to overcome the problem of poor water solubility and non-specific toxicity associated with STAT3 inhibitor cucurbtacins, PEO-*b*-PCL based micellar formulation of cucurbitacins were developed and characterized (chapter five)[25]. PEO-*b*-PCL based micelles especially those with longer PCL or benzyl

substituent on the PCL block, i.e., PBCL, efficiently improved the water solubility of cucurbitacins and controlled the rate of drug release for the more hydrophobic derivative, i.e., cucurbitacin B. Encapsulation of STAT3 inhibitor cucurbitacins in PEO-*b*-PCL based micelles didn't significantly affect the anticancer and STAT3 inhibitory activity of cucurbitacins against B16 cancer both *in vitro* and *in vivo* (after intra-tumoral application). The micellar solution was; however, able to restrict the distribution of encapsulated cucurbitacin out of tumor in a B16 mouse melanoma model. These observations suggest that the development of PEO-*b*-PCL based micelles of STAT3 inhibitor cucurbitacins is a promising approach for overcoming the limitations associated with clinical application of this important category of STAT3 inhibitors.

DCs have been the target of most cancer immunotherapy strategies due to their determinative role in the induction of immunity versus tolerance [26]. Cancer affected immunosuppressed DCs with hyperactive STAT3 are found to be crucial in the establishment of an immunosuppressive network inside tumor [6,27]. Blocking STAT3 in immunosuppressed DCs is considered to be an efficient strategy to restore their function and reverse cancer immunosuppression. Thus, we proposed to target STAT3 inhibitor JSI-124 to DCs using PLGA, a nano-carrier widely used for targeting therapeutic agents to these cells. PLGA NPs containing chemically conjugated JSI-124 was developed and found to be capable of delivering functional JSI-124 to DCs and B16 cancer cells, *in vitro*. Importantly, PLGA-JSI-124 NPs were able to suppress the level of p-STAT3 in immunosuppressed $STAT3^{high}$DCs and restore their function in stimulating T cell

proliferation in MLR reaction, *in vitro.* These observations suggest that PLGA NPs is a potentially suitable nano-carrier for delivery of JSI-124 to DCs as well as cancer cells. In the context of targeted delivery of therapeutics agents to DCs, PLGA-JSI-124 NPs can provide a useful platform for co-delivery of JSI-124 and antigens and/or adjuvants to DCs (Figure 7-1). These findings can have important implications in the development of clinically successful cancer vaccines.

As demonstrated in Figure 7-1 a nanoparticulate formulation carrying STAT3 inhibitor JSI-124, an adjuvant (i.e CpG), and a cancer antigen can be injected intra-tumorally for in situ manipulation of immunosuppression inside tumor and induction of potent anti-tumor immunity. Incorporation of a tumor specific antigen in the cancer vaccine formulation provides a useful tool for characterization of antigen specific immune responses induced by intra-tumoral cancer vaccination. Induction of anticancer immune response by in situ manipulation of tumor environment or intra-tumoral cancer vaccination seems to have better therapeutic efficacy as compared with the vaccines which are injected to a site far from a tumor. The better therapeutic outcome of an intra-tumorally injected cancer vaccine results from its effect on overcoming immunosuppression inside tumor. In other word, intra-tumoral injection of a cancer vaccine containing an STAT3 inhibitory agent and a TLR9 ligand (i.e CpG) can change the immunosuppressive tumor environment to an immunosupportive one facilitating the effector phase of anti-tumor immunity.

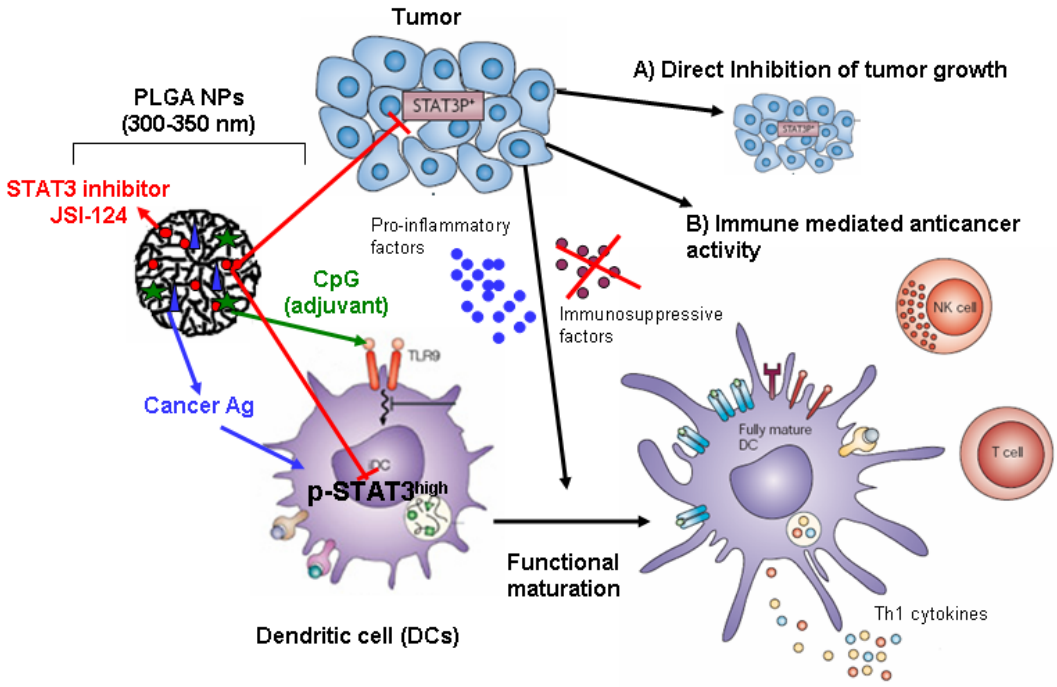

Figure 7-1. The schematic picture showing the potential of PLGA-JSI-124 NPs loaded with CpG and cancer Ag for development of an effective cancer vaccine

7.2 Conclusions

This research has developed a highly sensitive and specific LC-MS method for quantitative analysis of STAT3 inhibitor cucurbitacins *in vitro* and *in vivo*. Our observations on superior anticancer activity of TLR4 and TLR9-based cancer immunotherapy in combination with JSI-124 induced STAT3 inhibition provide a proof of principle for inhibition of STAT3 activation to enhance the therapeutic efficacy of cancer immunotherapy. Moreover, polymeric micelles of cucurbitacins were developed and characterized *in vitro* and in a mouse melanoma model. Our findings showed that PEO-*b*-PCL based micelles can provide a suitable vehicle for solubilization and controlled delivery of cucurbitacins to tumor. Finally, PLGA-JSI-124 NPs were developed and shown to be a potentially useful platform for sustained delivery of JSI-124 in tumor and its targeted delivery to DCs. While polymeric micelles are promising nano-carriers for sustained JSI-124 delivery to the tumor microenvironment, their small size and the dense hydrophilic coating of PEO can restrict their interaction with DCs. On the other hand PLGA NPs are naturally targeted to DCs through phagocytosis since their size is comparable to that of pathogens and their surface is not protected by a hydrophilic palisade [28]. With respect to successful use of PLGA NPs for of delivery of several antigens, adjuvants and small molecules to DCs [16,29-32], this type of nano-carriers is expected to provide a promising platform for co-delivery of cancer vaccines and STAT3 inhibitors to DCs.

7.3 Future studies

Several studies have suggested that STAT3 inhibition in tumor and/or immunosuppressed DCs is a promising strategy for enhancing the therapeutic efficacy of cancer immunotherapy [6,27]. Our findings presented in chapter two and three support the notion that STAT3 activation restricts the therapeutic efficacy of TLR-based cancer immunotherapy. These studies suggest that JSI-124 induced inhibition of STAT3 can be an effective strategy for improving the therapeutic outcome of TLR9-based immunotherapy.

An important limitation to our studies on the immunomodulatory and anticancer effects of JSI-124 + TLR9 combination therapy is the use of mice carrying subcutaneously implanted tumor. Transplantable tumors have been extensively used in immunotherapeutic studies, but there are important limitations to the use of these models [33]. First of all, subcutaneously injected cancer cells grow in the anatomically inappropriate site so the immune system is not exposed to the tumor in a manner that naturally happens. Moreover, subcutaneous tumors grow faster so the kinetic variation can lead to different immunological outcomes. Besides, premalignant lesions, which might already induce immune responses, cannot be found in s.c. growing tumors. Finally, transplantable tumors are not metastatic. With respect to the high prevalence and impotence of tumor metastasis as a major cause of death in cancer patients, the effect of any cancer therapy approach should be evaluated in metastatic tumor models. Therefore, further studies are suggested to investigate the immunomodulatroy and anticancer effects of JSI-124 + TLR9-based cancer immunotherapy in animal spontaneous tumor

models, which mimic as closely as possible the human cancer for which the therapy is designed.

The use of only one mouse cancer model with B16 tumor having constitutively activated STAT3 represents another limitation for our study. JSI-124 shows potent anticancer activity in tumors with constitutively active STAT3 since it directly inhibits tumor growth and survival through the suppression of STAT3 activity. Therefore, the immunomodulatory effects of JSI-124 are needed to be investigated in other tumor models without hyperactive STAT3.

Another limitation for studying the immunomodulatory effects of JSI-124 + CpG in a mouse model is related to different expression pattern of TLR9 in human and mouse system [18]. In human TLR9 expression profile in immune cells is narrower than that in mouse immune system. While the expression of TLR9 ligand is only limited to B cells and pDCs in human immune system, B cells, monocytes, and probably all DC subsets express TLR9 in mouse. Consequently, the mouse immune system produces different cytokines and chemokines when exposed to unmethylated CpG motifs, making it extremely difficult to predict the effects of TLR9 activation in humans by drawing conclusions from results with mice.

The lack of our knowledge on the contribution of STAT3 hyperactivation in tumor and DCs to tumor-induced immunosuppression in human malignances is another limitation for. While several studies in mouse cancer models have consistently shown the critical role of STAT3 in the induction of cancer immunosuppression [6], no definitive date has been reported for the effect of

STAT3 hyperactivation in tumor or DCs on tumor-induced immunosuppression in human cancers. Therefore clinical application of JSI-124 + TLR9-based cancer immunotherapy is dependent on further studies on the role of constitutively activated STAT3 in the induction of immunosuppression in human cancers.

Polymeric micellar formulations have been extensively investigated for of the solubilization of poorly water soluble anticancer agents with non-specific toxicity. The current research demonstrates that PEO-*b*-PCL based micelles may potentially provide a suitable vehicle for the solublizaiton and controlled delivery of STAT3 inhibitor cucurbitcins. Further studies are required to develop an optimized polymeric micellar formulation capable of solubilization and tumor targeted delivery of JSI-124 after systemic administration. Because of the relatively rapid release of JSI-124 from polymeric micelles shown *in vitro*, a premature release of JSI-124 from these nano-carriers upon i.v. administration, *in vivo*, was envisioned. However, further biodistribution and pharmacokinetic studies are needed to evaluate the potential of PEO-*b*-PCL based micelle formulation in actual *in vivo* studies after i.v. administration. As an alternative strategy to reduce the premature release of JSI-124 from its polymeric micellar carrier, chemical conjugation of JSI-124 to PEO-b-PCCL can be pursued. Preliminary studies conducted in our group have shown the successful attachment of JSI-124 to PEO-*b*-PCCL using DCC and DMAP as catalysts (appendix).

PLGA NPs has been extensively investigated for the delivery of therapeutic agents to DCs and tumor. PLGA NPs containing JSI-124 were developed. The capability of the developed formulation in restoring the function

of immunosuppressed STAT3^{high}DCs in stimulating T cell proliferation *in vitro* demonstrate the potential of PLGA NPs for targeted delivery of JSI-124 to cancer and affected immunosuppressed DCs for effective immunotherapy of cancer. An important limitation for this study is the evaluation of the effects of our formulation on DCs and T cells in culture, *in vitro*. Indeed all the cells and mediators of immune systems are working in a close interaction with each others in a complex network, *in vivo*. Moreover, there is a complicated interaction between immune cells and cancer cells, *in vivo*. Therefore, the immunomodulatory and anticancer effects of PLGA NPs delivery of JSI-124 must be investigate in relevant cancer models, *in vivo.*

Furthermore, in our study the adjuvant activator of DCs (i.e. CpG) was encapsulated in a separate PLGA NP not in NPs containing chemically conjugated JSI-124. We believe that encapsulation of the adjuvants in the same NP as the one with chemically conjugated STAT3 inhibitor JSI-124, can provide a better formulation for co-delivery of JSI-124 and CpG. Such a formulation can be loaded with tumor specific/associated antigens for the development of peptide-based cancer vaccines. Thus additional pharmaceutical studies are suggested to develop and characterize PLGA-JSI-124 NPs loaded with CpG for co-delivery of CpG and JSI-124 to DCs. This type of nano-carrier can have potential application in the development of effective cancer vaccine delivering adjuvant (CpG), cancer antigen, and STAT3 inhibitor JSI-124 to DCs.

7.4 References

1. Rosenberg SA, Yang JC, Restifo NP: Cancer immunotherapy: moving beyond current vaccines. Nat Med 2004;10:909-915.
2. Pejawar-Gaddy S, Finn OJ: Cancer vaccines: Accomplishments and challenges. Crit Rev Oncol Hematol 2008.
3. Slingluff CL, Speiser DE: Progress and controversies in developing cancer vaccines. J Transl Med 2005;3:18-27.
4. Gajewski TF, Meng Y, Blank C, Brown I, Kacha A, Kline J, Harlin H: Immune resistance orchestrated by the tumor microenvironment. Immunol Rev 2006;213:131-145.
5. Zou W: Immunosuppressive networks in the tumour environment and their therapeutic relevance. Nat Rev Cancer 2005;5:263-274.
6. Yu H, Kortylewski M, Pardoll D: Crosstalk between cancer and immune cells: role of STAT3 in the tumour microenvironment. Nat Rev Immunol 2007;7:41-51.
7. Kortylewski M, Xin H, Kujawski M, Lee H, Liu Y, Harris T, Drake C, Pardoll D, Yu H: Regulation of the IL-23 and IL-12 balance by Stat3 signaling in the tumor microenvironment. Cancer Cell 2009;15:114-123.
8. Stewart CA, Trinchieri G: Reinforcing suppression using regulators: a new link between STAT3, IL-23, and Tregs in tumor immunosuppression. Cancer Cell 2009;15:81-83.
9. Al Zaid Siddiquee K, Turkson J: STAT3 as a target for inducing apoptosis in solid and hematological tumors. Cell Res 2008;18:254-267.

10. Yu H, Jove R: The STATs of cancer--new molecular targets come of age. Nat Rev Cancer 2004;4:97-105.

11. Jing N, Tweardy DJ: Targeting Stat3 in cancer therapy. Anticancer Drugs 2005;16:601-607.

12. Blaskovich MA, Sun J, Cantor A, Turkson J, Jove R, Sebti SM: Discovery of JSI-124 (cucurbitacin I), a selective Janus kinase/signal transducer and activator of transcription 3 signaling pathway inhibitor with potent antitumor activity against human and murine cancer cells in mice. Cancer Res 2003;63:1270-1279.

13. Sun J, Blaskovich MA, Jove R, Livingston SK, Coppola D, Sebti SM: Cucurbitacin Q: a selective STAT3 activation inhibitor with potent antitumor activity. Oncogene 2005;24:3236-3245.

14. Van Kester MS, Out-Luiting JJ, von dem Borne PA, Willemze R, Tensen CP, Vermeer MH: Cucurbitacin I Inhibits Stat3 and Induces Apoptosis in Sezary Cells. J Invest Dermatol 2008.

15. Nefedova Y, Nagaraj S, Rosenbauer A, Muro-Cacho C, Sebti SM, Gabrilovich DI: Regulation of dendritic cell differentiation and antitumor immune response in cancer by pharmacologic-selective inhibition of the janus-activated kinase 2/signal transducers and activators of transcription 3 pathway. Cancer Res 2005;65:9525-9535.

16. Hamdy S, Elamanchili P, Alshamsan A, Molavi O, Satou T, Samuel J: Enhanced antigen-specific primary CD4+ and CD8+ responses by codelivery of ovalbumin and toll-like receptor ligand monophosphoryl

lipid A in poly(D,L-lactic-co-glycolic acid) nanoparticles. J Biomed Mater Res A 2007;81:652-662.

17. Hamdy S, Haddadi A, Somayaji V, Ruan D, Samuel J: Pharmaceutical analysis of synthetic lipid A-based vaccine adjuvants in poly (D,L-lactic-co-glycolic acid) nanoparticle formulations. J Pharm Biomed Anal 2007;44:914-923.

18. Krieg AM: Development of TLR9 agonists for cancer therapy. J Clin Invest 2007;117:1184-1194.

19. Kortylewski M, Kujawski M, Herrmann A, Yang C, Wang L, Liu Y, Salcedo R, Yu H: Toll-like receptor 9 activation of signal transducer and activator of transcription 3 constrains its agonist-based immunotherapy. Cancer Res 2009;69:2497-2505.

20. Molavi O, Ma Z, Hamdy S, Lai R, Lavasanifar A, Samuel J: Synergistic antitumor effects of CpG oligodeoxynucleotide and STAT3 inhibitory agent JSI-124 in a mouse melanoma tumor model. Immunol Cell Biol 2008;86:506-514.

21. Johnson BF, Clay TM, Hobeika AC, Lyerly HK, Morse MA: Vascular endothelial growth factor and immunosuppression in cancer: current knowledge and potential for new therapy. Expert Opin Biol Ther 2007;7:449-460.

22. Mimura K, Kono K, Takahashi A, Kawaguchi Y, Fujii H: Vascular endothelial growth factor inhibits the function of human mature dendritic

cells mediated by VEGF receptor-2. Cancer Immunol Immunother 2007;56:761-770.

23. Chen Z, Han ZC: STAT3: A critical transcription activator in angiogenesis. Med Res Rev 2007.

24. Kortylewski M, Kujawski M, Wang T, Wei S, Zhang S, Pilon-Thomas S, Niu G, Kay H, Mule J, Kerr WG, Jove R, Pardoll D, Yu H: Inhibiting Stat3 signaling in the hematopoietic system elicits multicomponent antitumor immunity. Nat Med 2005;11:1314-1321.

25. Molavi O, Ma Z, Mahmud A, Alshamsan A, Samuel J, Lai R, Kwon GS, Lavasanifar A: Polymeric micelles for the solubilization and delivery of STAT3 inhibitor cucurbitacins in solid tumors. Int J Pharm 2008;347:118-127.

26. Novak N, Bieber T: 2. Dendritic cells as regulators of immunity and tolerance. J Allergy Clin Immunol 2008;121:S370-374; quiz S413.

27. Nefedova Y, Gabrilovich DI: Targeting of Jak/STAT pathway in antigen presenting cells in cancer. Curr Cancer Drug Targets 2007;7:71-77.

28. Foged C, Sundblad A, Hovgaard L: Targeting vaccines to dendritic cells. Pharm Res 2002;19:229-238.

29. Elamanchili P, Diwan M, Cao M, Samuel J: Characterization of poly(D,L-lactic-co-glycolic acid) based nanoparticulate system for enhanced delivery of antigens to dendritic cells. Vaccine 2004;22:2406-2412.

30. Elamanchili P, Lutsiak CM, Hamdy S, Diwan M, Samuel J: "Pathogen-mimicking" nanoparticles for vaccine delivery to dendritic cells. J Immunother 2007;30:378-395.

31. Samuel J, Kwon GK: Polymeric Nanoparticle Delivery of Cancer Vaccines. USA, Informa Healthcare, 2005.

32. Gerelchuluun T, Lee YH, Lee YR, Im SA, Song S, Park JS, Han K, Kim K, Lee CK: Dendritic cells process antigens encapsulated in a biodegradable polymer, poly(D,L-lactide-co-glycolide), via an alternate class I MHC processing pathway. Arch Pharm Res 2007;30:1440-1446.

33. Ostrand-Rosenberg S: Animal models of tumor immunity, immunotherapy and cancer vaccines. Curr Opin Immunol 2004;16:143-150.

Appendix

Development of other formulations for depot release of JSI-124

A) Temperature-responsive hydrogel formulations for in situ delivery of JSI-124

Methods:

Preparation of chitosan and Pluronic F127 hydrogel containing JSI-124: PEO-*b*-PBCL micelles of JSI-124 were prepared as described in chapter 5 section 5.2.2. Then 50 µl of aqueous solution of JSI-124 micelles containing (15 µg JSI-124) was mixed with 400 mL of either 1.8% chitosan or 20% Pluronic F127 solution at 4°C. The level of JSI-124 in each formulation was measured using LC-MS as described in chapter 4 section 4.2.2. Almost 100% of added JSI-124 was soluble in both hydrogel formulations.

***In vitro* release of JSI-124 from chitosan and Pluronic F127 hydrogel**. The release study was performed at 25°C for F127 formulation and at 37°C for chitosan gel. Diffusion cells with a cellulose membrane separating donor and acceptor phase were used. The gel formulations were applied evenly on the surface of the membrane in the donor compartment. The receptor compartment was filled with ddH_2O, stirred at 300 rpm, and maintained at 37°C for chitosan hydrogel and at room temperature for F127 formulation. At predetermined time intervals 20 µl were taken from the receptor compartment consisting of ddH_2O, and JSI-124 content of the samples was analyzed by LC-MS as described in chapter 4 section 4.4.2.

Results:
The results of this study indicated a relatively rapid release of JSI-124 from both formulations. Drug release from micelles incorporated in the F127 hydrogel was particularly very rapid (Figure 1). This may reflect the intraction of F127 block copolymers leading to instabilization of micelles in the gel formulation.

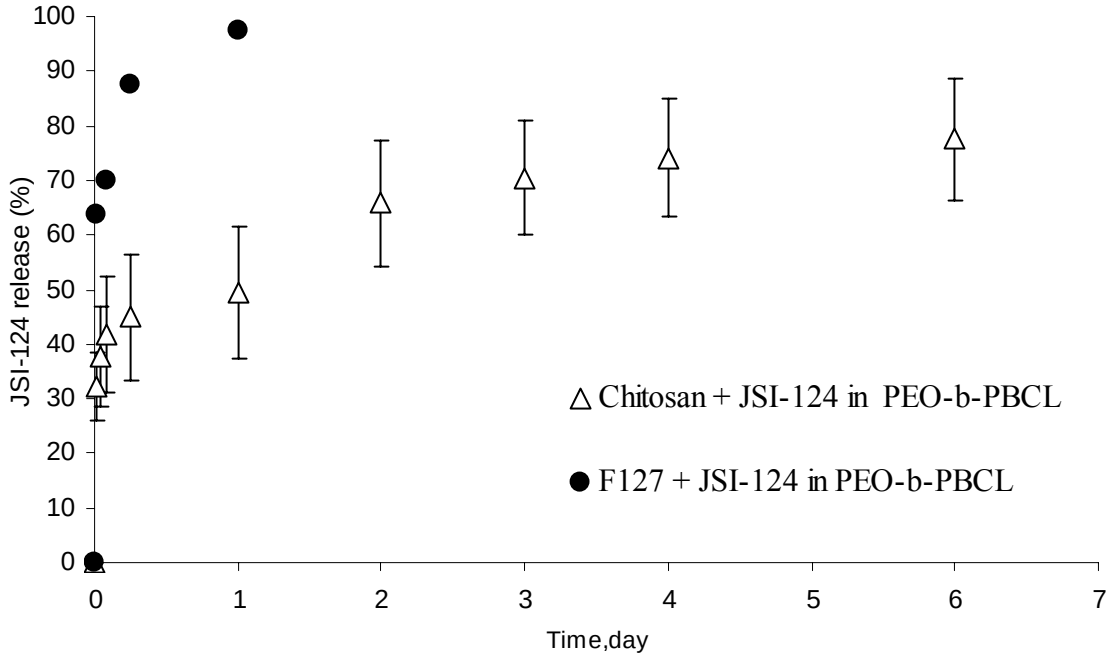

Figure 1. *In vitro* release profile of JSI-124 from hydrogel formulations

B) Chemical conjugation of JSI-124 to PEO-b-α-carboxyl-ε-caprolactone (PCCL) block copolymer

Method:

Chemical Conjugation of JSI-124 to PEO-*b*-PCCL:

To prepare PEO-*b*-PCCL copolymer, PEO-*b*-PBCL was synthesized as described in chapter 5, section 5.2.2. PEO-*b*-PCCL was obtained by the catalytic debenzylation of PEO-*b*- PBCL in the presence of hydrogen gas. Briefly, a solution of PEO-*b*-PBCL (200 mg in 25 mL of THF) was placed into a 100 mL round-bottom flask. Charcoal coated with palladium (300 mg) was dispersed in this solution. The flask was sealed with a septum, and vacuum was applied through a needle for 10 min. The reaction flask was filled with hydrogen gas and maintained a continuous supply of hydrogen gas. The mixture was stirred vigorously with a magnetic stirrer and reacted with hydrogen for 24 h at room temperature. The reaction mixture was centrifuged at 3000 rpm to remove the catalyst. The supernatant was collected, condensed under reduced pressure, precipitated in diethyl ether, and washed repeatedly to remove impurities. The final product was collected and dried under vacuum at room temperature for 48 h. The ^{1}H NMR spectrum of reduced block copolymer in DMSO-d_6 at 300 MHz was used to assess the conversion of benzyl carboxylate to carboxyl group following the disappearance of the characteristic aromatic peak at *ä*) 7.4 ppm (Figure 2). The conjugation of JSI-124 to PEO-*b*-PCCL was carried out with DCC and DMAP as coupling agent and catalyst. Briefly DMAP (52.41 mg , 0.429 mM) and DCC (88.5 mg, 0.429 mM) were added to a stirring solution of PEO-*b*-PCCL (25 mg, 0.0033 mM) in anhydrous THF (25 mL) under argon gas. The reaction mixture was stirred for 1 h at room temperature. A solution of JSI-124 (8 mg ~ 0.0165 mM) in anhydrous THF (10 mL) was then added to the reaction mixture and the reaction was continued for an additional 96 h. Evaporation of the reaction mixture gave a residue that was dissolved in a 1:5 ratio of HPLC grade THF and methanol (10 mL). The solution of PEO-PCCL-JSI-124 polymer was then added to 20 mL water in a drop-wise manner while stirring. The resulting solution was dialyzed against water for 48 h to remove the unreacted JSI-124 and any other by-product. PEO-*b*-PCCL-JSI-124 conjugate was lyophilized to a bright yellow solid. JSI-124 esters of PEO-*b*-PCCL were characterized by ^{1}H NMR.

Results:

Chemical conjugation of JSI-124 to PEO-*b*-PCCL copolymer

JSI-124 has several hydroxyl groups in its structure. For generation of cleavable ester bond between JSI-124 and the polymer, A hydroxyl group form JSI-124 was reacted with carboxyl group repeated over PCL block of PEO-*b*-PCCL polymer using DMAP and DCC as coupling agent and catalyst. The conjugation of the JSI-124 molecule to PEO-*b*-PCCL copolymer was confirmed by the ^{1}H NMR spectrum of PEO-*b*-PCCL copolymer (Figure 2B), free JSI-124 (Figure 3A), and PEO-*b*-PCCL-JSI-124 in DMSO-d_6 (Figure 3B). ^{1}H NMR spectrum of PEO-*b*-PCCL-JSI-124 shows the characteristic JSI-124 peaks at 5.6 and 0.8 ppm (Figure 3B). Similar peaks were also present in the ^{1}H NMR spectrum of the free JSI-124 (Figure 3A).

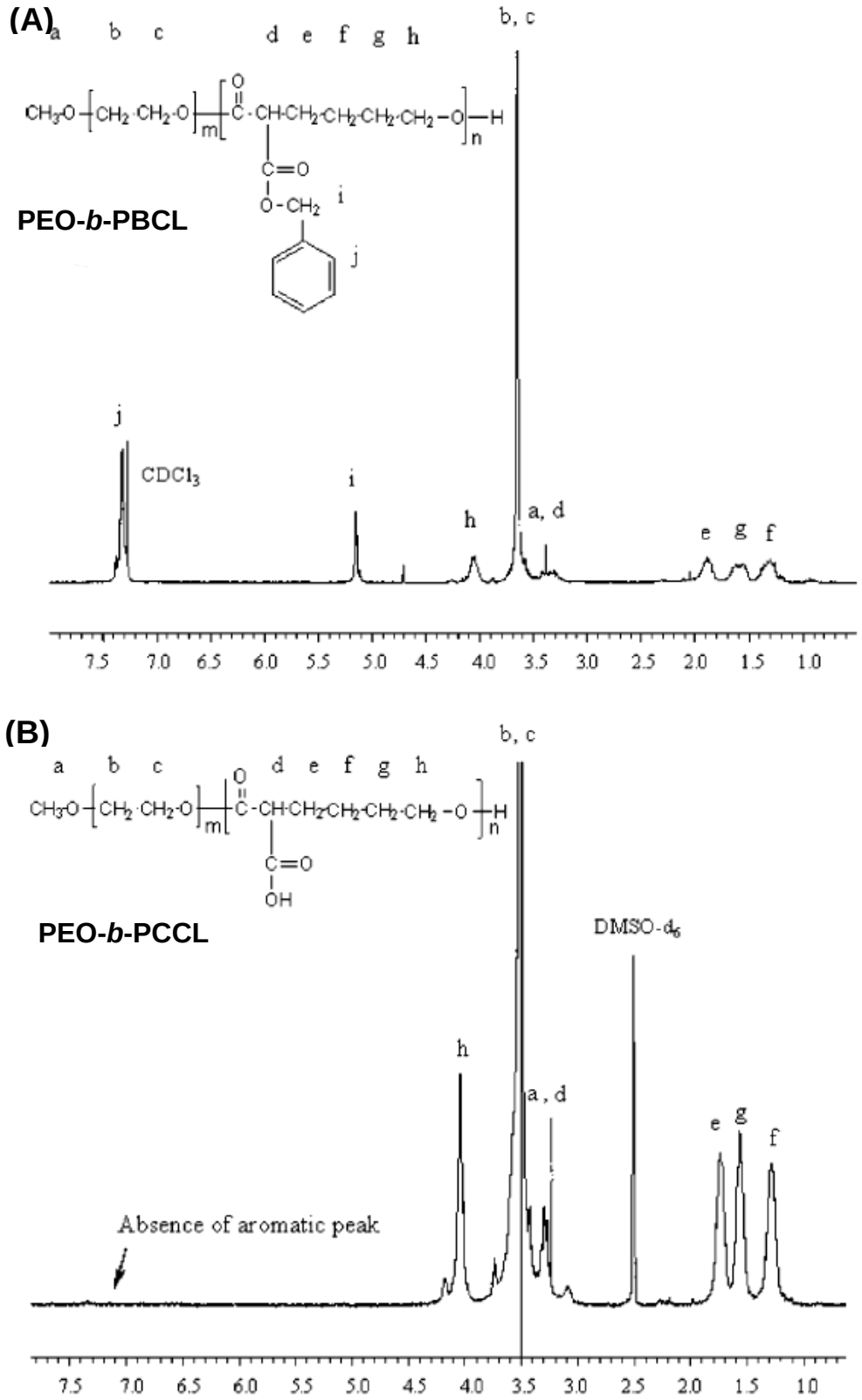

Figure 2: ^{1}H NMR spectrum for A) PEO-*b*-PBCL in $CDCl_3$ B) PEO-*b*-PCCL in DMSO-d_6

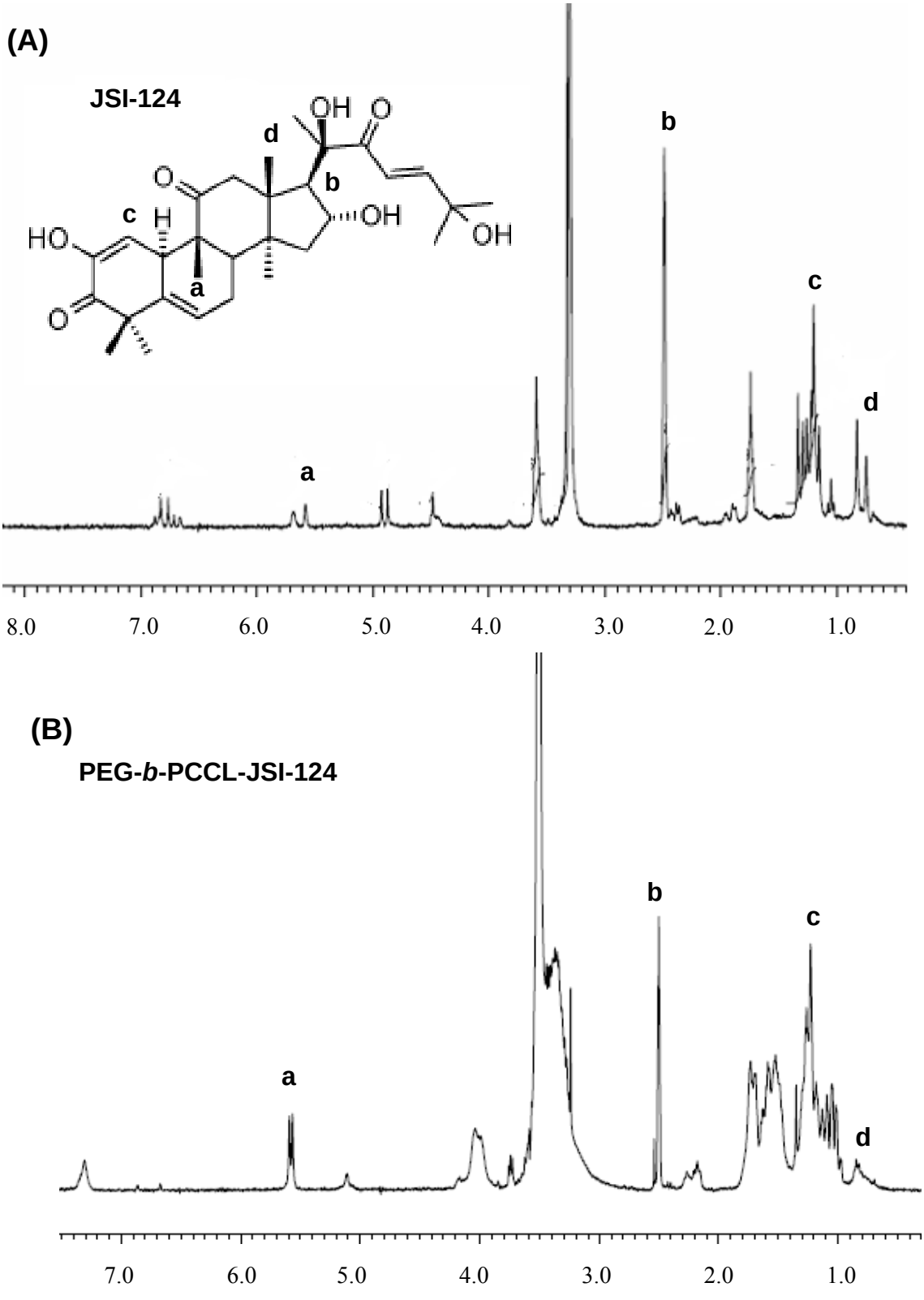

Figure 3: ^{1}H NMR spectrum for A) JSI-124 B) PEO-*b*-PCCL-JSI-124 in DMSO-d_6